It’s like Dis!

Ribonucleases associated with the human RNA exosome

Raymond H.J. Staals

Cover illustration:
Gerard W.M. Staals
www.gerardstaalsart.nl

Printed & Lay Out by:
Proefschriftmaken.nl || Uitgeverij BOXPress

ISBN 9789462950511

It’s like Dis!

Ribonucleases associated with the human RNA exosome

Proefschrift

ter verkrijging van de graad van doctor
aan de Radboud Universiteit Nijmegen
op gezag van de rector magnificus prof. dr. Th.L.M. Engelen,
volgens besluit van het college van decanen
in het openbaar te verdedigen op vrijdag 9 januari 2015
om 16.30 uur precies

door
Raymond Hubert Josèphe Staals
geboren op 16 oktober 1979
te Grubbenvorst

Promotor:

Prof. dr. G.J.M. Pruijn

Manuscriptcommissie:

Prof. dr. R.J.M. Nolte
Prof. dr. R. Agami (Nederlands Kanker Instituut, Amsterdam)
Dr. A. Aschrafi

The research presented in this thesis was performed at the Department of Biomolecular Chemistry, Institute for Molecules and Materials and Nijmegen Centre for Molecular Life Sciences, Radboud University Nijmegen, The Netherlands

TABLE OF CONTENTS

CHAPTER 1

General introduction

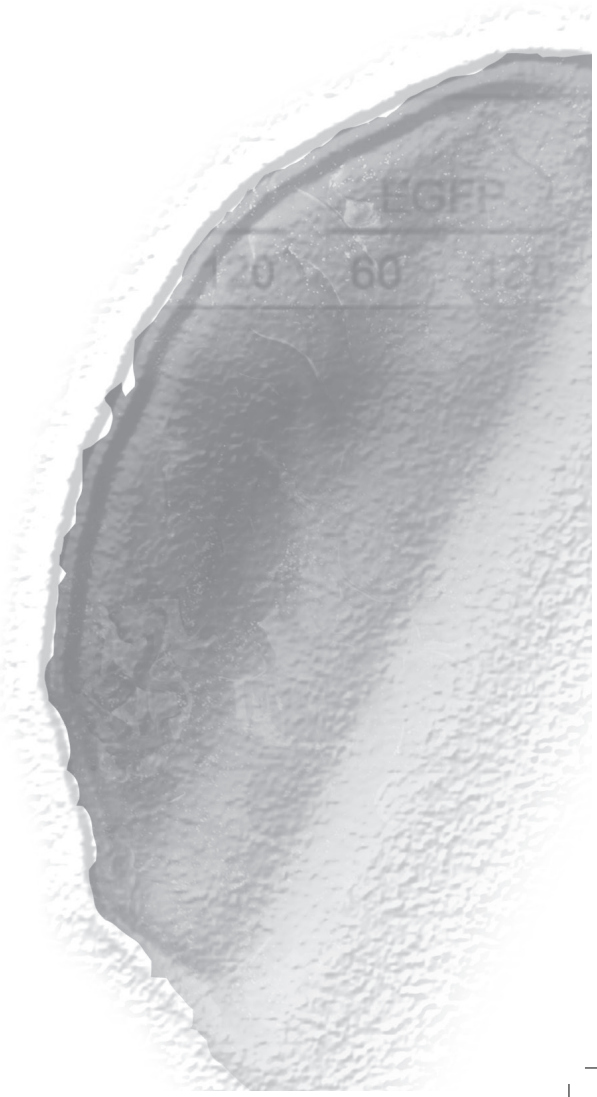

It is feasible that RNA is one of the oldest biomacromolecules still present in living cells today. The versatility of RNA is perhaps one of the most important reasons why it still has such a central position. Arguably, the most well-known function of RNA is to confer the genomic information embedded in the DNA into functional proteins, but RNAs can be utilized for many other different purposes. Examples of this include the use of RNA as a structural component (e.g. the tRNAs), the use of RNA as a catalytic subunit (i.e. ribozymes) and the use of RNA as a regulatory element (e.g. miRNAs). This great variety of functions also implies that the metabolism of these important biomolecules must be tightly regulated within a cell. One of the many different factors that govern this regulation is a protein complex with associated 3'-5' exoribonuclease activity called the RNA exosome, which has been conserved in archaea and eukarya, while eubacteria contain a similar protein complex called the degradosome. This chapter will give an outline of the thesis combined with a brief review of our current knowledge on the RNA exosome, addressing its structure and function in different species.

Discovery of the exosome

While the discovery of the human RNA exosome complex was facilitated by its association with disease (see Chapter 2), the first indication of the presence of such a protein complex came from studies in yeast. Around 1990, research focused on the most abundant type of RNA species: the ribosomal RNAs (or rRNAs). The rRNAs are believed to constitute as much as 75% of the total RNA content of a cell, and since they are essential components of the ribosomes, they are directly involved in the production of virtually all proteins operating in a living cell. One of the constituents that make up the large subunit (60S) of the yeast ribosome is the 5.8S rRNA. It is initially transcribed as a large precursor rRNA (also pre-rRNA), which is modified by several endonucleases and exonucleases to produce the mature 5.8S rRNA and the two larger RNA components of ribosomes. This process is often referred to as 'maturation', and much effort was put into finding and characterizing the protein(s) that are involved in this process. For this reason, temperature-sensitive yeast mutants were screened for defects in pre-rRNA maturation by northern blot hybridization experiments, which revealed aberrant 5.8S rRNA species that were extended at either their 5' or 3' end.

The 5'-extended pre-5.8S rRNA species were found to be a result of a mutation in the Pop1 gene, which was later shown to be a part of a large multi-protein complex with associated endonuclease activity called RNase MRP (Lygerou *et al*, 1996). The gene associated with the mutation that led to aberrant 5.8S rRNA species extended at their 3'-end was cloned and designated Rrp4 (rRNA processing defective). The discovery that this protein was associated with 3'-5' exoribonuclease activity led to the hypothesis that Rrp4 is responsible for generating the mature 3'-end of the 5.8S rRNA species (Mitchell *et al*, 1996). Analogous to Pop1, the Rrp4 protein appeared to be a constituent of a 300-400 kDa protein complex, as determined by glycerol gradient sedimentation analysis. Aided by the advances in protein purification and protein identification by nanoelectrospray mass spectrometry, four other constituents of the

complex were readily identified: Rrp41, Rrp42, Rrp43 and Rrp44 (Mitchell *et al*, 1997). Analysis of their amino acid sequences showed that Rrp4, Rrp41, Rrp42 and Rrp43 shared homology to the bacterial exonuclease RNase PH, which is a relatively well-known protein belonging to the PDX superfamily of 3'-5' phosphorolytic exonucleases (Table 1).

The hallmark of a phosphorolytic enzyme is that it uses inorganic phosphate to attack the nucleotide-nucleotide bond, while a hydrolytic enzyme will activate a water molecule to establish this (schematically illustrated in Figure 1). As a result, phosphorolytic enzymes will release nucleotide diphosphates (NDPs), while hydrolytic enzymes will release nucleotide monophosphates (NMPs). An example of such a hydrolytic enzyme is the fourth identified component of the complex, Rrp44 (also called Dis3), which shares homology to the bacterial RNase R and RNase II, and is therefore placed in the RNR superfamily of exonucleases.

Screening the yeast genome for open reading frames (ORFs) encoding proteins with homology to RNase PH, allowed the identification of three additional proteins: Rrp45, Rrp46 and Mtr3 (Mian, 1997), which were later found to be constituents of the same complex (Allmang *et al*, 1999b). In the latter study, two additional protein subunits of the complex were identified: Rrp40 and Csl4 (an overview of all the different exosome components is given in Table 2). These two proteins were grouped together with Rrp4 in a separate superfamily of exonucleases (RRP4), because of their S1 and/or KH RNA binding domains and their lack of homology to any of the RNase PH-like proteins. Further evidence that these proteins are functionally related came from experiments in yeast, which demonstrated that all of them are essential for proper 3' end formation of the 5.8S rRNA. For obvious reasons, this protein complex with exoribonuclease activity was designated 'the exosome'. Shortly hereafter, the human exosome was identified as well, after Allmang and colleagues realized that a previously identified complex in humans, frequently targeted by autoantibodies in the serum of patients suffering from the polymyositis/scleroderma-overlap syndrome showed striking similarities with the yeast exosome (Allmang *et al*, 1999b; Brouwer *et al*, 2001).

Table 1. Overview of exoribonuclease superfamilies.[1]

Superfamily	Exoribonucleases (examples)	Activity
5PX	Xrn1, Rat1	5'-3' hydrolytic
DEDD	RNase D, RNase T, Rrp6 (PM/Scl-100)	3'-5' hydrolytic
PDX	PNPase, RNase PH, 'exosome ring'	3'-5' phosphorolytic
RNB	RNase BN	3'-5' hydrolytic
RNR	RNase R, RNase II, Dis3, Dis3-like 1	3'-5' hydrolytic
RRP4	Rrp4, Rrp40, Csl4	3'-5' phosphorolytic[2]

[1] Table is adapted from Zuo and colleagues (Zuo and Deutscher, 2001)

[2] Only activity of the plant Rrp4 has been demonstrated

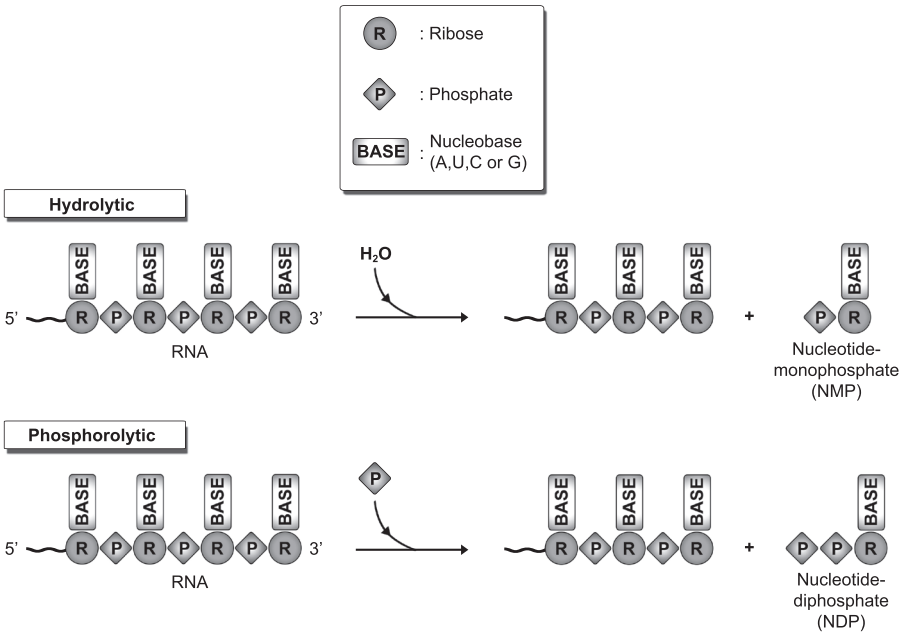

Figure 1. Hydrolytic versus phosphorolytic exoribonuclease activity.

Although exoribonucleolytic RNA degradation can be performed in two different directions (either 3' to 5' or 5' to 3') and can involve many different enzymes, there are only two underlying mechanisms to establish this. In hydrolytic RNA degradation, a water molecule will be used for a nucleophilic attack on the RNA ribose-phophate backbone, and as a result will generate NMPs. Phosphorolytic RNA degradation entails the usage of inorganic phosphate to establish this, leading to the formation of NDPs.

Structure of the exosome

The complex formation of proteins with RNase PH-like domains (RPDs) and proteins containing S1 and/or KH RNA-binding domains was reminiscent of a protein complex originally identified in eubacteria, called polynucleotide phosphorylase, or PNPase (Figure 2A). This complex is composed of three PNPase molecules, each containing two different RNase PH-like domains (RPD1 and RPD2), a S1 and a KH RNA binding domain (Symmons *et al*, 2000). Although each PNPase molecule has two RPDs, only one of them (RPD2) was found to be phosphorolytically active, in agreement with the lack of conservation of key residues in RPD1. RPD1 seems to be of structural importance, as the active sites as well as the RNA-binding surfaces are formed at the interface between RPD1 and RPD2. This protein complex adopts a ring-like structure, formed by the alternating RPD1 and RPD2 domains, while the RNA-binding domains are positioned on one side of the ring.

Although PNPase was originally discovered as the first enzyme synthesizing RNA (Grunberg-Manago *et al*, 1955), it later became clear that the primary function of PNPase, like that of the exosome, is the processing and degradation of RNA (Yehudai-Resheff *et al*, 2001). It is also

Table 2. Exosome core components and exosome-associated proteins and complexes.

Exosome core proteins						
Protein name (subcellular localization[1])					**Domain(s)[2]**	**Remarks**
Archaea	***S. cerevisiae***		**Human**			
Rrp41	Rrp41	(N/C)	Rrp41	(N/C)	RPD2	(Putative) phosphorolytic 3'-5 exoribonuclease
	Rrp46		Rrp46			
	Mtr3		Mtr3			
Rrp42	Rrp42	(N/C)	Rrp42	(N/C)	RPD1	(Putative) phosphorolytic 3'-5 exoribonuclease
	Rrp43		OIP2			
	Rrp45		PM/Scl-75			
Rrp4	Rrp4	(N/C)	Rrp4	(N/C)	S1, KH	RNA binding
Rrp40	Rrp40		Rrp40			
Csl4	Csl4	(N/C)	Csl4	(N/C)	S1	RNA binding
Exosome-associated proteins						
Exonucleases						
-	Dis3	(N/C)	Dis3	(N)	RNB	Hydrolytic 3'-5' exoribonuclease
					PIN	Endonuclease
-	-	-	Dis3-like 1	(C)	RNB	Hydrolytic 3'-5' exoribonuclease
-	Rrp6	(N)	PM/Scl-100	(N/C)	35EXOc	Hydrolytic 3'-5' exoribonuclease
TRAMP complex						
-	Trf4	(N)	Trf4-2	(N)	PAP	Poly(A) polymerase
	Trf5					
-	Air1	(N)	ZCCHC7	(N)	Znf	RNA binding (Zinc finger)
	Air2					
-	Mtr4	(N)	Mtr4	(N)	DEXDc	DEAD-like helicase
NEXT complex						
-	-	-	RBM7	(N)	RRM	RNA binding
-	-	-	ZCCHC8	(N)	Znf	RNA binding (Zinc finger)
-	-	-	Mtr4	(N)	DEXDc	DEAD-like helicase
Ski complex						
-	Ski2	(C)	SkiV2	(C/N)	DEXDc	DEAD-like helicase
-	Ski3	(C)	Ski3	(C/N)	TPR	Protein-protein interactions?
-	Ski8	(C)	Ski8	(C/N)	WD40	Protein-protein interactions?

CBCA complex						
-	Cbc2	(C/N)	CBP20	(C/N)	RRM	(capped) RNA binding
-	Cbc1	(C/N)	CBP80	(C/N)	MIF4G	Structural protein
-	-	-	ARS2	(C/N)	-	Protein-protein interactions
Ccr4-Not complex						
-	Not(1-5)	(C/N)	Cnot(1-5)	(C/N)	-	-
-	Ccr4	(C/N)	Cnot6	(C/N)	LRR	Deadenylase
-	Caf1	(C/N)	Cnot7	(C/N)	-	Deadenylase
-	Caf40	(C/N)	Cnot9	(C/N)	-	-
-	Caf130	(C/N)	Cnot10	(C/N)	-	-
Others						
-	Rrp47	(N)	C1D	(N)	-	Interacts with Rrp6 (PM/Scl-100)
-	MPP6	(N)	MPP6	(N)	-	Interacts with Rrp6 (PM/Scl-100)
AU-binding proteins						
-	-	-	KSRP	(C/N)	KH	Destabilization
-	-	-	AUF1/ hnRNP D	(C/N)	RRM	Stabilization / destabilization
-	-	-	TTP	(C/N)	CCCH zinc finger	Destabilization
-	-	-	RHAU	(C/N)	DExH/D	RNA helicase / destabilization
-	-	-	HuR	(N)	RRM	Stabilization

[1] Subcellular localization of the protein (C = cytoplasm, N = nucleus)

[2] RPD1/2 (RNase PH-like domain 1/2), S1 (RNA-binding domain, S1), KH (K Homology domain), RNB (catalytic domain of ribonuclease II), PIN (PilT N terminus), 35EXOc (3' to 5' exonuclease domain), PAP (polynucleotide adenylyltransferases polymerase), Znf (Zinc finger domain), DEXDc (Helicase-like, DEXD box c2 type domain), TPR (Tetratricopeptide repeat domain), WD40 (WD40-repeat-containing domain), RRM (RNA recognition motif domain), MIF4G (Middle domain of eukaryotic initiation factor 4G), LRR (leucine-rich repeats), CCCH zinc finger (Zinc finger, CCCH-type domain), DExH/D (DEXH box helicase, DNA ligase-associated domain).

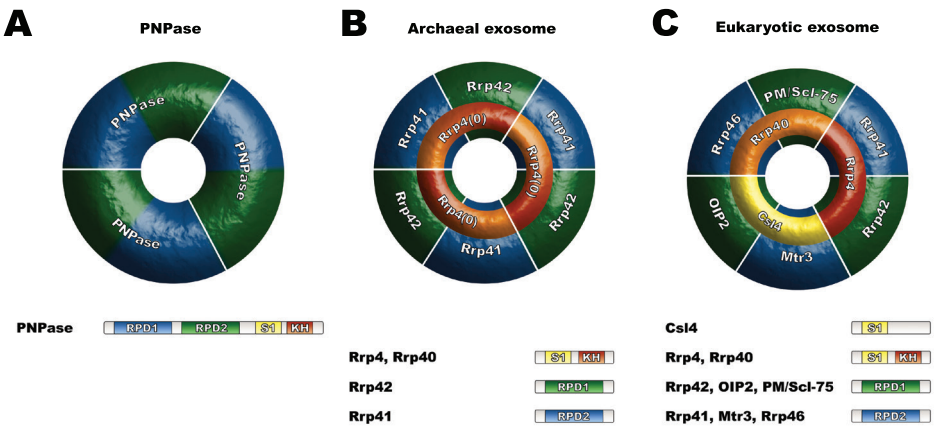

Figure 2. Comparison of the bacterial PNPase with the archaeal and eukaryotic exosome complexes.

Schematic representation of three structurally similar protein complexes involved in RNA processing and degradation. (A) In PNPase, the RPD1 and RPD2 domains are clustered together with the RNA binding domains S1 and KH into one single PNPase protein. Three of these PNPase molecules are used to form the donut-shaped protein complex. (B) In the archaeal exosome, the RPD domains are found in two different proteins: Rrp41 and Rrp42. As a result, three Rrp41/Rrp42 dimers are used to construct the ring structure, while the S1 and KH binding domains are represented by the Rrp4 and Rrp40 proteins that are clustered on one side of the donut structure, guiding substrate RNAs towards the catalytic center of the exosome formed by the Rrp41-Rrp42 dimer. (C) The eukaryotic exosome has a similar configuration in terms of domain organization, with the difference that 6 different proteins are used to form the ring-structure. Please note that the human nomenclature has been used in this illustration (also see Table 2).

noteworthy that the above-mentioned RNase PH can be found in a similar barrel-shaped complex, consisting out of six RNase PH subunits, each containing a single RNase PH domain, although in comparison with the PNPase complex the S1 and/or KH RNA binding domains appear to be absent from the RNase PH complex (Ishii *et al*, 2003).

The structures of the eubacterial exoribonuclease complexes suggest that there appears to be a reoccurring theme in the structure of complexes that control 3'-5' degradation of RNA. Considering that 3'-5' degradation is the main route for RNA turnover in bacteria and the fact that PNPase is present in the chloroplasts and mitochondria of higher eukaryotes, it can be hypothesized that RNase PH, PNPase and the exosome are evolutionary related complexes (Lin-Chao *et al*, 2007). This hypothesis was extended by Van Hoof and Parker (van Hoof and Parker, 1999), who also described similarities with a complex involved in the correct processing and degradation of proteins, the proteasome. The individual components that make up the proteasome were each found to be essential, as depletion of one resulted in the failure in the assembly of the whole complex, thereby abrogating its function. A similar explanation could therefore be applied to the observations that depletion of each individual subunit of the exosome complex resulted in defects in 3' end formation of the 5.8S rRNA,

indicating that each subunit might be important for the structural integrity of the complete complex.

Initial results supporting the idea that the exosome adopts a PNPase-like structure came from electron microscopy (EM) studies with the yeast exosome, which was consistent with such a model (Aloy *et al*, 2002). More direct evidence came from two-hybrid studies with the human exosome, showing interactions between six of the RNase PH-domain-containing proteins: Rrp41, Rrp42, OIP2 (Rrp43), Rrp45, Rrp46 and Mtr3 (Raijmakers *et al*, 2002), suggesting that these proteins indeed form a ring-like structure. After another 3 years, the first crystal structure of an intact exosome complex, from the archaeon *Sulfolobus solfataricus*, was solved (Lorentzen *et al*, 2005).

Analogous to PNPase, the ring-like structure of the archaeal exosome complex is composed of proteins containing RPDs (Figure 2B). Unlike PNPase however, the ring-structure is not formed by oligomerization of one single protein, but by a set of two different proteins, Rrp41 and Rrp42, which trimerize to form the ring. The RPD of Rrp41 shares sequence similarities with the RPD2 of PNPase, while the RPD of Rrp42 is more similar to the RPD1 of PNPase, resulting in a PNPase-like ring with alternating RPD1 and RPD2 domains. The archaeal exosome also harbors S1 and KH RNA-binding domains, which are found in two associated proteins, Rrp4 and Csl4, positioned on one side of the ring-like structure (Buttner *et al*, 2005; Lorentzen *et al*, 2007; Navarro *et al*, 2008).

Not long after the crystal structure of the archaeal exosome, the crystal structures of the yeast and human exosome complexes were resolved (Liu *et al*, 2006), and these displayed many similarities with the archaeal exosome and PNPase complexes. The ring-structure of the eukaryotic exosome is composed of six different proteins. Based on sequence conservation and comparison with the archaeal Rrp41 and Rrp42 proteins, these six proteins can be divided into 2 groups. One group (Rrp41, Rrp46 and Mtr3) is very similar to the RPD2-containing, archaeal Rrp41 protein, whereas the other group is more similar to the RPD1-containing, archaeal Rrp42 protein (Rrp42, OIP2 and PM/Scl-75). These six proteins constitute the ring-structure, whereas the S1 and KH RNA binding domains are found in three different proteins that cap the ring-structure, Rrp4, Rrp40 and Csl4 (Figure 2C). In contrast to the archaeal exosome, these three proteins were found to be essential for the structural integrity of the complex. This feature explains why depletion of each of the exosome subunits in eukaryotes resulted in similar defects in 3'-end maturation of the 5.8S rRNA.

Activity of the exosome

The structural similarities between the exosome and PNPase, as described above, strongly suggested that its mode of action would be similarly as well. Indeed, initial data supporting

this idea came from studies on the archaeal exosome (Lorentzen *et al*, 2005). While the individual components (Rrp41, Rrp42, Rrp4 and Csl4) were found to be catalytically inert, reconstitution of the Rrp41-Rrp42 dimer from *S. solfataricus* showed that phoshorolytic exoribonuclease activity was indeed associated with the dimer. More specifically, the activity seemed to originate from the RPD2 domain of Rrp41. Mutations in this domain were sufficient to abrogate the activity of the dimer, whereas similar mutations in the RPD1 domain of Rrp42 did not interfere with this particular activity. Analogous to PNPase, where the active site is formed by the interface of the two RPD domains, Rrp42 seems to be of structural importance for the activity of the archaeal exosome. This indicates that the hexameric ring-structure is phoshorolytically active, harboring three active sites residing in the three Rrp41-Rrp42 dimers that are present in the ring-structure.

The RNA binding proteins (Rrp4, Csl4, or combinations hereof) probably play a role in the modulation of the exosome's exoribonuclease activity and contribute to the substrate specificity of the exosome (Buttner *et al*, 2005; Ramos *et al*, 2006). Recently, it was shown that Rrp4 of *S. solfataricus* has a preference for RNA substrates containing a homopolymeric tail of adenosine residues at their 3' end, whereas Csl4 prefers RNA substrates lacking such a tail (Roppelt *et al*, 2010). In addition, the RNA-binding proteins may contribute to the unwinding of secondary structures in RNA substrates, which otherwise would prevent access to the narrow channel in the ring-structure (Evguenieva-Hackenberg *et al*, 2008). These data support a model where substrate RNA is recruited by the RNA binding proteins, which guide the substrate into the central channel of the ring-structure, where it will be degraded by the Rrp41-Rrp42 dimer. A similar mechanism for RNA degradation by the bacterial PNPase has also been suggested (Shi *et al*, 2008).

It is noteworthy to mention that the archaeal exosome also displays polyadenylation activity, depending on the availability of nucleotide diphosphates (NDPs), similar to what was originally demonstrated for PNPase (Mohanty and Kushner, 2000). The 3'-end tailing of RNA substrates with a homopolymeric tract of adenosine residues appears to be a recurring mechanism for enhanced 3'-5' RNA decay in various species. Examples of this include the tailing of RNA substrates by the TRAMP-complex, which functions in nuclear RNA quality control (see below) and the transient polyadenylation of rRNA species discussed in Chapter 4.

In 2006, the activity of the yeast and human exosome complexes was studied by reconstitution experiments (Liu *et al*, 2006). The reconstituted human exosome complex was initially found to be phosphorolytically active, but this appeared to be due to contamination of the bacterially expressed protein subunits with PNPase, which copurified with these exosome components. Given the structural similarities shared by the yeast and human exosome complexes with the archaeal exosome and PNPase, it was rather surprising that the reconstituted yeast

and human exosome complexes were shown to be devoid of any catalytically activity. Nevertheless, this is in agreement with the poor conservation of several residues in the yeast and human Rrp41 proteins (Figure 3) that are involved in the coordination of the inorganic phosphate needed for the nucleophilic attack of the substrate RNA (Figure 1) (Dziembowski *et al*, 2007; Lorentzen and Conti, 2005). Exosome complexes from higher eukaryotes thus seem to have lost their ability to degrade RNA in a phosphorolytic fashion. An exception to this is the plant exosome, which displays phosphorolytic activity, consistent with the conservation of phosphate coordinating residues in Rrp41 (Figure 3) (Chekanova *et al*, 2000).

The lack of activity found for the yeast and human exosome complexes complicated the interpretation of previous results, which showed that depletion of any of the exosome subunits had similar effects on 5.8S rRNA maturation and cell viability. Furthermore, experiments with the yeast exosome had shown that exoribonuclease activity was associated with the complex. An explanation for these paradoxical results came from experiments showing that exosomes from higher eukaryotes serve as a scaffold for the association of hydrolytic ribonucleases, which are responsible for the exosome-associated exoribonuclease activity.

Figure 3. Conservation of important functional residues in Rrp41 in different species.

Sequence alignment of part of the Rrp41 protein from *Arabidopsis thaliana* (At), *Sulfolobus solfataricus* (Ss), *Saccharomyces cerevisiae* (Sc), *Homo sapiens* (Hs) and *Pyrococcus furiosis* (Pf). Note the lack of conservation of some essential residues involved in phosphate binding (highlighted in black) in the human and yeast Rrp41.

Exosome-associated proteins and protein complexes

Dis3

An obvious candidate providing the yeast exosome with ribonuclease activity was Rrp44, which copurified with the exosome (Mitchell *et al*, 1997), but was found to be not required for the reconstitution of the exosome core (Liu *et al*, 2006). It should be stressed that, throughout this thesis, the term 'exosome core protein' is exclusively reserved for the proteins that constitute the ring-structure (Rrp41-like and Rrp42-like proteins) and the RNA binding proteins that cap this structure (Rrp4, Rrp40, Csl4).

Rrp44 appeared to be a homologue of the fission yeast Dis3 protein (Chromosome disjunction protein 3), which was originally identified as an essential protein for mitotic progression, (Kinoshita *et al*, 1991). Sequence analysis showed that Rrp44/Dis3 was homologous to the bacterial RNase R and RNase II, important 3'-5' exoribonucleases belonging to the RNR

family of processive, hydrolytic exoribonucleases (Table 1). The term processive stands for the ability of an enzyme to remain attached to its substrate, performing multiple rounds of substrate conversion, whereas a distributive enzyme dissociates after only one round of catalysis (Von Hippel *et al*, 1994).
Yeast Dis3 can be found in both the cytoplasm and the nucleus, where is has been shown to associate with the exosome core complex (Synowsky *et al*, 2009). The activity of Dis3 correlated well with the activity associated with the yeast exosome, and substitution of the wild-type Dis3 with a catalytically inactive mutant of the protein resulted in an inactive exosome complex (Dziembowski *et al*, 2007). These results strongly suggested that Dis3 was responsible for the majority of the activity of the yeast exosome. Surprisingly, the yeast Dis3 protein appeared to be capable of degrading RNA substrates in two different ways. Besides its exoribonuclease activity, which is associated with the centrally located RNB domain, it was shown to possess endoribonuclease activity, for which the PIN domain is required (Lebreton *et al*, 2008; Schaeffer *et al*, 2009). This PIN domain also mediates the interaction between Dis3 and the exosome, allowing it to bind to one side of the exosome core structure (opposite to the side where Rrp4, Rrp40 and Csl4 are attached) (Bonneau *et al*, 2009; Hernandez *et al*, 2006; Schneider *et al*, 2009). Based on these findings, a model for RNA degradation by the eukaryotic exosome has been proposed (Bonneau *et al*, 2009; Malet *et al*, 2010). In this model, an RNA substrate will be recruited by the RNA-binding proteins, guided to the central channel of the complex, and after passing through this channel will be degraded by Dis3. This mechanism also allows the degradation of structured RNA substrates in which the exosome facilitates in the unwinding of the substrate before it gets degraded by Dis3 (Bonneau *et al*, 2009). It is noteworthy to add that Dis3 can unwind and degrade structured RNA substrates itself without the help of the exosome core. When challenged with a structured RNA substrate with a sufficiently long 3'-overhang, Dis3 utilizes the energy of several rounds of nucleotide hydrolysis of this 'free' 3' end to unwind structured regions (Lee *et al*, 2012).

Several observations indicated that the role of Dis3 in the function of the human exosome is different. Although the human homologue of yeast Dis3 was shown to rescue the growth defect phenotype in yeast, induced by depletion of Dis3 (Shiomi *et al*, 1998), Dis3 was never found to be stably associated with the human exosome core complex (Allmang *et al*, 1999b; Chen *et al*, 2001; Lejeune *et al*, 2003; Lim *et al*, 1997). Also the subcellular localization of Dis3 is partially different between the two species. Whereas yeast Dis3 can be found in the nucleus as well as the cytoplasm, human Dis3 seems to be confined to the nucleoplasm (Staals *et al*, 2010; Synowsky *et al*, 2009; Tomecki *et al*, 2010). This raised the question which proteins contributed to the activity of the cytoplasmic exosome in human and possibly other mammalian cells.

PM/Scl-100 (Rrp6)

Before the association between PM/Scl-100 and the human exosome was demonstrated, its orthologue in yeast, Rrp6, was already known for its involvement in the maturation of rRNA. Similar to the experiments leading to the discovery of the exosome, the depletion of PM/Scl-100 (Rrp6) resulted in the accumulation of a 5.8S rRNA precursor, which was extended at the 3' end (Briggs *et al*, 1998).

PM/Scl-100 (Rrp6) is a hydrolytic 3'-5' exoribonuclease with structural homology to the bacterial RNase D and is therefore placed in the DEDD family of exoribonucleases (Table 1). The name for this family is derived from the 4 negatively charged residues (3 aspartic acids and 1 glutamic acid) that are each part of different sequence motifs of the protein. These residues are crucial for the coordination of divalent metal cofactors (Mg^{2+} and/or Mn^{2+}), which facilitate the activation of a water molecule needed for the hydrolytic attack of the nucleotide-nucleotide bond (Midtgaard *et al*, 2006; Steitz and Steitz, 1993).

Yeast Rrp6 contains a nuclear localization signal and immunofluorescence experiments demonstrated that it accumulates in the nucleoli. In this subnuclear compartment also a high concentration of exosome complexes has been found. The same holds true for its human counterpart PM/Scl-100, although the latter has also been reported to localize to the cytoplasm (Lejeune *et al*, 2003; van Dijk *et al*, 2007). Interestingly, plants express three different forms of this protein, each having a completely different subcellular localization (Lange *et al*, 2008).

The nuclease activity of PM/Scl-100 (Rrp6) is used in many RNA processing and degradation pathways, in which it generally acts in association with the exosome core structure. Experiments using a truncated version of Rrp6, which prevents the binding to the exosome core, have shown that the interaction is not essential for all of its biological activities (Callahan and Butler, 2008). The activity of PM/Scl-100 (Rrp6) is heavily influenced by the binding of two other proteins: Rrp47 (C1D in humans) and MPP6, especially when rRNA maturation is considered (Schilders *et al*, 2005; Schilders *et al*, 2007; Stead *et al*, 2007). These and other studies gave rise to the idea that PM/Scl-100 (Rrp6) might have exosome-independent roles as well (Callahan and Butler, 2008; Graham *et al*, 2009).

Although Rrp6 is a hydrolytic exoribonuclease like Dis3, they show some interesting differences between their modes of action and substrate specificities. First, Rrp6 is a distributive enzyme, whereas Dis3 was shown to act in a processive fashion. In addition, *in vivo* experiments have shown that Rrp6 has difficulties degrading structured areas of an RNA substrate, while Dis3 doesn't seem to be hampered by this (Liu *et al*, 2006). The association of these two different ribonucleases thus provides the eukaryotic exosome with a broad repertoire of exoribonucleolytic activities. Distributive and processive ribonucleases often act in concert with each other (Deutscher, 2006; Dziembowski *et al*, 2007; Li *et al*, 1998).

TRAMP complex

As mentioned above, 3' poly(A) tailing followed by 3'-5' degradation of an RNA substrate is a recurring phenomenon throughout many domains of life. In bacteria for instance, a complex called the degradosome is an assembly of different proteins that facilitate this process: a DEAD-box helicase called RhlB, the endonuclease RNase E, enolase and the abovementioned PNPase (Py *et al*, 1996; Raynal and Carpousis, 1999; Xu and Cohen, 1995). Degradation is often initiated by an endonucleolytic cleavage within the RNA substrate (RNase E), followed by polyadenylation to create a 'landing-pad' for exoribonuclease (PNPase) to begin degradation of the RNA body. RNA binding proteins and/or secondary structures, which might interfere with degradation, can be removed by the enzymatic function of the helicase (RhlB). A general model for this mechanism is depicted in Figure 4.

A similar system has been found in the nucleus of eukaryotes, where RNA degradation by the exosome is facilitated by the actions of the TRAMP complex, which harbors a similar 'repertoire' of proteins needed to perform this: a poly(A) polymerase, either Trf4 or Trf5, the DEAD-box helicase Mtr4, and the RNA binding proteins Air1 and Air2 (Table 2). The TRAMP complex resides in the nucleus, where it is involved in RNA quality control and 3'-end processing events (Kadaba *et al*, 2006; LaCava *et al*, 2005; Vanacova *et al*, 2005; Wyers *et al*, 2005). A human homologue of this complex (the NEXT complex) has recently been characterized, showing some interesting differences in terms of spatial distribution of its subunits when compared to its yeast counterpart (Lubas *et al*, 2011).

Other exosome-associated proteins

There are many other proteins and complexes that interact with the exosome. Several of these have been shown to aid the exosome in its role in cytoplasmic mRNA turnover. In yeast for instance, the Ski-complex (Ski2, Ski3 and Ski8) has been shown to be essential for exosome-mediated 3'-5' decay of mRNAs (Anderson and Parker, 1998; Brown *et al*, 2000), probably by playing a role in substrate selection (Houseley *et al*, 2006). The Ski complex is positioned on top of the Rrp4/Rrp40/Csl4 ring structure, forming an extension of the exosome core channel. This couples the helicase activity of the Ski complex (Ski2) to the ribonuclease activities associated with the exosome (Halbach *et al*, 2013). Human homologues of Ski proteins have been identified, but experimental evidence linking them to mRNA turnover is limited. Paradoxically, the human Ski complex exists in the nucleus as well, suggesting that differences exist between the substrates of the human and yeast Ski complex (Zhu *et al*, 2005).

Other proteins involved in exosome-mediated mRNA turnover are proteins which bind a specific sequence element in the 3'-UTR (3'-untranslated region) of some mRNAs, termed ARE (AU-rich element). AREs have a dramatic impact on the stability of the mRNA, depending on which ARE-binding proteins are present (Chen and Shyu, 1995; Mukherjee *et al*, 2002; Parker and Song, 2004). All currently known ARE-binding proteins that can bind to the exosome

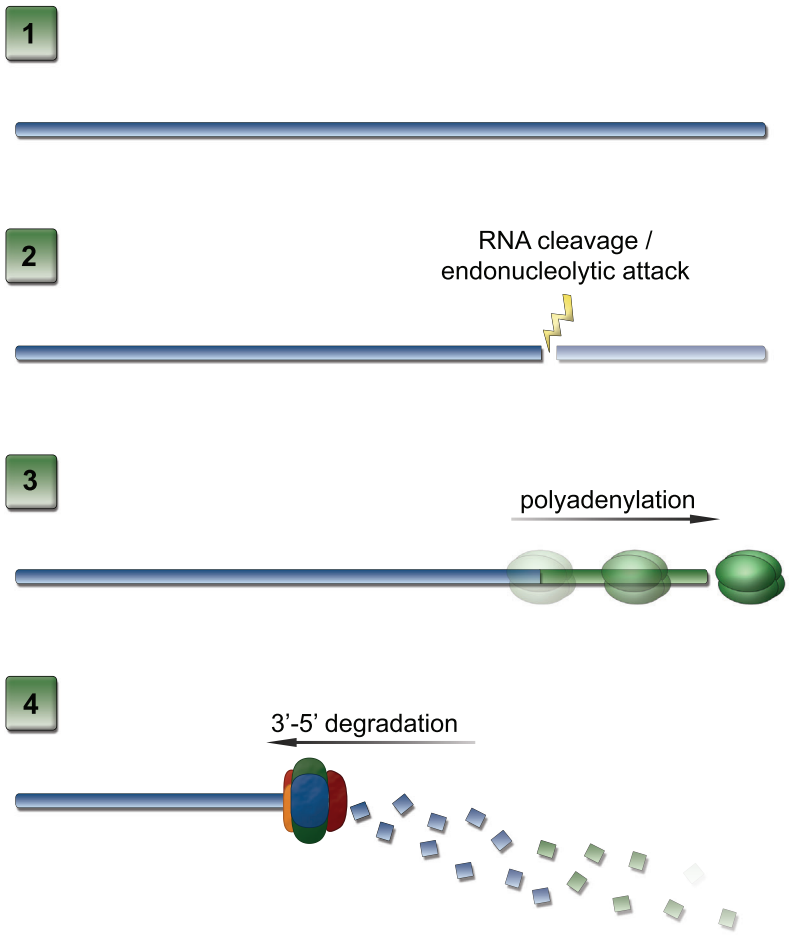

Figure 4. Model for polydenylation-stimulated 3'-5' degradation of RNA.

Degradation of the RNA body is often initiated by an endonucleolytic cleavage event (step 2), after which the newly formed 3' end will be using as starting point for exonucleolytic degradation. When degradation is stalled (eg. by encountering secondary RNA structures or RNA-bound proteins) a polyadenosine tail will be added (step 3). This tail will subsequently be used as a 'landing pad' for another round of exonucleolytic degradation (step 4).

are listed in Table 2. AREs as well as the ARE-binding proteins have been shown to recruit the exosome to the ARE-containing mRNAs (Chen *et al*, 2001; Gherzi *et al*, 2004). A similar mechanism was demonstrated for the ZAP protein. This protein specifically recognizes and binds viral RNA sequences and presents them to the exosome for degradation, implicating the exosome in viral resistance (Guo *et al*, 2007).

The Nrd1–Nab3–Sen1 (NNS) complex in yeast associates with AREs, where it serves as an important regulator of transcriptional termination (Creamer *et al*, 2011). The NNS complex copurifies with the nuclear exosome and TRAMP complexes, suggesting a role in the

recruitment of RNA quality control factors (exosome and TRAMP) for degradation or trimming. With the exception of Sen1, no human homologues for the yeast NNS complex components have been found. However, recent copurification experiments with the human exosome and the abovementioned NEXT complex have identified the CBCA complex (cap-binding proteins CBP20 and CBP80 and arsenic-resistance protein ARS2), which is associated with the 5' cap structure of nuclear mRNAs. Since CBCA was found to promote transcriptional termination, this finding hints at the coupling of transcriptional termination with RNA degradation and therefore might be functionally related to the activity of the yeast NNS complex (Andersen *et al*, 2013).

The exosome has also been reported to be associated with a protein complex that is often found at the 3' end of RNAs: the Ccr4-Not complex. This latter complex has an important role in transcriptional regulation and mRNA decay (Ccr4 is the deadenylase that initiates mRNA decay by shortening of the poly(A) tail). It was postulated that the Ccr4-Not complex serves as a platform for bridging the nuclear exosome with the TRAMP complex, as Caf40 (one of the constituents of the Ccr4-Not complex) was found to be required for the interaction between Mtr4 and Rrp6 (Azzouz *et al*, 2009).

Functions of the exosome

Exosomes or exosome-like complexes (e.g. PNPase) are evolutionary highly conserved protein assemblies that are present in a broad range of different species, reflecting their central role in RNA metabolism. The complex seems to have adapted to the changing complexity in RNA processing and degradation events, given the still growing list of potential RNA substrates that have been identified over the years. With that said, it's not unthinkable that virtually every RNA species will encounter the exosome somewhere in its lifecycle. Part of the explanation why the exosome is capable of handling so many different RNA species is the equally impressive list of known exosome-associated proteins and complexes (Table 2). Covering all known RNA species that are affected by the exosome would therefore be beyond the scope of this chapter. Instead, a brief overview of the most well established functions of the exosome, together with recent developments will be covered here. To keep everything in perspective, the 'core activities' of the exosome complex can roughly be divided into two major categories: complete RNA degradation and 3'-end processing.

RNA degradation is required in many different stages in the 'lifecycle' of an RNA molecule. Starting from the synthesis, the initial pre-RNA molecule often has to undergo several maturation events, in which parts of the pre-RNA molecule are cleaved off or excised, followed by the complete degradation of the released fragments. A good example is the degradation of the 5'ETS fragment resulting from the processing of the ribosomal RNA precursor (Allmang *et al*, 2000). Complete RNA degradation also occurs when errors during the maturation steps or other damaging agents lead to the formation of aberrant RNA molecules. Over the years, many examples showing the involvement of the exosome in the surveillance of

RNA molecules have been reported, including the clearance of hypomethylated tRNAs, improperly processed rRNAs (Allmang *et al*, 2000; Vanacova *et al*, 2005) and aberrant pre-mRNA molecules (Houseley *et al*, 2006). These processes are often referred to as "RNA quality control", in which the TRAMP complex, Rrp6 as well as Rrp44 play an important role. A role for Rrp6 during mRNA transcription has recently been established, where it was shown that Rrp6 ensures the tethering of the transcript to the DNA until full pre-mRNA processing has occurred (de Almeida *et al*, 2010).

Even when aberrant mRNAs escape early quality control mechanisms, additional cytoplasmic quality control mechanisms (Isken and Maquat, 2007), involving the exosome, prevent these abnormal mRNAs from doing damage. These mechanisms are often activated upon events that occur during the translation process of these aberrant mRNAs. In NMD (nonsense-mediated decay), aberrant mRNAs containing a premature stop codon will cause the stalling of the ribosome at an unusual location, e.g. distant from the poly(A) tail and/or the presence of exon junction complexes upstream of the stop codon. These serve as important cues for recognition by the Upf proteins, which in turn recruit enzymes to promote the initial endonucleolytic cleavage (SMG6 in humans), resulting in 3' fragments which will be degraded by Xrn1 and 5' fragments that are degraded by the exosome in concert with the Ski complex (Eberle *et al*, 2009; Kervestin and Jacobson, 2012; Mitchell and Tollervey, 2003).

In NSD (nonstop decay) and NGD (no-go decay), the ribosome will also stall at either the poly(A) tail (due to the lack of a stop codon) or at internal locations (due to inhibitory mRNA structures, rare codons, etc) respectively (Doma and Parker, 2006; Frischmeyer *et al*, 2002). In both cases, the stalled ribosomes will be sensed by the Hbs1-Dom34 protein complex (Carr-Schmid *et al*, 2002; Saito *et al*, 2013). These proteins are known to interact directly with the "A" site of the stalled ribosome, which is believed to stimulate cleavage of the mRNA substrate by a currently unknown endoribonuclease, again followed by degradation of the resulting fragments by Xrn1 and the exosome. Since many components of the NSD and NGD pathways seem to overlap, it is currently under discussion whether these pathways should be considered as separate entities (Shoemaker and Green, 2012).

Even when an mRNA molecule has been properly processed, it will eventually be broken down by the exosome when it reaches the end of its lifespan (Schaeffer and van Hoof, 2011; van Dijk *et al*, 2007). Although 'normal' mRNA turnover can also be achieved by decapping, followed by seemingly uncontrolled 5'-3' degradation by Xrn1, it has been shown that the 3'-5' degradation route, involving the exosome, is more tightly regulated (Garneau *et al*, 2007). Sequential or structured elements located in the 3'UTR (e.g. AREs) as well as the length of the poly(A) tail can serve as important regulatory signals for exosome-mediated degradation of these molecules.

The enzymatic activities of ribonucleases do not always result in the degradation of the RNA substrate. In some cases, only partial degradation is required, which is referred to as (exonucleolytic) processing or trimming. Some steps in rRNA maturation, for instance, require

the complete degradation of released RNA fragments (e.g. the excised 5'ETS fragment), while other steps require the trimming of only a part of the pre-RNA sequence. In one of the final steps in the maturation of the 5.8S rRNA the molecule is still extended at its 3' end. Removal of this sequence by the exosome has been shown to be dependent on Dis3, Rrp6, Mtr4 and Rrp47 in yeast (Allmang *et al*, 1999a; de la Cruz *et al*, 1998; Mitchell *et al*, 1997), as demonstrated by the accumulation of 3' extended 5.8S rRNA molecules in the absence of these proteins. While the same repertoire of proteins have been shown to be involved in the processing of pre-rRNAs in humans, the exact mechanism and proteins involved are thought to be slightly different (Schilders *et al*, 2007; Sloan *et al*, 2013). Of course, 3' processing in not restricted to the maturation of rRNAs, as the 3' processing of snRNA and snoRNAs was also shown to be dependent of the exosome (Mitchell *et al*, 2003; van Hoof *et al*, 2000). Similar to the rRNAs, the absence of especially Rrp6 and Mtr4 resulted in 3' polyadenylated sn(o) RNA species, suggesting that the biosynthesis of these RNA species includes the formation of transient, TRAMP-induced, polyadenylated pre-sn(o)RNA intermediates, which are then targeted for processing by the exosome (LaCava *et al*, 2005).

More recent work has shown that the exosome is also responsible for the removal of non-coding RNA transcripts, that arise from transcription at noncanonical regions in the genome (such as intergenic and heterochromatin regions), which were previously considered to be transcriptionally silent. Nowadays, aided by the advances in sequencing-technologies, it is generally accepted that as much as 90% of the human genome is transcribed (Wilhelm *et al*, 2008). Examples of such transcripts include the CUTs (cryptic unstable transcripts) in yeast, and PROMPTs (promotor-upstream transcripts) in humans (Neil *et al*, 2009; Preker *et al*, 2008). Their expression levels are very low and they are rapidly degraded, which explains why they weren't identified before. Their detection was facilitated by silencing several exosome and exosome-associated components, which points to an important role for the exosome in the regulation of their expression levels (Gudipati *et al*, 2012; Schmidt *et al*, 2012; Schneider *et al*, 2012).

Outline of this thesis

Roughly 15 years have passed since the discovery of the RNA exosome complex. During this period, our knowledge about its structure and function in different species has enormously increased. Nevertheless, there are still many aspects left uncovered considering the enzymatic activities associated with exosome, particularly the mammalian exosome. As has been described in this chapter, while the overall structure of the exosome complex is evolutionary highly conserved, the nature and distribution of catalytic subunits varies to a large extent among different species. The main aim of the research described in this

thesis was to provide more insight into the function of the exosome in human cells and the regulation of its activities.

In **Chapter 2** the discovery of the human exosome will be covered from a medical perspective. The implications of autoantibodies targeting various components of the exosome complex in autoimmune disease patients will be addressed. In addition, a putative link between aberrant expression of exosome subunits and/or auxiliary proteins and cancer will be discussed.
In **Chapter 3** the identification and functional characterization in human cells of a newly identified exosome-associated exoribonuclease, Dis3-like 1, will be described. In contrast to Dis3, Dis3-like 1 showed a stable interaction with the human exosome and was shown to contribute to the activity of the exosome complex. In addition to Dis3-like 1 another gene homologous to Dis3 was identified in the human genome and the corresponding protein was termed Dis3-like 2.
The studies in **Chapter 4** are focused on the biological role of Dis3-like 1. The results indicated that at least one of the functions of this newly discovered protein in human cells is its role in polyadenylation-stimulated rRNA degradation in the cytoplasm. Although examples of polyadenylation-stimulated RNA degradation are fairly well known to occur in the nucleus, this is the first example of a similar RNA degradation mechanism operating in the cytoplasm. Since the human exosome core appears to function as a scaffold for the stable association of at least two exoribonucleases (Dis3-like 1 and PM/Scl-100) and the transient or weak association of Dis3, the relative contribution of each of these enzymes to the activity of the complex as a whole was investigated and the results of these experiments are described in **Chapter 5**. These not only indicated that the expression levels of these three exoribonucleases can affect each other, but also provide evidence that their association with the exosome complex might be mutually exclusive. We also show evidence that the activity of PM/Scl-100 can be modulated by proteins (other than Dis3 and Dis3-like 1) that co-purify with the exosome.
Since previous observations indicated that both Dis3 and Dis3-like 2 have no or only a very weak interaction with the exosome core, the studies in **Chapter 6** and **Chapter 7** address their biological function independent of the exosome. Microarray analyses revealed that depletion of Dis3 results in a set of affected mRNAs that differs from that resulting from depletion of other exosome(associated) proteins. Furthermore, we show that Dis3 associates with proteins involved in pre-mRNA splicing and processing. The role of Dis3-like 2 was studied in transiently transfected human cells and the effect on cell viability and morphology were determined. Based upon the results and currently available literature, we discuss the possible cellular role of Dis3-like 2.
Finally, the results of all chapters will be recapitulated in **Chapter 8**, followed by a more general discussion of the impact of these findings on our current understanding of the exosome, its enzymatic activity and its involvement in biochemical processes.

References

Allmang C, Kufel J, Chanfreau G, Mitchell P, Petfalski E, Tollervey D (1999a) Functions of the exosome in rRNA, snoRNA and snRNA synthesis. *EMBO J* **18:** 5399-5410

Allmang C, Mitchell P, Petfalski E, Tollervey D (2000) Degradation of ribosomal RNA precursors by the exosome. *Nucleic Acids Res* **28:** 1684-1691

Allmang C, Petfalski E, Podtelejnikov A, Mann M, Tollervey D, Mitchell P (1999b) The yeast exosome and human PM-Scl are related complexes of 3' --> 5' exonucleases. *Genes Dev* **13:** 2148-2158

Aloy P, Ciccarelli FD, Leutwein C, Gavin AC, Superti-Furga G, Bork P, Bottcher B, Russell RB (2002) A complex prediction: three-dimensional model of the yeast exosome. *EMBO Rep* **3:** 628-635

Andersen PR, Domanski M, Kristiansen MS, Storvall H, Ntini E, Verheggen C, Schein A, Bunkenborg J, Poser I, Hallais M, Sandberg R, Hyman A, LaCava J, Rout MP, Andersen JS, Bertrand E, Jensen TH (2013) The human cap-binding complex is functionally connected to the nuclear RNA exosome. *Nat Struct Mol Biol* **20:** 1367-1376

Anderson JS, Parker RP (1998) The 3' to 5' degradation of yeast mRNAs is a general mechanism for mRNA turnover that requires the SKI2 DEVH box protein and 3' to 5' exonucleases of the exosome complex. *EMBO J* **17:** 1497-1506

Azzouz N, Panasenko OO, Colau G, Collart MA (2009) The CCR4-NOT complex physically and functionally interacts with TRAMP and the nuclear exosome. *PLoS One* **4:** e6760

Bonneau F, Basquin J, Ebert J, Lorentzen E, Conti E (2009) The yeast exosome functions as a macromolecular cage to channel RNA substrates for degradation. *Cell* **139:** 547-559

Briggs MW, Burkard KT, Butler JS (1998) Rrp6p, the yeast homologue of the human PM-Scl 100-kDa autoantigen, is essential for efficient 5.8 S rRNA 3' end formation. *J Biol Chem* **273:** 13255-13263

Brouwer R, Pruijn GJ, van Venrooij WJ (2001) The human exosome: an autoantigenic complex of exoribonucleases in myositis and scleroderma. *Arthritis Res* **3:** 102-106

Brown JT, Bai X, Johnson AW (2000) The yeast antiviral proteins Ski2p, Ski3p, and Ski8p exist as a complex in vivo. *RNA* **6:** 449-457

Buttner K, Wenig K, Hopfner KP (2005) Structural framework for the mechanism of archaeal exosomes in RNA processing. *Mol Cell* **20:** 461-471

Callahan KP, Butler JS (2008) Evidence for core exosome independent function of the nuclear exoribonuclease Rrp6p. *Nucleic Acids Res* **36:** 6645-6655

Carr-Schmid A, Pfund C, Craig EA, Kinzy TG (2002) Novel G-protein complex whose requirement is linked to the translational status of the cell. *Mol Cell Biol* **22:** 2564-2574

Chekanova JA, Shaw RJ, Wills MA, Belostotsky DA (2000) Poly(A) tail-dependent exonuclease AtRrp41p from Arabidopsis thaliana rescues 5.8 S rRNA processing and mRNA decay defects of the yeast ski6 mutant and is found in an exosome-sized complex in plant and yeast cells. *J Biol Chem* **275:** 33158-33166

Chen CY, Gherzi R, Ong SE, Chan EL, Raijmakers R, Pruijn GJ, Stoecklin G, Moroni C, Mann M, Karin M (2001) AU binding proteins recruit the exosome to degrade ARE-containing mRNAs. *Cell* **107:** 451-464

Chen CY, Shyu AB (1995) AU-rich elements: characterization and importance in mRNA degradation. *Trends Biochem Sci* **20:** 465-470

Creamer TJ, Darby MM, Jamonnak N, Schaughency P, Hao H, Wheelan SJ, Corden JL (2011) Transcriptome-wide binding sites for components of the Saccharomyces cerevisiae non-poly(A) termination pathway: Nrd1, Nab3, and Sen1. *PLoS Genet* **7:** e1002329

de Almeida SF, Garcia-Sacristan A, Custodio N, Carmo-Fonseca M (2010) A link between nuclear RNA surveillance, the human exosome and RNA polymerase II transcriptional termination. *Nucleic Acids Res* **38:** 8015-8026

de la Cruz J, Kressler D, Tollervey D, Linder P (1998) Dob1p (Mtr4p) is a putative ATP-dependent RNA helicase required for the 3' end formation of 5.8S rRNA in Saccharomyces cerevisiae. *EMBO J* **17:** 1128-1140

Deutscher MP (2006) Degradation of RNA in bacteria: comparison of mRNA and stable RNA. *Nucleic Acids Res* **34:** 659-666

Doma MK, Parker R (2006) Endonucleolytic cleavage of eukaryotic mRNAs with stalls in translation elongation. *Nature* **440:** 561-564

Dziembowski A, Lorentzen E, Conti E, Seraphin B (2007) A single subunit, Dis3, is essentially responsible for yeast exosome core activity. *Nat Struct Mol Biol* **14:** 15-22

Eberle AB, Lykke-Andersen S, Muhlemann O, Jensen TH (2009) SMG6 promotes endonucleolytic cleavage of nonsense mRNA in human cells. *Nat Struct Mol Biol* **16:** 49-55

Evguenieva-Hackenberg E, Roppelt V, Finsterseifer P, Klug G (2008) Rrp4 and Csl4 are needed for efficient degradation but not for polyadenylation of synthetic and natural RNA by the archaeal exosome. *Biochemistry* **47:** 13158-13168

Frischmeyer PA, van Hoof A, O'Donnell K, Guerrerio AL, Parker R, Dietz HC (2002) An mRNA surveillance mechanism that eliminates transcripts lacking termination codons. *Science* **295:** 2258-2261

Garneau NL, Wilusz J, Wilusz CJ (2007) The highways and byways of mRNA decay. *Nat Rev Mol Cell Biol* **8:** 113-126

Gherzi R, Lee KY, Briata P, Wegmuller D, Moroni C, Karin M, Chen CY (2004) A KH domain RNA binding protein, KSRP, promotes ARE-directed mRNA turnover by recruiting the degradation machinery. *Mol Cell* **14:** 571-583

Graham AC, Kiss DL, Andrulis ED (2009) Core exosome-independent roles for Rrp6 in cell cycle progression. *Mol Biol Cell* **20:** 2242-2253

Grunberg-Manago M, Oritz PJ, Ochoa S (1955) Enzymatic synthesis of nucleic acidlike polynucleotides. *Science* **122:** 907-910

Gudipati RK, Xu Z, Lebreton A, Seraphin B, Steinmetz LM, Jacquier A, Libri D (2012) Extensive degradation of RNA precursors by the exosome in wild-type cells. *Mol Cell* **48:** 409-421

Guo X, Ma J, Sun J, Gao G (2007) The zinc-finger antiviral protein recruits the RNA processing exosome to degrade the target mRNA. *Proc Natl Acad Sci U S A* **104:** 151-156

Halbach F, Reichelt P, Rode M, Conti E (2013) The yeast ski complex: crystal structure and RNA channeling to the exosome complex. *Cell* **154:** 814-826

Hernandez H, Dziembowski A, Taverner T, Seraphin B, Robinson CV (2006) Subunit architecture of multimeric complexes isolated directly from cells. *EMBO Rep* **7:** 605-610

Houseley J, LaCava J, Tollervey D (2006) RNA-quality control by the exosome. *Nat Rev Mol Cell Biol* **7:** 529-539

Ishii R, Nureki O, Yokoyama S (2003) Crystal structure of the tRNA processing enzyme RNase PH from Aquifex aeolicus. *J Biol Chem* **278:** 32397-32404

Isken O, Maquat LE (2007) Quality control of eukaryotic mRNA: safeguarding cells from abnormal mRNA function. *Genes Dev* **21:** 1833-1856

Kadaba S, Wang X, Anderson JT (2006) Nuclear RNA surveillance in Saccharomyces cerevisiae: Trf4p-dependent polyadenylation of nascent hypomethylated tRNA and an aberrant form of 5S rRNA. *RNA* **12:** 508-521

Kervestin S, Jacobson A (2012) NMD: a multifaceted response to premature translational termination. *Nat Rev Mol Cell Biol* **13:** 700-712

Kinoshita N, Goebl M, Yanagida M (1991) The fission yeast dis3+ gene encodes a 110-kDa essential protein implicated in mitotic control. *Mol Cell Biol* **11:** 5839-5847

LaCava J, Houseley J, Saveanu C, Petfalski E, Thompson E, Jacquier A, Tollervey D (2005) RNA degradation by the exosome is promoted by a nuclear polyadenylation complex. *Cell* **121:** 713-724

Lange H, Holec S, Cognat V, Pieuchot L, Le Ret M, Canaday J, Gagliardi D (2008) Degradation of a polyadenylated rRNA maturation by-product involves one of the three RRP6-like proteins in Arabidopsis thaliana. *Mol Cell Biol* **28:** 3038-3044

Lebreton A, Tomecki R, Dziembowski A, Seraphin B (2008) Endonucleolytic RNA cleavage by a eukaryotic exosome. *Nature* **456:** 993-996

Lee G, Bratkowski MA, Ding F, Ke A, Ha T (2012) Elastic coupling between RNA degradation and unwinding by an exoribonuclease. *Science* **336:** 1726-1729

Lejeune F, Li X, Maquat LE (2003) Nonsense-mediated mRNA decay in mammalian cells involves decapping, deadenylating, and exonucleolytic activities. *Mol Cell* **12:** 675-687

Li Z, Pandit S, Deutscher MP (1998) 3' exoribonucleolytic trimming is a common feature of the maturation of small, stable RNAs in Escherichia coli. *Proc Natl Acad Sci U S A* **95:** 2856-2861

Lim J, Kuroki T, Ozaki K, Kohsaki H, Yamori T, Tsuruo T, Nakamori S, Imaoka S, Endo M, Nakamura Y (1997) Isolation of murine and human homologues of the fission-yeast dis3+ gene encoding a mitotic-control protein and its overexpression in cancer cells with progressive phenotype. *Cancer Res* **57:** 921-925

Lin-Chao S, Chiou NT, Schuster G (2007) The PNPase, exosome and RNA helicases as the building components of evolutionarily-conserved RNA degradation machines. *J Biomed Sci* **14:** 523-532

Liu Q, Greimann JC, Lima CD (2006) Reconstitution, activities, and structure of the eukaryotic RNA exosome. *Cell* **127:** 1223-1237

Lorentzen E, Conti E (2005) Structural basis of 3' end RNA recognition and exoribonucleolytic cleavage by an exosome RNase PH core. *Mol Cell* **20:** 473-481

Lorentzen E, Dziembowski A, Lindner D, Seraphin B, Conti E (2007) RNA channelling by the archaeal exosome. *EMBO Rep* **8:** 470-476

Lorentzen E, Walter P, Fribourg S, Evguenieva-Hackenberg E, Klug G, Conti E (2005) The archaeal exosome core is a hexameric ring structure with three catalytic subunits. *Nat Struct Mol Biol* **12:** 575-581

Lubas M, Christensen MS, Kristiansen MS, Domanski M, Falkenby LG, Lykke-Andersen S, Andersen JS, Dziembowski A, Jensen TH (2011) Interaction profiling identifies the human nuclear exosome targeting complex. *Mol Cell* **43:** 624-637

Lygerou Z, Allmang C, Tollervey D, Seraphin B (1996) Accurate processing of a eukaryotic precursor ribosomal RNA by ribonuclease MRP in vitro. *Science* **272:** 268-270

Malet H, Topf M, Clare DK, Ebert J, Bonneau F, Basquin J, Drazkowska K, Tomecki R, Dziembowski A, Conti E, Saibil HR, Lorentzen E (2010) RNA channelling by the eukaryotic exosome. *EMBO Rep* **11:** 936-942

Mian IS (1997) Comparative sequence analysis of ribonucleases HII, III, II PH and D. *Nucleic Acids Res* **25:** 3187-3195

Midtgaard SF, Assenholt J, Jonstrup AT, Van LB, Jensen TH, Brodersen DE (2006) Structure of the nuclear exosome component Rrp6p reveals an interplay between the active site and the HRDC domain. *Proc Natl Acad Sci U S A* **103:** 11898-11903

Mitchell P, Petfalski E, Houalla R, Podtelejnikov A, Mann M, Tollervey D (2003) Rrp47p is an exosome-associated protein required for the 3' processing of stable RNAs. *Mol Cell Biol* **23:** 6982-6992

Mitchell P, Petfalski E, Shevchenko A, Mann M, Tollervey D (1997) The exosome: a conserved eukaryotic RNA processing complex containing multiple 3'-->5' exoribonucleases. *Cell* **91:** 457-466

Mitchell P, Petfalski E, Tollervey D (1996) The 3' end of yeast 5.8S rRNA is generated by an exonuclease processing mechanism. *Genes Dev* **10:** 502-513

Mitchell P, Tollervey D (2003) An NMD pathway in yeast involving accelerated deadenylation and exosome-mediated 3'-->5' degradation. *Mol Cell* **11:** 1405-1413

Mohanty BK, Kushner SR (2000) Polynucleotide phosphorylase functions both as a 3' right-arrow 5' exonuclease and a poly(A) polymerase in Escherichia coli. *Proc Natl Acad Sci U S A* **97:** 11966-11971

Mukherjee D, Gao M, O'Connor JP, Raijmakers R, Pruijn G, Lutz CS, Wilusz J (2002) The mammalian exosome mediates the efficient degradation of mRNAs that contain AU-rich elements. *EMBO J* **21:** 165-174

Navarro MV, Oliveira CC, Zanchin NI, Guimaraes BG (2008) Insights into the mechanism of progressive RNA degradation by the archaeal exosome. *J Biol Chem* **283:** 14120-14131

Neil H, Malabat C, d'Aubenton-Carafa Y, Xu Z, Steinmetz LM, Jacquier A (2009) Widespread bidirectional promoters are the major source of cryptic transcripts in yeast. *Nature* **457:** 1038-1042

Parker R, Song H (2004) The enzymes and control of eukaryotic mRNA turnover. *Nat Struct Mol Biol* **11:** 121-127

Preker P, Nielsen J, Kammler S, Lykke-Andersen S, Christensen MS, Mapendano CK, Schierup MH, Jensen TH (2008) RNA exosome depletion reveals transcription upstream of active human promoters. *Science* **322:** 1851-1854

Py B, Higgins CF, Krisch HM, Carpousis AJ (1996) A DEAD-box RNA helicase in the Escherichia coli RNA degradosome. *Nature* **381:** 169-172

Raijmakers R, Egberts WV, van Venrooij WJ, Pruijn GJ (2002) Protein-protein interactions between human exosome components support the assembly of RNase PH-type subunits into a six-membered PNPase-like ring. *J Mol Biol* **323:** 653-663

Ramos CR, Oliveira CL, Torriani IL, Oliveira CC (2006) The Pyrococcus exosome complex: structural and functional characterization. *J Biol Chem* **281:** 6751-6759

Raynal LC, Carpousis AJ (1999) Poly(A) polymerase I of Escherichia coli: characterization of the catalytic domain, an RNA binding site and regions for the interaction with proteins involved in mRNA degradation. *Mol Microbiol* **32:** 765-775

Roppelt V, Klug G, Evguenieva-Hackenberg E (2010) The evolutionarily conserved subunits Rrp4 and Csl4 confer different substrate specificities to the archaeal exosome. *FEBS Lett* **584:** 2931-2936

Saito S, Hosoda N, Hoshino S (2013) The Hbs1-Dom34 protein complex functions in non-stop mRNA decay in mammalian cells. *J Biol Chem* **288:** 17832-17843

Schaeffer D, Tsanova B, Barbas A, Reis FP, Dastidar EG, Sanchez-Rotunno M, Arraiano CM, van Hoof A (2009) The exosome contains domains with specific endoribonuclease, exoribonuclease and cytoplasmic mRNA decay activities. *Nat Struct Mol Biol* **16:** 56-62

Schaeffer D, van Hoof A (2011) Different nuclease requirements for exosome-mediated degradation of normal and nonstop mRNAs. *Proc Natl Acad Sci U S A* **108:** 2366-2371

Schilders G, Raijmakers R, Raats JM, Pruijn GJ (2005) MPP6 is an exosome-associated RNA-binding protein involved in 5.8S rRNA maturation. *Nucleic Acids Res* **33:** 6795-6804

Schilders G, van Dijk E, Pruijn GJ (2007) C1D and hMtr4p associate with the human exosome subunit PM/Scl-100 and are involved in pre-rRNA processing. *Nucleic Acids Res* **35:** 2564-2572

Schmidt K, Xu Z, Mathews DH, Butler JS (2012) Air proteins control differential TRAMP substrate specificity for nuclear RNA surveillance. *RNA* **18:** 1934-1945

Schneider C, Kudla G, Wlotzka W, Tuck A, Tollervey D (2012) Transcriptome-wide analysis of exosome targets. *Mol Cell* **48:** 422-433

Schneider C, Leung E, Brown J, Tollervey D (2009) The N-terminal PIN domain of the exosome subunit Rrp44 harbors endonuclease activity and tethers Rrp44 to the yeast core exosome. *Nucleic Acids Res* **37:** 1127-1140

Shi Z, Yang WZ, Lin-Chao S, Chak KF, Yuan HS (2008) Crystal structure of Escherichia coli PNPase: central channel residues are involved in processive RNA degradation. *RNA* **14:** 2361-2371

Shiomi T, Fukushima K, Suzuki N, Nakashima N, Noguchi E, Nishimoto T (1998) Human dis3p, which binds to either GTP- or GDP-Ran, complements Saccharomyces cerevisiae dis3. *J Biochem* **123:** 883-890

Shoemaker CJ, Green R (2012) Translation drives mRNA quality control. *Nat Struct Mol Biol* **19:** 594-601

Sloan KE, Mattijssen S, Lebaron S, Tollervey D, Pruijn GJ, Watkins NJ (2013) Both endonucleolytic and exonucleolytic cleavage mediate ITS1 removal during human ribosomal RNA processing. *J Cell Biol* **200:** 577-588

Staals RH, Bronkhorst AW, Schilders G, Slomovic S, Schuster G, Heck AJ, Raijmakers R, Pruijn GJ (2010) Dis3-like 1: a novel exoribonuclease associated with the human exosome. *EMBO J* **29:** 2358-2367

Stead JA, Costello JL, Livingstone MJ, Mitchell P (2007) The PMC2NT domain of the catalytic exosome subunit Rrp6p provides the interface for binding with its cofactor Rrp47p, a nucleic acid-binding protein. *Nucleic Acids Res* **35:** 5556-5567

Steitz TA, Steitz JA (1993) A general two-metal-ion mechanism for catalytic RNA. *Proc Natl Acad Sci U S A* **90:** 6498-6502

Symmons MF, Jones GH, Luisi BF (2000) A duplicated fold is the structural basis for polynucleotide phosphorylase catalytic activity, processivity, and regulation. *Structure* **8:** 1215-1226

Synowsky SA, van Wijk M, Raijmakers R, Heck AJ (2009) Comparative multiplexed mass spectrometric analyses of endogenously expressed yeast nuclear and cytoplasmic exosomes. *J Mol Biol* **385:** 1300-1313

Tomecki R, Kristiansen MS, Lykke-Andersen S, Chlebowski A, Larsen KM, Szczesny RJ, Drazkowska K, Pastula A, Andersen JS, Stepien PP, Dziembowski A, Jensen TH (2010) The human core exosome interacts with differentially localized processive RNases: hDIS3 and hDIS3L. *EMBO J* **29:** 2342-2357

van Dijk EL, Schilders G, Pruijn GJ (2007) Human cell growth requires a functional cytoplasmic exosome, which is involved in various mRNA decay pathways. *RNA* **13:** 1027-1035

van Hoof A, Lennertz P, Parker R (2000) Yeast exosome mutants accumulate 3'-extended polyadenylated forms of U4 small nuclear RNA and small nucleolar RNAs. *Mol Cell Biol* **20:** 441-452

van Hoof A, Parker R (1999) The exosome: a proteasome for RNA? *Cell* **99:** 347-350

Vanacova S, Wolf J, Martin G, Blank D, Dettwiler S, Friedlein A, Langen H, Keith G, Keller W (2005) A new yeast poly(A) polymerase complex involved in RNA quality control. *PLoS Biol* **3:** e189

Von Hippel PH, Fairfield FR, Dolejsi MK (1994) On the processivity of polymerases. *Ann N Y Acad Sci* **726:** 118-131

Wilhelm BT, Marguerat S, Watt S, Schubert F, Wood V, Goodhead I, Penkett CJ, Rogers J, Bahler J (2008) Dynamic repertoire of a eukaryotic transcriptome surveyed at single-nucleotide resolution. *Nature* **453:** 1239-1243

Wyers F, Rougemaille M, Badis G, Rousselle JC, Dufour ME, Boulay J, Regnault B, Devaux F, Namane A, Seraphin B, Libri D, Jacquier A (2005) Cryptic pol II transcripts are degraded by a nuclear quality control pathway involving a new poly(A) polymerase. *Cell* **121:** 725-737

Xu F, Cohen SN (1995) RNA degradation in Escherichia coli regulated by 3' adenylation and 5' phosphorylation. *Nature* **374:** 180-183

Yehudai-Resheff S, Hirsh M, Schuster G (2001) Polynucleotide phosphorylase functions as both an exonuclease and a poly(A) polymerase in spinach chloroplasts. *Mol Cell Biol* **21:** 5408-5416

Zhu B, Mandal SS, Pham AD, Zheng Y, Erdjument-Bromage H, Batra SK, Tempst P, Reinberg D (2005) The human PAF complex coordinates transcription with events downstream of RNA synthesis. *Genes Dev* **19:** 1668-1673

CHAPTER 2

The human exosome and disease

Raymond H.J. Staals[1] and Ger J.M. Pruijn[1]

[1] Department of Biomolecular Chemistry, Nijmegen Center for Molecular Life Sciences, Institute for Molecules and Materials, Radboud University Nijmegen, Nijmegen, The Netherlands

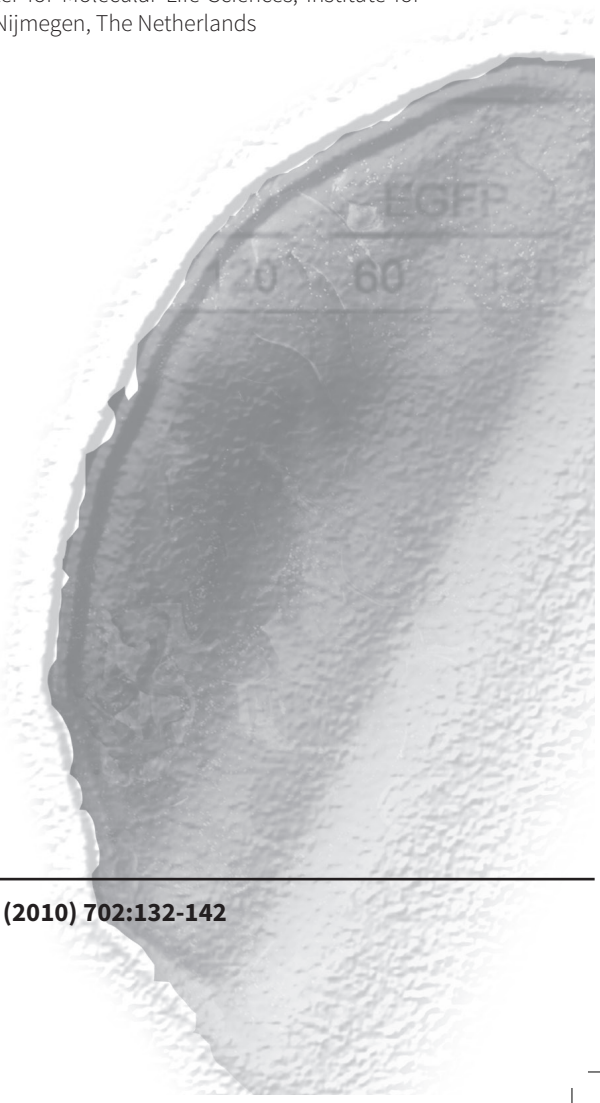

Advances in experimental medicine and biology (2010) 702:132-142

Abstract

Long before the RNA degrading exosome was first described in the yeast Saccharomyces cerevisiae, the use of autoantibodies found in the sera of certain autoimmune patients allowed the identification of a complex of polypeptides which later appeared to be the human exosome. Today, the most extensively documented association of the exosome with disease is still its targeting by the immune system of such patients. The highest frequency of autoantibodies to components of the exosome complex is found in polymyositis-scleroderma overlap patients and therefore the exosome is termed PM/Scl autoantigen in the autoimmune field. More recently, one of the core components of the exosome was identified as a protein associated with chronic myelogenous leukemia. In this Chapter we will describe the identification of the PM/Scl autoantigen from a historical perspective, discuss our current knowledge on the occurrence of autoantibodies to exosome components in autoimmune diseases and end with the data that connect the exosome with cancer.

Introduction

As described in the other chapters of this book, the exosome is implicated in the processing/maturation and degradation of many different species of RNA. The exosome complex is evolutionary conserved and can therefore be found in virtually all eukaryotic and archaeal forms of life, although the composition of the complex might differ to some extent from one species to another. In eubacteria a similar complex in terms of structure and function can be discerned, which is called the degradosome. The presence of exosome or exosome-like complexes in these different species suggests that it fulfills an essential role in RNA metabolism. In agreement with the assumption that eukaryotic cells can probably not survive without a functional exosome, studies in yeast and humans have shown that an intact exosome core is required for normal cell growth (Allmang *et al*, 1999; Mitchell *et al*, 1997; van Dijk *et al*, 2007).

The discovery of the human exosome complex was facilitated by its association with autoimmunity. A response of the immune system to self-components is observed in a plethora of diseases, in particular connective tissue diseases. The autoimmune response can be directed to a variety of biomolecules, including proteins, nucleic acids and lipids. In most cases, it is neither known how immunological tolerance to self-components is broken, nor whether the immune response plays a pathophysiological role or is merely an epiphenomenon. Autoimmunity is generally detected by the appearance of autoantibodies in the serum of patients. Autoantibodies in a distinct group of autoimmune patients target components of the exosome complex and these autoantibodies have been instrumental in the identification of a complex of proteins that was later found to represent the human exosome complex.

Identification of the PM/Scl complex

As already mentioned above, the first indication of the existence of a human exosome complex dates back from 1977 when Wolfe and colleagues showed that autoantibodies in the sera of patients suffering from certain muscle disorders were capable of precipitating an antigen from a calf thymus extract as determined by an immunodiffusion assay (Wolfe *et al*, 1977). This antigen was initially called "PM-1", as 17 out of the 28 sera (61%) that were scored as 'positive' (in terms of successfully precipitating the antigen) were derived from patients that were diagnosed with polymyositis.

Polymyositis, literally meaning "many muscle inflammations", is a progressive, chronic disorder that belongs to the group of connective tissue diseases (CTD), along with other diseases including dermatomyositis (DM) and systemic sclerosis (SSc, also referred to as scleroderma, Scl). Symptoms of PM include weakening and/or loss of mass of the muscles, which is particularly evident in the legs, shoulders and pelvis of the patient, thereby severely hampering the patient's abilities in everyday's activities such as climbing stairs, standing up or even walking. While some of these PM-symptoms are shared with DM and SSc, the latter two disorders have more prominent visual effects on the skin, such as the appearance of rash, hardening of the skin and disposition of calcium under the skin (Figure 1). When patients have symptoms of both SSc and PM or DM, the disorder is referred to as polymyositis/scleroderma-overlap syndrome (PM/Scl). A total of 8 patients suffering from this overlap syndrome were also included in Wolfe's study and all but one of these appeared to contain anti-PM-1 antibodies, indicating that these autoantibodies are more common in this group of patients. More importantly however, the disease-specificity of the autoantibodies indicated that they might be exploited as a biomarker for clinical diagnosis, which was not yet available for these patients at that time. In view of the strongest association of the autoantibodies

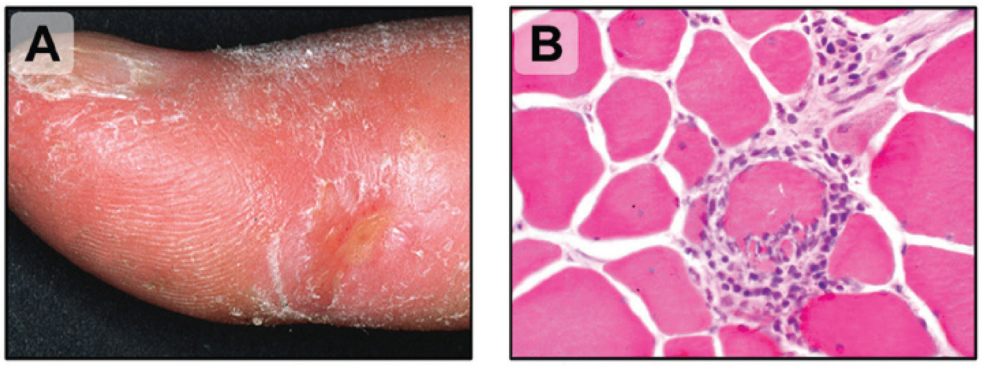

Figure 1. Clinical features of scleroderma and polymyositis.

A) Sclerodactyly, a typical symptom often seen in patients suffering from scleroderma, which is characterized by thickening and tightening of the skin. B) Muscle fibers of a polymyositis patient, showing the infiltration of inflammatory cells (a.o. lymphocytes) in the endomysium.

with PM/Scl patients, the antigen was renamed "PM/Scl-antigen" in 1984. In the same period other research groups confirmed the high prevalence of these autoantibodies in patients suffering from the PM/Scl-overlap syndrome (Reichlin *et al*, 1984; Treadwell *et al*, 1984).

An obvious next step was the identification and characterization of the molecules that make up this particular antigen. By immunoprecipitation experiments it was demonstrated that the PM/Scl-antigen consists of at least 11 polypeptides, with relative molecular masses ranging from 20,000 to 110,000. Subsequently, it took about 5 years before two of the major autoantigenic proteins targeted by the sera of PM/Scl-patients were identified and their cDNAs were cloned (Alderuccio *et al*, 1991; Bluthner and Bautz, 1992; Ge *et al*, 1992). The identified proteins were named according to their relative molecular mass as determined by SDS-PAGE: a M_r 75,000 protein designated PM/Scl-75 and a M_r 100,000 protein designated PM/Scl-100. It should be noted that the PM/Scl-75 protein migrates aberrantly in SDS-PAGE gels, most likely due to the clustering of charged amino acids in its C-terminal region (Raijmakers *et al*, 2003). In addition, four isoforms of the PM/Scl-75 protein have been described. The original cDNA reported by Alderuccio and coworkers (Alderuccio *et al*, 1991) was probably incomplete in the region corresponding to the N-terminus, which was substantiated by the lack of association with the exosome complex in two-hybrid experiments (Raijmakers *et al*, 2002). By screening human EST databases sequences encoding 84 additional amino acids in the N-terminal region were found. Importantly, the polypeptide corresponding to the longer isoform did show two-hybrid interactions with components of the exosome core complex (Raijmakers *et al*, 2003). Another variation in the PM/Scl-75 sequence is resulting from an alternative splicing event, which leads to the incorporation of a 17 amino acids encoding optional exon in the C-terminal region of the protein.

When the yeast exosome complex was identified (Mitchell *et al*, 1997) and Allmang and colleagues found that two of its protein components, Rrp45 and Rrp6, were homologous to the human PM/Scl-75 and PM/Scl-100 proteins, respectively (Allmang *et al*, 1999), the suggestion was raised that the PM/Scl complex might in fact represent the human counterpart of the yeast exosome. This was confirmed by the cloning of cDNAs encoding the other components of the human exosome, which was based upon either the homology with their yeast counterparts or the copurification with the human exosome during affinity-purifications (Brouwer *et al*, 2001; Chen *et al*, 2001).

Autoantibodies to the exosome / PM/Scl-antigen

Originally, the detection of autoantibodies in patient sera was mainly performed by immunodiffusion (or the related technique counterimmunoelectrophoresis) and by indirect immunofluorescence (IF). With the latter technique a typical nucleolar staining pattern was indicative for the presence of anti-PM/Scl autoantibodies and therefore anti-PM/Scl autoantibodies were categorized as anti-nucleolar antibodies (ANoA), together with anti-Th/

To (antibodies to protein components of the RNase MRP and RNase P particles) and anti-U3 (antibodies to proteins of the U3 snoRNP particle, in particular to fibrillarin). Although this method is not very specific for the detection of anti-PM/Scl autoantibodies, ANoA and ANA (anti-nuclear antibodies) are at least indicative for many CTD, especially since they are usually absent from healthy controls (Reimer *et al*, 1988; von Muhlen and Tan, 1995). For this reason, this technique was often used as an initial screening method, which was followed by either immunodiffusion (ID), immunoprecipitation (IP), immunoblotting (IB) or enzyme-linked immunosorbent assays (ELISA).

A combination of the data from many studies addressing anti-PM/Scl reactivity in patient sera by either ID, IF and/or IP showed that this reactivity can be found in 31% of PM/Scl patients (Table 1). The frequency of anti-PM/Scl reactivity in patients diagnosed with PM, DM and SSc was 8%, 11% and 2%, respectively.

The cloning of cDNAs encoding individual protein subunits of the exosome and the production of the corresponding recombinant proteins in various expression systems created new possibilities to characterize the anti-PM/Scl autoimmune response and to screen patient sera for the occurrence of anti-PM/Scl autoantibodies. This facilitated the detection of autoantibodies to individual protein components of the exosome, e.g., by ELISA. Since IP assays can be quite laborious, especially when large cohorts of patients have to be analyzed and due to the poor recognition of the main antigens (PM/Scl-75 in particular)

Table 1. Anti-PM/Scl reactivity in PM, DM, Scl, PM/Scl-overlap and nondifferentiated idiopathic inflammatory myopathy (IIM) patients monitored by ID, IF and/or IP

Study	IIM	PM	DM	Scl	PM/Scl	Method
Wolfe (1977)		9/14 (64)	1/6 (17)		7/8 (88)	ID
Treadwell (1984)		2/22 (9)		2/32 (6)	9/77 (12)	ID
Reichlin (1984)	9/114 (8)					ID
Reimer (1988)				8/646 (1)		IF/IP
Reichlin (1988)		8/168 (5)				ID
Oddis (1992)	5/106 (5)			6/359 (2)	10/41 (24)	ID/IF
Hausmanowa (1997)		0/19 (0)	0/21 (0)		19/25 (76)	ID
O'Hanlon (2006)	65/603 (11)	13/227 (6)	19/177 (11)		32/101 (32)	ID
Selva-O'Callaghan (2006)	10/88 (11)	1/27 (4)	8/59 (14)			IP
Total	**89/991 (10)**	**33/477 (8)**	**28/263 (11)**	**16/1037 (2)**	**77/252 (31)**	

by the patient sera on IB, ELISA has become the method of choice to detect anti-exosome autoantibodies. During the last decade also a number of exosome-associated proteins, that are not considered to be part of the exosome core complex, but (transiently) associate with a subset of the exosome, have been identified and their cDNAs have been cloned and expressed (Chen *et al*, 2001; Lehner and Sanderson, 2004; Schilders *et al*, 2007a; Schilders *et al*, 2005; Schilders *et al*, 2007c). A number of these proteins have been used as well to investigate whether they are also targeted by autoantibodies in (anti-PM/Scl-positive) patient sera (Table 2). A schematic overview of the targeting of exosome core components and of exosome-associated/auxiliary proteins by autoantibodies (as determined by ELISA) in PM/Scl-overlap sera is given in Figure 2.

The majority of anti-PM/Scl-positive patients appeared to have autoantibodies directed against PM/Scl-100 and/or PM/Scl-75 (Table 3). The other exosome core components are less frequently targeted, with the exception of Rrp4, which is recognized by 64% of the anti-PM/Scl-positive patients (Brouwer *et al*, 2002; Raijmakers *et al*, 2004). A combination of ELISA data for PM/Scl-100 and PM/Scl-75 leads to similar sensitivity scores as the conventional ID, IF, IB and IP assays (approximately 31% of PM/Scl patients are positive). After mapping a major autoepitope of PM/Scl-100 (Bluthner *et al*, 2000), a synthetic peptide corresponding to this epitope, designated "PM1-alpha", was produced to set up an ELISA, which allowed the detection of autoantibodies in 55% of the PM/Scl-overlap patients (Mahler *et al*, 2005). In addition, the C1D protein, a RNA-binding protein which binds to PM/Scl-100 and participates in exosome-mediated pre-rRNA processing, was found to be a major autoantigen in PM/Scl patients (Schilders *et al*, 2007a; Schilders *et al*, 2007c).

Because many of the autoantibody studies described above have not yet been replicated with other cohorts of patients, the frequencies by which these antibody specificities occur should be interpreted with care. It is known that ethnic differences and genetic variation

Table 2. Anti-exosome(-associated) protein reactivity in PM, DM, Scl and PM/Scl-overlap patients monitored by ELISA.[a,b]

	Antigen						
Diagnosis	**PM/Scl-75**	**PM/Scl-100**	**MPP6**	**C1D**	**Mtr4**	**Ski2**	**hSki8**
PM	0–3	2–8	0	5	2	5	0
DM	2–3	2–6	2	0	0	2	2
Scl	10	2–13	0	0	0	0	0
PM/Scl	27–28	23–55	0	23	7	0	3

[a] Reactivity values are given in percentages.

[b] References used for PM/Scl-75: (Brouwer *et al,* 2002; Raijmakers *et al,* 2004; Schilders *et al,* 2007a), PM/Scl-100: (Brouwer *et al,* 2002; Raijmakers *et al,* 2004; Schilders *et al,* 2007a), MPP6, C1D, Mtr4, Ski2 and hSki8: (Schilders *et al,* 2007a)

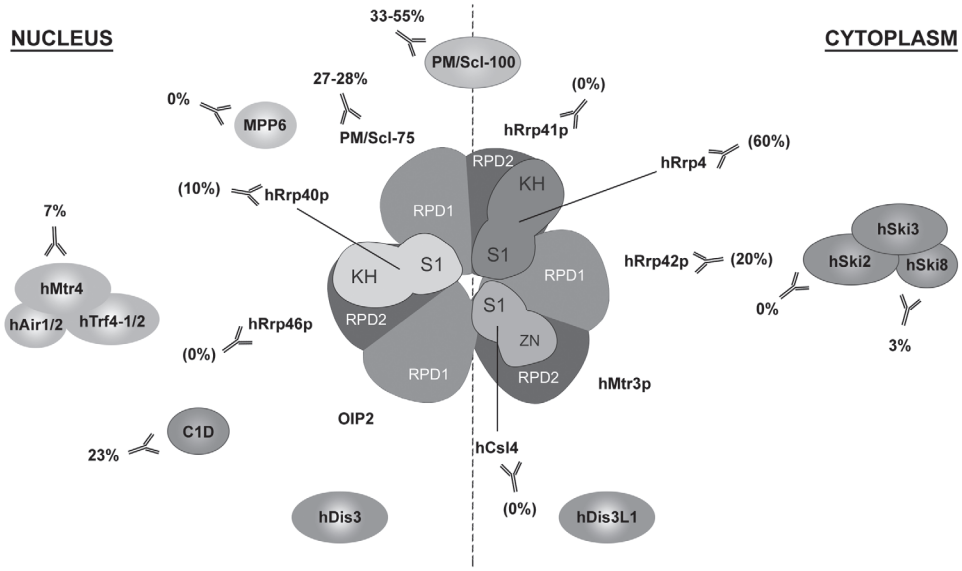

Figure 2. Targeting of exosome and exosome-associated proteins by autoantibodies from PM/Scl-overlap patients.

Schematic structure of the human exosome. The nine core subunits assemble into a ring-like structure (central). RPD1 and RPD2 refer to two groups of RNase PH domains; KH, S1 and ZN to RNA-binding domains. Exosome-associated/auxiliary proteins and protein complexes that have been reported to interact with the exosome core are shown at the periphery. Proteins for which the presence of autoantibodies in PM/Scl sera has been investigated are indicated by the schematic antibody structures. Numbers (in percentages) represent the frequency of autoantibodies in patient sera. Numbers between brackets represent the frequencies for sera that were preselected based upon the reactivity with either PM/Scl-75 or PM/Scl-100.

Table 3. Anti-exosome core protein reactivity in anti-PM/Scl-positive PM, DM, Scl and PM/Scl-overlap patients monitored by ELISA.[a]

	Antigen							
Diagnosis	**PM/Scl-75**	**PM/Scl-100**	**hRrp4**	**hRrp40**	**hRrp41**	**hRrp42**	**hRrp46**	**hCsl4**
PM	nd	nd	nd	nd	nd	nd	nd	nd
DM	nd	nd	nd	nd	nd	nd	nd	nd
Scl	64	100	64	0	0	36	0	0
PM/Scl	90	100	60	10	0	20	0	0

[a] Reactivity values are given in percentages.

may affect the incidence of autoantibody production. The frequency of patients with anti-PM/Scl reactivity, for example, appears to be quite variable, as this reactivity was not found in a large cohort of 275 Japanese patients (Kuwana *et al*, 1994). This may at least in part be due to the fact that the presence of anti-PM/Scl antibodies seems to be associated with certain MHC alleles, HLA-DRB1*0301, HLA-DQA1*0501 and HLA-DQB1*02,26,27 whereas HLA-DRB1*15/*16 and HLA-DQA1*0101 might prevent the production of these autoantibodies (O'Hanlon *et al*, 2006).

Initiation of the anti-exosome / PM/Scl autoimmune response

It is still an open question what triggers the anti-PM/Scl response in the initial stages of these autoimmune diseases. Several studies have proposed a role for unusual protein modifications, in particular those occurring during apoptosis and necrosis, which might play a role in breaking immunological tolerance to these proteins (Hof *et al*, 2007; Utz *et al*, 2000). One of the core subunits of the exosome, PM/Scl-75, which is also one of the most frequently targeted proteins by anti-PM/Scl-positive sera, has been demonstrated to be cleaved by caspases in apoptotic cells (Schilders *et al*, 2007b). Moreover, PM/Scl-100 appeared to be cleaved by granzyme B *in vitro* (Casciola-Rosen *et al*, 1999). It is not known yet whether these changes lead to the formation of neo-epitopes. An alternative mechanism might be molecular mimicry, in which structural similarities between epitopes of foreign and self-proteins result in the cross-activation of autoreactive T or B cells by pathogen-derived peptides.

The targeting of multiple exosome subunits and exosome associated proteins is most likely the result of a phenomenon called intermolecular epitope spreading. When an immune response towards a particular protein is elicited, it can extend to another molecule that resides in the same complex. Data supporting this hypothesis regarding the human exosome is still scarce, although two bodies of evidence point in that direction. Firstly, immunization of rabbits with a synthetic peptide corresponding to a major epitope of PM/Scl-100 led to the generation of antibodies that targeted other components of the exosome complex as well (Mahler and Raijmakers, 2007). Secondly, the serum of a patient with high anti-PM/Scl reactivity was shown to stain a single, 100 kDa polypeptide in IB. Three months later, the serum was found to stain an additional, 29 kDa polypeptide in IB, which was suggested to correspond to an aberrant form of PM/Scl-75, but might be one of the other core components as well (Gutierrez-Ramos *et al*, 2008).

The human exosome and cancer

As already mentioned in the introduction, the viability of cells is severely impaired when the integrity of the exosome complex is disturbed. This strongly suggests that at least one of the functions of the exosome is essential to keep the cell in a proliferating state. On the other hand, when the activity of the exosome would be rate limiting in the maturation or turnover

of RNAs that are crucial for cell proliferation, an overactive exosome may lead to a higher rate of proliferation. Although rather speculative, this is supported by observations of Yang and coworkers who examined patients who received a donor lymphocyte infusion (DLI) as a treatment for chronic myelogenous leukemia (CML) (Yang *et al*, 2002). CML is characterized by the uncontrolled production of myeloid cells, resulting in a strong accumulation of these cells in the blood and is associated with a typical chromosomal translocation resulting in the so-called Philadelphia chromosome. This translocation leads to the production of an aberrant, overactive tyrosine kinase fusion protein, Bcr-Abl, which is thought to affect several substrate proteins involved in cell division, DNA repair and genomic instability. Of all the known cases of adult leukemia in the Western countries, about 15 to 20% have been classified as CML (Faderl *et al*, 1999). Before the introduction of Imatinib, a drug that specifically counteracts the activity of the Bcr-Abl fusion protein, patients suffering from CML often received a bone marrow transplantation (BMT). The patients who relapsed after this transplantation were further treated with DLI, resulting in a durable remission of the disease in 70 to 80% of the cases (Collins *et al*, 1997). The success of this treatment is a result of a phenomenon called the graft-versus-tumor (GVT) effect, in which the infused lymphocytes attack any remaining cancerous cells in the bone marrow.

When Yang and colleagues used the serum of DLI-responding patients for an antibody-based screening of a CML cDNA expression library, new putative tumor-related antigens were identified (Wu *et al*, 2000). Among these was a M_r 28,000 protein, which was designated CML28. Sequence analysis revealed that this protein is identical to hRrp46, a constituent of the exosome core complex (Figure 2), although the 5' coding region of the CML28 is 33 amino acids longer than that of hRrp46. To confirm that hRrp46 is immunogenic in these patients, serum samples derived from a CML patient before and after BMT and DLI were analyzed with IB and ELISA using recombinant hRrp46. While anti-hRrp46 reactivity couldn't be detected in healthy controls and in the CML patient prior to DLI, this reactivity significantly increased 2 to 6 months post-DLI, after which the reactivity gradually declined to undetectable levels 2 years post-DLI. Moreover, the temporal pattern of anti-hRrp46 reactivity correlated well with the onset of cytogenetic remission, which is indicated by the disappearance of the Philadelphia chromosome. Since the patient didn't appear to have any symptoms indicating the development of an autoimmune disease, the anti-hRrp46 reactivity seemed to be associated with tumor rejection instead. The immune response towards hRrp46 was shown to be a common feature of other types of cancer, such as lung and prostate cancer and melanoma, in which the antibodies could be detected in 10% to 33% of the cases. The anti-hRrp46 response might at least in part be due to the overexpression of hRrp46 in these different cancers, as it was demonstrated by northern blot hybridization and IB that highly proliferating cell lines express high levels of hRrp46 when compared to normal tissues or even stable-phase CML. These findings might also prove useful for the development of an antigen-specific immunotherapy and progress in the development of such strategies has

already been made (Mao *et al*, 2008; Xie *et al*, 2008; Zhou *et al*, 2006). The anti-hRrp46 immune response and elevated hRrp46 expression levels in cancer raise the question whether these phenomena are specific for hRrp46 or also occur for other exosome components. Further experiments will be required to clarify this issue.

Interestingly, the antimetabolite 5-fluorouracil, which is frequently used to treat solid tumors in a variety of cancers, was shown to inhibit the function of the exosome. Originally this drug was selected for its hypothetical ability to inhibit cell proliferation, presumably by causing thymidine starvation and thus negatively affecting DNA synthesis. However, Fang and coworkers reported that also rRNA processing was impaired by this drug (Fang *et al*, 2004). The accumulated pre-rRNA precursors were similar to the precursors accumulating in exosome mutant yeast strains. Possibly related to these observations, it was demonstrated that the absence of Rrp6 (the yeast counterpart of PM/Scl-100) enhanced the 5-fluorouracil-induced defects (Lum *et al*, 2004). Taken together, these results suggest that 5-fluorouracil exerts its effect on rRNA processing at least in part by inhibiting the exosome.

Conclusion

In view of the central role of the human exosome in the processing and degradation of many RNAs, it is intriguing to investigate to what extent a disturbance of its function can interfere with normal cellular physiology and is associated with diseases. The two best documented examples, autoimmunity and cancer, have been discussed in this chapter, although there are still many questions that need to be addressed. It is, for example, still unclear what causes the targeting of PM/Scl-75 and PM/Scl-100 by the immune system in patients suffering from the PM/Scl-overlap syndrome and why this response is particularly associated with this autoimmune disease. In view of the physical barrier of the plasma membrane, autoantibodies are not likely to interfere with the functions of the exosome in RNA metabolism, but once exosome components are released from (dying) cells the resulting immune complexes may contribute to the progression of autoimmunity and tissue damage. In case of cancer dysfunctioning of the exosome may play a direct role, but it is clear that more work has to be done to investigate the effects of increased or decreased exosome activity on cell proliferation. It is currently not known whether exosome core subunits other than hRrp46 are overexpressed in solid tumors as well. Alternatively, a pool of non-exosome associated hRrp46 may exist and might have a completely other role independent of the exosome. In this respect, also the importance of the N-terminal extension, which may be specific for a particular isoform of hRrp46, needs to be studied.

The exosome is known to play an important role in the degradation of a special class of mRNAs, containing cis-acting adenylate-uridylate-rich sequence elements (AREs) in their

3'UTR. Transcripts containing such elements are often involved in important biological processes and their levels are therefore often tightly regulated. In theory, a perturbation of exosome function is likely to affect these levels and, as a consequence, might cause a wide variety of pathological conditions (Khabar, 2005).

In this Chapter we focused on human diseases, but one should realize that the exosome is expressed is many other species and thus might also here be associated with disease. In plants, for instance, it was found that the effects of deletion of a particular exosome component mimicked a disorder that induced cell death in the tip of the leafs when plants are inoculated with *Blumeria graminis*, a fungus that causes mildew on grasses and that is frequently used to infect plants in a laboratory setting. Intriguingly, the deleted exosome component was Rrp46 (Xi *et al*, 2009).

We conclude that although targeting of exosome components in autoimmunity is known for many years, our knowledge on the involvement of the exosome, of its individual components or of its auxiliary factors in other diseases is still in its infancy and much work needs to be done to obtain more insight in this topic.

Acknowledgements

We thank Reinout Raijmakers as well as present and former members of our laboratory for stimulating discussions and contribution of ideas and information to this article.

References

Alderuccio F, Chan EK, Tan EM (1991) Molecular characterization of an autoantigen of PM-Scl in the polymyositis/scleroderma overlap syndrome: a unique and complete human cDNA encoding an apparent 75-kD acidic protein of the nucleolar complex. *J Exp Med* **173:** 941-952

Allmang C, Petfalski E, Podtelejnikov A, Mann M, Tollervey D, Mitchell P (1999) The yeast exosome and human PM-Scl are related complexes of 3' --> 5' exonucleases. *Genes Dev* **13:** 2148-2158

Bluthner M, Bautz FA (1992) Cloning and characterization of the cDNA coding for a polymyositis-scleroderma overlap syndrome-related nucleolar 100-kD protein. *J Exp Med* **176:** 973-980

Bluthner M, Mahler M, Muller DB, Dunzl H, Bautz FA (2000) Identification of an alpha-helical epitope region on the PM/Scl-100 autoantigen with structural homology to a region on the heterochromatin p25beta autoantigen using immobilized overlapping synthetic peptides. *J Mol Med (Berl)* **78:** 47-54

Brouwer R, Allmang C, Raijmakers R, van Aarssen Y, Egberts WV, Petfalski E, van Venrooij WJ, Tollervey D, Pruijn GJ (2001) Three novel components of the human exosome. *J Biol Chem* **276:** 6177-6184

Brouwer R, Vree Egberts WT, Hengstman GJ, Raijmakers R, van Engelen BG, Seelig HP, Renz M, Mierau R, Genth E, Pruijn GJ, van Venrooij WJ (2002) Autoantibodies directed to novel components of the PM/Scl complex, the human exosome. *Arthritis Res* **4:** 134-138

Casciola-Rosen L, Andrade F, Ulanet D, Wong WB, Rosen A (1999) Cleavage by granzyme B is strongly predictive of autoantigen status: implications for initiation of autoimmunity. *J Exp Med* **190:** 815-826

Chen CY, Gherzi R, Ong SE, Chan EL, Raijmakers R, Pruijn GJ, Stoecklin G, Moroni C, Mann M, Karin M (2001) AU binding proteins recruit the exosome to degrade ARE-containing mRNAs. *Cell* **107:** 451-464

Collins RH, Jr., Shpilberg O, Drobyski WR, Porter DL, Giralt S, Champlin R, Goodman SA, Wolff SN, Hu W, Verfaillie C, List A, Dalton W, Ognoskie N, Chetrit A, Antin JH, Nemunaitis J (1997) Donor leukocyte infusions in 140 patients with relapsed malignancy after allogeneic bone marrow transplantation. *J Clin Oncol* **15:** 433-444

Faderl S, Talpaz M, Estrov Z, Kantarjian HM (1999) Chronic myelogenous leukemia: biology and therapy. *Ann Intern Med* **131:** 207-219

Fang F, Hoskins J, Butler JS (2004) 5-fluorouracil enhances exosome-dependent accumulation of polyadenylated rRNAs. *Mol Cell Biol* **24:** 10766-10776

Ge Q, Frank MB, O'Brien C, Targoff IN (1992) Cloning of a complementary DNA coding for the 100-kD antigenic protein of the PM-Scl autoantigen. *J Clin Invest* **90:** 559-570

Gutierrez-Ramos R, Gonz Lez-Diaz V, Pacheco-Tovar MG, Lopez-Luna A, Avalos-Diaz E, Herrera-Esparza R (2008) A dermatomyositis and scleroderma overlap syndrome with a remarkable high titer of anti-exosome antibodies. *Reumatismo* **60:** 296-300

Hof D, Pruijn GJ, van Venrooij WJ, Raats JM (2007) The role of cell death-specific modifications in breaking tolerance to self-antigens. In *Cell apoptosis research advances*, Kettleworth CR (ed), pp 179-202. New York: Nova Biomedical Books

Khabar KS (2005) The AU-rich transcriptome: more than interferons and cytokines, and its role in disease. *J Interferon Cytokine Res* **25:** 1-10

Kuwana M, Okano Y, Kaburaki J, Tojo T, Medsger TA, Jr. (1994) Racial differences in the distribution of systemic sclerosis-related serum antinuclear antibodies. *Arthritis Rheum* **37:** 902-906

Lehner B, Sanderson CM (2004) A protein interaction framework for human mRNA degradation. *Genome Res* **14:** 1315-1323

Lum PY, Armour CD, Stepaniants SB, Cavet G, Wolf MK, Butler JS, Hinshaw JC, Garnier P, Prestwich GD, Leonardson A, Garrett-Engele P, Rush CM, Bard M, Schimmack G, Phillips JW, Roberts CJ, Shoemaker DD (2004) Discovering modes of action for therapeutic compounds using a genome-wide screen of yeast heterozygotes. *Cell* **116:** 121-137

Mahler M, Raijmakers R (2007) Novel aspects of autoantibodies to the PM/Scl complex: clinical, genetic and diagnostic insights. *Autoimmun Rev* **6:** 432-437

Mahler M, Raijmakers R, Dahnrich C, Bluthner M, Fritzler MJ (2005) Clinical evaluation of autoantibodies to a novel PM/Scl peptide antigen. *Arthritis Res Ther* **7:** R704-713

Mao H, Geng Z, Liu W, Sun H, Huang W (2008) Selection of HLA-A2 restricted CML28 peptide by artificial antigen-presenting cells. *J Immunother* **31:** 487-490

Mitchell P, Petfalski E, Shevchenko A, Mann M, Tollervey D (1997) The exosome: a conserved eukaryotic RNA processing complex containing multiple 3'-->5' exoribonucleases. *Cell* **91:** 457-466

O'Hanlon TP, Carrick DM, Targoff IN, Arnett FC, Reveille JD, Carrington M, Gao X, Oddis CV, Morel PA, Malley JD, Malley K, Shamim EA, Rider LG, Chanock SJ, Foster CB, Bunch T, Blackshear PJ, Plotz PH, Love LA, Miller FW (2006) Immunogenetic risk and protective factors for the idiopathic inflammatory myopathies: distinct HLA-A, -B, -Cw, -DRB1, and -DQA1 allelic profiles distinguish European American patients with different myositis autoantibodies. *Medicine (Baltimore)* **85:** 111-127

Raijmakers R, Egberts WV, van Venrooij WJ, Pruijn GJ (2002) Protein-protein interactions between human exosome components support the assembly of RNase PH-type subunits into a six-membered PNPase-like ring. *J Mol Biol* **323:** 653-663

Raijmakers R, Egberts WV, van Venrooij WJ, Pruijn GJ (2003) The association of the human PM/Scl-75 autoantigen with the exosome is dependent on a newly identified N terminus. *J Biol Chem* **278:** 30698-30704

Raijmakers R, Renz M, Wiemann C, Egberts WV, Seelig HP, van Venrooij WJ, Pruijn GJ (2004) PM-Scl-75 is the main autoantigen in patients with the polymyositis/scleroderma overlap syndrome. *Arthritis Rheum* **50:** 565-569

Reichlin M, Maddison PJ, Targoff I, Bunch T, Arnett F, Sharp G, Treadwell E, Tan EM (1984) Antibodies to a nuclear/nucleolar antigen in patients with polymyositis overlap syndromes. *J Clin Immunol* **4:** 40-44

Reimer G, Steen VD, Penning CA, Medsger TA, Jr., Tan EM (1988) Correlates between autoantibodies to nucleolar antigens and clinical features in patients with systemic sclerosis (scleroderma). *Arthritis Rheum* **31:** 525-532

Schilders G, Egberts WV, Raijmakers R, Pruijn GJ (2007a) C1D is a major autoantibody target in patients with the polymyositis-scleroderma overlap syndrome. *Arthritis Rheum* **56:** 2449-2454

Schilders G, Raijmakers R, Malmegrim KC, Vande Walle L, Saelens X, Vree Egberts W, van Venrooij WJ, Vandenabeele P, Pruijn GJ (2007b) Caspase-mediated cleavage of the exosome subunit PM/Scl-75 during apoptosis. *Arthritis Res Ther* **9:** R12

Schilders G, Raijmakers R, Raats JM, Pruijn GJ (2005) MPP6 is an exosome-associated RNA-binding protein involved in 5.8S rRNA maturation. *Nucleic Acids Res* **33:** 6795-6804

Schilders G, van Dijk E, Pruijn GJ (2007c) C1D and hMtr4p associate with the human exosome subunit PM/Scl-100 and are involved in pre-rRNA processing. *Nucleic Acids Res* **35:** 2564-2572

Treadwell EL, Alspaugh MA, Wolfe JF, Sharp GC (1984) Clinical relevance of PM-1 antibody and physiochemical characterization of PM-1 antigen. *J Rheumatol* **11:** 658-662

Utz PJ, Gensler TJ, Anderson P (2000) Death, autoantigen modifications, and tolerance. *Arthritis Res* **2:** 101-114

van Dijk EL, Schilders G, Pruijn GJ (2007) Human cell growth requires a functional cytoplasmic exosome, which is involved in various mRNA decay pathways. *RNA* **13:** 1027-1035

von Muhlen CA, Tan EM (1995) Autoantibodies in the diagnosis of systemic rheumatic diseases. *Semin Arthritis Rheum* **24:** 323-358

Wolfe JF, Adelstein E, Sharp GC (1977) Antinuclear antibody with distinct specificity for polymyositis. *J Clin Invest* **59:** 176-178

Wu CJ, Yang XF, McLaughlin S, Neuberg D, Canning C, Stein B, Alyea EP, Soiffer RJ, Dranoff G, Ritz J (2000) Detection of a potent humoral response associated with immune-induced remission of chronic myelogenous leukemia. *J Clin Invest* **106:** 705-714

Xi L, Moscou MJ, Meng Y, Xu W, Caldo RA, Shaver M, Nettleton D, Wise RP (2009) Transcript-based cloning of RRP46, a regulator of rRNA processing and R gene-independent cell death in barley-powdery mildew interactions. *Plant Cell* **21:** 3280-3295

Xie LH, Sin FW, Cheng SC, Cheung YK, Chan KT, Xie Y, Xie Y (2008) Activation of cytotoxic T lymphocytes against CML28-bearing tumors by dendritic cells transduced with a recombinant adeno-associated virus encoding the CML28 gene. *Cancer Immunol Immunother* **57:** 1029-1038

Yang XF, Wu CJ, Chen L, Alyea EP, Canning C, Kantoff P, Soiffer RJ, Dranoff G, Ritz J (2002) CML28 is a broadly immunogenic antigen, which is overexpressed in tumor cells. *Cancer Res* **62:** 5517-5522

Zhou H, Zhang D, Wang Y, Dai M, Zhang L, Liu W, Liu D, Tan H, Huang Z (2006) Induction of CML28-specific cytotoxic T cell responses using co-transfected dendritic cells with CML28 DNA vaccine and SOCS1 small interfering RNA expression vector. *Biochem Biophys Res Commun* **347:** 200-207

CHAPTER 3

Dis3-like 1: a novel exoribonuclease associated with the human exosome

Raymond H.J. Staals[1], Alfred W. Bronkhorst[1], Geurt Schilders[1], Shimyn Slomovic[2], Gadi Schuster[2], Albert J.R. Heck[3], Reinout Raijmakers[3], Ger J.M. Pruijn[1]

[1] Department of Biomolecular Chemistry, Nijmegen Center for Molecular Life Sciences, Institute for Molecules and Materials, Radboud University Nijmegen, Nijmegen, The Netherlands

[2] Faculty of Biology, Technion – Israel Institute of Technology, Haifa 32000, Israel

[3] Biomolecular Mass Spectrometry and Proteomics Group, Bijvoet Center for Biomolecular Research, Utrecht University and Netherlands Proteomics Centre, Utrecht, The Netherlands

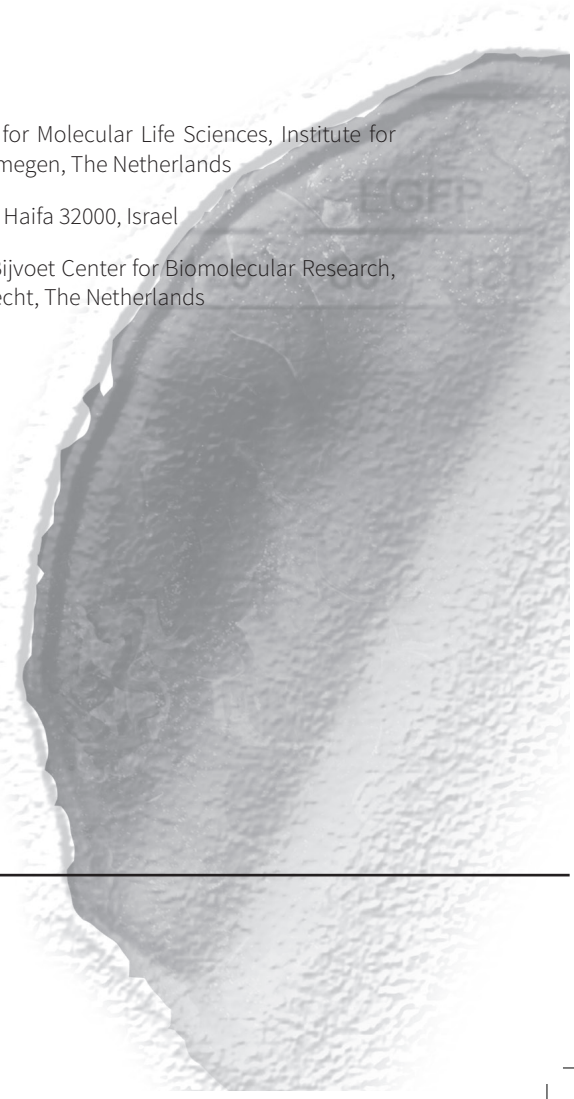

The EMBO Journal (2010) Jul 21;29(14):2358-2367

Abstract

The exosome is an exoribonuclease complex involved in the degradation and maturation of a wide variety of RNAs. The nine-subunit core of the eukaryotic exosome is catalytically inactive and may play an architectural role and mediate substrate binding. In Saccharomyces cerevisiae the associated Dis3 and Rrp6 provide the exoribonucleolytic activity. The human exosome-associated Rrp6 counterpart contributes to its activity, whereas the human Dis3 protein is not detectably associated with the exosome. Here, a proteomic analysis of immunoaffinity-purified human exosome complexes identified a novel exosome-associated exoribonuclease, hDis3L1, which was confirmed to associate with the exosome core by co-immunoprecipitation. In contrast to the nuclear localization of Dis3, hDis3L1 exclusively localized to the cytoplasm. hDis3L1 isolated from transfected cells degraded RNA in an exoribonucleolytic fashion, and its RNB domain appeared to mediate this activity. The siRNA-mediated knockdown of hDis3L1 in HeLa cells resulted in elevated levels of poly(A)-tailed 28S rRNA degradation intermediates, indicating the involvement of hDis3L1 in cytoplasmic RNA decay. Taken together, these data indicate that hDis3L1 is a novel exosome-associated exoribonuclease in the cytoplasm of human cells.

Introduction

RNA is one of the most fundamental and versatile biomolecules present in the cell, with many different roles, including the translation of genetic information into proteins, the replication of DNA and structural roles in large complexes. Perhaps one of the key features which accounts for the diverse biological roles that can be performed by RNA is the fact that it can be heavily modified after synthesis of the original precursors. As such, proper maturation of RNA molecules is of crucial importance for its function and can involve many different steps, such as splicing, polyadenylation, capping, as well as cleavage and/or trimming by endo- and exoribonucleases. One of the main players in the latter is the exosome, a conserved protein complex with 3' to 5' exoribonuclease activity.

Originally identified in yeast as a complex generating the 3' end of the 5.8S rRNA in the nucleolus (Mitchell *et al*, 1997), it has become clear that the exosome complex is implicated in many processes of RNA metabolism. In the nucleoplasm and nucleolus, for instance, the maturation of many small RNAs (e.g. snRNAs and snoRNAs) is dependent on processing steps by the exosome. In addition, the exosome fulfills a role in degrading improperly processed RNAs (such as aberrant pre-mRNA and pre-tRNA species), as well as in the 'normal' turnover of cytoplasmic mRNAs (van Dijk *et al*, 2007), and it is involved in specific mRNA decay pathways, including non-stop decay and nonsense mediated decay (Schilders *et al*, 2006; van Hoof *et al*, 2002).

The doughnut-shaped core of the exosome consists of nine proteins, six of which are homologous to the 3' to 5' exonuclease RNase PH and three proteins with RNA binding domains (each containing a S1 RNA-binding domain and two of which contain an additional KH domain). While the archaeal and probably also the plant exosome core seem to have retained their activity during the course of evolution, reconstitution experiments showed that the core of the yeast and human exosome are catalytically inactive (Chekanova *et al*, 2000; Liu *et al*, 2006; Lorentzen *et al*, 2005). However, two other types of hydrolytic RNases associated with exosome complexes in eukaryotes are thought to be responsible for the activity of the complex. Rrp6 (designated PM/Scl-100 in humans), an enzyme belonging to the RNase D family of hydrolytic exoribonucleases, associates with a subset of exosome cores and contributes to its activity (Brouwer *et al*, 2001b; Synowsky *et al*, 2009). Rrp6 has been reported to reside exclusively in the nucleus of yeast cells (Allmang *et al*, 1999b), whereas in human cells PM/Scl-100 was found both in the nucleus and cytoplasm (Brouwer *et al*, 2001a; Lejeune *et al*, 2003). Depletion of Rrp6 from cells has been shown to give rise to phenotypes markedly different from when core exosome components are depleted in various experimental setups, suggesting that its function is at least partially uncoupled to that of the core exosome (Callahan and Butler, 2008; Graham *et al*, 2009; van Dijk *et al*, 2007). Another hydrolytic exoribonuclease, Dis3 (also known as Rrp44), which belongs to the RNase R family of RNases, was recently shown to be essential for the activity of the yeast exosome (Dziembowski *et al*, 2007). In yeast, the Dis3 protein can be detected in both the nucleolus as well as the cytoplasm (Synowsky *et al*, 2009). Recently, Dis3 was found to display endonuclease activity as well, in agreement with the presence of a functional PIN domain in its N-terminal region (Lebreton *et al*, 2008; Schaeffer *et al*, 2009). The recently determined crystal structure of the yeast Dis3-Rrp41-Rrp45 complex led, in combination with the results of biochemical analyses, to a model in which RNA substrates thread through the central channel of the exosome core to reach the Dis3 exoribonuclease site (Bonneau *et al*, 2009).
Although a human homologue of Dis3 was described more than a decade ago and was shown to complement yeast Dis3 (Shiomi *et al*, 1998), a stable association of this protein with the exosome core could not be shown (Chen *et al*, 2001). During our studies to identify proteins stably associated with the human exosome core, we detected another homologue of the yeast Dis3 protein, designated Dis3-like exoribonuclease 1 (Dis3L1). Here, we characterize its association with the exosome core, its subcellular localization and its enzymatic activities.

Results

Identification of Dis3L1 as a novel exosome-associated protein

To identify proteins associated with the core of the human exosome, which may be involved in its exoribonuclease activity or the regulation thereof, antibodies to a core component were

used to isolate exosome complexes by immuno-affinity chromatography. These complexes were isolated from total HeLa cell extracts using polyclonal anti-hRrp40 antibodies (Brouwer *et al*, 2001a). Proteins that remained bound to the immobilized antibodies at 1 M NaCl were eluted and analyzed by SDS-PAGE. Following Coomassie Brilliant Blue staining, the gel lane was cut in 19 slices, which were subjected to in-gel digestion and analyzed by nano-reversed phase liquid chromatography coupled to a high-resolution LTQ-Orbitrap mass spectrometer. Analysis of the resulting MS/MS spectra against the Swissprot database using Mascot revealed the presence of all nine core exosome subunits (Table 1), as well as two additional proteins, known to associate with the exosome: PM/Scl-100 and MPP6. MPP6 has previously been shown to be involved in the exosome-mediated maturation of the 5.8S rRNA (Schilders *et al*, 2005). The sequence coverage of the identified exosome proteins ranged from 7 to 44%. In accordance with previous results, no peptides indicating the presence of the human Dis3 protein (hDis3) in the exosome preparation were detected. However, we identified with very high confidence (26% coverage and 29 unique peptides) a protein homologous to Dis3 that was designated Dis3-like exonuclease 1 (hDis3L1).

In the genome of humans and other higher eukaryotes (including mice, zebrafish and frogs) in total three genes homologous to the yeast Dis3 protein are present: Dis3, Dis3-like exonuclease 1 (Dis3L) and Dis3-like exonuclease 2 (Dis3L2), of which only Dis3L1 was found in the immuno-affinity purified exosome fraction. Based upon cDNA sequence data 4 isoforms of hDis3L1 can be discerned, which are most likely resulting from alternative splicing events. The largest isoform (GenBank acc. nr. NM_001143688) consists of 1,054 amino acids with a calculated molecular mass of 120,787 Da. For the human Dis3L2 (hDis3L2) five potential

Table 1. Exosome-associated proteins identified by LC-MS/MS in immunoaffinity-purified human exosome complexes.

Gene	Accession no.	Protein name(s)	MW (kDa)	Unique peptides	Sequence coverage (%)
EXOSC1	Q9Y3B2	CSL4	21 kD	4	25
EXOSC2	Q13868	RRP4	33 kD	3	11
EXOSC3	Q9NQT5	RRP40	30 kD	15	38
EXOSC4	Q9NPD3	RRP41	26 kD	6	29
EXOSC5	Q9NQT4	RRP46	25 kD	4	14
EXOSC6	Q5RKV6	MTR3	28 kD	8	24
EXOSC7	Q15024	RRP42	32 kD	11	36
EXOSC8	Q96B26	RRP43 / OIP2	30 kD	11	33
EXOSC9	Q06265	RRP45 / PM/Scl-75	49 kD	5	12
EXOSC10	Q01780	RRP6 / PM/Scl-100	101 kD	5	7
MPHOSPH6	Q99547	MPP6	19 kD	6	44
DIS3L	Q8TF46	hDis3L1	121 kD	29	26

isoforms have been identified, the largest of which (GenBank acc. nr. NM_152383) contains 885 amino acids with a calculated molecular mass of 99,210 Da. An alignment of the 'canonical' isoforms of the three human Dis3 variants and their yeast equivalent (yDis3) is shown in Supplementary Figure S1. In terms of sequence conservation, hDis3 is more closely related to yDis3 (42% sequence similarity) than the two Dis3-like proteins (29% and 26% for hDis3L1 and hDis3L2, respectively). To obtain insight into the domain structure of these proteins their amino acid sequences were analyzed by the online tool SMART (Letunic *et al*, 2009). This revealed the presence of several domains, some of which were, however, poorly conserved. Like many members of the RNase II/R-family of hydrolytic nucleases, the three hDis3 variants contain a highly conserved RNB domain (which is known to contain the exonuclease activity) and three OB-fold-type nucleic acid binding domains: two CSDs (cold shock domains) and one S1 RNA binding domain. The conservation of the latter domains is generally more evident at the secondary structure level than at the level of the amino acid sequence (Theobald *et al*, 2003). All β-strands and α-helixes detected in hDis3L1 with the PsiPred protein structure prediction tool are depicted below the alignment (Supplementary Figure S1). Typical for OB-fold-like domains are the five β-strands forming a β-barrel. Finally, a PIN (PilT N terminus) domain is present in the N-terminal regions of hDis3 and yDis3. PIN domains were originally thought to be involved in signaling events (Noguchi *et al*, 1996), but were recently shown to confer endonucleolytic activity. This was shown for several proteins involved in NMD and RNAi pathways, such as the SMG protein (Clissold and Ponting, 2000; Glavan *et al*, 2006) and yDis3 (Lebreton *et al*, 2008). PIN domains are characterized by two or three nearly invariant aspartic acid residues. Both hDis3 and yDis3 contain all three aspartic acids, whereas in hDis3L1 only two and in hDis3L2 only one of these residues are conserved (Supplementary Figure S1). The domain structure of yDis3, hDis3, hDis3L1 and hDis3L2 is schematically illustrated in Figure 1.

To confirm the interaction of hDis3L1 with the exosome, the full-length coding sequence of the largest isoform of hDis3L1 was cloned from a teratocarcinoma cDNA library and was inserted in different mammalian expression vectors. HEp-2 cells were transiently transfected with a construct expressing hDis3L1 fused to either an N- or C-terminal GFP tag. After forty-eight hours, the fusion proteins were immunoprecipitated from cell lysates using anti-GFP antibodies and analyzed by SDS/PAGE and immunoblotting. The results showed that both the N- and C-terminally GFP-tagged hDis3L1 proteins were expressed, although the expression of the C-terminally tagged protein was less efficient. The association with the exosome core was monitored by anti-Rrp4 antibodies and showed the co-precipitation of Rrp4 with both hDis3L1 fusion proteins, but not with GFP alone (Figure 2), confirming the interaction between hDis3L1 and the core of the exosome complex. To rule out the possibility that this interaction is mediated by RNA, similar experiments were performed in which either the cell lysates or the immunoprecipitates were treated with nucleases (RNase A and micrococcal nuclease). The co-precipitation of hRrp4 was not affected by these treatments

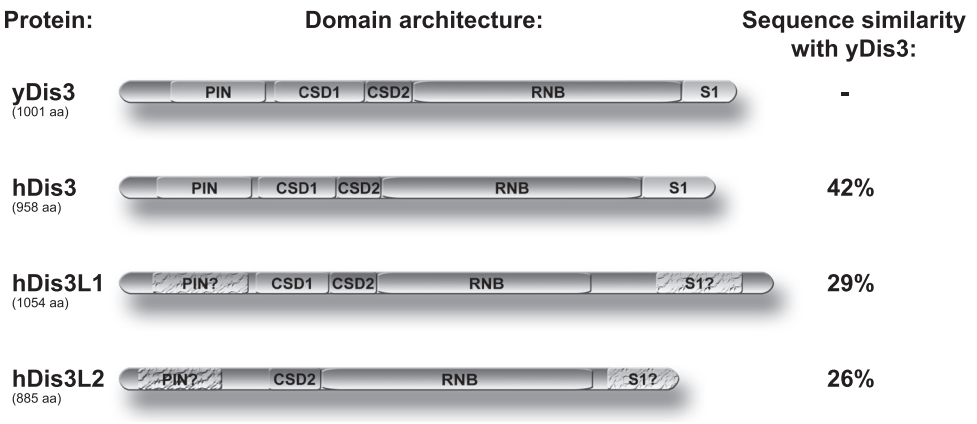

Figure 1. Schematic structure of Dis3 and Dis3-like proteins in yeast and humans.

Schematic diagram of *Saccharomyces cerevisiae* Dis3 (yDis3), human Dis3 (hDis3), human Dis3-like 1 (hDis3L1) and human Dis3-like 2 (hDis3L2) with the identified domains indicated: the PIN domain, two cold shock domains (CSD1, CSD2), a RNB domain and a S1 RNA binding domain. Crackled boxes and question marks indicate domains with a low level of conservation (see Supplementary Figure S1 for details). The level of sequence similarity between the human Dis3 proteins and yDis3 is indicated on the right.

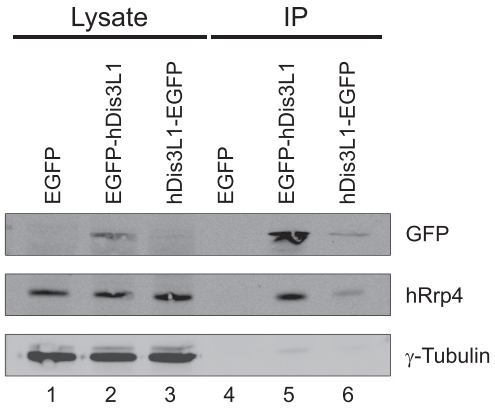

Figure 2. Association of hDis3L1 with the exosome core complex.

Total cell extracts were prepared from HEp-2 cells transiently transfected with expression constructs encoding EGFP, EGFP-hDis3L1 or hDis3L1-EGFP, after which immunoprecipitation was performed using polyclonal anti-GFP antibodies. Both the complete cell extracts (Lysate) and the anti-GFP (co-)precipitated proteins (IP) were separated by SDS-PAGE and analyzed by western blotting, using monoclonal anti-GFP antibodies and monoclonal anti-hRrp4 antibodies to visualize the co-precipitation of the exosome core complex with hDis3L1. Monoclonal anti-γ-tubulin antibodies were used as loading control.

(data not shown), indicating that the association of hDis3L1 with the exosome core is not bridged by RNA.

hDis3L1 is localized to the cytoplasm

To analyze the subcellular localization of hDis3L1, human HEp-2 cells were transiently transfected with constructs encoding either GFP-hDis3L1, hDis3L1-GFP or VSV-hDis3L1, the latter resulting in the formation of a N-terminally VSV-tagged (vesicular stomatitis virus G epitope) protein. The localization of tagged hDis3L1 was determined by fluorescence microscopy either directly (EGFP-tagged, Figures 3A, B) or indirectly (VSV-tagged, Figure 3C) using anti-VSV-tag antibodies. All three tagged hDis3L1 proteins localized exclusively to the cytoplasm (Figures 3A-3C). To compare its localization with that of hDis3, we also transfected cells with N-terminally GFP-tagged hDis3, the localization of which was confined to the nucleoplasm (Figure 3D), in agreement with our previous observations (Schilders *et al.*, manuscript in preparation). Because the localization of overexpressed, tagged proteins may not completely reflect the localization of the corresponding endogenous proteins, the subcellular localization of hDis3L1 was also determined by confocal immunofluorescence microscopy using antibodies to hDis3L1 (Figure 3E-G). Antibodies to exosome core component hRrp40 were used in parallel (Figure 3H-J). Although some staining of hDis3L1 within the nucleus was observed, the results of these experiments confirm the cytoplasmic accumulation of hDis3L1. In agreement with previous observations, the highest concentration of hRrp40 was observed in the nucleoli.

hDis3L1 displays exoribonuclease activity

The lack of exoribonuclease activity associated with the core of the human exosome raised the question whether the exosome-associated hDis3L1 protein might be responsible for at least part of the activity of the human exosome. This would be consistent with the presence of the RNase II-type RNB domain in this protein. To test this hypothesis, RNA degradation assays were performed with GFP-hDis3L1 immunoaffinity-purified from transiently transfected HEp-2 cells. Following immunoprecipitation with anti-GFP antibodies, the precipitate was incubated for 2 hours with a radiolabeled RNA substrate in the presence of various concentrations of Mg^{2+}, which is known to be involved in the nucleophilic attack by these types of hydrolytic enzymes (Frazao *et al*, 2006). Denaturating gel analysis of the reaction products (Figure 4A) showed that the substrate RNA indeed was converted to mononucleotides, more specifically nucleotide monophosphates, by EGFP-hDis3L1-containing precipitates, whereas no activity was found in EGFP precipitates. The activity appeared to be dependent on the Mg^{2+} concentration with an optimum at about 0.05 mM, which is very similar to the optimal Mg^{2+} concentration described for yeast Dis3 (Dziembowski *et al*, 2007). To further demonstrate that the mononucleotide products were resulting from the presumed 3'-5'

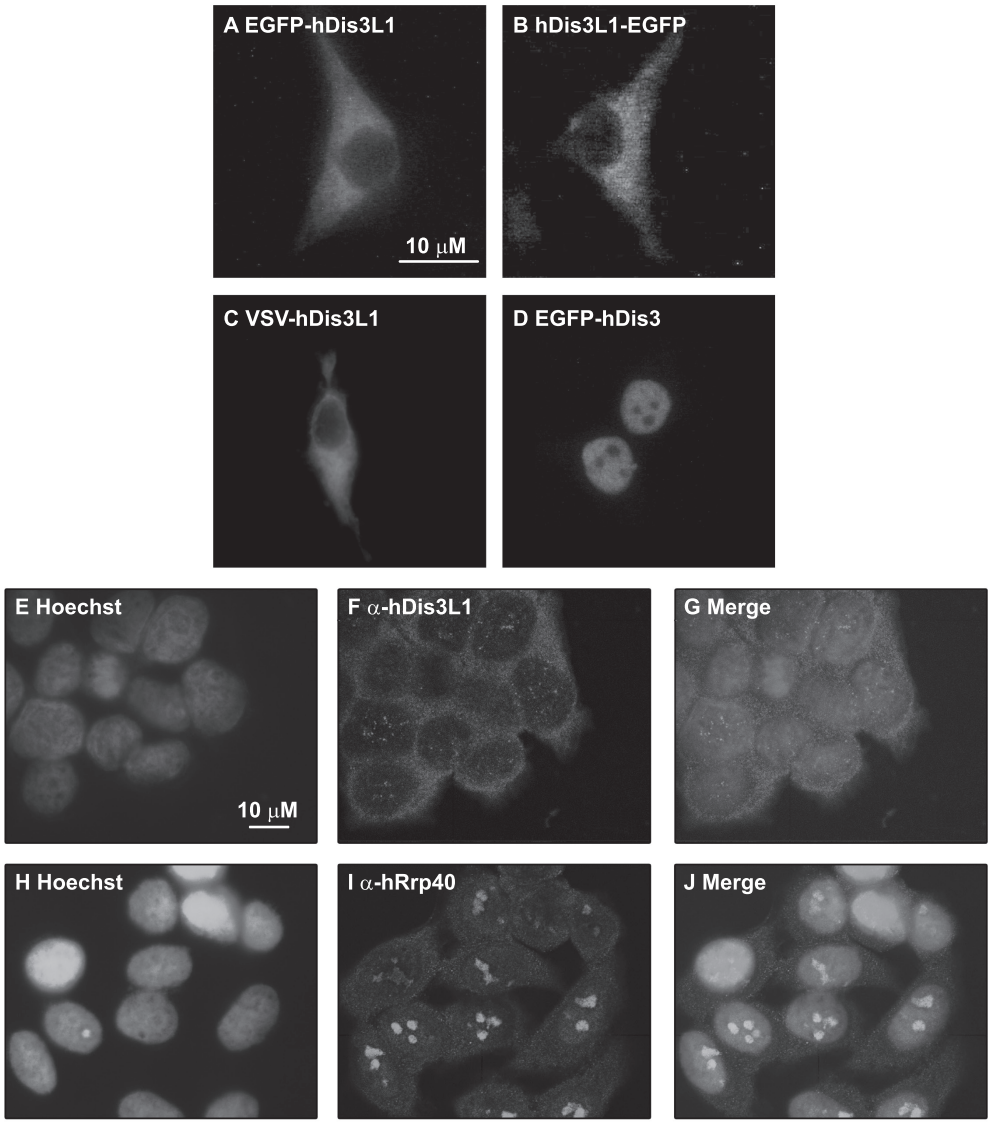

Figure 3. Localization of hDis3L1 and hDis3 in HEp-2 cells.

HEp-2 cells were transiently transfected with expression constructs encoding EGFP-hDis3L1 (A), hDis3L1-EGFP (B), VSV-hDis3L1 (C) or EGFP-hDis3 (D). Forty-eight hours after transfection the cells were fixed and EGFP-fusion proteins were visualized directly by fluorescence microscopy. The VSV-tagged hDis3L1 protein was visualized by incubating the cells with monoclonal anti-VSV-tag antibodies, followed by Alexa Fluor 555-conjugated goat anti-mouse antibodies and fluorescence microscopy. (E-J) Fixed HEp-2 cells were incubated with polyclonal antibodies to hDis3L1 (F-G) or to hDis3 (I-J) and bound antibodies were visualized by Alexa Fluor 488-conjugated secondary antibodies and confocal immunofluorescence microscopy. Nuclei were visualized by Hoechst staining (E and H). (G) and (J) show the merged images of Hoechst and antibody staining. Bar: 10 μm.

exoribonuclease activity of EGFP-hDis3L1 the radiolabeled substrate was pre-incubated with DNA oligonucleotides complementary to either the 5' or the 3' terminal part of the substrate. Since blocking of the 3' end, in contrast to that of the 5' end, impaired the degradation of the substrate RNA (data not shown), the results of these experiments are consistent with 3'-5' exoribonuclease activity.

Since the Dis3 protein in yeast contains endonucleolytic activity as well, mediated by the PIN domain, a similar activity assay was performed to investigate whether also hDis3L1 acts as an endoribonuclease. These experiments were performed in the presence of Mn^{2+}, rather than Mg^{2+}, because this was previously shown to be required for the endonucleolytic activity of PIN domain-containing proteins. The results showed that under these conditions no endonucleolytic activity could be detected in these EGFP-hDis3L1 precipitates (Supplementary Figure S2).

To investigate whether the exoribonuclease activity associated with hDis3L1 is also associated with the exosome core, similar activity assays were performed, but now with material immunoaffinity-purified with antibodies to exosome core component hRrp40. In addition, the lysates used for these experiments were prepared from cells treated with a hDis3L1-specific siRNA or with a control siRNA. If hDis3L1 is responsible for the exosome-associated exoribonuclease activity, knocking-down the expression level of hDis3L1 was expected to reduce this activity. In agreement with previous observations, exosome complexes isolated with the anti-hRrp40 antibodies displayed exoribonuclease activity (Figure 4B). The siRNA-mediated depletion of hDis3L1 (the efficiency of which is shown in Supplementary Figure S3) led to a reduced exoribonuclease activity of anti-hRrp40 precipitates, strongly suggesting that hDis3L1 indeed contributes to the activity of the human exosome.

The RNB domain of hDis3L1 is mediating its exoribonuclease activity

The identification of a RNB domain in hDis3L1 (described above) suggested that this domain might be necessary for its exoribonuclease activity. To investigate this in more detail, one the most highly conserved residues in this domain, the aspartate at position 486 was replaced by an asparagine (D486N). Substitution of the corresponding residue in other RNB domains has been demonstrated to inhibit their exonuclease activity without interfering with RNA binding, as was initially found for RNase II (Amblar and Arraiano, 2005). This residue also corresponds to the D551 in the yeast Dis3 protein. Substitution of D551 of yeast Dis3 abolished its exoribonuclease activity, whereas the endonuclease activity remained unaffected (Dziembowski *et al*, 2007). Likewise, two additional hDis3L1 mutants were generated in which the two conserved aspartates in the putative PIN-domain were substituted for asparagines (D62N and D166N). The expression of EGFP-fused hDis3L1 mutants in transfected HEp-2 cells was monitored by western blotting, revealing similar expression levels for all hDis3L1 constructs (Figure 4C). A ribonuclease assay with the immunoaffinity-purified hDis3L1 mutants (Figure 4D) showed that the D486N mutant was completely inactive, in contrast to the wild type protein and the PIN domain mutants, which showed similar levels of

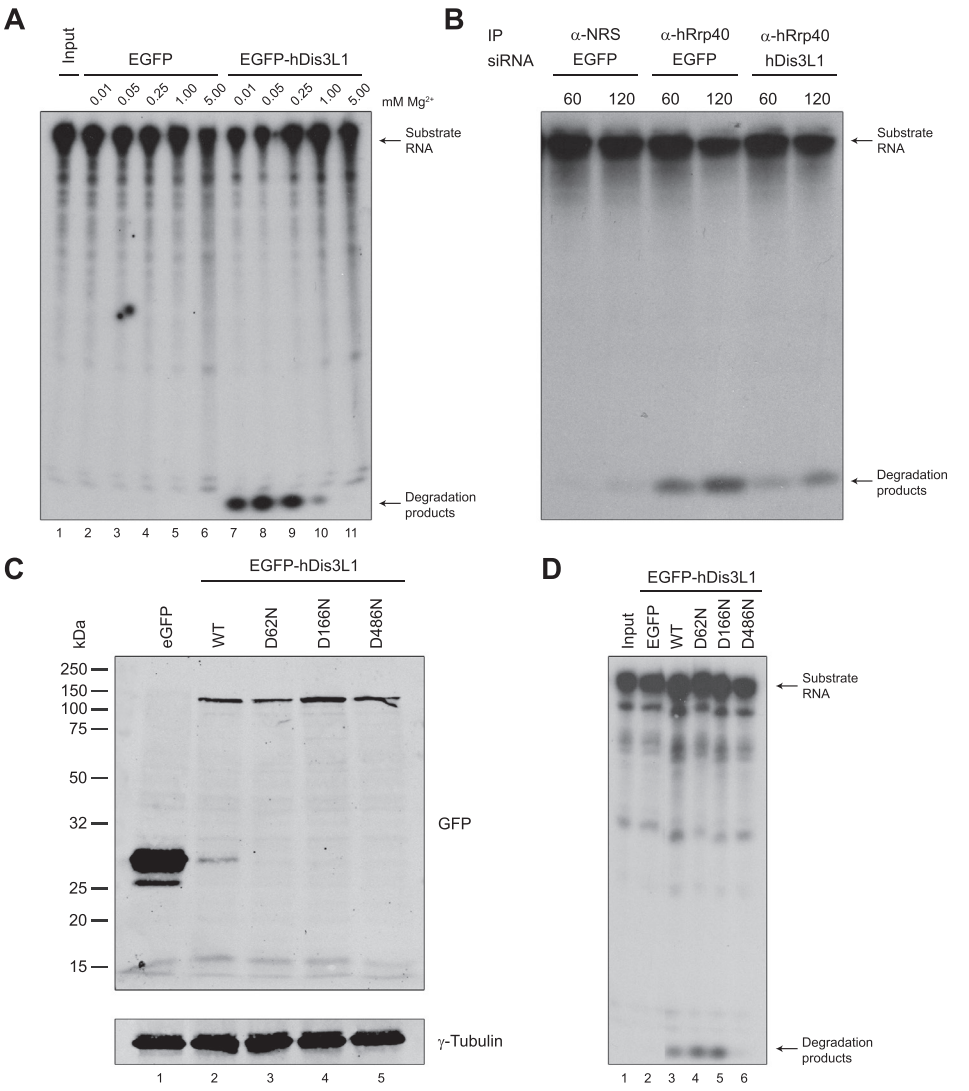

Figure 4. In vitro RNA degradation by hDis3L1.

(A) HEp-2 cells were transfected with expression constructs encoding EGFP-hDis3L1 or EGFP and after 48 hrs cell lysates were subjected to immunoprecipitation with anti-GFP antibodies. Precipitated proteins/complexes were incubated with a radiolabeled RNA substrate (Input) and the reaction products were subsequently analyzed by denaturing polyacrylamide gel electrophoresis followed by autoradiography. The incubations were performed in the presence of increasing concentrations of Mg^{2+}. (B) A similar assay was performed with endogenous exosome complexes after precipitation with anti-hRrp40 antibodies or antibodies from normal rabbit serum (NRS) antibodies and lysates from cells which transfected with siRNAs downregulating either EGFP (used as a control) or hDis3L1. (C) Expression efficiency of EGFP-tagged hDis3L1 proteins monitored by western blotting using anti-GFP antibodies. WT: wild-type hDis3L1. D62N, D166N, D486N: hDis3L1 amino acid substitution mutants. Anti-γ-tubulin antibodies were used as a loading control. (D) Activity assay as described above (A) with immunoprecipitated hDis3L1 mutants D62N, D166N, D486N in the presence of 0.05 mM Mg^{2+}. Precipitates from cell lysates containing EGFP and wild type (WT) hDis3L1 were used as negative and positive control, respectively.

exonucleolytic degradation of the substrate RNA. These results indeed indicate that the RNB domain is involved in exonucleolytic RNA degradation by hDis3L1.
The abrogation of the exonucleolytic activity by the RNB domain mutation confirms that the activity observed in the *in vitro* ribonuclease assay is due to the presence of hDis3L1 and is not caused by a contaminating ribonuclease, which may non-specifically co-purify with hDis3L1.

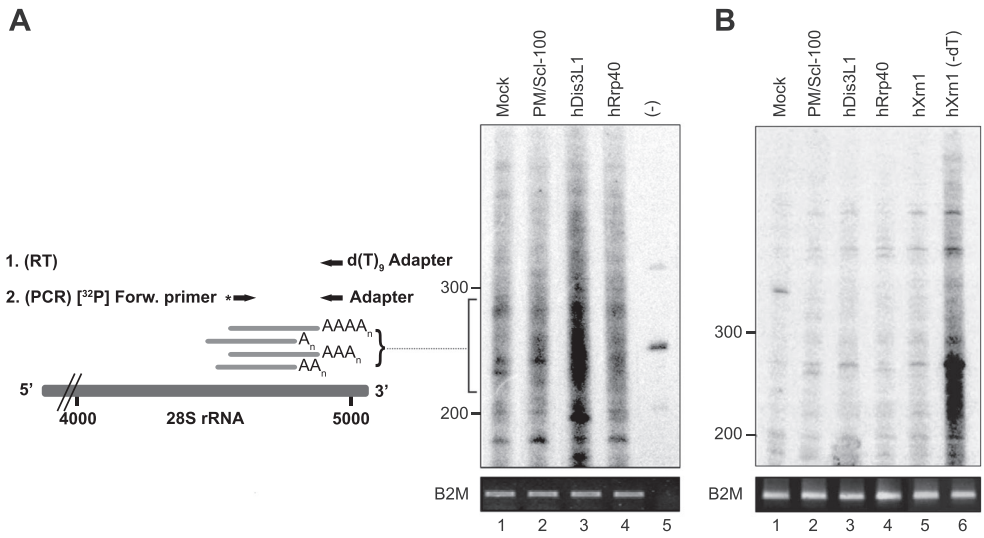

Figure 5. Cytoplasmic accumulation of adenylated degradation intermediates upon hDis3L1 knock-down.

(A) Cytoplasmic RNA from cells in which the indicated proteins were silenced by RNAi was subjected to oligo(dT) RT-PCR labeling, followed by fractionation by denaturing polyacrylamide gel electrophoresis and autoradiography. A schematic representation of the labeling procedure is shown on the left. First, cDNA was generated using a $d(T)_9$-adapter primer. Products from these reactions were amplified by PCR using a [^{32}P]-labeled forward (F) primer corresponding to a sequence element of the 28S rRNA and a reverse primer corresponding to the adapter sequence. Material from a control reaction, in which the reverse transcriptase was omitted (-), is shown in lane 5. The positions of dsDNA markers are indicated on the left of the gel. For normalization, RT-PCR products obtained with PCR primers specific for the B2M gene are shown in the lower panel. (B) A similar oligo(dT) RT-PCR labeling experiment as in panel A, but now the isolated RNA was incubated with oligo(dT) and RNase H prior to the RT reactions. RNA isolated from cells in which hXrn1 was knocked-down, which like silencing of hDis3L1 leads to accumulation of poly(A) containing degradation intermediates, was used as a control to show that treatment with RNase H in the absence of oligo(dT) (lane 6) did not lead to the disappearance of the intermediates.

hDis3L1 is involved in rRNA degradation

The cytoplasmic localization of hDis3L1 suggested that it might be involved in the exoribonucleolytic degradation of RNAs in the cytoplasm. To investigate this possibility, the effect of hDis3L1 depletion on ribosomal RNA was studied. Degradation of rRNA in human cells involves the formation of truncated, transiently poly(A)-tailed molecules (Slomovic *et al*, 2006). An oligo(dT)-primed RT-PCR labeling procedure allows the detection of these truncated, poly(A)-tailed molecules derived from cytoplasmic 28S rRNA (Slomovic *et al*, 2010). hRrp40, PM/Scl-100 and hDis3L1 were knocked-down and the effect of reduced levels of these proteins on the 28S rRNA degradation intermediates was determined by the RT-PCR procedure, which is schematically illustrated in Figure 5A. Controls for the cell fractionation are shown in Supplementary Figure S4, panel A). Western blotting or RT-PCR quantification, in case appropriate antibodies were lacking, showed a strong reduction of the silenced proteins (Supplementary Figure S4, panel B). The RT-PCR products were analyzed by denaturing gel electrophoresis, which showed that knocking down hDis3L1 resulted in the accumulation of truncated 28S rRNA fragments, whereas no or only a very weak accumulation of these molecules was observed when hRrp40 or PM/Scl-100 were knocked down (Figure 5A). To verify whether the accumulated products were not artifacts of nonspecific reverse transcription, the purified RNA purified was incubated with RNase H and oligo(dT) before the oligo(dT)-primed RT reaction. In this way, no cDNA can be produced as this treatment removes the poly(A) tails that are needed for the subsequent oligo(dT)-primed cDNA synthesis. The results of this experiment showed that this treatment indeed reduced the observed amplified signals to background levels (Figure 5B).
These results strongly suggest that hDis3L1 plays a role in the degradation of rRNA and possibly other RNAs in the cytoplasm of human cells.

Discussion

The evidence that the core of the eukaryotic exosome complex lacks exoribonuclease activity raised the question which proteins are responsible for this activity of the exosome. Paradoxically, the canonical human homologue of one of the main exosome-associated exoribonucleases in the yeast *Saccharomyces cerevisiae*, Dis3, does not detectably associate with the core of the exosome. In this study, a proteomic approach led to the identification of a novel human Dis3-like exonuclease (hDis3L1), which is stably associated with human exosome complexes. The sequence of the Dis3L1 protein was first added to the databases in 2002, which may explain why it was not found in previous proteomic analyses of purified exosome complexes (Chen *et al*, 2001). The failure to detect the association of hDis3 with the exosome complexes in the study of Chen and collaborators and also in other studies (Allmang *et al*, 1999a; Raijmakers *et al*, 2002) suggested that hDis3 is either weakly associated with the exosome core or not al all. The identification of hDis3L1 as an exosome-associated

exoribonuclease indeed suggests that hDis3L1 shares more functional features with the yeast Dis3 protein than hDis3.

The ribonuclease assays presented in this study show that hDis3L1 is a Mg^{2+}-dependent exoribonuclease and that this activity is dependent on its RNB domain. On the other hand, no endoribonuclease activity was observed under conditions identical or similar to those previously applied to study the endoribonuclease activity of the yeast Dis3 protein (Lebreton *et al*, 2008; Schaeffer *et al*, 2009). The failure to detect this activity is consistent with the relatively poor conservation of the PIN domain in hDis3L1, in which one of the three highly conserved aspartic acids is not present. These aspartic acids have been demonstrated to be crucial for the endonucleolytic potential of PIN domains, as substitution of only one of these residues can severely reduce this activity (Glavan *et al*, 2006; Lebreton *et al*, 2008).

Since hDis3L1 appears to accumulate in the cytoplasm, its subcellular localization only partially overlaps with that of the core exosome components, which are found in both the cytoplasm and the nucleus. Although the cytoplasmic accumulation of hDis3L1 was observed both with ectopically expressed GFP- and VSV-tagged proteins and with a polyclonal antibody to hDis3L1, our results to not exclude the possibility that a specific isoform of hDis3L1 displays another subcellular distribution. The sequence databases provide evidence for the existence of 4 isoforms, which most likely result from alternative splicing events. Future experiments will have to clarify potential differences between their localization and function.

The results of our localization studies not only suggest that hDis3L1 is specifically associated with cytoplasmic exosome complexes, but also implicate that the RNA substrates for hDis3L1 are restricted to the cytoplasm. Paradoxically, the yeast exosome-associated Dis3 protein is found both in the cytoplasm and in the nucleus (Synowsky *et al*, 2009). In view of the observations that the exosome core itself is catalytically inactive, it is tempting to speculate on the differentiation between ribonucleases associated with the nuclear and cytoplasmic core complexes. PM/Scl-100, which seems to be more concentrated in the nuclear compartment, might be more important for the nuclear functions of the exosome, whereas hDis3L1 might be more important for its cytoplasmic activities (such as the turnover of rRNAs and mRNAs). Interestingly, hDis3 appears to be mainly nucleoplasmic, suggesting that the function of the Dis3 protein in yeast is performed by separate homologous proteins, hDis3 and hDis3L1, in the nucleus and cytoplasm, respectively. In the nucleus, hDis3 seems to act independently of the core of the exosome, although an instable association that is not resistant to cell lysis and fractionation can not be excluded (see also Supplementary Figure S5). The relationship with the third human member of the Dis3 protein family, hDis3L2, is currently enigmatic. The proteomic data suggest that also this protein is not stably associated with the core of the exosome, but more studies will be required to elucidate its function.

Besides differences in subcellular localization, the capacity of different exoribonucleases to degrade RNA substrates completely or to process RNA substrates to the mature 3' end may differ from one enzyme to another. Indeed, it has been suggested previously that one enzyme may take over from another to remove the last few nucleotides from a RNA substrate and the

dependence on the activity of the TRAMP complex appears to be different for the yeast Dis3 and Rrp6 proteins (LaCava *et al*, 2005).

The stable association of hDis3L1 with the human exosome suggests that it acts in concert with the core of the exosome in the degradation of cytoplasmic RNAs. Depletion of hDis3L1 led to a strong reduction of the exoribonuclease activity of immunoaffinity-purified exosome complexes, indicating that hDis3L1 is indeed mediating part of the RNA-degrading activity of the exosome. This does, however, not exclude the possibility that a subset of hDis3L1 is not exosome-associated and degrades RNAs independently of the exosome. Interestingly, the binding of yeast Dis3 to the exosome core is mediated mainly by the PIN domain (Schneider *et al*, 2009) and in view of the structural similarity it is likely that the interaction of hDis3L1 and the human exosome core is mediated by the same element. The exosome core may function to bind RNA substrates in its central channel and to lead these RNAs to the exoribonuclease site of hDis3L1 (Bonneau *et al*, 2009).

One of the RNA substrates that are degraded by the exosome-associated hDis3L1 appeared to be 28S rRNA. The degradation of this RNA proceeds through polyadenylated intermediates, which accumulated upon hDis3L1 knock-down. Although these molecules were detected in the cytoplasmic fraction, our data do not rule out the possibility that they are generated in the nucleus and enter the cytoplasm in the hDis3L1 knock-down cells. The depletion of one of the exosome core components had a less pronounced effect on the accumulation of these molecules, which may indicate that the association of hDis3L1 with the exosome core is either not necessary for this activity or that the knock-down of PM/Scl-100 and hRrp40 was not efficient enough to produce a similar level of accumulation. Further studies will be required to investigate the requirement of the exosome core in hDis3L1-mediated RNA degradation in more detail, to shed more light on the ratio between exosome-associated and free hDis3L1, and to identify additional cellular RNA substrates for hDis3L1.

Recently, we were informed about an independent study by other investigators, who also identified hDis3L1 (termed hDis3L in their study) as an exoribonuclease associated with the cytoplasmic exosome (Tomecki *et al*, 2010). The results of this study confirm our conclusions on the subcellular localization, exosome-association and enzymatic activities of hDis3L1.

It is clear that more studies have to be performed to elucidate the possible differences between the nucleases associated with the nuclear and cytoplasmic exosome. The data presented in this study demonstrate that hDis3L1, rather than hDis3, is an exoribonuclease which is stably associated with exosome core complexes and this protein is mainly localized in the cytoplasm of human cells.

Materials and methods

Purification of exosome complexes

Polyclonal anti-hRrp40 (H70) antibodies, affinity-purified from rabbit serum H70 (Brouwer *et al*, 2001a) were coupled to protein A-agarose beads (Kem-En-Tec, Denmark) by incubation for 2 hours at room temperature in PBS. After washing the beads three times with 0.2 M sodium borate, pH 9.0, the beads were incubated twice with 20 mM DMP (dimethyl pimelinidate dihydrochloride [Sigma]) in 0.2 M sodium borate, pH 9.0, by end-over-end rotation for 30 minutes. DMP was inactivated by washing the beads four times with 0.2 M ethanolamine, pH 8.0, after which the beads were washed three more times with PBS.

Five billion HeLa cells were resuspended in 6 volumes of lysis buffer (25 mM Tris-HCl, pH 7.5, 100 mM KCl, 1 mM dithiotreitol (DTT), 2 mM EDTA, 0.5 mM PMSF, 2 mM Na_3VO_4, 2 mM NaF, 10 mM $NaHPO_4$, 0.05% NP-40, containing a protease inhibitor cocktail [Complete, Roche]), and incubated for 30 minutes on ice. After sonication (3 times 30 seconds at 0 ºC), cell lysates were centrifuged at 100,000g for 1 hour at 4 ºC and the supernatants were used immediately or stored at -70 ºC.

The anti-hRrp40 beads were washed twice with wash buffer (PBS, 0.35 M NaCl, 0.05% NP-40), followed by washing with elution buffer A (0.1 M glycine-HCl, pH 2.5, 0.05% NP-40, 0.5 M NaCl) and two additional wash steps with wash buffer. Subsequently, HeLa S100 extract (1×10^9 cell equivalents) was added and incubated overnight at 4 ºC by end-over-end rotation. The beads were then washed twice with wash buffer, once with wash buffer containing 1 M NaCl, and again three times with wash buffer. Bound proteins were eluted by applying elution buffer A. Eluted fractions were neutralized immediately by adding 1M Tris base and the proteins were concentrated by acetone precipitation. Precipitated proteins were dissolved in SDS sample buffer, separated by 12% SDS-PAGE and stained with colloidal Coomassie Brilliant Blue.

LC-MS/MS

The gel containing the immunoaffinity-purified proteins was cut into 19 slices, proteins were reduced with 1,4-dithiothreitol (6.5 mM) and alkylated with iodoacetamide reagent (54 mM). After thorough washing, the gel slices were rehydrated in trypsin solution (10 ng/μl) on ice. After addition of 30 μl of NH_4HCO_3 (50 mM, pH 8.5), samples were digested for 16 h at 37 °C. The supernatant of the digest was collected and the gel slices were washed for 15 min in 5% formic acid at room temperature, after which the supernatant was combined with the earlier fraction and stored at –20º C. All LC-MS/MS analyses were performed on an LTQ-Orbitrap mass spectrometer (Thermo, San Jose, CA) connected to an Agilent 1200 series nano LC system. Peptides were fractionated on C18 with a multi-step gradient of 0.6% HAc (solution A) and 0.6% HAc/80% acetonitrile (ACN) (solution B). The mass spectrometer was operated in the data-dependent mode to automatically switch between MS and MS/MS. Raw MS data were converted to peak lists using Bioworks Browser software, version 3.1.1. The spectra

were searched with Mascot against all human proteins in the Swissprot (v56.2) database with a precursor mass tolerance of 15 ppm and a product mass tolerance of 0.9 Da with trypsin as an enzyme, allowing 2 miscleavages. Peptide identifications were accepted with a Mascot score greater than 25 and a p value smaller than 0.005, corresponding to 1% false discovery rate as determined by decoy database searching.

cDNA cloning and generation of the hDis3L1 expression constructs

The complete coding sequence of the largest isoform of hDis3L1 (GenBank accession number: NM_001143688) was isolated from a teratocarcinoma cDNA library by PCR using the following oligonucleotides: 5' - GGATCCCTCGAGATGCTGCAGAAGCGGGAGAA - 3' and 5' - GTCGACTCACCCGGGTATTCCATAATTGTTTGAAAC - 3'. The resulting amplicon of 3229 basepairs was subsequently cloned into the pCR4-TOPO vector according to the manufacturer's guidelines (Invitrogen). The sequence of the selected clone was confirmed by DNA sequencing. N-terminal EGFP- and VSV-tagged hDis3L1 expression constructs and a C-terminal EGFP-tagged expression construct were made by subcloning the coding sequence into the pEGFP-C3 (Clontech), pCI-neo-5'-VSV (Promega) and pEGFP-N2 vectors (Clontech), respectively, using the restriction enzyme combinations: Xho I/Sal I, Xho I/Sal I and Xho I/Sma I, respectively.

Transient transfection of HEp-2 cells and fluorescence microscopy

To express tagged hDis3L1 in a human cell line, 4 x 10^6 HEp-2 cells were transfected with 20 μg of plasmid DNA in 1 ml DMEM supplemented with 10% FCS by electroporation at 260V and 950μF using a Gene-Pulsar II (Bio-Rad). To increase expression levels, 5 mM sodium butyrate was added to the medium 24 hours after transfection. Forty-eight hours after transfection the cells were harvested by trypsinization, resuspended in lysis-buffer (25 mM Tris-HCl, pH 7.5, 100 mM KCl, 1 mM EDTA, 0.5 mM PMSF, 0.05% NP-40, 1 mM DTT) and sonicated 3 times 30 seconds on ice. To study the subcellular localization of hDis3L1 and hDis3, HEp-2 cells were transfected in a similar fashion, seeded on glass coverslips and fixed after forty-eight hours with 3.7% paraformaldehyde. EGFP fusion proteins were visualized directly, while the VSV-tagged proteins were detected indirectly by incubation with a monoclonal anti-VSV antibody after permeabilization of the cells, followed by Alexa Fluor 555-conjugated goat anti-mouse antibodies (Invitrogen). Incubations with antibodies were performed in PBS supplemented with 1% sheep serum. The localization of EGFP- and VSV-tagged proteins was monitored by fluorescence microscopy. For the localization of the endogenous proteins hDis3L1 and hRrp40, HEp-2 cells were seeded on glass coverslips and fixed with methanol. Antibody incubations (anti-hRrp40; anti-hDis3L1, H00115752-B01P (Abnova)) were performed as described above with the exception that Alexa Fluor 488-conjugated goat anti-rabbit or anti-mouse secondary antibodies (Invitrogen) were used for the detection of hRrp40. The nuclei of the cells were stained by incubation with the Hoechst 33342 (Invitrogen), diluted in PBS,

for 3 minutes. Images were made on a confocal laser scanning microscope (TCS SP2 AOBS System, Leica-microsystems).

siRNA treatment

siRNAs were purchased from Eurogentec. The sequences of the siRNAs for EGFP and hDis3L1 are 5' - CCAUGUAACCGUAAGAAUAdTdT - 3' and 5' - CGAGAAGCGCGAUCACAUGdTdT - 3', respectively. Transfection of HEp-2 cells with these siRNAs was performed essentially as described previously (Schilders *et al*, 2005).

Immunoprecipitation

Polyclonal rabbit anti-GFP antibodies or polyclonal rabbit anti-hRrp40 antibodies were coupled to protein A-agarose beads (Kem-En-Tec, Denmark) in IPP500 (500 mM NaCl, 10 mM Tris-HCl, pH 8.0, 0.05% NP-40) at room temperature for 1 h. Beads were washed once with IPP500 and twice with IPP150 (150 mM NaCl, 10 mM Tris-HCl, pH 8.0, 0.05% NP-40). HEp-2 cell extract was incubated with the antibody-coupled beads for 2 h at 4°C. After washing the beads twice with IPP150 (or IPP1000 for the anti-hRrp40-coupled beads), bound proteins were either eluted with sample buffer for SDS-PAGE analysis, or were washed two more times with RNA degradation assay buffer (described below).

Immunoblotting

For the detection of proteins on western blots, polyclonal rabbit antibodies (anti-GFP, anti-γ-tubulin, GTU-88 [Abcam]), polyclonal mouse antibodies (anti-hDis3L1) or monoclonal mouse antibodies (anti-hRrp4, 15B3 [ModiQuest], anti-GFP, JL-8 [BD Biosciences]) were diluted in blocking buffer (5% skimmed milk, PBS, 0.05% NP-40). Blots were incubated with these antibodies for 1 hour at room temperature. Bound antibodies were detected by incubation with IRDye 800CW-conjungated polyclonal goat anti-mouse or goat anti-rabbit antibodies (Li-Cor) for 1 hour in blocking buffer and visualization using an Odyssey® Infrared Imaging System (Li-Cor).

***In vitro* RNA degradation assays**

RNA degradation assays were performed using a radiolabeled 267 nucleotide RNA substrate, which was obtained by *in vitro* transcription in the presence of ^{32}P α-UTP. This substrate RNA contained the human 5.8S rRNA sequence and the most 5' 100 nucleotides of ITS2 (Schilders *et al*, 2005). After gel-purification of the RNA substrate, it was incubated for 2 hours with the immunoprecipitated material at 37˚C in RNA degradation buffer (20 mM HEPES, pH 7.5, 50 mM KCl, 1 mM DTT, 1 mM Na_2HPO_4) containing different concentrations of Mg^{2+} or Mn^{2+}. Reactions were stopped by the addition of RNA-loading buffer (9 M urea, 0.1% bromophenol

blue, 0.1% xylene cyanol), supplemented with 20% v/v phenol. Samples were analyzed by denaturing polyacrylamide gel electrophoresis followed by autoradiography.

In vivo 28S rRNA degradation analysis

HeLa cells were grown as a monolayer at 37°C, 5% CO2 in DMEM (Sigma) supplemented with 10% fetal calf serum, 2 mM L-glutamine, and penicillin–streptomycin (Slomovic *et al*, 2008). Cells were transfected with 400 pmole siRNA duplex (PM/Scl-100: 5' – GUUUCGAGAGAAGAUUGAUdTdT – 3', hRrp40: 5' – CACGCACAGUACUAGGUCAdTdT – 3') using lipofectamine 2000 (Invitrogen). After 24 h, cells were detached with trypsin and replated, followed 24 hours later by a second transfection with 800 pmole siRNA. 72 hours after the initial transfection, cytoplasmic fractions were obtained from HeLa cells as previously described (van Dijk *et al*, 2007). To assess accumulation of truncated adenylated 28S rRNA, oligo(dT)-primed cDNA was subjected to 25 PCR cycles with a 28S rRNA specific forward primer coupled with the adapter oligo as follows: 1 min 95°C, 1 min 58°C and 1 min 72°C. Products of this PCR were used as templates in a second round of PCR-labeling using the same 28S rRNA primer which was 5' end [^{32}P]-labeled by polynucleotide kinase and γ-[^{32}P] ATP and the adapter. This second round was performed as described above but consisted of 5 cycles and was followed by 10 min of extension at 72°C. PCR-labeled products were resolved by 6% denaturing PAGE and autoradiography. Ethidium bromide-stained DNA markers were run on the same gels and used as length markers.

Acknowledgements

We would like to thank Wiljan Hendriks (Department of Cell Biology, University of Nijmegen, The Netherlands) for the anti-GFP antibodies and Elisabeth Pierson (Department of General Instrumentation, University of Nijmegen, The Netherlands) for assistance with confocal microscopy. This work was supported in part by the Council for Chemical Sciences (NWO-CW) of The Netherlands Organization for Scientific Research.

References

Allmang C, Kufel J, Chanfreau G, Mitchell P, Petfalski E, Tollervey D (1999a) Functions of the exosome in rRNA, snoRNA and snRNA synthesis. *EMBO J* **18:** 5399-5410

Allmang C, Petfalski E, Podtelejnikov A, Mann M, Tollervey D, Mitchell P (1999b) The yeast exosome and human PM-Scl are related complexes of 3' --> 5' exonucleases. *Genes Dev* **13:** 2148-2158

Amblar M, Arraiano CM (2005) A single mutation in Escherichia coli ribonuclease II inactivates the enzyme without affecting RNA binding. *FEBS J* **272:** 363-374

Bonneau F, Basquin J, Ebert J, Lorentzen E, Conti E (2009) The yeast exosome functions as a macromolecular cage to channel RNA substrates for degradation. *Cell* **139:** 547-559

Brouwer R, Allmang C, Raijmakers R, van Aarssen Y, Egberts WV, Petfalski E, van Venrooij WJ, Tollervey D, Pruijn GJ (2001a) Three novel components of the human exosome. *J Biol Chem* **276:** 6177-6184

Brouwer R, Pruijn GJ, van Venrooij WJ (2001b) The human exosome: an autoantigenic complex of exoribonucleases in myositis and scleroderma. *Arthritis Res* **3:** 102-106

Callahan KP, Butler JS (2008) Evidence for core exosome independent function of the nuclear exoribonuclease Rrp6p. *Nucleic Acids Res* **36:** 6645-6655

Chekanova JA, Shaw RJ, Wills MA, Belostotsky DA (2000) Poly(A) tail-dependent exonuclease AtRrp41p from Arabidopsis thaliana rescues 5.8 S rRNA processing and mRNA decay defects of the yeast ski6 mutant and is found in an exosome-sized complex in plant and yeast cells. *J Biol Chem* **275:** 33158-33166

Chen CY, Gherzi R, Ong SE, Chan EL, Raijmakers R, Pruijn GJ, Stoecklin G, Moroni C, Mann M, Karin M (2001) AU binding proteins recruit the exosome to degrade ARE-containing mRNAs. *Cell* **107:** 451-464

Clissold PM, Ponting CP (2000) PIN domains in nonsense-mediated mRNA decay and RNAi. *Curr Biol* **10:** R888-890

Dziembowski A, Lorentzen E, Conti E, Seraphin B (2007) A single subunit, Dis3, is essentially responsible for yeast exosome core activity. *Nat Struct Mol Biol* **14:** 15-22

Edgar RC (2004) MUSCLE: multiple sequence alignment with high accuracy and high throughput. *Nucleic Acids Res* **32:** 1792-1797

Frazao C, McVey CE, Amblar M, Barbas A, Vonrhein C, Arraiano CM, Carrondo MA (2006) Unravelling the dynamics of RNA degradation by ribonuclease II and its RNA-bound complex. *Nature* **443:** 110-114

Glavan F, Behm-Ansmant I, Izaurralde E, Conti E (2006) Structures of the PIN domains of SMG6 and SMG5 reveal a nuclease within the mRNA surveillance complex. *EMBO J* **25:** 5117-5125

Graham AC, Kiss DL, Andrulis ED (2009) Core exosome-independent roles for Rrp6 in cell cycle progression. *Mol Biol Cell* **20:** 2242-2253

LaCava J, Houseley J, Saveanu C, Petfalski E, Thompson E, Jacquier A, Tollervey D (2005) RNA degradation by the exosome is promoted by a nuclear polyadenylation complex. *Cell* **121:** 713-724

Lebreton A, Tomecki R, Dziembowski A, Seraphin B (2008) Endonucleolytic RNA cleavage by a eukaryotic exosome. *Nature* **456:** 993-996

Lejeune F, Li X, Maquat LE (2003) Nonsense-mediated mRNA decay in mammalian cells involves decapping, deadenylating, and exonucleolytic activities. *Mol Cell* **12:** 675-687

Letunic I, Doerks T, Bork P (2009) SMART 6: recent updates and new developments. *Nucleic Acids Res* **37:** D229-232

Liu Q, Greimann JC, Lima CD (2006) Reconstitution, activities, and structure of the eukaryotic RNA exosome. *Cell* **127:** 1223-1237

Lorentzen E, Walter P, Fribourg S, Evguenieva-Hackenberg E, Klug G, Conti E (2005) The archaeal exosome core is a hexameric ring structure with three catalytic subunits. *Nat Struct Mol Biol* **12:** 575-581

Mitchell P, Petfalski E, Shevchenko A, Mann M, Tollervey D (1997) The exosome: a conserved eukaryotic RNA processing complex containing multiple 3'-->5' exoribonucleases. *Cell* **91:** 457-466

Noguchi E, Hayashi N, Azuma Y, Seki T, Nakamura M, Nakashima N, Yanagida M, He X, Mueller U, Sazer S, Nishimoto T (1996) Dis3, implicated in mitotic control, binds directly to Ran and enhances the GEF activity of RCC1. *EMBO J* **15:** 5595-5605

Raijmakers R, Egberts WV, van Venrooij WJ, Pruijn GJ (2002) Protein-protein interactions between human exosome components support the assembly of RNase PH-type subunits into a six-membered PNPase-like ring. *J Mol Biol* **323:** 653-663

Schaeffer D, Tsanova B, Barbas A, Reis FP, Dastidar EG, Sanchez-Rotunno M, Arraiano CM, van Hoof A (2009) The exosome contains domains with specific endoribonuclease, exoribonuclease and cytoplasmic mRNA decay activities. *Nat Struct Mol Biol* **16:** 56-62

Schilders G, Raijmakers R, Raats JM, Pruijn GJ (2005) MPP6 is an exosome-associated RNA-binding protein involved in 5.8S rRNA maturation. *Nucleic Acids Res* **33:** 6795-6804

Schilders G, van Dijk E, Raijmakers R, Pruijn GJ (2006) Cell and molecular biology of the exosome: how to make or break an RNA. *Int Rev Cytol* **251:** 159-208

Schneider C, Leung E, Brown J, Tollervey D (2009) The N-terminal PIN domain of the exosome subunit Rrp44 harbors endonuclease activity and tethers Rrp44 to the yeast core exosome. *Nucleic Acids Res* **37:** 1127-1140

Shiomi T, Fukushima K, Suzuki N, Nakashima N, Noguchi E, Nishimoto T (1998) Human dis3p, which binds to either GTP- or GDP-Ran, complements Saccharomyces cerevisiae dis3. *J Biochem* **123:** 883-890

Slomovic S, Fremder E, Staals RH, Pruijn GJ, Schuster G (2010) Addition of poly(A) and poly(A)-rich tails during RNA degradation in the cytoplasm of human cells. *Proc Natl Acad Sci U S A* **107:** 7407-7412

Slomovic S, Laufer D, Geiger D, Schuster G (2006) Polyadenylation of ribosomal RNA in human cells. *Nucleic Acids Res* **34:** 2966-2975

Slomovic S, Portnoy V, Schuster G (2008) Detection and characterization of polyadenylated RNA in Eukarya, Bacteria, Archaea, and organelles. *Methods Enzymol* **447:** 501-520

Synowsky SA, van Wijk M, Raijmakers R, Heck AJ (2009) Comparative multiplexed mass spectrometric analyses of endogenously expressed yeast nuclear and cytoplasmic exosomes. *J Mol Biol* **385:** 1300-1313

Theobald DL, Mitton-Fry RM, Wuttke DS (2003) Nucleic acid recognition by OB-fold proteins. *Annu Rev Biophys Biomol Struct* **32:** 115-133

Tomecki R, Kristiansen MS, Lykke-Andersen S, Chlebowski A, Larsen KM, Szczesny RJ, Drazkowska K, Pastula A, Andersen JS, Stepien PP, Dziembowski A, Jensen TH (2010) The human core exosome interacts with differentially localized processive RNases: hDIS3 and hDIS3L. *EMBO J* **29:** 2342-2357

van Dijk EL, Schilders G, Pruijn GJ (2007) Human cell growth requires a functional cytoplasmic exosome, which is involved in various mRNA decay pathways. *RNA* **13:** 1027-1035

van Hoof A, Frischmeyer PA, Dietz HC, Parker R (2002) Exosome-mediated recognition and degradation of mRNAs lacking a termination codon. *Science* **295:** 2262-2264

Waterhouse AM, Procter JB, Martin DM, Clamp M, Barton GJ (2009) Jalview Version 2--a multiple sequence alignment editor and analysis workbench. *Bioinformatics* **25:** 1189-1191

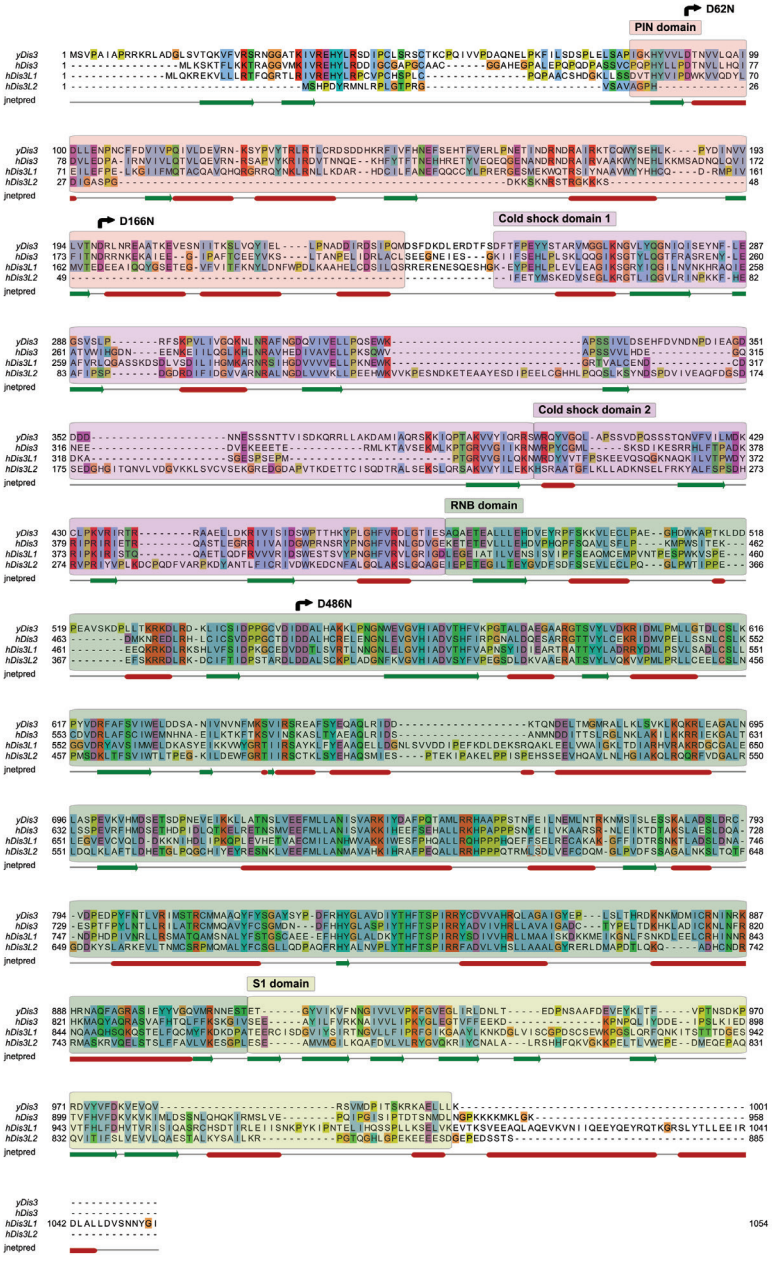

Figure S1. Yeast and human Dis3 and Dis3-like sequence alignment.

A multiple alignment of the amino acid sequences of yeast Dis3 (yDis3), human Dis3 (hDis3), human Dis3-like 1 (hDis3L1) and human Dis3-like 2 (hDis3L2) was generated by the MUSCLE algorithm (Edgar, 2004). The secondary structure of hDis3L1, as predicted by PsiPred, is depicted below the sequence alignment; β-strands are represented with green arrows and α-helices with red bars. Protein domains predicted by SMART are indicated by colored boxes surrounding the sequences. The graphical presentation of the alignments was generated with Jalview (Waterhouse *et al*, 2009) using the default color scheme used for alignments in Clustal X.

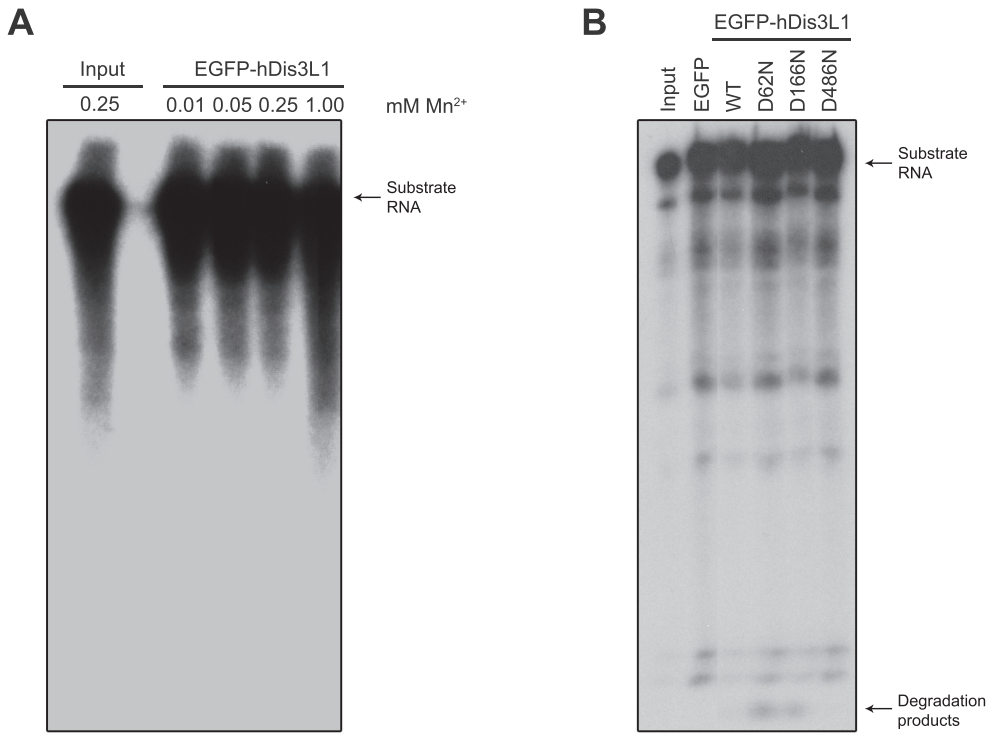

Figure S2. hDis3L1 lacks endonuclease activity.

(A) HEp-2 cells were transfected with expression constructs encoding EGFP or EGFP-hDis3L1 and after 48 hrs cell lysates were subjected to immunoprecipitation with anti-GFP antibodies. Precipitated material was incubated with a radiolabeled substrate RNA (Input) and the reaction products were subsequently analyzed by denaturing polyacrylamide gel electrophoresis followed by autoradiography. The incubations were performed in the presence the indicated concentrations of $Mn2^{+}$. (B) Ribonuclease assay as described above (A), but with immunoprecipitated hDis3L1 mutants D62N, D166N, D486N (in addition to the wild type protein) in the presence of 1 mM $Mn2^{+}$. Mononucleotide degradation products, most likely resulting from low levels of exoribonuclease activity, are indicated.

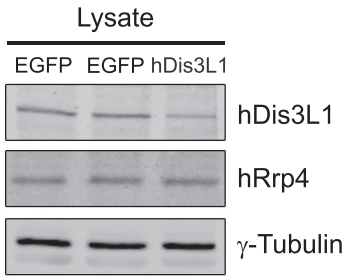

Figure S3. SiRNA-mediated hDis3L1 knock-down.

The lysates from HEp-2 cells transfected with siRNAs for EGFP or hDis3L1 that were used for the activity assay, as depicted in Figure 4B, were analyzed by incubating western blots with anti-hDis3L1 and anti-hRrp4 antibodies. Anti-γ-tubulin antibodies were used as a loading control.

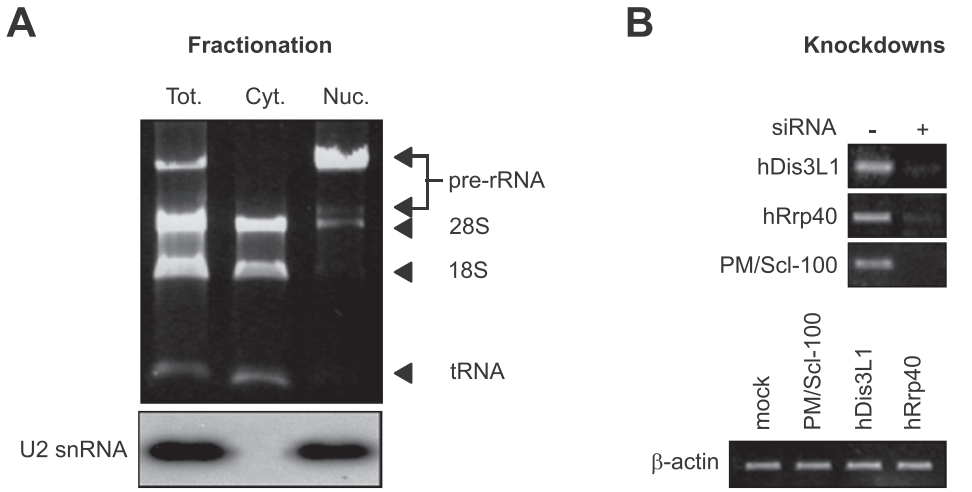

Figure S4. Analysis of cell fractionation and efficiency of knock-down for cells used to study cytoplasmic rRNA degradation.

(A) Following cell fractionation, RNA purified from the cytoplasmic and nuclear fractions was stained with EtBr and the rRNA and tRNA distribution was compared with that of total cellular RNA. Tot., total cell RNA; Cyt., cytoplasmic RNA; Nuc., nuclear RNA. In addition, the RNA samples were subjected to northern blot hybridization using a probe for the nuclear U2 snRNA. The positions of the various RNAs are indicated. (B) The efficiency of siRNA-mediated silencing of exosome subunits hDis3L1, hRrp40 and PM/Scl-100 was monitored by RT-PCR using RNA isolated from the respective cells. RT-PCR analysis of β-actin mRNA was performed in parallel to control for equal amounts of starting material with the RNA from mock and siRNA-transfected cells.

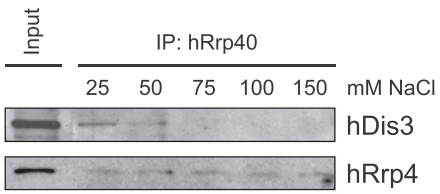

Figure S5. hDis3 does not stably interact with the exosome core.

Anti-hRrp40 antibodies were used to precipitate exosome complexes from a HEp-2 cell lysate in the presence of NaCl concentrations ranging from 25 mM to 150 mM, as indicated. The coprecipitation of hDis3 and hRrp4 (exosome core control) was monitored by western blotting using polyclonal and monoclonal antibodies, respectively, to these proteins. In the 'Input' lane the total cell lysate was loaded.

CHAPTER 4

Addition of poly(A) and poly(A)-rich tails during RNA degradation in the cytoplasm of human cells

Shimyn Slomovic[1,a], Ella Fremder[1,a], Raymond H.J. Staals[2], Ger J.M. Pruijn[2], and Gadi Schuster[1]

[1] Faculty of Biology, Technion–Israel Institute of Technology, Haifa 32000, Israel

[2] Department of Biomolecular Chemistry, Nijmegen Center for Molecular Life Sciences, Institute for Molecules and Materials, Radboud University Nijmegen, NL-6525 GA, Nijmegen, The Netherlands

[a] contributed equally

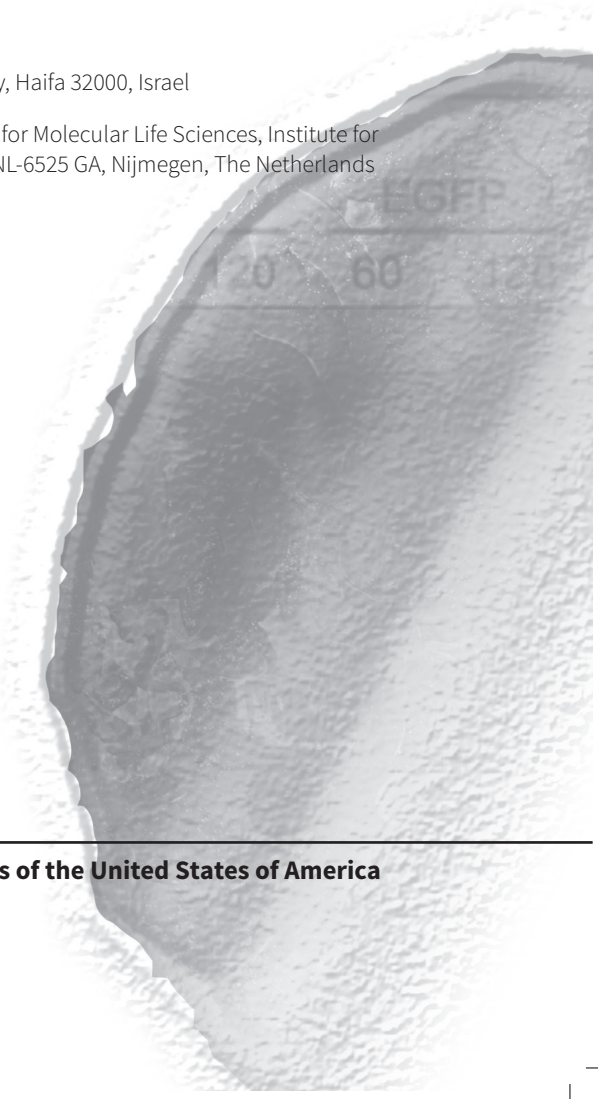

Proceedings of the National Academy of Sciences of the United States of America (2010) Apr 20;107(16):7407-7412

Abstract

Polyadenylation of RNA is a posttranscriptional modification that can play two somewhat opposite roles: stable polyadenylation of RNA encoded in the nuclear genomes of eukaryote cells contributes to nuclear export, translation initiation, and possibly transcript longevity as well. Conversely, transient polyadenylation targets RNA molecules to rapid exonucleolytic degradation. The latter role has been shown to take place in prokaryotes and organelles, as well as the nucleus of eukaryotic cells. Here we present evidence of hetero- and homopolymeric adenylation of truncated RNA molecules within the cytoplasm of human cells. RNAi-mediated silencing of the major RNA decay machinery of the cell resulted in the accumulation of these polyadenylated RNA fragments, indicating that they are degradation intermediates. Together, these results suggest that a mechanism of RNA decay, involving transient polyadenylation, is present in the cytoplasm of human cells.

Introduction

RNA polyadenylation occurs throughout the biological world. Stable poly(A) is associated with the mature 3′ end of most mRNAs encoded in the nuclear genome of eukaryotes. It is important for nuclear export and efficient translation initiation and may also contribute to transcript longevity (Edmonds, 2002). In turn, mRNA degradation in the cytoplasm usually initiates with deadenylation of the stable poly(A) tail, followed by either further degradation of the mRNA body by the exosome (3′–5′ pathway) or removal of the 5′ cap and subsequent 5′–3′ degradation by hXrn1 (exoribonuclease 1; 5′–3′ pathway) (Doma and Parker, 2007; Garneau *et al*, 2007; Houseley and Tollervey, 2009).

Unlike stable poly(A), transient poly(A) is not associated with the mature 3′ end of the transcript. RNA decay pathways that use transient poly(A) include a stage in which poly(A) or poly (A)-rich tails are added to the 3′ ends of truncated degradation intermediates and are believed to assist exoribonucleases in their rapid degradation. As the tail addition can occur after endonucleolytic cleavage of the RNA or repetitive adenylation and 3′-5′ digestion, it often appears to be at “internal” positions relative to the full RNA sequence (Deutscher, 2006; Slomovic *et al*, 2006b). The term “transient” is used because the short-lived tail is degraded along with the RNA fragment. Transient poly(A) was first disclosed in *Escherichia coli* and then in additional bacteria, organelles, archaea and, eventually, in yeast and human nuclei (Deutscher, 2006; Houseley and Tollervey, 2009; Slomovic *et al*, 2008b; Vanacova and Stefl, 2007; Wilusz and Wilusz, 2008). In all systems in which truncated, polyadenylated RNA fragments were initially detected, they were later found to be correlated to poly(A)- assisted RNA decay (Houseley and Tollervey, 2009; Slomovic *et al*, 2008b; Wilusz and Wilusz, 2008).

In yeast nuclei, transient poly(A) was found to play a role in RNA quality control wherein polyadenylation, initiated by the TRAMP complex, targets incorrectly folded tRNA molecules to degradation by the nuclear exosome (LaCava *et al*, 2005; Vanacova *et al*, 2005). In human cells, cotranscriptionally cleaved 3′ regions of an introduced β-globin gene and a class of short, highly unstable RNAs, dubbed PROMPTs (promoter upstream transcripts), were found to be adenylated and accumulated when the exosome was downregulated (Preker *et al*, 2008; West *et al*, 2006). It has recently become clear that almost the entire genome is transcribed, which results in the production of antisense and noncoding RNAs (Arigo *et al*, 2006; Lykke-Andersen and Jensen, 2006; Preker *et al*, 2008; Thiebaut *et al*, 2006; Wyers *et al*, 2005). These cryptic unstable transcripts were found to undergo rapid poly(A)-assisted decay as well (LaCava *et al*, 2005; Vanacova *et al*, 2005; Wyers *et al*, 2005). However, although such nuclear mechanisms have been reported, poly(A)-assisted RNA decay has not been found in the cytoplasm of eukaryote cells.

Previously, we isolated truncated, poly(A)-tailed ribosomal RNA molecules from total RNA of human cells (Slomovic *et al*, 2006a). Interestingly these tails were either of homopolymeric [poly(A)] or heteropolymeric [poly(A)-rich] nature. The heteropolymeric extensions were dominantly adenylated but contained other nucleotides as well and resembled the poly(A)-rich tails produced in bacteria, chloroplasts, and archaea (Slomovic *et al*, 2006b; Slomovic *et al*, 2008b). However, neither the cellular location nor the function of these adenylation events was deciphered.

Here, we show the presence of truncated mRNAs and rRNAs, bearing homopolymeric or heteropolymeric tails, in the cytoplasm of human cells. RNAi-mediated silencing of 3′-5′ exoribonucleases and hXrn1 resulted in the accumulation of these molecules in the cytoplasm, strongly suggesting that poly(A)- assisted RNA decay occurs in the cytoplasm of human cells.

Results

Fragmented 28S rRNA molecules containing homo-or heteropolymeric tails are present in both the cytoplasm and nucleus of human cells

In earlier work, we detected truncated 28S and 18S rRNAs containing homo- or heteropolymeric tails (Slomovic *et al*, 2006a). It was plausible that these rRNA fragments are degradation intermediates of the nuclear process mentioned earlier, but a second option could not be ignored: transient, perhaps degradation-assisting, adenylation of RNA within the cytoplasm, coexisting with the stable poly(A) tails that characterize this cellular location.

Hence, our first goal was to determine whether these tailed, truncated molecules are present in the nucleus, cytoplasm, or both.

RNA and protein were obtained from cytoplasmic and nuclear fractions which were prepared from HeLa cells. A clear fractionspecific distribution of mature rRNA and pre-rRNA (and tRNA) was observed upon ethidium bromide staining of total, cytoplasmic, and nuclear RNA (Figure S1). To assess purity of fractions, Northern blots and immunoblots were prepared, and Figure 1A shows that the RNA and protein markers were detected exclusively in the corresponding fractions. Next, the presence of fragmented polyadenylated 28S rRNA was evaluated by oligo (dT) RT-PCR. The results disclosed 28S rRNA fragments, with either homo- or heteropolymeric extensions in both the nucleus and cytoplasm (Figure 1B). To our knowledge, this is the first detection of internally adenylated RNA in the cytoplasm of human cells.

To evaluate the truncated molecules in both fractions by means unbiased to poly(A) extensions, circularized reverse transcription (cRT) was applied to the same region of 28S rRNA (Figure 1C). Truncated molecules were successfully isolated from both the cytoplasmic and nuclear fractions. Although most fragments were tail-less, a small number had extensions of 1 to 4 nt; however, there are cases in which it is not clear whether the adenosine is part of the encoded sequence or was posttranscriptionally added. These molecules could reflect oligo(A) addition, or could be either at a stage before tail synthesis or amid 3′-5′ degradation. Therefore, as in many previous studies of transient adenylation, biased methods such as oligo(dT) RT-PCR are necessary to view long internal tails and assess their nt composition, which can often lead to the identity of the polyadenylating factor (Slomovic *et al*, 2008a; Slomovic *et al*, 2008b).

Truncated, intron-Less β-actin transcripts harboring homo- or heteropolymeric tails

To check if, in addition to rRNA, mRNA can undergo this process, the presence of truncated adenylated β-actin mRNA molecules was analyzed using oligo(dT) RT-PCR. Gene-specific primers were applied; some of which targeted the mRNA sequence immediately upstream of introns, potentially allowing the isolation of both spliced and unspliced adenylated β-actin fragments. As shown in Figure 2A, truncated adenylated β-actin fragments were isolated and similar to rRNA, both homo- and heteropolymeric tails were observed. Also, such molecules were obtained from both nuclear and cytoplasmic fractions (Table S1). No introns were present among the isolated sequences, disclosing that these are (partially, if not fully) spliced transcripts. These results show that like rRNA, mRNA can undergo transient adenylation.

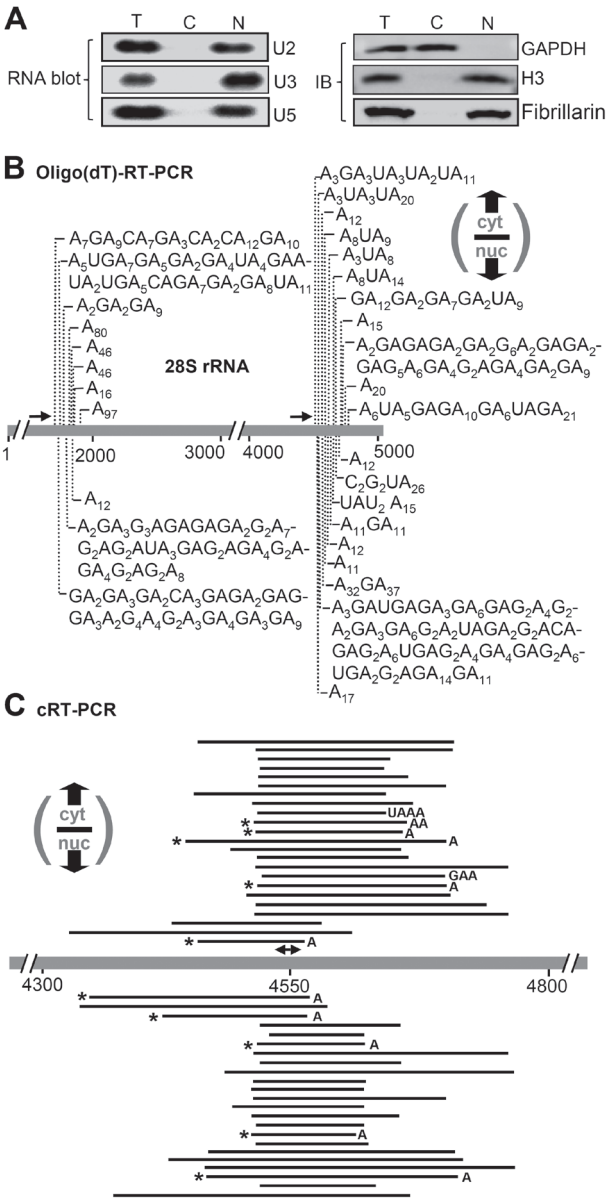

Figure 1. 28S rRNA fragments with homo- or heteropolymeric poly(A) tails in the cytoplasm and nuclei of human cells.

(A) Fractionation purity was determined by Immunoblots (IBs) and RNA blots using fraction-specific markers: C, cytoplasm: GAPDH. N, nucleus: histone H3 (H3), fibrillarin, and U2/U3/U5-snoRNAs. T, total cell RNA/proteins. (B) Oligo(dT) RT-PCR isolation of truncated, adenylated 28S rRNA molecules from cyt (above) and nuc (below) fractions. 28S rRNA is schematically presented with arrows indicating primer locations and vertical lines showing tail sites and content (Table S1). (C) cRT-PCR isolation of truncated 28S rRNA molecules from cyt (above) and nuc (below) fractions. Cases in which it is not known whether the "A" is encoded or added posttranscriptionally are marked with an asterisk (Table S2).

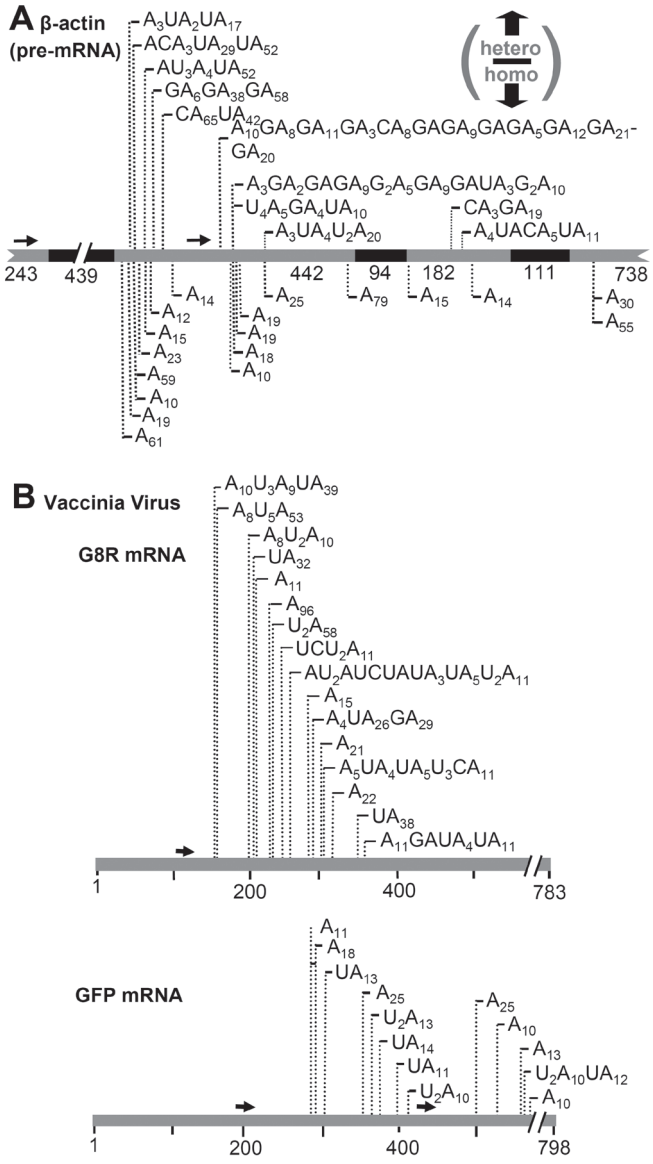

Figure. 2. Homo- or heteropolymeric poly(A) tails in eukaryotic and viral (pre-) mRNAs.

(A) Spliced β-actin fragments with homo- or heteropolymeric poly(A) tails, isolated from human cells. Primary β-actin mRNA is schematically presented (introns in black, exons in gray). Lengths of each exon/intron are shown. Homo- and heteropolymeric tails are presented above and below the gene, respectively (Table S1). (B) Oligo(dT) RT-PCR isolation of truncated, adenylated VV RNA molecules [G8R (a viral mRNA) and GFP (integrated into the viral genome)] from HeLa cells 4 h after transfection (Table S3).

Truncated vaccinia virus RNAs bearing homo- or heteropolymeric tails were isolated from infected cells.

In addition to the fractionation purity assays (Figure 1A), to further ensure that the RNA molecules obtained from cytoplasmic fractions as described earlier were not intermediates of a nuclear process that had "leaked" to the cytoplasm, either *in vivo* or during our experimental procedures, we adopted an additional approach: vaccinia virus (VV) belongs to the poxvirus family and contains a doublestranded DNA genome, encoding more than 200 proteins. Poxviruses are unique among most DNA viruses in that they do not enter the nucleus during their entire life cycle (Broyles, 2003). To check if viral RNA is subjected to transient adenylation within the cytoplasm, RNA was purified from infected HeLa cells and analyzed for the presence of truncated, polyadenylated transcripts of genes encoded in the viral genome. Figure 2B displays the results of the analysis of G8R mRNA, an intermediate viral gene and GFP mRNA, produced from a GFP gene inserted into the viral genome (Hsiao *et al*, 2006). Truncated transcripts originating from these genes, with either homo- or heteropolymeric tails, were detected. These results provide additional support that a mechanism involving transient RNA polyadenylation is present in the cytoplasm and applies not only to rRNA, but mRNA as well. Accordingly, the next step was to check if there is a link between this type of RNA adenylation and RNA decay, as in all previously studied systems in which such molecules were found.

Are the truncated, polyadenylated transcripts degradation intermediates?

In all systems in which truncated, adenylated RNA molecules were detected, they were later shown to be intermediates in a poly(A)- assisted RNA decay pathway. We asked if the tails observed here, in the cytoplasm, are indeed telltale signs of such a process. If so, inhibition of exonucleolytic activity would result in their accumulation, as observed in bacteria, plant mitochondria, and the nuclei of yeast and human cells (Kushner, 2004; Preker *et al*, 2008; West *et al*, 2006; Wyers *et al*, 2005). To this end, we used RNAi to knock down (KD) hXrn1 and the exosome subunits. For the latter, PM/Scl-100, an exoribonuclease associated with the exosome and hRrp41, an exosome core protein, were targeted. Immunoblots disclosed significant KD of the targeted proteins (Figure 3A). A reduction in exosome activity was validated by 5.8S rRNA precursor accumulation in both the PM/Scl-100 and hRrp41-silenced cells (Figure 3B) (Preker *et al*, 2008; Stoecklin *et al*, 2006).

Degradation intermediates are nonabundant and rapidly degraded; hence it is beneficial to analyze highly expressed transcripts for such related molecules. Therefore, we chose to focus on the region of 28S rRNA from which adenylated fragments had been isolated by oligo(dT) RT-PCR, as described earlier. To visually evaluate fragmented, adenylated 28S rRNA accumulation, a radiolabeling assay was applied; loading amounts were normalized according to B2M mRNA via RT-PCR (Figure 4A). Following oligo (dT) reverse transcription, the same primers with which the truncated molecules were previously isolated were used but this time, an extra PCR-stage in which the products were labeled via a 5′ end [^{32}P] 28S rRNA primer,

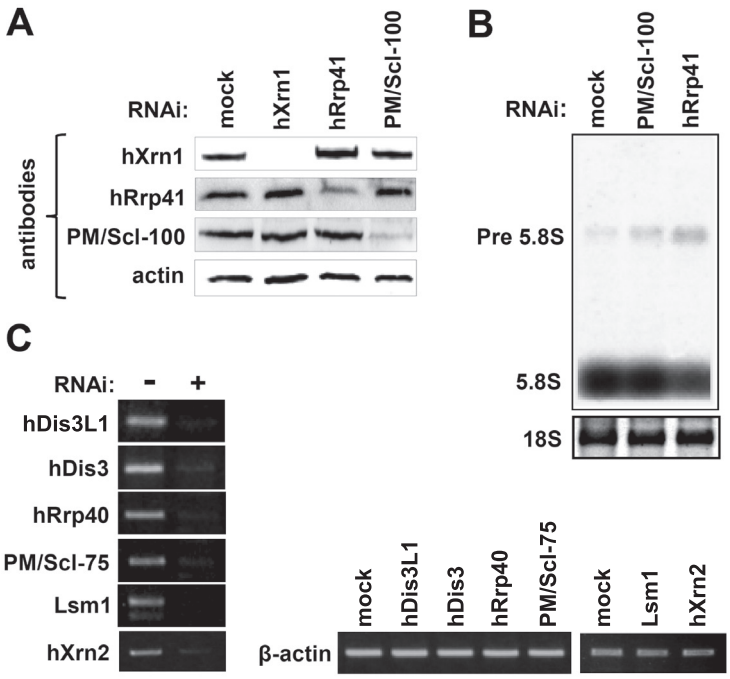

Figure 3. RNAi-mediated silencing of exosome subunits, hXrn1, hXrn2, and Lsm1.

(A) Efficiency of silencing was measured via immunoblot with specific antibodies. (B) Loss of exosome activity was validated by the accumulation of the 5.8S rRNA precursor as detected by Northern blot. (C) KD efficiency of RNAi-silenced proteins for which antibodies were not available was monitored by RT-PCR. Immunoblots and RT-PCR were normalized with β-actin.

was included. Fractionation on denaturing polyacrylamide gel, allowed sensitive assessment of accumulation of the labeled amplification products. As the truncated molecules were polyadenylated at varying sites along the 28S rRNA (Figure 1B), and the extensions were of different lengths, accumulation did not result in a single band, but a smeared signal instead. Substantial accumulation of truncated 28S rRNA fragments was observed in the lanes representing the RNAi silencing of PM/Scl- 100 and hXrn1 (Figure 4B). Although PM/Scl-100 (Rrp6 in yeast) has been reported to exist in the cytoplasm, it is mainly found in the nucleus of human cells in association with the nuclear exosome (Lykke-Andersen *et al*, 2009; van Dijk *et al*, 2007). Therefore, the corresponding signal in this lane is most likely the result of the accumulation of nucleus-localized degradation intermediates. In contrast, accumulation of truncated 28S rRNA fragments was much less drastic in the hRrp41-silenced cells.

hXrn1 plays a central role in 5′-3′ RNA degradation in the cytoplasm. Counter intuitively, its silencing resulted in significant accumulation of the polyadenylated molecules. A cytoplasmic localization of these transcripts is implied by that of hXrn1 but the obvious question is why the inhibition of a 5'-3' exonuclease results in the accumulation of degradation intermediates

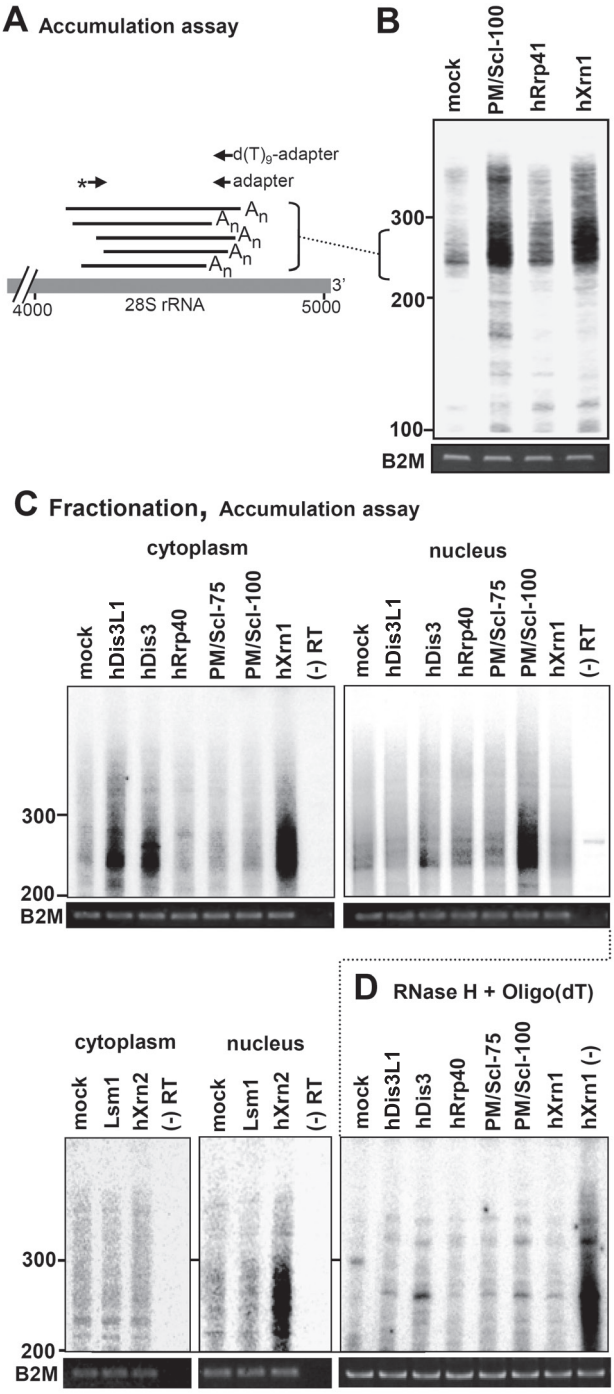

Figure 4. Adenylated 28S rRNA degradation intermediates significantly accumulated in cells upon RNAi silencing of major exonucleases.

(A) Schematic presentation of PCR-labeling assay to detect accumulation of adenylated, truncated 28S rRNA molecules after exonuclease KD. Briefly, following oligo(dT) RT of RNA from different KD cells, PCR with [^{32}P]-labeled gene-specific primer (asterisk; same as used to isolate molecules as shown in Figure 1B) and adapter oligo was performed. (B) RNA purified from the mock and KD HeLa cells was subjected to this analysis to assess the accumulation of polyadenylated, fragmented 28S rRNA. The migration of DNA markers is shown to the left (nucleotide numbers). (C) Cytoplasmic or nuclear RNA from cells in which the indicated proteins were silenced by RNAi, was subjected to oligo(dT) RT-PCR labeling. A control, with reverse transcript was omitted from the reaction, is shown in the far right lane of each panel. (D) To verify that the PCR products originated from polyadenylated transcripts, a control was performed in which the poly(A) tails of the cytoplasmic fractions were removed by incubation with oligo(dT) and RNase H before oligo(dT)-primed RT-PCR labeling. This resulted in reduction of amplification signals to background levels, as compared with the hXrn1 sample that was treated with RNase H but without oligo(dT) [lane labeled hXrn1 (-)].

with 3' end poly(A) tails. This issue will be addressed in the Discussion. Together, the information obtained using this assay suggests that the isolated polyadenylated 28S rRNA fragments are indeed degradation intermediates. To definitively determine cellular location, the analyses described here were repeated after fractionation of the nucleus and cytoplasm. Also, to further investigate whether the exosome core is involved in this process, several additional subunits and exoribonucleases were down-regulated.

RNAi silencing of exoribonucleases confirmed that poly(A)-assisted RNA decay exists in the cytoplasm of human cells

To confirm that degradation of transiently adenylated RNA occurs in the cytoplasm of human cells, the analysis was repeated after nuclear and cytoplasmic fractions were prepared. Two additional exosome core components, hRrp40 and PM/Scl-75, and two exoribonucleases, hDis3 and hDis3L1, were knocked down. hDis3 is a homologue of the yeast Dis3 protein; a hydrolytic 3′-5′ exoribonuclease with additional endonuclease activity that is associated with the exosome in both the nucleus and cytoplasm in yeast. This protein serves as the only catalytic subunit in the cytoplasmic yeast exosome (Dziembowski *et al*, 2007; Lykke-Andersen *et al*, 2009). While this work was in progress, an additional Dis3 homologue in human cells, hDis3L1, was discovered, and unlike hDis3, was found to be strongly associated with the exosome core and to localize to the cytoplasm. Therefore, it is the more likely Dis3 orthologue in human cells and its silencing was included (Staals *et al*, 2010). Two additional enzymes were silenced: hXrn2 and Lsm1. The former is a major, nucleus-localized 5′-3′ exonuclease and so its KD could be anticipated to cause accumulation in the nucleus but not in the cytoplasm (Houseley and Tollervey, 2009). The Lsm proteins play a role similar to the bacterial Hfq proteins, involved in bacterial mRNA decay via tail addition. Lsm1 is associated with hXrn1, decapping enzymes (Dcp1/Dcp2), and mRNA decay in the cytoplasm. Also, it was shown to be directly involved in histone mRNA oligo(U)-mediated decay. Thus, the effect of its RNAi silencing was evaluated as well (Mullen and Marzluff, 2008). RT-PCR quantification, for lack of appropriate antibodies, showed significant reduction in the mRNA levels of the silenced proteins (Figure 3C).

No accumulation was observed in the cytoplasm of cells silenced of the exosome components, hRrp40 or PM/Scl-75, and only minor accumulation could be observed in their nuclear fractions (Figure 4C). In contrast, KD of either hDis3 or hDis3L1 resulted in distinct cytoplasmic accumulation of truncated 28S rRNA fragments, suggesting that these two proteins are involved in the degradation process. As anticipated, hXrn1 and PM/Scl-100 silencing caused substantial accumulation in the cytoplasmic and nuclear fraction, respectively, and KD of hXrn2 resulted in accumulation only in the nuclear fraction. Silencing of Lsm1 did not result in accumulation within either fraction. To be sure that the labeled products observed in the gel were indeed obtained by the amplification of polyadenylated 28S rRNA molecules and not artifacts of nonspecific reverse transcription, RNA purified from

the cytoplasm was incubated with RNase H and oligo(dT) before the oligo(dT)-primed reverse transcription (Figure 4D). This way, all poly(A) tails would be removed and no cDNA would be produced during the subsequent oligo(dT)-primed RT. Indeed, this treatment reduced the observed amplified signals to the background level. It is especially evident when comparing the result obtained for RNA purified from hXrn1-silenced cells that was either incubated with RNase H alone or with RNase H together with oligo(dT) (Figure 4D).

Together, these results confirm that rRNA can be transiently adenylated, not only in the nucleus of human cells, but in the cytoplasm as well, and this is linked to rRNA decay. In the cytoplasm, the involved exoribonucleases include hDis3L1, hDis3, and hXrn1, as the adenylated degradation intermediates accumulate upon their down-regulation.

Exosome or hPNPase silencing does not cause a decrease in the percentage of hetero-adenylated clones

At this stage, we attempted to identify the enzyme responsible for the addition of the tails, in particular those of heteropolymeric nature. PNPase and the archaeal exosome are responsible for both hetero-tailing and degrading bacterial, organellar, and archaeal RNA (Slomovic *et al*, 2008b). The structurally similar eukaryotic exosome was initially a candidate for the hetero- activity observed here and if it were responsible for producing the hetero-tails, a shift in favor of the homoextensions would be expected to occur upon its KD. However, the exosome was reported to lack phosphorolytic activity (Lykke-Andersen *et al*, 2009) and in agreement with this, we found that the percentage of homo- tails within the total amount of isolated and sequenced clones did not increase upon KD of exosome subunits, hRrp41, PM/Scl-100, and PM/Scl-75 (Figure 5).

PNPase is present in human cells (hPNPase) and phosphorolytically active (Portnoy *et al*, 2008). Although localized to the mitochondrial intermembrane space (IMS) (Chen *et al*, 2007), we considered the possibility that hPNPase, similar to other IMS proteins such as cytochrome C and endonuclease G (Widlak and Garrard, 2005), could be liberated from this compartment and enter the cytoplasm(and/or nucleus), where it could polymerize hetero- tails. However, no increase in homo- tail rate was observed in cells with constant hPNPase shRNA silencing either (Slomovic and Schuster, 2008).

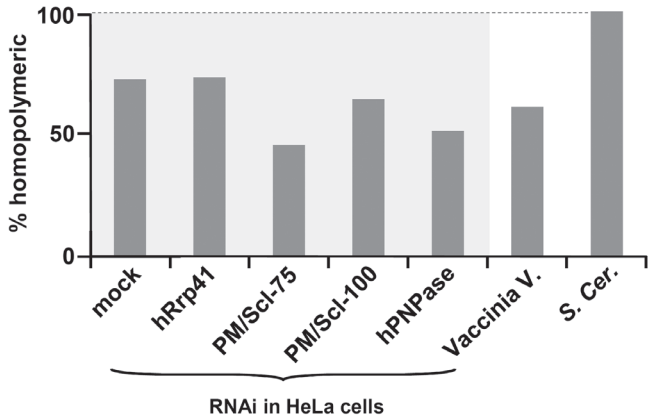

Figure. 5. Percentage of homopolymerically tailed molecules isolated from HeLa cells with RNAi silencing of exosome components or hPNPase, cells infected with VV, and yeast.

Percentage of homopolymerically tailed molecules among the total number of sequenced molecules isolated from HeLa cells did not increase upon RNAi silencing of: hRrp41, PM/Scl-75, PM/Scl-100, or hPNPase (28S rRNA was analyzed). In VV-infected cells, the viral G8R RNA was analyzed, and in S. cerevisiae, 25S rRNA, CYH2 and Actin1 (Tables S3, S4, and S5).

Discussion

Poly(A)-assisted RNA decay occurs in the cytoplasm of human cells.

A nuclear RNA surveillance mechanism involving polyadenylation and rapid degradation of nonfunctional, antisense, and noncoding RNAs has been described in yeast and human cells (Houseley and Tollervey, 2009; Neil *et al*, 2009; Proudfoot and Gullerova, 2007; Thompson and Parker, 2007; Vanacova and Stefl, 2007; Xu *et al*, 2009). We initially assumed that the truncated, polyadenylated rRNA molecules that we had previously detected in human cells (Slomovic *et al*, 2006a) are solely related to this process, but in this study we found that transient adenylation can occur in the cytoplasm as well, as such molecules were detected in cytoplasmic fractions. However, in yeast, unstable transcripts derived from intergenic regions (i.e., nuclear) were reported to be stabilized upon inhibition of Xrn1 and Dcp1 (i.e., cytoplasmic). In such a case, export from the nucleus would be entailed (Thompson and Parker, 2007). To ensure this was not the case in our work, besides assays that demonstrated fractionation purity, both at protein and RNA levels, additional cytoplasmic localization evidence was obtained by analyzing the RNA of VV, a virus that spends its entire life cycle in the cytoplasm. Analysis of the β-actin transcript was applied as well, demonstrating that endogenous mRNA can undergo this process.

If indeed the observed molecules are degradation intermediates of poly(A)-assisted RNA decay, we expected to observe their accumulation upon exoribonuclease down-regulation. Silencing of three of the nine exosome core proteins caused only slight accumulation of adenylated rRNA in the nucleus and no noticeable accumulation in the cytoplasm. PM/Scl-100 silencing resulted in accumulation only in the nuclear fraction and therefore, although reported to partially reside in the cytoplasm of human cells, PM/Scl-100 does not seem to be involved in this cytoplasmic process (Lejeune *et al*, 2003; Schmid and Jensen, 2008; van Dijk *et al*, 2007). Conversely, RNAi silencing of the two Dis3 (Rrp44) homologues, hDis3 and hDis3L1, resulted in cytoplasmic accumulation of truncated adenylated rRNA. The fact that silencing of hDis3, the previously identified yeast Dis3 orthologue (Schmid and Jensen, 2008), had this effect, suggests that this Dis3 family member, although most likely not associated with the exosome, acts as a 3′-5′ exonuclease. hDis3L1, however, is most likely associated with the cytoplasmic exosome core (Staals *et al*, 2010), and the accumulation of truncated adenylated rRNA in the cytoplasm upon its silencing suggests either exosome involvement in this process (despite no such effect when silencing core subunits) or a level of exosome-independent activity of hDis3L1. In previous studies, although substantially knocked down by RNAi (validated by assessment of 5.8S rRNA processing), not all exosome subunits that were silenced caused a substantial effect on AU-rich element (ARE)–mediated decay, and a similar situation could occur in this case (Stoecklin *et al*, 2006). hXrn2 KD led to accumulation within the nucleus but not in the cytoplasm, in correlation with its cellular localization.

Lsm1 silencing did not result in the accumulation of adenylated rRNA fragments. This result is somewhat surprising, as Lsm1 is known to play a central role in mRNA degradation following stable poly(A) tail shortening . Also, recent work disclosed a novel oligo(U)-mediated histone mRNA decay pathway with Lsm1 as an integral component (Mullen and Marzluff, 2008). There, its silencing greatly stabilized histone mRNA (i.e., hampered its degradation), as did that of Xrn1 and Dcp2. Here, its apparent uninvolvement in poly (A)-mediated rRNA decay could be interpreted as the following: Lsm1 is known to recruit the decapping enzymes and allow Xrn1 5′-3′ degradation after the cap is removed. However, rRNA (uncapped) was the focus of the assay presented here. The poly (A)-mediated decay of rRNA may differ from that of mRNA (capped). First, Lsm1 could well be involved in cap removal of mRNA, allowing hXrn1 activity. Second, hXrn1 may not be involved in mRNA decay. Third, in any case, in previous work, we traced truncated adenylated 28S rRNA molecules to an endonucleolytically cleaved region of the 28S transcript (Slomovic *et al*, 2006a). Multiple endonucleolytic cleavage events of rRNA or mRNA before transient tail addition, as in other poly(A)-mediated RNA decay pathways, could provide bare 5′ (and 3′) ends, thereby bypassing the need to decap the molecule (Slomovic *et al*, 2006a). More studies are needed to characterize any differences between poly(A)-mediated rRNA and mRNA decay.

Why did silencing of hXrn1 result in the accumulation of truncated transcripts, adenylated at the 3′ end?

If the tails observed here provide the same function as in all known cases of transient adenylation, to assist in 3′-5′ degradation, why did inhibition of hXrn1's 5′-3′ activity result in the accumulation of these 3′ tailed molecules? Perhaps this case resembles ARE-mediated mRNA decay in the sense that, although AREs are present in the 3′ UTR, Xrn1 is required to fully degrade the substrates (Stoecklin *et al*, 2006). Also, oligo (U)-mediated histone mRNA degradation was shown to include degradation from both the 5′ and 3′ ends of the transcript (Mullen and Marzluff, 2008). Moreover, if endonucleolytic cleavage events were to precede poly (A) tail addition, hXrn1 would be a likely candidate to degrade the distal cleavage products, starting from their unprotected 5′ ends.

Interestingly, recent studies have questioned the necessity of polyadenylation of nuclear exosome substrates by Trf4/5 of the TRAMP complex, as a polyadenylation-defective form of Trf4 (Trf4-DADA) can activate exosomal degradation of RNA substrates and rescue the lethality of Trf4/5 double mutants (San Paolo *et al*, 2009; Wyers *et al*, 2005). This suggests that the general addition of poly(A) tails to nuclear degradation intermediates may only be necessary to promote the degradation of certain structured RNAs. If cytoplasmic poly(A)- assisted RNA decay is similar in this manner, more weight would be placed on the 5′-3′ pathway; hence, hXrn1's involvement.

Which enzyme produces the homo- and heteropolymeric tails?

Neither hPNPase nor exosome silencing caused an increase in the percentage of homo-tailed molecules within the total amount isolated and sequenced. Theoretically, this could indicate two alternatives: (i) neither enzyme produces the heteropolymeric tails or (ii) one of the enzymes produces both homo- and heteropolymeric tails. The latter scenario is highly unanticipated as, traditionally, polyadenylating enzymes in such pathways are known to synthesize a single type of tail, as far as nucleotide composition. Furthermore, the exosome's reported lack of phosphorolytic activity and "inconvenient" IMS localization of hPNPase agree with their lack of involvement. Possible candidates, especially for producing the observed A/U-rich heteropolymeric tails, could be among the seven noncanonical poly(A) polymerases recently identified in human cells, as nc-PAPs have been shown to add either As or Us (Heo *et al*, 2009; Martin and Keller, 2007; Mullen and Marzluff, 2008). However, many of the isolated heteropolymeric sequences are A/G-rich and could possibly be produced by a different factor. Initial results obtained by RNAi silencing of the seven human ncPAPs are yet inconclusive in terms of their possible involvement in the transient tail addition (Figure S2 and Table S6). Degenerative or overlapping activities may necessitate combinatorial RNAi KD of these proteins in future analysis. Interestingly, only homopolymeric tails were found in *Saccharomyces cerevisiae* (Figure 5), suggesting that the component responsible for heteropolymeric tails is not present in *S. cerevisiae*. Clear identification of the polyadenylating

elements involved will assist in understanding the apparently complex model that governs this pathway.

In summary, in this work, we revealed transient homo- and heteropolymeric adenylation of rRNA and mRNA fragments within the cytoplasm of human cells. The adenylated rRNA fragments accumulated upon KD of RNA degradation machinery, showing that they are intermediates in an RNA decay process that involves transient poly(A). Although much remains to be done to decipher the specific functionality of the two tail types, the enzyme(s) that produce them, and the precise mechanism of decay, we have identified a number of exonucleases involved in their degradation.

Materials and methods

Cells

HeLa and HEp-2 cells were grown as a monolayer at 37 °C, 5% CO2, in DMEM (Sigma) supplemented with 10% FCS, 2 mM L-glutamine, and penicillin– streptomycin (Slomovic and Schuster, 2008). Growing and infection of cells with recombinant viruses containing GFP was performed as described (Hsiao *et al*, 2006).

Transient siRNA application

Cells were transfected with 400 pmol siRNA duplex (Table S7) using Lipofectamine 2000 (Invitrogen). After 24 h, cells were detached with trypsin and replated, followed 24 h later by a second transfection with 800 pmol siRNA. Seventy-two hours after the initial transfection, total RNA was harvested with MasterPure kit (Epicentre) or total protein was harvested with an SDS-lysis buffer (1% SDS, 10% glycerol, and 0.1 M DTT).

Cell fractionation

Nuclear and cytoplasmic fractions were obtained from HeLa cells as previously described (van Dijk *et al*, 2007). Briefly, detached cells were washed in PBS solution, resuspended in lysis buffer, incubated on ice for 10 min, and centrifuged for 10 min at 3,000 × g. The supernatant (cytoplasmic fraction) was transferred to a new tube and the pellet (nuclear fraction) was resuspended in lysis buffer and lysed via sonication. Following centrifugation at 12,000 × g for 10 min at 4 °C, RNA was purified from both fractions by the MasterPure kit (Epicenter).

Random-primed RT-PCR and Northern blots

Random-primed RT was performed on 3 μg total RNA using AffinityScript RT (Stratagene) with 500 ng random primers (Amersham Biosciences) and normalized with β-actin by PCR. RNAi silencing efficiency was measured via semiquantitative RT-PCR using random primed cDNA. RNA blot was performed as described previously (Slomovic and Schuster, 2008). The [^{32}P] uniformly labeled antisense riboprobe (beginning at +1 of the mature 5.8S rRNA and ending 48 nt downstream of its 3′ end) was used. The Northern blot to validate cell fractionation was probed with a [^{32}P]-labeled U2, U3, or U5 snoRNA oligonucleotide (Table S7).

Western blot analysis

Proteins were analyzed by 8% to 10% SDS/PAGE gel, transferred to a nitrocellulose membrane, blotted with appropriate antibody (Table S7), and normalized with actin rabbit polyclonal antibody (Santa Cruz Biotechnology).

Oligo(dT) RT-PCR isolation and sequencing of truncated polyadenylated RNA

Briefly, cDNA was generated with dT^{10}-adapter. PCR was applied to cDNA with a gene-specific primer and adapter followed by T/A cloning and sequencing (Slomovic *et al*, 2008a).

PCR labeling assays

For all reactions RNA amounts were measured with ND-1000 NanoDrop and cDNA was normalized according to B2M. The normalized oligo(dT)-primed cDNA was then subjected to 25 PCR cycles with a 28S rRNA-specific forward primer coupled with adapter oligo. Products were used as templates in a second round of PCR-labeling using the same 28S rRNA primer, which was 5′-end [^{32}P]-labeled by PNK and γ-[^{32}P]ATP, and the adapter. The second round lasted five cycles followed by 10 min extension at 72 °C. PCR-labeled products were resolved by 6% denaturing PAGE and autoradiography. EtBr-stained DNA and [^{32}P]-labeled RNA molecules were run on the gels as length markers.

Acknowledgments

We thank Dr. Wen Chang (Academia Sinica, Taiwan) for help with the VV experiments and Dr. Mark Christensen (Georgetown College, Georgetown, Kentucky) for providing us with the fibrillarin antibody. This work was supported by grants from the Israel Science Foundation, the Niedersachsen Foundation, and The Israel Ministry of Science (Israel- Taiwan Collaboration Program).

References

Arigo JT, Eyler DE, Carroll KL, Corden JL (2006) Termination of cryptic unstable transcripts is directed by yeast RNA-binding proteins Nrd1 and Nab3. *Mol Cell* **23:** 841-851

Broyles SS (2003) Vaccinia virus transcription. *J Gen Virol* **84:** 2293-2303

Chen HW, Koehler CM, Teitell MA (2007) Human polynucleotide phosphorylase: location matters. *Trends Cell Biol* **17:** 600-608

Christensen ME, Banker N (1992) Mapping of monoclonal antibody epitopes in the nucleolar protein fibrillarin (B-36) of Physarum polycephalum. *Cell Biol Int Rep* **16:** 1119-1131

Deutscher MP (2006) Degradation of RNA in bacteria: comparison of mRNA and stable RNA. *Nucleic Acids Res* **34:** 659-666

Doma MK, Parker R (2007) RNA quality control in eukaryotes. *Cell* **131:** 660-668

Dziembowski A, Lorentzen E, Conti E, Seraphin B (2007) A single subunit, Dis3, is essentially responsible for yeast exosome core activity. *Nat Struct Mol Biol* **14:** 15-22

Edmonds M (2002) A history of poly A sequences: from formation to factors to function. *Prog Nucleic Acid Res Mol Biol* **71:** 285-389

Garneau NL, Wilusz J, Wilusz CJ (2007) The highways and byways of mRNA decay. *Nat Rev Mol Cell Biol* **8:** 113-126

Heo I, Joo C, Kim YK, Ha M, Yoon MJ, Cho J, Yeom KH, Han J, Kim VN (2009) TUT4 in concert with Lin28 suppresses microRNA biogenesis through pre-microRNA uridylation. *Cell* **138:** 696-708

Houseley J, Tollervey D (2009) The many pathways of RNA degradation. *Cell* **136:** 763-776

Hsiao JC, Chao CC, Young MJ, Chang YT, Cho EC, Chang W (2006) A poxvirus host range protein, CP77, binds to a cellular protein, HMG20A, and regulates its dissociation from the vaccinia virus genome in CHO-K1 cells. *J Virol* **80:** 7714-7728

Kushner SR (2004) mRNA decay in prokaryotes and eukaryotes: different approaches to a similar problem. *IUBMB Life* **56:** 585-594

LaCava J, Houseley J, Saveanu C, Petfalski E, Thompson E, Jacquier A, Tollervey D (2005) RNA degradation by the exosome is promoted by a nuclear polyadenylation complex. *Cell* **121:** 713-724

Lejeune F, Li X, Maquat LE (2003) Nonsense-mediated mRNA decay in mammalian cells involves decapping, deadenylating, and exonucleolytic activities. *Mol Cell* **12:** 675-687

Lykke-Andersen S, Brodersen DE, Jensen TH (2009) Origins and activities of the eukaryotic exosome. *J Cell Sci* **122:** 1487-1494

Lykke-Andersen S, Jensen TH (2006) CUT it out: silencing of noise in the transcriptome. *Nat Struct Mol Biol* **13:** 860-861

Martin G, Keller W (2007) RNA-specific ribonucleotidyl transferases. *RNA* **13:** 1834-1849

Mullen TE, Marzluff WF (2008) Degradation of histone mRNA requires oligouridylation followed by decapping and simultaneous degradation of the mRNA both 5' to 3' and 3' to 5'. *Genes Dev* **22:** 50-65

Neil H, Malabat C, d'Aubenton-Carafa Y, Xu Z, Steinmetz LM, Jacquier A (2009) Widespread bidirectional promoters are the major source of cryptic transcripts in yeast. *Nature* **457:** 1038-1042

Portnoy V, Palnizky G, Yehudai-Resheff S, Glaser F, Schuster G (2008) Analysis of the human polynucleotide phosphorylase (PNPase) reveals differences in RNA binding and response to phosphate compared to its bacterial and chloroplast counterparts. *RNA* **14:** 297-309

Preker P, Nielsen J, Kammler S, Lykke-Andersen S, Christensen MS, Mapendano CK, Schierup MH, Jensen TH (2008) RNA exosome depletion reveals transcription upstream of active human promoters. *Science* **322:** 1851-1854

Proudfoot N, Gullerova M (2007) Gene silencing CUTs both ways. *Cell* **131:** 649-651

San Paolo S, Vanacova S, Schenk L, Scherrer T, Blank D, Keller W, Gerber AP (2009) Distinct roles of non-canonical poly(A) polymerases in RNA metabolism. *PLoS Genet* **5:** e1000555

Schilders G, Pruijn GJ (2008) Biochemical studies of the mammalian exosome with intact cells. *Methods Enzymol* **448:** 211-226

Schmid M, Jensen TH (2008) The exosome: a multipurpose RNA-decay machine. *Trends Biochem Sci* **33:** 501-510

Slomovic S, Laufer D, Geiger D, Schuster G (2006a) Polyadenylation of ribosomal RNA in human cells. *Nucleic Acids Res* **34:** 2966-2975

Slomovic S, Portnoy V, Liveanu V, Schuster G (2006b) RNA polyadenylation in prokaryotes and organelles; Different tails tell different tales. *Critical Reviews in Plant Sciences* **25:** 65-77

Slomovic S, Portnoy V, Schuster G (2008a) Detection and characterization of polyadenylated RNA in Eukarya, Bacteria, Archaea, and organelles. *Methods Enzymol* **447:** 501-520

Slomovic S, Portnoy V, Yehudai-Resheff S, Bronshtein E, Schuster G (2008b) Polynucleotide phosphorylase and the archaeal exosome as poly(A)-polymerases. *Biochim Biophys Acta* **1779:** 247-255

Slomovic S, Schuster G (2008) Stable PNPase RNAi silencing: its effect on the processing and adenylation of human mitochondrial RNA. *RNA* **14:** 310-323

Staals RH, Bronkhorst AW, Schilders G, Slomovic S, Schuster G, Heck AJ, Raijmakers R, Pruijn GJ (2010) Dis3-like 1: a novel exoribonuclease associated with the human exosome. *EMBO J* **29:** 2358-2367

Stoecklin G, Mayo T, Anderson P (2006) ARE-mRNA degradation requires the 5'-3' decay pathway. *EMBO Rep* **7:** 72-77

Thiebaut M, Kisseleva-Romanova E, Rougemaille M, Boulay J, Libri D (2006) Transcription termination and nuclear degradation of cryptic unstable transcripts: a role for the nrd1-nab3 pathway in genome surveillance. *Mol Cell* **23:** 853-864

Thompson DM, Parker R (2007) Cytoplasmic decay of intergenic transcripts in Saccharomyces cerevisiae. *Mol Cell Biol* **27:** 92-101

Tomecki R, Dmochowska A, Gewartowski K, Dziembowski A, Stepien PP (2004) Identification of a novel human nuclear-encoded mitochondrial poly(A) polymerase. *Nucleic Acids Res* **32:** 6001-6014

Trippe R, Guschina E, Hossbach M, Urlaub H, Luhrmann R, Benecke BJ (2006) Identification, cloning, and functional analysis of the human U6 snRNA-specific terminal uridylyl transferase. *RNA* **12:** 1494-1504

van Dijk EL, Schilders G, Pruijn GJ (2007) Human cell growth requires a functional cytoplasmic exosome, which is involved in various mRNA decay pathways. *RNA* **13:** 1027-1035

Vanacova S, Stefl R (2007) The exosome and RNA quality control in the nucleus. *EMBO Rep* **8:** 651-657

Vanacova S, Wolf J, Martin G, Blank D, Dettwiler S, Friedlein A, Langen H, Keith G, Keller W (2005) A new yeast poly(A) polymerase complex involved in RNA quality control. *PLoS Biol* **3:** e189

West S, Gromak N, Norbury CJ, Proudfoot NJ (2006) Adenylation and exosome-mediated degradation of cotranscriptionally cleaved pre-messenger RNA in human cells. *Mol Cell* **21:** 437-443

West S, Gromak N, Proudfoot NJ (2004) Human 5' --> 3' exonuclease Xrn2 promotes transcription termination at co-transcriptional cleavage sites. *Nature* **432:** 522-525

Widlak P, Garrard WT (2005) Discovery, regulation, and action of the major apoptotic nucleases DFF40/CAD and endonuclease G. *J Cell Biochem* **94:** 1078-1087

Wilusz CJ, Wilusz J (2008) New ways to meet your (3') end oligouridylation as a step on the path to destruction. *Genes Dev* **22:** 1-7

Wyers F, Rougemaille M, Badis G, Rousselle JC, Dufour ME, Boulay J, Regnault B, Devaux F, Namane A, Seraphin B, Libri D, Jacquier A (2005) Cryptic pol II transcripts are degraded by a nuclear quality control pathway involving a new poly(A) polymerase. *Cell* **121:** 725-737

Xu Z, Wei W, Gagneur J, Perocchi F, Clauder-Munster S, Camblong J, Guffanti E, Stutz F, Huber W, Steinmetz LM (2009) Bidirectional promoters generate pervasive transcription in yeast. *Nature* **457:** 1033-1037

Supplementary Figures

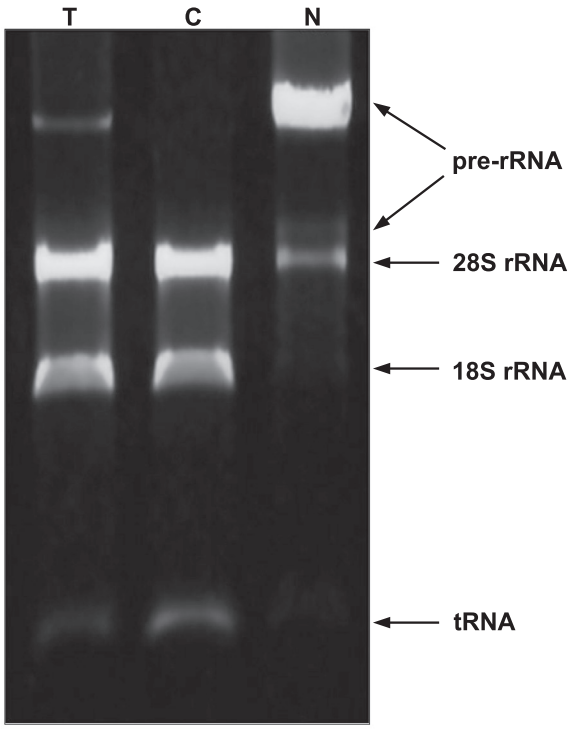

Figure S1. The distribution of rRNAs and tRNAs in the cytoplasm and nucleus.

Following fractionation, RNA purified from the cytoplasm and nucleus was stained with EtBr and the profile (rRNA and tRNA distribution) was compared between the two fractions and total RNA. T, total cell RNA; C, cytoplasmic RNA; N, nuclear RNA.

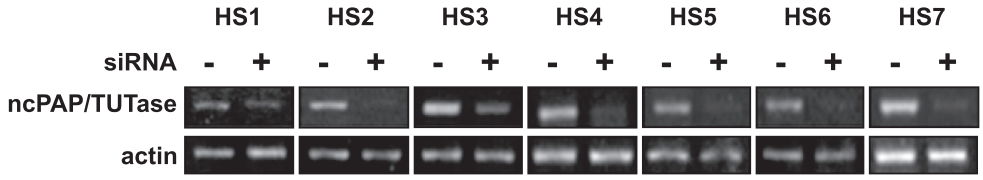

Figure S2. RNAi-mediated silencing of the seven-member ncPAP family in HeLa cells: HS1–HS7.

HeLa cells were transfected with siRNA targeting each of theseven human noncanonical PAPs. RT-PCR was used to evaluate KD of the expression levels of the targeted mRNAs in the RNAi cells compared with the mock transfection cells.

Supplementary Tables

Table S1. Truncated, polyadenylated 28S rRNA and β-actin mRNA molecules isolated from HeLa cells using oligo(dT) RT-PCR.

Fraction	Gene	Clone	Poly(A) site	Tail length and content
Cytoplasm	28S rRNA	1	1565	$A_7GA_9CA_7GA_3CA_2CA_{12}GA_{10}$
		2	1615	$A_5UGA_7GA_5GA_2GA_4UA_4GA_8GA_4$ $UA_2UGA_5CAGA_7GA_2GA_8UA_{11}$
		3	1679	$A_2GA_2GA_9$
		4	1695	A_{80}
		5	1698	A_{46}
		6	1699	A_{16}
		7	1777	A_{97}
		8	4598	$A_3GA_3UA_3UA_2UA_{11}$
		9	4607	A_{12}
		10	4610	A_8UA_9
		11	4620	$A_3UA_3UA_{20}$
		12	4623	A_3CA_8
		13	4640	A_8UA_{14}
		14	4646	$GA_{12}GA_2GA_7GA_2UA_9$
		15	4699	A_{15}
		16	4700	$A_2GAGAGA_2GA_2G_6A_2GAGA_2GAG_5$ $A_6GA_4G_2AGA_4GA_2GA_9$
		17	4700	A_{20}
		18	4701	$A_6UA_5GAGA_{10}GA_6UAGA_{21}$
Nucleus		1	1615	$GA_2GA_3GA_2CA_3GAGA_2GAGAGA_3A_2$ $G_4A_4G_2A_3GA_4GA_3GA_9$
		2	1685	$A_2GA_3G_3AGAGAGA_2G_2A_7G_2AG_2AUA_3$ $GAG_2AGA_4G_2AGA_4G_2AG_2A_8$
		3	1700	A_{12}
		4	4599	A_{17}
		5	4620	$A_3GAUGAGA_3GA_6GAG_2A_4G_2A_2GA_3GA_6$ $G_2A_2UAGA_2G_2ACAGA$ $G_2A_6UGAG_2A_4GA_4GAG_2A_6UGA_2G_2$ $AGA_{14}GA_{11}$
		6	4623	$A_{32}GA_{37}$
		7	4623	A_{11}
		8	4634	A_{12}
		9	4656	$C_2G_2UA_{26}$
		10	4678	UAU_2A_{15}
		11	4681	$A_{11}GA_{11}$
		12	4687	A_{12}
Total	β-actin	1	1875	A_{61}
		2	1877	$A_3UA_2UA_{17}$
		3	1878	A_{19}
		4	1879	A_{59}
		5	1879	A_{10}
		6	1881	$ACA_3UA_{29}UA_{52}$
		7	1885	A_{23}
		8	1887	A_{15}
		9	1903	$AU_3A_4UA_{12}$

Fraction	Gene	Clone	Poly(A) site	Tail length and content
		10	1910	A_{12}
		11	1927	$GA_6GA_{38}GA_{58}$
		12	1948	$CA_{65}UA_{42}$
		13	2093	A_{14}
		14	2207	$A_{10}GA_8GA_{11}GAAACA_8GAGA_9$ $GAGA_5GA_{12}GA_{21}GA_{20}$
		15	2258	A_{10}
		16	2259	A_{18}
		17	2259	$U_4A_5GA_4UA_{10}$
		18	2259	$A_3GA_2GAGA_9G_2A_5GA_9GAUA_3G_2A_{10}$
		19	2260	A_{19}
		20	2261	A_{19}
		21	2266	A_{25}
		22	2266	$A_3UA_4U_2A_{20}$
		23	2277	A_{79}
		24	2425	A_{15}
		25	2468	CA_3GA_{19}
		26	2492	$A_4UACA_5UA_{11}$
		27	2556	A_{14}
		28	2923	A_{55}
		29	2923	A_{30}
Cytoplasm		1	1876	A10
		2	1901	A_{61}
		3	1976	A_{22}
		4	2005	A_{10}
		5	2923	A_{18}
		6	2923	A_{10}
Nucleus		1	1873	A_2GA_{81}
		2	1901	$UA_{14}CA_{25}$
		3	1901	A_{25}
		4	1911	A_{11}
		5	2921	CA_{15}
		6	2923	A_{38}

Table S2. Truncated, 28S rRNA molecules isolated from cytoplasmic or nuclear fractions from HeLa cells using circularized RT-PCR.

Clone	Fraction	Start	End	Tail	Comment
6	nuc	4345	4568	A	or 4569 no A
49		4335	4594		
66		4421	4553	A	or 4554 no A
15		4523	4659		
37		4528	4624		
38		4519	4623	A	or 4518 no A
40		4510	4758		
44		4523	4659		
46		4486	4766		
97		4511	4624		
99		4510	4623		
100		4511	4702		
104		4492	4623		
109		4510	4660		
112		4522	4623		
114		4510	4620	A	or 4621 no A
25		4522	4628		
26		4461	4702		
27		4416	4710		
28		4457	4754		
30		4451	4703	A	or 4450 no A
31		4511	4624		
33		4361	4658		
19	cyt	4459	4552	A	or 4458 no A
20		4321	4610		
64		4435	4587		
7		4510	4757		
26		4511	4741		
27		4501	4710		
28		4519	4697	A	or 4518 no A or 4698 no A
31		4526	4691	GAA	
34		4510	4757		
35		4520	4667		
36		4492	4650		
74		4448	4691	A	or 4447 no A or 4692 no A
80		4524	4653	A	or 4523 no A or 4654 no A
82		4522	4660	AA	or 4662 no A
85		4526	4631	UAAA	
86		4513	4666		or 4664 +GC
87		4456	4648		
90		4522	4701		
93		4521	4653		
94		4524	4623		
19		4522	4630		
20		4510	4705		
22		4455	4705		

*In many cases it is not certain whether the observed adenosine is encoded in the corresponding transcript sequence (either at the 5' or 3' end of the sequenced molecule) or post-transcriptionally added.

Table S3. Truncated, polyadenylated G8R (viral mRNA) and GFP (gene integrated into VV genome) molecules isolated from HeLa cells 4 h after VV infection using oligo(dT) RT-PCR.

Gene/clone	Poly(A) site	Tail length and content
G8R		
1	164	$A_{10}U_3A_9UA_{39}$
2	166	$A_8U_5A_{53}$
3	204	$A_8U_2A_{10}$
4	210	UA_{32}
5	214	A_{11}
6	227	A_{96}
7	233	U_2A_{58}
8	246	UCU_2A_{11}
9	255	$AU_2AUCUAUA_3UA_5U_2A_{11}$
10	289	A_{15}
11	293	$A_4UA_{26}GA_{29}$
12	299	A_{21}
13	301	$A_{10}UA_5U_3CA_{11}$
14	307	A_{22}
15	348	UA_{38}
16	365	$A_{11}GAUA_4UA_{11}$
GFP		
1	289	A_{11}
2	298	A_{18}
3	303	UA_{13}
4	354	A_{15}
5	367	U_2A_{13}
6	378	UA_{14}
7	392	UA_{11}
8	416	U_2A_{14}
9	496	A_{25}
10	529	A_{10}
11	561	A_{13}
12	564	$U_2A_{10}UA_{12}$
13	578	A_{10}

Table S4. Truncated, polyadenylated transcripts detected in S. cerevisiae.

Clone	Gene	Poly(A) site	Tail length and content
1	CYH2	347	A_{13}
2	Actin1	373	AGA_{12}
3	Actin1	431	A_{10}
4	Actin1	466	A_{11}
5	Actin1	569	A_{11}
6	25S rRNA	2082	A_{12}
7	25S rRNA	2091	A_{10}
8	25S rRNA	2147	A_{12}
9	25S rRNA	2154	A_{10}
10	25S rRNA	2159	A_{11}
11	25S rRNA	2174	A_{14}
12	25S rRNA	2192	A_{10}
13	25S rRNA	2249	A_{15}
14	25S rRNA	2269	A_{12}
15	25S rRNA	2275	A_{14}
16	25S rRNA	2275	A_3UA_{25}
17	25S rRNA	2302	A_{11}
18	25S rRNA	2312	A_{13}
19	25S rRNA	2313	A_{10}

*CYH2-ribosomal protein gene CYH2.

Table S5. Truncated, polyadenylated 28S rRNA molecules isolated from HeLa cells subjected to siRNA silencing of the proteins as indicated.

Clone	RNAi- silenced gene	Poly(A) site	Poly(A) tail length and content
1	mock	2540	UA_{20}
2	mock	2586	A_{16}
3	mock	4534	A_{14}
4	mock	4536	$A_{20}UA_2$
5	mock	4598	AUA_{18}
6	mock	4598	$AG_2AGA_2GA_3G_3A_9$
7	mock	4598	$A_8GA_2CA_{15}$
8	mock	4600	A_{12}
9	mock	4600	A_{23}
10	mock	4604	A_{26}
11	mock	4617	A_{44}
12	mock	4619	$A_9G_2A_4GAGAGAGA_2UGA_{21}$
13	mock	4638	A_{12}
14	mock	4645	A_9
15	mock	4647	A_{14}
16	mock	4653	A_{11}
17	mock	4662	A_{17}
18	mock	4669	AGA_5GA_{13}
19	mock	4681	$GA_4CA_{10}G_2A_6CA_4GA_3GAG_2AGAGA_5CA_{10}G_2A_{10}$
20	mock	4691	GA_{11}
21	mock	4692	A_3GA_{11}
22	mock	4692	A_{18}
23	mock	4699	A_{20}
24	mock	4701	A_{20}
25	mock	4710	$A_2GA_2G_2AGCAGAGA_3G_3AG_2AG_2A_2G_2A_3UA_{10}GA_{22}$
26	mock	4713	$AC_2GA_6GAG_2A_3GA_2GAG_3AUA_3UGUCGACUCA_3GAGA_2UA_6$
1	hRrp41	4596	A_{17}
2	hRrp41	4598	A_{21}
3	hRrp41	4598	A_4GA_9
4	hRrp41	4598	A_{33}
5	hRrp41	4598	AGA_{13}
6	hRrp41	4598	A_3GUGA_9
7	hRrp41	4599	A_{14}
8	hRrp41	4603	A_{23}
9	hRrp41	4603	$A_{13}GA_9$
10	hRrp41	4605	$A_{12}GA_{14}$
11	hRrp41	4611	ACA_{12}
12	hRrp41	4626	A_{22}
13	hRrp41	4627	$A_4GA_6GA_{11}GA_{33}$
14	hRrp41	4647	$ACGA_{26}$
15	hRrp41	4652	$A_{10}GA_5CA_8GA_4UG_2AG_2A_6GA_3CA_2GA_2CA_{20}$
16	hRrp41	4686	A_{26}
17	hRrp41	4693	$A_{17}GA_3$
18	hRrp41	4728	A_4CA_{12}
19	hRrp41	4729	$A_4GA_2GA_{15}$

1	PM/Scl-75	4547	AUA_{10}
2	PM/Scl-75	4551	$GA_6GAG_3AGAG_3AGAGA_5UA_{20}$
3	PM/Scl-75	4585	A_{19}
4	PM/Scl-75	4586	A_7UACA_8
5	PM/Scl-75	4599	A_{54}
6	PM/Scl-75	4599	GA_7GA_{15}
7	PM/Scl-75	4599	A_{10}
8	PM/Scl-75	4599	A_5CA_6GA
9	PM/Scl-75	4601	A_{20}
10	PM/Scl-75	4603	A_{16}

Clone	RNAi- silenced gene	Poly(A) site	Poly(A) tail length and content
11	PM/Scl-75	4607	$A_7UA_6GA_7GA_7UA_{17}$
12	PM/Scl-75	4609	A_{19}
13	PM/Scl-75	4612	A_{26}
14	PM/Scl-75	4619	A_{16}
15	PM/Scl-75	4621	A_{12}
16	PM/Scl-75	4676	$AU_4AUA_2UA_6CA_8U_2A_5GA_{11}$
17	PM/Scl-75	4681	$GA_{10}GA_9$
18	PM/Scl-75	4687	$A_7GA_5CA_8$
19	PM/Scl-75	4687	AGA_8GA_7
20	PM/Scl-75	4690	AGA_8
21	PM/Scl-75	4691	$A_3G_2A_4CA_3UA_9$
22	PM/Scl-75	4694	$AGUAUA_6GA_4GA_{20}GA_2$
23	PM/Scl-75	4696	$AG_3A_3GAGAGAGAGAUAG_2AG_2A_5GA_8GAGA_{20}$
24	PM/Scl-75	4712	$A_5GA_2GA_{40}$
1	PM/Scl-100	4533	A_{17}
2	PM/Scl-100	4590	A_5CA_{18}
3	PM/Scl-100	4593	A_{12}
4	PM/Scl-100	4594	$A_6UA_9GA_{19}$
5	PM/Scl-100	4597	A_{18}
6	PM/Scl-100	4598	A_3GAUA_{12}
7	PM/Scl-100	4598	ACA_{15}
8	PM/Scl-100	4598	A_{10}
9	PM/Scl-100	4599	A_{10}
10	PM/Scl-100	4601	A_{16}
11	PM/Scl-100	4603	$A_2GA_{17}GA$
12	PM/Scl-100	4603	A_6GA_{15}
13	PM/Scl-100	4604	AGA_{17}
14	PM/Scl-100	4609	$GAUA_{11}$
15	PM/Scl-100	4618	$A_2GA_3GA_2GAGAGA_{14}$
16	PM/Scl-100	4619	A_{20}
17	PM/Scl-100	4620	A_{12}
18	PM/Scl-100	4620	A_{17}
19	PM/Scl-100	4621	A_{34}
20	PM/Scl-100	4650	A_{29}
21	PM/Scl-100	4674	$U_4A_{11}GA_{15}$

22	PM/Scl-100	4675	A_{37}
23	PM/Scl-100	4681	GA_2CGA_{10}
24	PM/Scl-100	4692	$A_5GA_5UGA_3UAGCA_6GA_6CA_6$
25	PM/Scl-100	4692	A_7CA_8
26	PM/Scl-100	4693	$A_3UA_2CUGA_2CA_4GA_2CUA_2CA_{18}$
27	PM/Scl-100	4697	$A_3UA_2UA_8UA_{12}$
28	PM/Scl-100	4698	A_{24}
29	PM/Scl-100	4699	A_8GA_{18}
30	PM/Scl-100	4702	A_{13}
31	PM/Scl-100	4702	$A_4GA_2CA_9$
32	PM/Scl-100	4702	$A_7GA_8GACA_7$
33	PM/Scl-100	4703	A_4UA_{14}
34	PM/Scl-100	4736	A_{33}
1	hPNPase	4595	A_{19}
2	hPNPase	4598	A_{15}
3	hPNPase	4602	$A_4GA_6GA_{14}CA_2GA_8G_2A_{18}$
4	hPNPase	4603	$A_2UA_2GCA_3GA_3GA_{10}$
5	hPNPase	4603	A_2CA_{12}
6	hPNPase	4604	$A_2UA_5UAGA_9$
7	hPNPase	4604	$A_2UGA_5CGA_2CA_{11}$
8	hPNPase	4604	$AUA_7GA_3UA_2CACGAUA_6GA_5GA_3GA_3GAGAG_4A_2G_2AGAGUA_3CA_{10}$
9	hPNPase	4605	$AGA_2GA_2GAG_2A_4GA_2GA_2GACGAGA_3UA_{13}$
10	hPNPase	4621	A_{11}
11	hPNPase	4681	GCA_9
12	hPNPase	4681	$GA_2CGAUA_5UA_{16}$
13	hPNPase	4687	AGA_{12}
14	hPNPase	4691	A_{10}
15	hPNPase	4691	$G_5A_3CA_{14}$
16	hPNPase	4692	A_{13}
17	hPNPase	4692	ACA_{14}
18	hPNPase	4693	A_{10}
19	hPNPase	4694	A_{13}
20	hPNPase	4694	A_{15}
21	hPNPase	4697	$A_5U_2GA_2GA_5GA_{20}$

*Tails with one non-A residue or less are termed homopolymeric.

Table S6. Truncated, polyadenylated 28S rRNA molecules isolated from HeLa cells subjected to siRNA silencing of the proteins as indicated (Hs1-7 of the ncPAP family in human cells).

RNAi-silenced gene	Tail site	Tail sequence
mock	4598	A_{20}
	4664	A_{53}
	4598	A_{18}
	4692	$A_{13}G_2A_5$
HS1	4740	UA_{12}
	4599	A_{12}
	4659	A_5UACA_{10}
	4678	UA_{11}
	4679	A_{97}
HS2	4598	A_{37}
	4681	$A_{24}GA_{21}$
	4583	$A_4UCA_2UA_2UACGAUA_5GA_9CA_9$
HS3	4572	A_{17}
	4691	$G_2A_2GA_{10}$
	4676	$AU_8A_2UA_8UA_{10}$
HS4	4722	$GA_6UA_6UA_8$
	4621	$A_3GA_2GA_4UAUGNGA_3CAC_2UCGA_3$ $UCAUA_2UC_3GC_3NAUA_{15}$
	4604	$AGA_2G_2AG_2A_5GA_7GAG_2AGA_2GA_5GA_2$ $GAG_2AG_3A_3GA_2GA_2GAG_2A_3GA_2GA_4$ $GAG_3AGA_2G_2A_2GA_2GA_2G_2A_2GA_5GA_2$ $G_3A_2G_2AGAGA_6UA_2GA_2G_2A_{17}$
	4678	UA_{11}
	4604	A_{30}
	4722	A_{104}
HS5	4640	A_5UA_{13}
	4599	$G_3AG_2A_3GAGA_4GAGA_2G_3A_2GA_2GA_2GAG_2A_3$ $GA_2GA_2GA_2GAG_3AGA_4GA_2GA_6GA_3GA_2UA_{10}$
	4656	$C_2G_2UA_{20}GA_{22}$
	4701	$A_{12}GA_{10}$
	4603	A_{16}
	4594	A_{13}
HS6	4696	A_{15}
	4756	$C_2A_3GA_2UA_{10}$
	4670	$A_{19}GA_8GUA_4GA_5GAUA_4GA_7GA_{10}$
	4535	$CA_2UA_{18}GA_{67}$
HS7	4619	$C_2A_2UG_2AGA_{75}$

Table S7. Oligonucleotides, antibodies, and RNAi target sequences used in this work.

Oligo name	Gene	Organism	Position	Direction	Application	Sequence 5' 3'
dT adapter	–	–	–	Reverse	dT-RT-PCR	GACTCGAGTCGACATCGAT10
adapter	–	–	–	Reverse	dT-RT-PCR	GACTCGAGTCGACATCGAT
28S rRNA A	28S rRNA	*H. sapiens*	1501	Forward	dT-RT-PCR	GAAAGATGGTGAACTATGCC
28S rRNA B	28S rRNA	*H. sapiens*	1529	Forward	dT-RT-PCR	GCGAAGCCAGAGGAAAC
28S rRNA C	28S rRNA	*H. sapiens*	1548	Forward	dT-RT-PCR	TGGTGGAGGTCCGTAGC
28S rRNA 2	28S rRNA	*H. sapiens*	4479	Forward	dT-RT-PCR	CGTGAGCTGGGTTTAGAC
28S rRNA 3	28S rRNA	*H. sapiens*	4497	Forward	dT-RT-PCR cRT-	CGTCGTGAGACAGGTTAG
28S rRNA last	28S rRNA	*H. sapiens*	4517	Forward	dT-RT-PCR cRT-	TTACCCTACTGATGATGTG
28S R101	28S rRNA	*H. sapiens*	4496	Reverse	cRT-PCR	GTCTAAACCCAGCTCACG
28S R102	28S rRNA	*H. sapiens*	4466	Reverse	cRT	GGGTGAACAATCCAACGC
28S int2	28S rRNA	*H. sapiens*	4561	Reverse	cRT	ACTGAGCAGGATTACCATG
28S int3	28S rRNA	*H. sapiens*	4538	Reverse	cRT	CAACACATCATCAGTAGGGT
28S F101	28S rRNA	*H. sapiens*	4573	Forward	cRT	CGCAGGTTCAGACATTTGG
28S F102	28S rRNA	*H. sapiens*	4592	Forward	cRT	TGTATGTGCTTGGCTGAGG
5.8S rRNA F1	5.8S rRNA	*H. sapiens*	1	Forward	Northern blot	CGACTCTTAGCGGTGGAT
5.8S rRNA R1	5.8S rRNA	*H. sapiens*	*	Reverse	Northern blot	CCGCGCACCCCGAGGAG
U2 snoRNA	U2 snoRNA	*H. sapiens*	188	Reverse	Northern blot	GGGTGCACCGTTCCTGGAGGTACTGCAATA
U3 snoRNA	U3 snoRNA	*H. sapiens*	217	Reverse	Northern blot	ACCACTCAGACCGCGTTCTCTCCCTCTCAC
U5 snoRNA	U5 snoRNA	*H. sapiens*	88	Reverse	Northern blot	TTGGGTTAAGACTCAGAGTTGTTCCTCTCC
PM/Scl-75 F	PM/Scl-75	*H. sapiens*	734	Forward	RT-PCR	CCAATGAACGAGAAGAACG
PM/Scl-75 R	PM/Scl-75	*H. sapiens*	1166	Reverse	RT-PCR	CCTTCATCATCTTCCTTCTCAG
β-actin N	actin	*H. sapiens*	309	Forward	dT-RT-PCR	GGGACGACATGGAGAAAATC
β-actin E	actin	*H. sapiens*	328	Forward	dT-RT-PCR	CTGGCACCACACCTTCTAC
β-actin M	actin	*H. sapiens*	346	Forward	dT-RT-PCR	CAATGAGCTGCGTGTGG
β-actin I	actin	*H. sapiens*	700	Forward	dT-RT-PCR	GCGTGACATTAAGGAGAAGC
β-actin W	actin	*H. sapiens*	730	Forward	dT-RT-PCR	CGCCCTGGACTTCGAG
β-actin S	actin	*H. sapiens*	747	Forward	dT-RT-PCR	AAGAGATGGCCACGGC
β-actin R3	actin	*H. sapiens*	632	Reverse	RT-PCR	GAGGATCTTCATGAGGTAGTC
hDis3 F2	Dis3	*H. sapiens*	1288	Forward	RT-PCR	GCGAGAAAATGTTGAAGCC
hDis3 R2	Dis3	*H. sapiens*	1670	Reverse	RT-PCR	CTTTTCAGTAATGCTCCAGG
hRrp40 F2	Rrp40	*H. sapiens*	586	Forward	RT-PCR	AATGGAATGGGTGTCATTGG
hRrp40 R1	Rrp40	*H. sapiens*	1011	Reverse	RT-PCR	ACAAAAGCGTGGGTGAAAAC
hDis3L1 F2	Dis3L	*H. sapiens*	2360	Forward	RT-PCR	TCCATCATTACGGTCTTGC
hDis3L1 R2	Dis3L	*H. sapiens*	2864	Reverse	RT-PCR	TGGTCAAACAAATGGAACG
Lsm1F1	Lsm1	*H. sapiens*	163	Forward	RT-PCR	GCATTGCAGCATTATTTC
Lsm1R1	Lsm1	*H. sapiens*	657	Reverse	RT-PCR	CCAGGATGTCACTTTCAC

Oligo name	Gene	Organism	Position	Direction	Application	Sequence 5' 3'
hXrn2F1	hXrn2	*H. sapiens*	1003	Forward	RT-PCR	TCCTTCGGCTTAATGTTCTTC
hXrn2R1	hXrn2	*H. sapiens*	1541	Reverse	RT-PCR	AGATGTGAAACTCGTATTAGG
HS1 F1	HS1	*H. sapiens*	551	Forward	RT-PCR	GCAGACTTGTCTAGAGCTGTG
HS1 R1	HS1	*H. sapiens*	1202	Reverse	RT-PCR	CTCGAATCAGCTGAGGTCTCTC
HS2 F1	HS2	*H. sapiens*	630	Forward	RT-PCR	GGTTATAGGTGGCAAGACACAAG
HS2 R1	HS2	*H. sapiens*	1166	Reverse	RT-PCR	CAGCCTCTGTTCCAAGTTCTC
HS3 F1	HS3	*H. sapiens*	594	Forward	RT-PCR	GGCAACCAGTTTACAGGCAAAAGC
HS3 R1	HS3	*H. sapiens*	946	Reverse	RT-PCR	CGTCCGATACGTCTTCAATTCC
HS4 F1	HS4	*H. sapiens*	879	Forward	RT-PCR	TTGCAACTCAGAAGATCC
HS4 R1	HS4	*H. sapiens*	1090	Reverse	RT-PCR	TCTTGAGTCTAGGGCACC
HS5 F1	HS5	*H. sapiens*	2052	Forward	RT-PCR	GGACAGAAAAACTGCTGTGAGG
HS5 R1	HS5	*H. sapiens*	2161	Reverse	RT-PCR	TGCACCATCTCTCCAACCTCTA
HS6 F1	HS6	*H. sapiens*	938	Forward	RT-PCR	GGTCCTATCCAAACAGAGACG
HS6 R1	HS6	*H. sapiens*	1472	Reverse	RT-PCR	GTTCCTTCTACACCAGCTTGTC
HS7 F1	HS7	*H. sapiens*	994	Forward	RT-PCR	GAGTAACAGATGAAGTTGCCAC
HS7 R1	HS7	*H. sapiens*	1489	Reverse	RT-PCR	GTTTGAGTTGTACCTTGGAAGC
G8R A	G8R	VV	105	Forward	dT-RT-PCR	GTATATTTTTGCCGCCTTG
G8R B	G8R	VV	121	Forward	dT-RT-PCR	TTGGGCGGATCTGTAAAC
G8R C	G8R	VV	140	Forward	dT-RT-PCR	TTTGGGCCATTATACCTCTC
GFP 1	GFP	VV	187	Forward	dT-RT-PCR	ACCACCCTGACCTACGGC
GFP 2	GFP	VV	218	Forward	dT-RT-PCR	GCCGCTACCCCGACC
GFP 3	GFP	VV	231	Forward	dT-RT-PCR	CCACATGAAGCAGCACG
GFP A	GFP	VV	391	Forward	dT-RT-PCR	TTCAAGGAGGACGGCAAC
GFP B	GFP	VV	409	Forward	dT-RT-PCR	ATCCTGGGGCACAAGC
GFP C	GFP	VV	431	Forward	dT-RT-PCR	ACAACTACAACAGCCACAACG
25S rRNA I	25S rRNA	*S. cerevisiae*	1959	Forward	dT-RT-PCR	GCAGGTCTCCAAGGTGAAC
25S rRNA L	25S rRNA	*S. cerevisiae*	1994	Forward	dT-RT-PCR	AATAATGTAGATAAGGGAAGTCG
25S rRNA M	25S rRNA	*S. cerevisiae*	2018	Reverse	dT-RT-PCR	CAAAATAGATCCGTAACTTCG
Act1 2	Act1	*S. cerevisiae*	253	Reverse	dT-RT-PCR	ATCTGGCATCATACCTTCTAC
Act1 3	Act1	*S. cerevisiae*	275	Forward	dT-RT-PCR	ACGAATTGAGAGTTGCCC
Act1 4	Act1	*S. cerevisiae*	289	Forward	dT-RT-PCR	GCCCCAGAAGAACACCC
CYH2 3	CYH2	*S. cerevisiae*	51	Forward	dT-RT-PCR	CGGTAAAGGTCGTATCGG
CYH2 4	CYH2	*S. cerevisiae*	69	Forward	dT-RT-PCR	TAAGCACAGAAAGCACCCC
CYH2 5	CYH2	*S. cerevisiae*	87	Forward	dT-RT-PCR	CGGTGGTAGAGGTATGGC

RNAi target mRNA (gene)	Target sequence	Source (ref.)
hPM/Scl100	guuucgagagaagauugau	(West *et al*, 2006)
hPM/Scl-75	caucgagagauuuguacua	(West *et al*, 2006)
hRrp41	ugugcaggugcuacaggca	(van Dijk *et al*, 2007)
hRrp40	cacgcacaguacuagguca	(Preker *et al*, 2008)
hDis3	agguagaguuguaggaaua	(Preker *et al*, 2008)
hDis3L	cagucagaaccuuaaauaa	Present study
Lsm1	ccagcaaguauccauugaa	(Mullen and Marzluff, 2008)
hXrn2	aagaguacagaugaucaug	(West *et al*, 2004)
hXrn1	ugaugauguucacuuuaga	(Stoecklin *et al*, 2006)
HS1	cguuagugcuggugauuaa	(Mullen and Marzluff, 2008)
HS2	gaaaagaggcacaagaaaa	(Mullen and Marzluff, 2008)
HS3	ugauagugcuucaggaauu	(Mullen and Marzluff, 2008)
HS4	gaucgaccuuccauaucaa	(Tomecki *et al*, 2004)
HS5	gcagccaauuacugccgaa	(Trippe *et al*, 2006)
HS6	cuacgguaccaauaauaaa	(Mullen and Marzluff, 2008)
HS7	ggacgacacuucaauuauu	(Mullen and Marzluff, 2008)

Antibody	Source (ref.)
Actin	Santa Cruz Biotechnology
GAPDH	Santa Cruz Biotechnology
Histone H3	Abcam
hPM/Scl100	(Schilders and Pruijn, 2008)
hRrp41	(Schilders and Pruijn, 2008)
fibrillarin	(Christensen and Banker, 1992)
hXrn1	Novus Biologicals

*48 nt downstream mature 3' end

CHAPTER 5

Exoribonuclease activity of the human RNA exosome

Raymond H.J. Staals[1], Erwin L. van Dijk[2], Judith Stammen-Vogelzangs[1], Victoria Horns[1], Geurt Schilders[1], Ger J.M. Pruijn[1]*

[1] Department of Biomolecular Chemistry, Nijmegen Center for Molecular Life Sciences and Institute for Molecules and Materials, Radboud University Nijmegen, Nijmegen, The Netherlands

[2] Centre de Génétique Moléculaire, Allée de la Terrasse, 91198 Gif-sur-Yvette, France

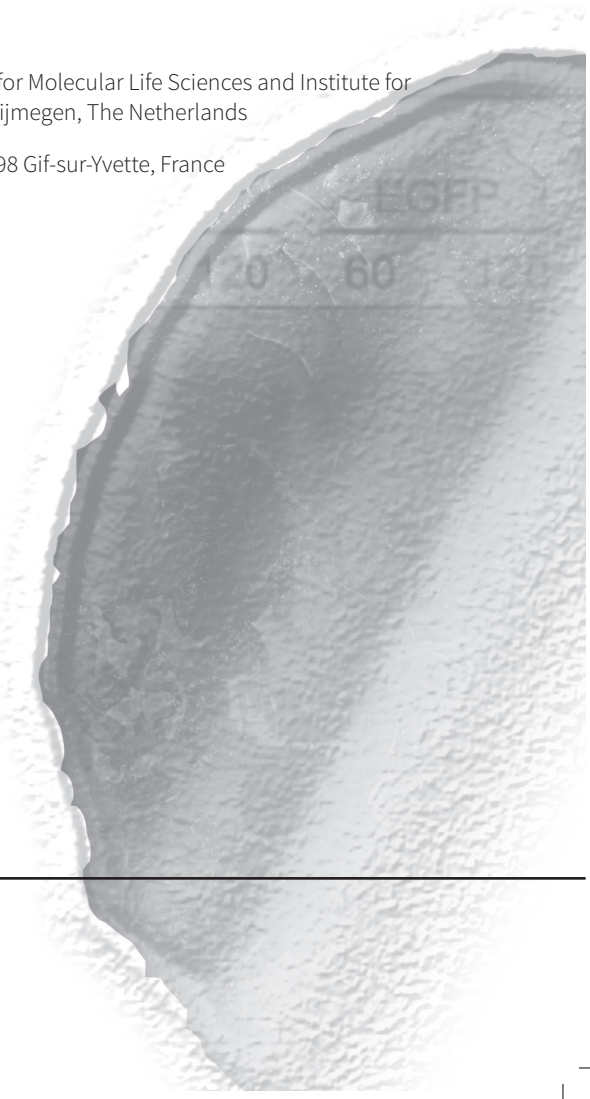

Manuscript in preparation

Abstract

The RNA exosome is a highly conserved protein complex with 3'-5' exoribonuclease activity, which plays a pivotal role in the degradation and maturation of a wide variety of RNAs. The enzymatic activity of the human exosome originates from the association of at least three different exoribonucleases: hDis3, hDis3L1 (Dis3-like exonuclease 1) and PM/Scl-100. Here, we addressed the question to what extent these enzymes contribute to the activity of the human exosome. The results show that the activity of immunoaffinity-purified exosome complexes at relatively high magnesium concentrations is mediated by the association of PM/Scl-100, whereas the activity at low magnesium concentrations can be attributed to hDis3 and hDis3L1. The activity of PM/Scl-100 is dependent on the 35EXOc and HRDC domains, but does not require the association with the exosome core. Our data suggest that the activity of exosome-associated PM/Scl-100 is modulated by other proteins that co-purify with the exosome. Furthermore, the associations of hDis3L1 and PM/Scl-100 with the exosome core seem to affect each other as suggested by the results of siRNA-mediated knock-down experiments. Taken together, our data indicate that the activity of the human RNA exosome is dependent on several exoribonucleases, which may act in concert, but which may also be active in a mutually exclusive manner depending on the microenvironment.

Introduction

Proper RNA metabolism is a fundamental aspect of all cellular forms of life. Next to the role of RNA in conferring the transition of the genetic information embedded in the genome into functional proteins, cellular RNAs are widely used for many different purposes. Structural frameworks (e.g. rRNAs), enzymatic activity (e.g. ribozymes) and gene regulation (e.g. miRNAs) are just a few examples to illustrate this. Central to the homeostasis of all these different RNA species is a protein complex that has been conserved from archaea to higher eukaryotes: the exosome.

The name for this protein complex is derived from the associated 3'-5' exoribonuclease activity. The cellular role of exosome complexes can be divided into two types of processes: maturation of cellular RNAs such as the ribosomal 5.8S RNA, snRNAs and snoRNAs and degradation of all kinds of RNA transcripts (Lykke-Andersen *et al*, 2009).

While its molecular composition might be different among species, the overall structure of the exosome is largely the same: a six-membered, donut-shaped ring, consisting of proteins that share homology with the RNase PH-like ribonucleases (Mitchell *et al*, 2003), and two or three other proteins with potential RNA-binding capacities that are stacked on one side of the donut (Liu *et al*, 2006; Raijmakers *et al*, 2002). Although eubacteria might not have an exosome complex per se, similar exoribonuclease complexes (e.g. RNase PH and PNPase) can be discerned. Given their structural similarities, it seems likely that these complexes are evolutionary conserved and have arisen from a common ancestor (Lin-Chao *et al*, 2007).

The human core exosome adopts a similar structure; a ring of six different proteins (hRrp41, hRrp42, hMtr3, OIP2, hRrp46 and PM/Scl-75), which is stabilized by the association of the three RNA-binding proteins (hRrp4, hRrp40 and hCsl4). Since exosomes, or exosome-like complexes, seem to be conserved in terms of structure, it is likely that their mechanisms to recruit and degrade RNA substrates is conserved as well (Buttner *et al*, 2005; Lorentzen *et al*, 2005). In the archaeal exosome model, substrate RNA is recruited by the RNA-binding proteins, which guide it into the central channel of the complex. Here, the active site is formed by the Rrp41-Rrp42 dimer, which has been shown to confer the phosphorolytic exoribonuclease activity associated with the complex. While this mechanism seems to hold true for the archaeal complex, eukaryotic exosome complexes (with the exception of plants) appear to have diverged from this way of degrading their RNA substrates, as the core of the yeast and human exosome were shown to be devoid of any ribonucleolytic activity (Dziembowski *et al*, 2007; Liu *et al*, 2006). Instead, the eukaryotic exosome core appears to function as a scaffold for the association of one or more hydrolytic exoribonucleases, which dock to the complex and provide it with ribonuclease activity. In yeast, two of such anchoring exoribonucleases, Rrp6 (counterpart of human PM/Scl-100) and Dis3, have been identified.

The Dis3 protein belongs to the RNR family of hydrolytic exoribonucleases (Mitchell *et al*, 2003), which includes well known members, like RNase R and RNase II. The overall domain architecture of these enzymes is largely the same: a central exoribonuclease domain, flanked by several RNA-binding domains. In addition, the Dis3 protein contains an N-terminal PIN domain, which provides the enzyme with endoribonuclease activity as well (Lebreton *et al*, 2008). This N-terminal region of Dis3 is also important for its binding to the core exosome (Schaeffer *et al*, 2012; Schneider *et al*, 2009). The Dis3 protein is ubiquitously expressed and its enzymatic activity was shown to be responsible for the majority of the activity associated with the yeast exosome (Dziembowski *et al*, 2007; Schaeffer *et al*, 2009). The human Dis3 protein is somewhat different from its yeast counterpart, since it is exclusively located in the nucleoplasm and has a relatively weak association with the exosome. Human cells appear to express two additional Dis3-like exonucleases: hDis3L1 (Dis3-like exonuclease 1) and hDis3L2 (Dis3-like exonuclease 2). Recent studies have shown that hDis3L1 stably associates with cytoplasmic exosome complexes and contributes to the exosome-mediated degradation of cytoplasmic RNA substrates (Slomovic *et al*, 2010; Staals *et al*, 2010; Tomecki *et al*, 2010). In contrast to hDis3 and hDis3L1, the hDis3L2 protein (covered in detail in Chapter 6) does not associate with the core exosome. Instead, this ribonuclease was found to interact with hXrn1 and colocalizes with P-bodies (cytoplasmic foci for the retention and degradation of translationally-inactive mRNAs) where it participates in a novel eukaryotic RNA degradation pathway, involving 3' oligouridylation of substrate RNAs (Lubas *et al*, 2013; Malecki *et al*, 2013). One of these uridylated substrate RNAs is the pre-let-7 miRNA, a pluripotency factor in stem cells (Chang *et al*, 2013). This might be relevant for the discovery that germline mutations in the gene encoding hDis3L2 are the cause for the Perlman syndrome. It was shown that

inactivation of hDis3L2 resulted in mitotic abnormalities in human cell lines (Astuti *et al*, 2012).

Rrp6 (PM/Scl-100) is a hydrolytic enzyme belonging to the DEDD family of exonucleases, which also includes RNase D and RNase T (Mitchell *et al*, 2003). Most of our understanding of the functions of Rrp6 comes from studies in yeast, where the protein has been found to be essential for many functions that are attributed to the nuclear exosome. For instance, 3' end formation of many non-coding RNAs, such as sn(o)RNAs and rRNAs are dependent on the activity of Rrp6 and for these processing events the binding of Rrp47 to Rrp6 seems to be crucial (Mitchell *et al*, 2003; Schilders *et al*, 2007b; van Hoof *et al*, 2000). In addition, Rrp6 plays a central role in nuclear RNA surveillance, where it targets aberrant RNAs for complete degradation together with a non-canonical polyadenylation complex called TRAMP (LaCava *et al*, 2005). Rrp6 also appears to be involved in various pathways that regulate cellular mRNA levels, either by stimulating degradation of the mRNA body itself (Roth *et al*, 2005) or by tethering immature pre-mRNAs near or at the site of transcription (de Almeida *et al*, 2010).

As stated above, the yeast exosome is strongly dependent on Dis3 for its activity, although several nuclear processing events are performed in concert with Rrp6. Human exosome complexes also require PM/Scl-100 to perform these tasks. However, PM/Scl-100 is also found in the cytoplasm, suggesting that it might have additional, and possibly exosome-independent roles (Callahan and Butler, 2008; Graham *et al*, 2009; Lejeune *et al*, 2003; van Dijk *et al*, 2007). The exosome-association of at least two distinct Dis3-like proteins underlines the idea that the activity of the human exosome complex is differently organized. This prompted us to study the contributions of hDis3, hDis3L1 and PM/Scl-100 to the activity of the human exosome in more detail.

Results

Exoribonuclease activity of PM/Scl-100

Even though the association of Rrp6 with the yeast exosome and its contribution to the exosome's activity have been established for quite some time now, the activity of the human orthologue PM/Scl-100 has only recently been addressed (Januszyk *et al*, 2011). To further characterize the enzymatic properties of PM/Scl-100, the activity of this protein was studied in an *in vitro* RNase assay. The PM/Scl-100 protein was immunoprecipitated from HEp-2 cell extracts using polyclonal anti-PM/Scl-100 antibodies. Subsequently, the associated ribonuclease activity was determined by incubating the precipitated protein with a radiolabeled single-stranded RNA substrate of 37 nucleotides, derived from a linearized plasmid template. Because PM/Scl-100 belongs to the DEDD superfamily of exonucleases, its activity was expected to be dependent on the binding of divalent metal ions to the active site (Cudny *et al*, 1981). Different divalent metal ions (Zn^{2+}, Mg^{2+}, Mn^{2+} and Cu^{2+}) were added

to the reaction mixture and the results showed that the highest activity was observed in the presence of Mg^{2+} (data not shown). The PM/Scl-100 exoribonuclease activity appeared to be stimulated by relatively high Mg^{2+} concentrations. Millimolar concentrations were required for the highest levels of substrate RNA degradation (Figure 1). The degradation products that were generated co-migrated with a nucleotide monophosphate marker in thin-layer chromatography (Supplementary Figure 1), which is consistent with a hydrolytic exoribonuclease activity, as expected for a member of the DEDD superfamily of RNases.

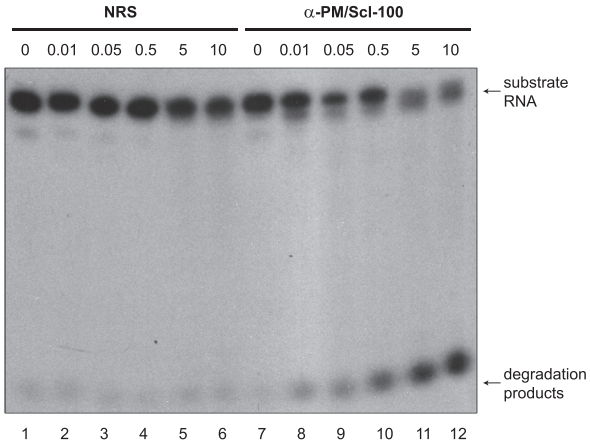

Figure 1. Mg^{2+}-dependent exoribonuclease activity of PM/Scl-100.

PM/Scl-100 was immunoprecipitated from a HEp-2 cell extract using a rabbit anti-PM/Scl-100 antiserum. Normal rabbit serum (NRS) was used as a control. The immunoprecipitate was incubated with a 37 nucleotide radiolabeled RNA substrate in the presence of different concentrations of Mg^{2+} (indicated in mM on top of the lanes). Reaction products were separated by denaturing polyacrylamide gel electrophoresis and visualized by autoradiography.

Association of PM/Scl-100 activity with the exosome core

To investigate whether a similar Mg^{2+}-dependent exoribonuclease activity is associated with the exosome, exosome complexes were immunoaffinity-purified from HEp-2 cell lysates using antibodies to the exosome core component hRrp40 (Raijmakers *et al*, 2002) and used to study RNase activity in the presence of 5 mM Mg^{2+}. Western blots demonstrated that the PM/Scl-100 protein was efficiently co-precipitated with the human exosome (Figure 2A; lane 3) and indeed these complexes displayed exoribonuclease activity (Figure 2B; lanes 7-9). To investigate the contribution of PM/Scl-100 to the appearance of the degradation products, PM/Scl-100 levels were down-regulated by RNAi using a PM/Scl-100-specific siRNA prior to preparation of the cell lysate for immunoprecipitation. The reduction of the PM/Scl-100 level was demonstrated by western blotting (Figure 2A; lanes 1-2). The results of the RNase assay showed that the down-regulation of PM/Scl-100 expression led to a reduced exosome-associated exoribonuclease activity under these conditions, indicating that PM/Scl-100 plays

an important role in this activity (Figure 2B; compare lanes 4-6 with lanes 7-9). To investigate whether the exoribonuclease activity of PM/Scl-100 is dependent on the association with the exosome core, the activity of immunoprecipitates from normal HEp-2 cell lysates obtained by antibodies specific for PM/Scl-100 was analysed in parallel. Western blotting analysis revealed that the amount of PM/Scl-100 in these precipitates was much higher than that in the anti-hRrp40 precipitates, whereas the amount of exosome core, as visualized by anti-hRrp4 antibodies, was lower (Figure 2A). The exoribonuclease activity displayed by the anti-PM/Scl-100 precipitate appeared to be higher than that observed with the anti-hRrp40 precipitate (Figure 2B), strongly suggesting that the activity of PM/Scl-100 is not dependent on the exosome core.

Structural elements of PM/Scl-100 required for its exoribonuclease activity

The amino acid sequence of PM/Scl-100 was analysed by the online SMART tool (Letunic *et al*, 2009), to obtain insight into its structural modules. As expected, this analysis revealed that its modular architecture is very similar to that of Rrp6: a central 3'-5' exonuclease domain (35EXOc), a PMC2NT domain close to its N-terminus, and a HRDC domain close to the C-terminus of the 35EXOc domain (Figure 3A). Typical for the DEDDy subgroup of the DEDD-family of exonucleases, the 35EXOc domain of PM/Scl-100 has a highly conserved tyrosine, which is predicted to be positioned close to the active site (Y436) and is thought to coordinate the water molecule for the nucleophilic attack on the phosphodiester backbone of the substrate RNA (Steitz and Steitz, 1993). The PMC2NT domain is often found in conjunction with HRDC domains in 3'-5' exoribonucleases. For Rrp6 it has been reported that this domain provides the interaction interface for Rrp47 (Stead *et al*, 2007), another protein involved in sn(o)RNA and pre-rRNA processing (Mitchell *et al*, 2003; Schilders *et al*, 2007b). The HRDC domain is believed to contribute to the recruitment to and proper positioning of the substrate RNA in the active site, as was originally proposed for bacterial RNase D (Zuo *et al*, 2005). Studies in yeast have shown that this domain seems to be required for some, but not all functions of Rrp6 (Phillips and Butler, 2003). A conserved amino acid in the HRDC domain, D525, has been shown to be involved in the contraction around the active site of Rrp6 upon substrate binding by forming hydrogen bonds with other conserved residues, Q184 and N193 (Midtgaard *et al*, 2006).

To investigate the importance of these elements for the exoribonuclease activity of PM/Scl-100, several VSV-tagged PM/Scl-100 expression constructs encoding single amino acid substitution mutants were generated: Q184A, N193A, Y436F and D525A. HEp-2 cells were transiently transfected with these constructs and the expression of the PM/Scl-100 mutants was monitored by western blotting of cell lysates (Figure 3B). The results showed that all mutants as well as the VSV-tagged, wild type PM/Scl-100 protein were expressed, albeit with different efficiencies. The mutant proteins were immunoprecipitated by anti-VSV-tag antibodies and their exoribonuclease activity was determined. Anti-PM/Scl-100 antibodies were used to visualize the PM/Scl-100 mutants in the precipitates by western

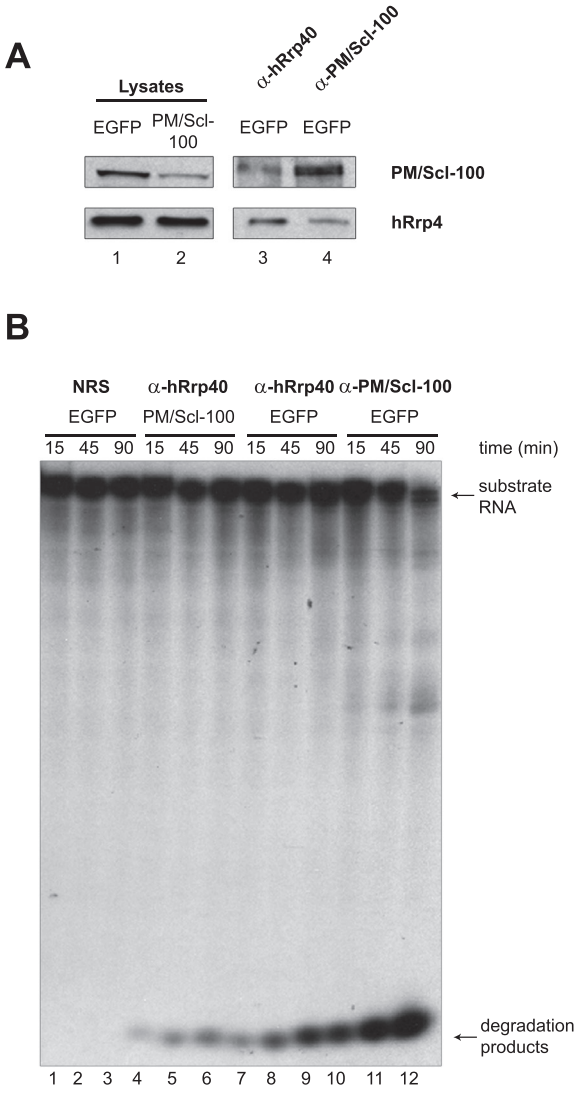

Figure 2. Exosome-association of PM/Scl-100.

(A) HEp-2 cells were transfected with siRNAs downregulating either EGFP (used as a control; lane 1) or PM/Scl-100 (lane 2) and 48 hours after transfection cell lysates were subjected to immunoprecipitation using anti-hRrp40 (lane 3) or anti-PM/Scl-100 antibodies (lane 4). Co-precipitated proteins as well as the efficiency of knockdown were determined by western blotting using anti-PM/Scl-100 and anti-hRrp4 antibodies (indicated at the right). (B) Ribonuclease activity was analysed by incubating equivalent amounts of the precipitated samples (obtained with antibodies and lysates from siRNA-treated cells as indicated on top of the lanes) with a 267 nucleotide, 5.8S rRNA-containing radiolabelled RNA substrate in RNA degradation buffer containing 5 mM Mg^{2+} for the indicated periods of time. Reaction products were separated by denaturing polyacrylamide gel electrophoresis and visualized by autoradiography.

blotting and anti-hRrp40 and anti-hRrp41 antibodies were used to demonstrate the co-precipitation of the exosome core. The results demonstrated that none of these mutations abolished the interaction with the exosome core, since both exosome core subunits were co-precipitated with similar efficiencies (Figure 3C). The exoribonuclease activity observed with the immunoprecipitated VSV-tagged, wild type PM/Scl-100 protein showed that the tag did not interfere with this activity (Figure 3D). All amino acid substitution mutations appeared to impair the activity of the PM/Scl-100 protein (Figure 3D). This not only confirmed that (part of) the exoribonuclease activity observed under these conditions is due to PM/Scl-100, but also indicates that all mutated residues are crucial for its exoribonuclease activity.

Human exosome-associated exoribonucleases

Although PM/Scl-100 appeared to be capable to exert its exoribonuclease activity independent of the exosome core, a subfraction of this protein acts in concert with the exosome. Previously, it has been shown that the exoribonuclease activity of hDis3 and hDis3L1 requires relatively low, submillimolar concentrations of Mg^{2+} (Staals *et al*, 2010; Tomecki *et al*, 2010). The differential requirement for Mg^{2+} of PM/Scl-100 and hDis3 or hDis3L1 allowed us to investigate the contributions of PM/Scl-100 on the one hand and hDis3 and hDis3L1 on the other hand to the exoribonuclease activity associated with the human exosome core. A concentration of 0.05 mM Mg^{2+} represents a condition with high hDis3 and hDis3L1 activity and very low PM/Scl-100 activity and at 5 mM Mg^{2+} mainly PM/Scl-100 is active. The rather weak association of hDis3 with the exosome was exploited to distinguish between hDis3 and hDis3L1 activities. The results in Figure 4 show that exosome complexes, immunoaffinity-purified by anti-hRrp40, display ribonuclease activity over a wide range of Mg^{2+} concentrations, which is in agreement with the association of exoribonucleases with varying optimal Mg^{2+} concentrations. Treatment of the precipitates with increasing concentrations of KCl allowed the selective removal of hDis3 from the precipitates (Figure 5A). hDis3 was barely detectable after treatment of the anti-hRrp40 precipitate with 150 mM KCl, whereas hDis3L1 and PM/Scl-100 remained bound to the exosome at concentrations up to 600 mM KCl. To investigate the contribution of these exonucleases to the activity of the human exosome, anti-hRrp40 precipitates pretreated with different KCl concentrations were used in RNase assays containing either 0.05 mM Mg^{2+} (Figure 5B) or 5 mM Mg^{2+} (Figure 5C). Much of the activity detected at 0.05 mM Mg^{2+} appeared to be due to hDis3, as most activity was lost after treatment with KCl concentrations higher than 100 mM. The remaining activity can be attributed to hDis3L1, although some reactivity of PM/Scl-100 under these conditions cannot be excluded. In contrast, the exoribonuclease activity at 5 mM Mg^{2+} was not decreased after treatment with any of the KCl concentrations, in agreement with the relatively stable association of PM/Scl-100. Moreover, incubations of the precipitate with 300-600 mM KCl appeared to enhance the activity slightly. Taken together, these data suggest that the majority of the exoribonuclease activity associated with the human exosome is due to hDis3 and PM/Scl-100 and that the cellular microenvironment may determine their relative contributions.

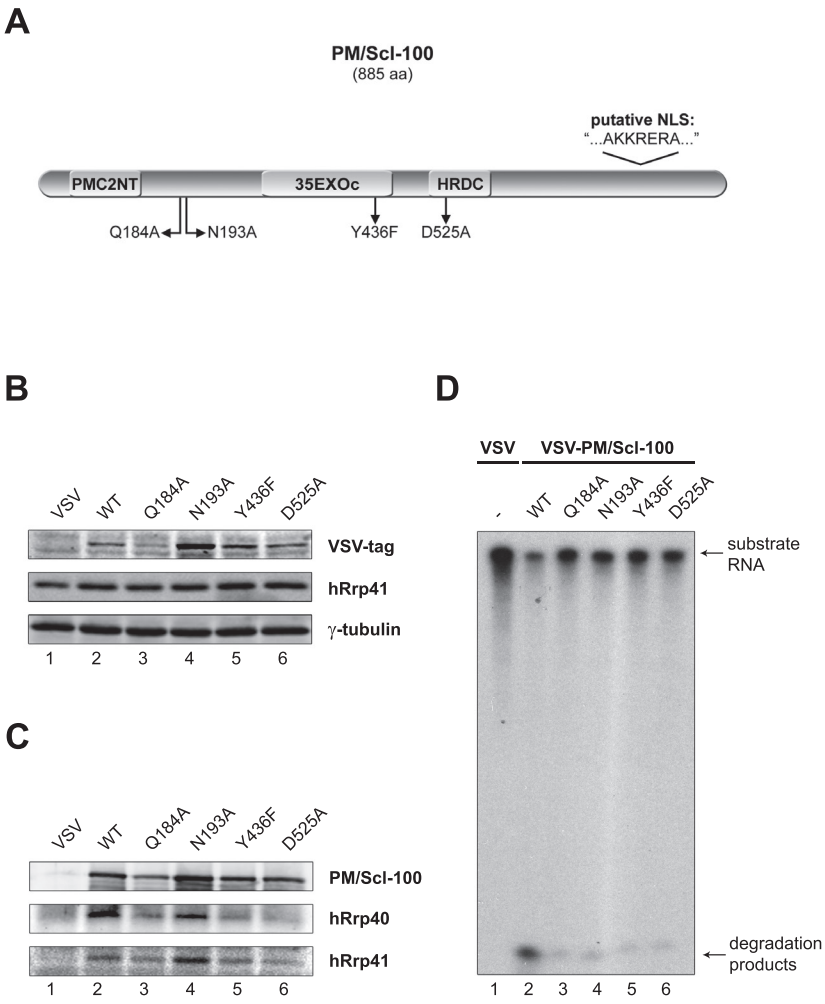

Figure 3. Ribonuclease activity of PM/Scl-100 mutants.

(A) Schematic representation of the PM/Scl-100 protein, showing the position of the PMC2NT (N-terminal domain in 3'-5'-exonucleases like polymyositis autoantigen 2), 35EXOc (3'-5' exonuclease) and HRDC (helicase and RNase D carboxy-terminal domain) domains. The position of a putative nuclear localization signal (NLS) is also indicated. Arrows mark the positions of residues that were mutated (Q184A, N193A, Y436F, D525A). (B) HEp-2 cells were transfected with constructs expressing either VSV-tagged wild-type PM/Scl-100 protein or single amino acid substitution mutants. Cells transfected with the 'empty' vector were used as a control (lane 1, VSV). Protein expression was verified by western blotting of cell lysates and detection by anti-VSV-tag antibodies. Anti-hRrp41 antibodies were used to detect the exosome core. Anti-γ-tubulin antibodies were used as loading control. (C) Anti-VSV antibodies were used to precipitate the tagged proteins from the extracts of the corresponding transfected cells. Immunoprecipitated PM/Scl-100 and the mutants thereof were visualized on western blot by anti-PM/Scl-100 antibodies. Co-precipitation of exosome core subunits was determined by staining the blot with anti-hRrp40 and anti-hRrp41 antibodies. (D) The immunoprecipitated PM/Scl-100 mutants were incubated for 2 hours with the 5.8S rRNA-containing radiolabelled RNA substrate in RNA degradation buffer containing 5 mM Mg^{2+}. Reaction products were separated by denaturing polyacrylamide gel electrophoresis and visualized by autoradiography.

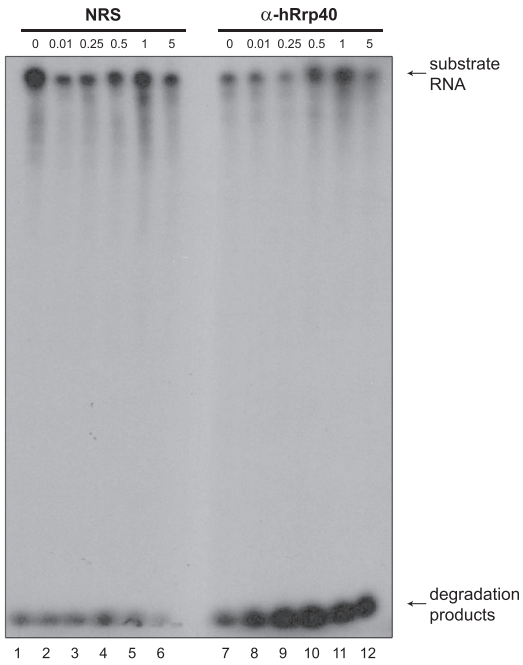

Figure 4. Mg^{2+}-dependent exoribonuclease activity of the human exosome complex.

Exosome complexes were immunoprecipitated by rabbit anti-hRrp40 antibodies from HEp-2 cell extracts and were incubated for 2 hours with the 5.8S rRNA-containingradiolabelled RNA substrate in the presence of various Mg^{2+} concentrations, as indicated above the lanes. Normal rabbit serum (NRS) was used as a control for background precipitation. Reaction products were separated by denaturing polyacrylamide gel electrophoresis and visualized by autoradiography.

Influence of the depletion of one exoribonuclease on the association of another with the exosome core

Previously published data suggest that the expression levels of hDis3, hDis3L1 and PM/Scl-100 influence each other (Tomecki *et al*, 2010). To investigate the consequences of alterations in the association of these proteins with the exosome core on the exoribonuclease activity associated with the exosome, hDis3, hDis3L1 or PM/Scl-100 were down-regulated by siRNA-mediated depletion. The KCl concentration in the experiments with lysates from these cells was kept at 50 mM to maintain the association of hDis3 with the exosome core. Western blotting confirmed the down-regulation of each of the exoribonucleases (Figure 6A). The knock-down of hDis3L1 resulted in a slight up-regulation of PM/Scl-100 and enhanced its association with the exosome. Vice versa, the down-regulation of PM/Scl-100 led to slightly increased hDis3L1 levels and elevated levels of exosome-associated hDis3L1. The depletion of hDis3 did not seem to have detectable effects on the levels of hDis3L1 and PM/Scl-100, nor did the down-regulation of either hDis3L1 or PM/Scl-100 result in notable changes in exosome-association by hDis3. The exosome-associated exoribonuclease activity of material

from the hDis3L1 siRNA-treated cells at 5 mM Mg^{2+} appeared to be slightly increased (Figure 6B-C), in agreement with the elevated levels of PM/Scl-100 associated with the exosome. Similarly, down-regulation of PM/Scl-100 resulted in enhanced exoribonuclease activity at 0.05 mM Mg^{2+} (Figure 6B-C), which is consistent with elevated levels of exosome-associated hDis3L1. Since previous results suggested only a minor contribution of hDis3L1 to the activity of the exosome core (Figure 5), these results indicate that either the increase of hDis3L1 association is sufficient to achieve this level of activity or that the depletion of PM/Scl-100 stimulates the activity of either hDis3 or hDis3L1. This might also explain the residual activity at 5 mM Mg^{2+} when PM/Scl-100 was depleted (Figure 6B; lane 8), although the activity both hDis3 and hDis3L1 was previously shown to be inhibited under these conditions (Staals *et al*, 2010; Tomecki *et al*, 2010). The observation that knock-down of one exosome-bound exonuclease resulted in an increase in the association of another one suggests that hDis3L1 and PM/Scl-100 have overlapping, mutually exclusive binding sites on the exosome, or that the binding of one of these nucleases affects the binding affinity and/or the activity of the other.

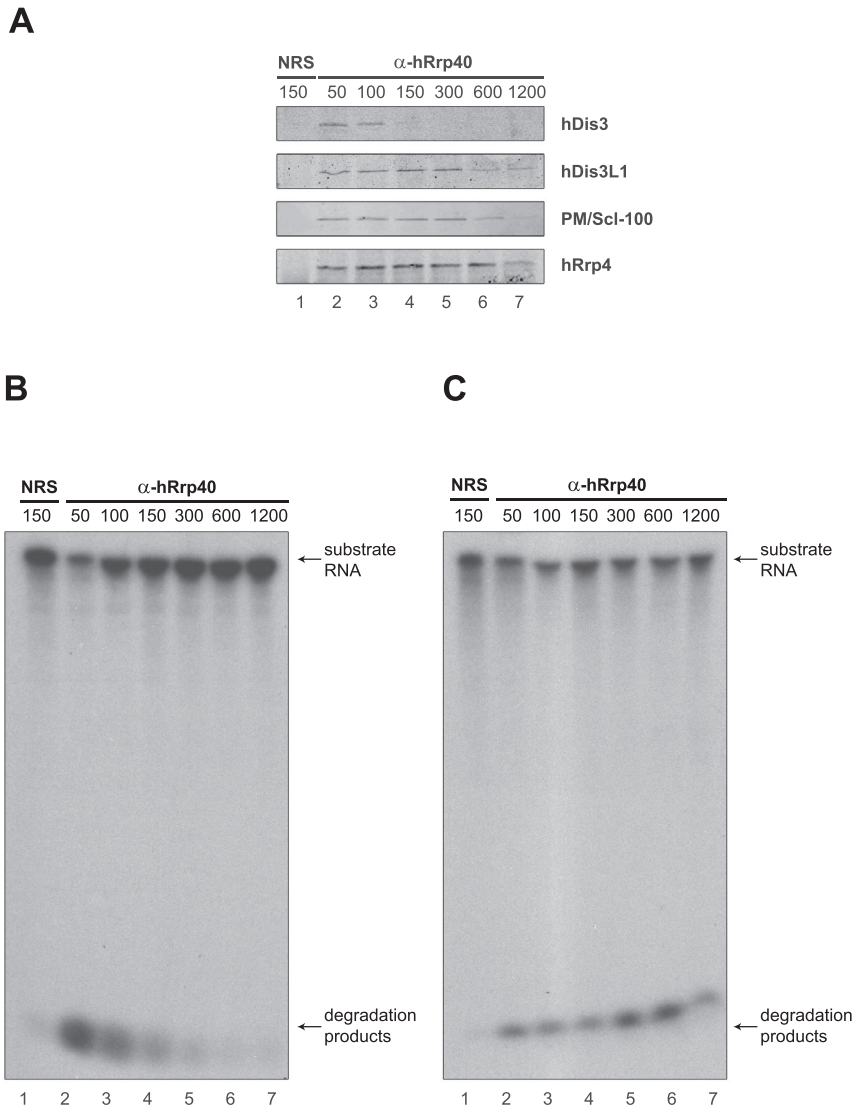

Figure 5. Differential stability of the association of hDis3, hDis3L1 and PM/Scl-100 with the exosome core.

Exosome complexes were immunoprecipitated from HEp-2 cell extracts using anti-hRrp40 antibodies and the precipitates were washed with a buffer containing increasing concentrations of KCl (as indicated above the lanes; concentration in mM). Normal rabbit serum (NRS) was used as a control. (A) Precipitated exosomes were visualized by western blotting using anti-hRrp4 antibodies. Co-precipitation of hDis3, hDis3L1 and PM/Scl-100 was determined by staining the blot with the corresponding antisera (indicated on the right). (B and C) Ribonuclease activity of the immunoprecipitated exosome complexes was determined by incubation with the 5.8S rRNA-containing radiolabelled RNA substrate in RNA degradation buffer containing 0.05 mM (B) or 5 mM Mg^{2+} (C).

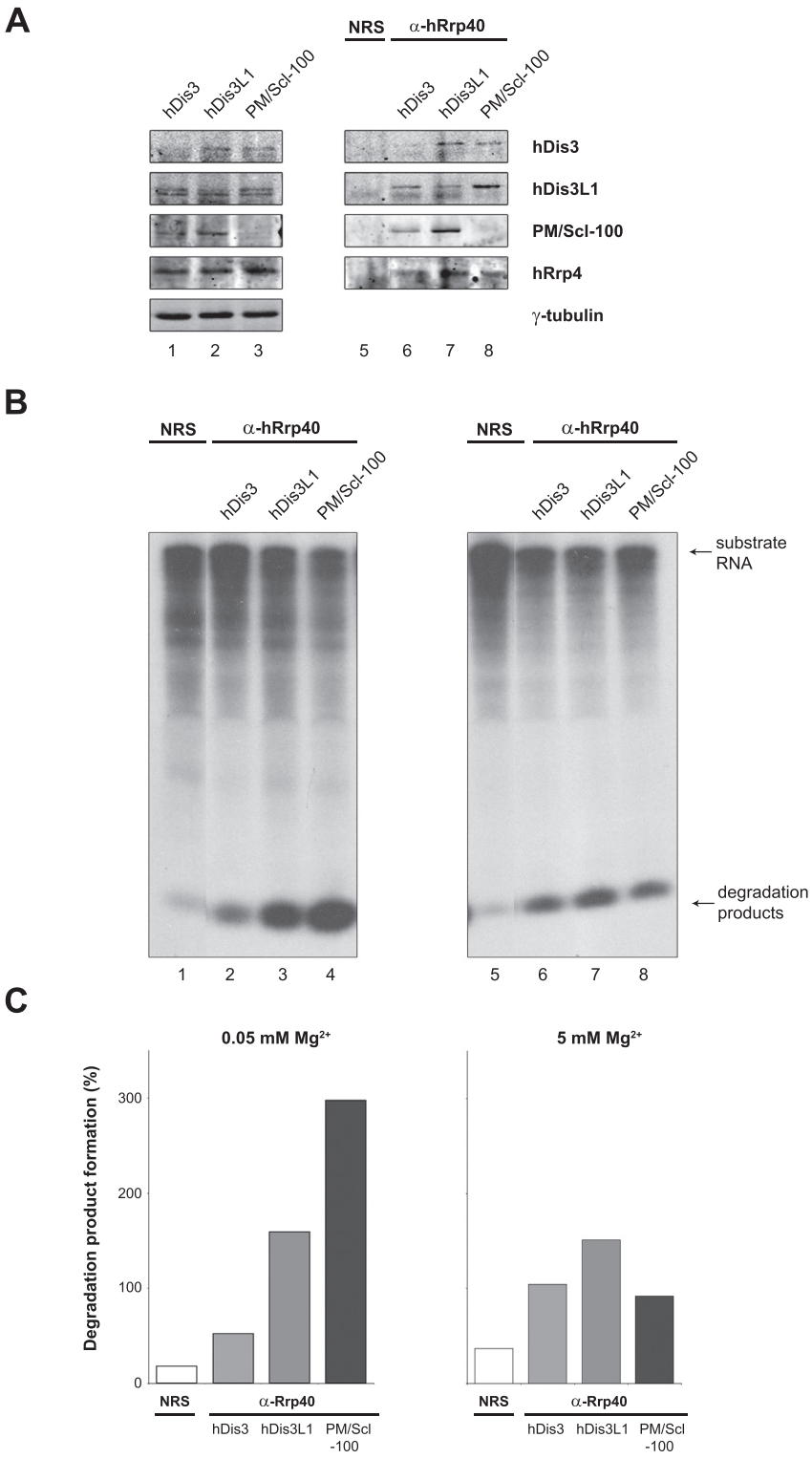
A
NRS
α-hRrp40
hDis3
hDis3L1
PM/Scl-100
hDis3
hDis3L1
PM/Scl-100
hDis3
hDis3L1
PM/Scl-100
hRrp4
γ-tubulin
1 2 3 5 6 7 8
B
NRS
α-hRrp40
hDis3
hDis3L1
PM/Scl-100
NRS
α-hRrp40
hDis3
hDis3L1
PM/Scl-100
substrate RNA
degradation products
1 2 3 4 5 6 7 8
C
0.05 mM Mg2+
5 mM Mg2+
Degradation product formation (%)
300
200
100
0
NRS
α-Rrp40
hDis3 hDis3L1 PM/Scl -100
NRS
α-Rrp40
hDis3 hDis3L1 PM/Scl -100

Figure 6. Effects of hDis3, hDis3L1 or PM/Scl-100 knockdown on exosome-associated exoribonuclease activity.

HEp-2 cells were transfected with siRNAs for hDis3, hDis3L1 or PM/Scl-100 (Schilders *et al*, 2007b) (indicated above the lanes). Forty eight hours after siRNA transfection exosome complexes were immunoprecipitated from cell lysates using anti-hRrp40 antibodies in a buffer containing 50 mM KCl. Normal rabbit serum (NRS) was used as an immunoprecipitation control. (A) hDis3, hDis3L1, PM/Scl-100 and hRrp4 were detected in the cell lysates (lanes 1-3) and the immunoprecipitates (lanes 5-8) by western blotting. Anti-γ-tubulin antibodies were used to visualize γ-tubulin as loading control. (B) Ribonuclease activity was determined by incubating equal amounts of the immunoprecipitated material with the 5.8S rRNA-containing radiolabelled RNA substrate in RNA degradation buffer containing 0.05 mM Mg^{2+} (lanes 1-4) or 5 mM Mg^{2+} (lanes 5-8). (C) The radioactivity of the degradation products in panel B was quantified by phosphorimaging. The data were normalized for the signals obtained with the material from control (EGFP) siRNA-treated cells.

Discussion

The catalytic subunits that determine the exoribonucleolytic activity of the RNA exosome vary markedly among species. In archaea, the core itself was shown to be enzymatically active and, perhaps for that reason, does not require the association of other (hydrolytic) enzymes (Lorentzen *et al*, 2005). Plants combine the activity of an active core (Chekanova *et al*, 2000) with three different versions of the Rrp6 protein, each with a specific subcellular localization (Lange *et al*, 2008). In budding yeast, the exosome core-associated Dis3 protein provides most of the activity to the catalytically inactive core, in concert with the nuclear Rrp6 protein. Mammals display yet another mode of exoribonuclease activity: the inactive core serves as a scaffold for the association of at least 3 distinct hydrolytic exonucleases: PM/Scl-100, hDis3, and hDis3L1. Here we determined the contribution of these enzymes to the activity of the human exosome.

PM/Scl-100 acts as a Mg^{2+}-dependent hydrolytic exonuclease and displays this activity both in association with the exosome core and independently. The requirement of relatively high Mg^{2+} concentrations is similar to what has been observed previously for the orthologous yeast Rrp6 protein (Liu *et al*, 2006; Phillips and Butler, 2003). Yeast Rrp6 has been reported to be activated by Mn^{2+} and Zn^{2+} as well (Midtgaard *et al*, 2006), but PM/Scl-100 did not show substantial activity in the presence of these divalent cations.
The results obtained with the PM/Scl-100 amino acid substitution mutants indicated that both the DEDDy motif and the elements that probably are involved in the recruitment and positioning of the substrate and/or the correct folding upon substrate binding are essential for the exonuclease activity of this enzyme. A mutation in the HRDC domain of the yeast Rrp6 protein resulted in 5.8S pre-rRNA and pre-snoRNA 3'-end processing defects, although its exonuclease activity appeared to be unaffected (Midtgaard *et al*, 2006; Phillips and Butler, 2003).

Most of the RNase assays in our study were performed using a highly structured RNA substrate, 5.8S rRNA extended at the 3' end by the most 5' 100 nucleotides of ITS2. In agreement with the results of a recent study (Januszyk *et al*, 2011) our data indicate that the activity of PM/Scl-100 is not hindered by secondary structures present in the RNA substrate. The apparent capacity of PM/Scl-100 to degrade structured RNA substrates (Januszyk *et al*, 2011) raises the question why PM/Scl-100 is also found in association with the exosome core and to what extent this association affects the enzymatic activity and/or substrate specificity. One possibility is that exosomes facilitate the recruitment of RNAs that are designated for destruction or truncation and present them in the proper way to the exoribonuclease, as has been demonstrated for the yeast exosome (Bonneau *et al*, 2009). Alternatively, although substrate unwinding might not be necessary for complete degradation by PM/Scl-100 *in vitro*, a role for the exosome core in unwinding highly structured RNA substrates is feasible as well.

PM/Scl-100 has a high affinity for binding to the exosome core, as this protein was shown to coprecipitate with the exosome under relatively stringent conditions. Surprisingly, the PM/Scl-100-mediated exosome activity appeared to be slightly increased when the immunoaffinity-purified complexes were subjected to relatively high salt concentrations prior to the analysis of exoribonuclease activity. Since immunoblotting data showed that this is not due to higher amounts of PM/Scl-100, these observations suggest that the activity of exosome-associated PM/Scl-100 might be regulated by other protein(s). Potential candidates for modulating the activity of PM/Scl-100 are C1D, hMPP6 and hMtr4, which have previously been shown to be associated with PM/Scl-100 (Schilders *et al*, 2005; Schilders *et al*, 2007b). However, these three proteins are expected to stimulate the activity of PM/Scl-100, as was demonstrated for the 3'end processing of the 5.8S rRNA *in vivo*, raising the possibility that other protein(s) are responsible for this phenomenon. Interestingly, the increase in activity of PM/Scl-100 inversely correlates with the association of hDis3 with the exosome core. This suggests that also hDis3 may somehow modulate the activity of PM/Scl-100, when associated with the exosome. In yeast, the binding of Dis3 did not seem to affect Rrp6's activity (Wasmuth and Lima, 2012). Further studies are required to clarify this issue.

The interaction of the human Dis3 with the exosome core is rather weak, especially when compared to its paralogue hDis3L1, suggesting that in human cells a substantial amount of hDis3 is not associated with the exosome core. In fact, the instability of the hDis3-exosome core association at physiological salt concentrations (~100 mM KCl) questions the biological significance of this interaction in human cells. Possibly, this association is rather dynamic and influenced by the microenvironment. In this respect it is important to note that the activity of the exosome *in vitro* at low magnesium concentration correlates with the association of hDis3. Moreover, knockdown of hDis3 resulted in reduced exosome activity under these conditions, substantiating that the human Dis3 may indeed provide an important contribution to the activity of the human exosome. In yeast, Dis3 has been shown to act as an endonuclease in addition to its function as an exonuclease (Lebreton *et al*, 2008; Schaeffer *et al*, 2009) and it

is likely that the human Dis3 protein displays the same activities. Since both PM/Scl-100 and hDis3L1 lack endonuclease activity, hDis3 is the only endonuclease currently known to be associated with the human exosome.

Taken together, PM/Scl-100, hDis3 and hDis3L1 have been shown to associate with the human exosome and are therefore likely to contribute to the ribonuclease activity of the complex. It is still not known, however, whether these ribonucleases can bind the human exosome core simultaneously. Recently, the crystal structure of the yeast exosome core in complex with both Dis3 and the C-terminal region of Rrp6 has been solved, demonstrating that simultaneous binding of these two nucleases is possible (Makino *et al*, 2013). As observed before, Dis3 is binding to one side of the donut structure of the exosome core, the central channel of which is connected to a path that leads to the exonucleolytic active site of Dis3. Rrp6 is positioned at another region of the exosome core, where it wraps around Csl4 and contacts the donut-structure. RNA substrates may follow two (partially overlapping) paths through the exosome followed by degradation by either Dis3 or Rrp6. Interestingly, the activity of Dis3 was positively affected by the binding of Rrp6 (irrespective of the activity of Rrp6), resulting in a conformational change in the Csl4 protein, which directs RNA substrates through the central channel towards Dis3 (Makino *et al*, 2013; Wasmuth and Lima, 2012).
The exact positioning of hDis3, hDis3L1 and PM/Scl-100 on the human exosome has not been determined so far. It also remains to be demonstrated whether the binding of hDis3 and hDis3L1 are mutually exclusive. Most likely the overall architecture is similar to that in yeast. The interaction of yeast Dis3 with the exosome core is mediated by its N-terminal region (Schaeffer *et al*, 2012; Schneider *et al*, 2009), which is conserved in the human Dis3 and Dis3L1 proteins. In view of their structural similarity hDis3 and hDis3L1 probably bind to the same region and thus are not expected to bind to the exosome core simultaneously. Furthermore, the C-terminal region of Rrp6 was shown to bind to a region of the exosome core containing conserved surface patches (Makino *et al*, 2013).

The results of the knock-down experiments suggest that alterations in the association of one of the exosome-associated ribonucleases may affect the level of association of another (Figure 6A). For instance, the knockdown of hDis3L1 led to an increased association of PM/Scl-100 with the exosome core and resulted in more activity at high magnesium concentrations. Conversely, knockdown of PM/Scl-100 resulted in elevated levels of hDis3L1 association and enhanced activity at low magnesium concentrations. Upon depletion of hDis3 such alterations were not observed. Paradoxically, the activity of yeast Dis3 was found to be stimulated by the association of Rrp6 with the exosome core (Wasmuth and Lima, 2012), while our results are suggesting the opposite effect: stimulation of hDis3 and/or hDis3L1 activity when PM/Scl-100 is depleted. It is difficult to explain these data based upon the predicted exosome complex architecture described above, for which mutual effects between hDis3 and hDis3L1 would be expected. It should, however, be noted that the N-terminal part of Rrp6 was lacking in

the analyses of the crystal structure of the yeast complex and it is possible that this domain is responsible for the observed effects. Additional studies will be required to clarify the interplay between the exosome core associated ribonucleases, which may be important for the regulation of exosome activity. In yeast for instance, Rrp6 is downregulated when cells progress through meiotic development to promote the stabilization of meiotic non-coding RNAs (Lardenois *et al*, 2011). In flies, it was shown that Rrp6 was dynamically redistributed in the cell during the different stages of mitosis, while exosome core subunits were found in close proximity to microtubuli during cell division (Graham *et al*, 2009). Furthermore, the interaction of the exosome with the complexes controlling the circadian clock is also indicative for temporal changes in the exosome-associated nuclease protein levels, which are needed for the degradation of specific RNAs in a periodical fashion (Guo *et al*, 2009). In conclusion, these results provide a rationale for the regulation of exosome activity *in vivo* and it is likely that this occurs by modulation of the association or activity of exosome-associated ribonucleases.

Materials and methods

Immunoprecipitation

Affinity purified polyclonal rabbit anti-PM/Scl-100 ("SN566") or anti-hRrp40 ("H70") antibodies (Brouwer *et al*, 2001) were coupled to protein A-agarose beads (Kem-En-Tec, Denmark) in IPP500 (500 mM NaCl, 10 mM Tris–HCl, pH 8.0, 0.05% NP-40) at room temperature for 1 h. Similar conditions were used to couple the monoclonal mouse anti-VSV antibodies (home-made) to protein G-agarose beads (Kem-En-Tec, Denmark). Beads were washed once with IPP500 and twice with the appropriate IPP-solution (same as IPP500, but KCl instead of NaCl, in which the concentration of KCl is depending on the assay). HEp-2 cell extract was made by resuspending the cells in six volumes of lysis buffer (25 mM Tris–HCl, pH 7.5, 50 or 100 mM KCl, 1 mM EDTA, 0.5 mM PMSF, 0.05% NP-40, 1 mM DTT), followed by sonication and centrifugation. The extract was incubated with the antibody-coupled beads for 2 h at 4°C. After washing the beads twice with the appropriate IPP-solution, bound proteins were washed two more times with RNA degradation assay buffer (described below), after which the beads were split for SDS-PAGE and the RNase assay.

Western blot analysis

Proteins were size-separated by SDS-PAGE (containing 12.5% acrylamide) and transferred to nitrocellulose membranes followed by 1 h of blocking (5% skimmed milk, PBS, 0.05% NP-40). For the detection of proteins on western blots, polyclonal rabbit antibodies (anti-PM/Scl-100, anti-hRrp40, anti-hRrp41), polyclonal mouse antibodies (anti-hDis3L1),

monoclonal mouse antibodies (anti-VSV, anti-hRrp4, anti-γ-tubulin, anti-hDis3) or a human patient serum ("Ven96") containing antibodies to PM/Scl-100 (Schilders *et al*, 2007a) were diluted in blocking buffer (5% skimmed milk, PBS, 0.05% NP-40). Blots were incubated with these antibodies for 1 h at room temperature. Bound antibodies were detected by incubation with IRDye-conjungated polyclonal goat anti-mouse, goat anti-rabbit or goat anti-human antibodies (Li-Cor) for 1 h in blocking buffer and visualized using an Odyssey Infrared Imaging System (Li-Cor).

Mutagenesis of PM/Scl-100

Point mutations in the coding sequence of the VSV-tagged PM/Scl-100 expression construct were introduced by site directed mutagenesis using the QuikChange Site-Directed Mutagenesis Kit (Stratagene) using the manufacturer's recommendations and the following primers:
(D525A) 5'CTCGCAGGGAAGCTGAAAGTTACGG 3'
and 5'CCGTAACTTTCAGCTTCCCTGCGAG 3',
(Y436F) 5'AGATGCTCAGCTTCGCCCGGGATGA 3'
and 5'TCATCCCGGGCGAAGCTGAGCATCT 3',
(Q184A) 5'CATCCGACCTGCGCTCAAGTTTC 3'
and 5'GAAACTTGAGCGCAGGTCGGATG 3'
(N193A) 5'GAGAGAAGATTGACGCTTCCAACACACC 3'
and 5'GGTGTGTTGGAAGCGTCAATCTTCTCTC 3'

RNase assays

RNase assays were performed using a radiolabelled 267 nucleotide RNA substrate, which was obtained by *in vitro* transcription in the presence of ^{32}P α-UTP. This substrate RNA contained the human 5.8S rRNA sequence and the most 5' 100 nucleotides of ITS2 (Schilders *et al*, 2005). The RNA substrate in Figure 1 was generated in a similar fashion, but with a XbaI-linearized pBS(-) plasmid as template for transcription by T3 RNA polymerase. After gel-purification the RNA substrate was incubated for 2 h with the immunoprecipitated material at 37°C in RNA degradation buffer (20 mM HEPES, pH 7.5, 50 mM KCl, 1 mM DTT, 1 mM Na_2HPO_4) containing different concentrations of Mg^{2+}, as indicated. Reactions were stopped by the addition of RNA-loading buffer (9M urea, 0.1% bromophenol blue, 0.1% xylene cyanol), supplemented with 20% (v/v) phenol. Samples were analysed by denaturing polyacrylamide gel electrophoresis followed by autoradiography. The results were quantified by phosphor-imaging, using Quantity One software (Bio-Rad).

siRNA-mediated knock-down

siRNAs were purchased from Eurogentec. The sequences of the siRNAs used in this study are as follows:
5'-CGAGAAGCGCGAUCACAUGdTdT-3' (EGFP),
5'-GCUGCAGCAGAACAGGCCAdTdT-3' (PM/Scl-100),
5'-GCCUACAGGUAGAGUUGUAdTdT-3' (hDis3),
5'-CCAUGUAACCGUAAGAAUAdTdT-3' (hDis3L1).
Transfection of HEp-2 cells with these siRNAs was performed essentially as described previously (Schilders *et al*, 2005).

Acknowledgments

We are grateful to Professor W. J. van Venrooij for critically reading this manuscript.

References

Astuti D, Morris MR, Cooper WN, Staals RH, Wake NC, Fews GA, Gill H, Gentle D, Shuib S, Ricketts CJ, Cole T, van Essen AJ, van Lingen RA, Neri G, Opitz JM, Rump P, Stolte-Dijkstra I, Muller F, Pruijn GJ, Latif F, Maher ER (2012) Germline mutations in DIS3L2 cause the Perlman syndrome of overgrowth and Wilms tumor susceptibility. *Nat Genet* **44:** 277-284

Bonneau F, Basquin J, Ebert J, Lorentzen E, Conti E (2009) The yeast exosome functions as a macromolecular cage to channel RNA substrates for degradation. *Cell* **139:** 547-559

Brouwer R, Allmang C, Raijmakers R, van Aarssen Y, Egberts WV, Petfalski E, van Venrooij WJ, Tollervey D, Pruijn GJ (2001) Three novel components of the human exosome. *J Biol Chem* **276:** 6177-6184

Buttner K, Wenig K, Hopfner KP (2005) Structural framework for the mechanism of archaeal exosomes in RNA processing. *Mol Cell* **20:** 461-471

Callahan KP, Butler JS (2008) Evidence for core exosome independent function of the nuclear exoribonuclease Rrp6p. *Nucleic Acids Res* **36:** 6645-6655

Chang HM, Triboulet R, Thornton JE, Gregory RI (2013) A role for the Perlman syndrome exonuclease Dis3l2 in the Lin28-let-7 pathway. *Nature* **497:** 244-248

Chekanova JA, Shaw RJ, Wills MA, Belostotsky DA (2000) Poly(A) tail-dependent exonuclease AtRrp41p from Arabidopsis thaliana rescues 5.8 S rRNA processing and mRNA decay defects of the yeast ski6 mutant and is found in an exosome-sized complex in plant and yeast cells. *J Biol Chem* **275:** 33158-33166

Cudny H, Zaniewski R, Deutscher MP (1981) Escherichia coli RNase D. Purification and structural characterization of a putative processing nuclease. *J Biol Chem* **256:** 5627-5632

de Almeida SF, Garcia-Sacristan A, Custodio N, Carmo-Fonseca M (2010) A link between nuclear RNA surveillance, the human exosome and RNA polymerase II transcriptional termination. *Nucleic Acids Res* **38:** 8015-8026

Dziembowski A, Lorentzen E, Conti E, Seraphin B (2007) A single subunit, Dis3, is essentially responsible for yeast exosome core activity. *Nat Struct Mol Biol* **14:** 15-22

Graham AC, Kiss DL, Andrulis ED (2009) Core exosome-independent roles for Rrp6 in cell cycle progression. *Mol Biol Cell* **20:** 2242-2253

Guo J, Cheng P, Yuan H, Liu Y (2009) The exosome regulates circadian gene expression in a posttranscriptional negative feedback loop. *Cell* **138:** 1236-1246

Januszyk K, Liu Q, Lima CD (2011) Activities of human RRP6 and structure of the human RRP6 catalytic domain. *RNA* **17:** 1566-1577

LaCava J, Houseley J, Saveanu C, Petfalski E, Thompson E, Jacquier A, Tollervey D (2005) RNA degradation by the exosome is promoted by a nuclear polyadenylation complex. *Cell* **121:** 713-724

Lange H, Holec S, Cognat V, Pieuchot L, Le Ret M, Canaday J, Gagliardi D (2008) Degradation of a polyadenylated rRNA maturation by-product involves one of the three RRP6-like proteins in Arabidopsis thaliana. *Mol Cell Biol* **28:** 3038-3044

Lardenois A, Liu Y, Walther T, Chalmel F, Evrard B, Granovskaia M, Chu A, Davis RW, Steinmetz LM, Primig M (2011) Execution of the meiotic noncoding RNA expression program and the onset of gametogenesis in yeast require the conserved exosome subunit Rrp6. *Proc Natl Acad Sci U S A* **108:** 1058-1063

Lebreton A, Tomecki R, Dziembowski A, Seraphin B (2008) Endonucleolytic RNA cleavage by a eukaryotic exosome. *Nature* **456:** 993-996

Lejeune F, Li X, Maquat LE (2003) Nonsense-mediated mRNA decay in mammalian cells involves decapping, deadenylating, and exonucleolytic activities. *Mol Cell* **12:** 675-687

Letunic I, Doerks T, Bork P (2009) SMART 6: recent updates and new developments. *Nucleic Acids Res* **37:** D229-232

Lin-Chao S, Chiou NT, Schuster G (2007) The PNPase, exosome and RNA helicases as the building components of evolutionarily-conserved RNA degradation machines. *J Biomed Sci* **14:** 523-532

Liu Q, Greimann JC, Lima CD (2006) Reconstitution, activities, and structure of the eukaryotic RNA exosome. *Cell* **127:** 1223-1237

Lorentzen E, Walter P, Fribourg S, Evguenieva-Hackenberg E, Klug G, Conti E (2005) The archaeal exosome core is a hexameric ring structure with three catalytic subunits. *Nat Struct Mol Biol* **12:** 575-581

Lubas M, Damgaard CK, Tomecki R, Cysewski D, Jensen TH, Dziembowski A (2013) Exonuclease hDIS3L2 specifies an exosome-independent 3'-5' degradation pathway of human cytoplasmic mRNA. *EMBO J* **32:** 1855-1868

Lykke-Andersen S, Brodersen DE, Jensen TH (2009) Origins and activities of the eukaryotic exosome. *J Cell Sci* **122:** 1487-1494

Makino DL, Baumgartner M, Conti E (2013) Crystal structure of an RNA-bound 11-subunit eukaryotic exosome complex. *Nature* **495:** 70-75

Malecki M, Viegas SC, Carneiro T, Golik P, Dressaire C, Ferreira MG, Arraiano CM (2013) The exoribonuclease Dis3L2 defines a novel eukaryotic RNA degradation pathway. *EMBO J* **32:** 1842-1854

Midtgaard SF, Assenholt J, Jonstrup AT, Van LB, Jensen TH, Brodersen DE (2006) Structure of the nuclear exosome component Rrp6p reveals an interplay between the active site and the HRDC domain. *Proc Natl Acad Sci U S A* **103:** 11898-11903

Mitchell P, Petfalski E, Houalla R, Podtelejnikov A, Mann M, Tollervey D (2003) Rrp47p is an exosome-associated protein required for the 3' processing of stable RNAs. *Mol Cell Biol* **23:** 6982-6992

Phillips S, Butler JS (2003) Contribution of domain structure to the RNA 3' end processing and degradation functions of the nuclear exosome subunit Rrp6p. *RNA* **9:** 1098-1107

Raijmakers R, Egberts WV, van Venrooij WJ, Pruijn GJ (2002) Protein-protein interactions between human exosome components support the assembly of RNase PH-type subunits into a six-membered PNPase-like ring. *J Mol Biol* **323:** 653-663

Roth KM, Wolf MK, Rossi M, Butler JS (2005) The nuclear exosome contributes to autogenous control of NAB2 mRNA levels. *Mol Cell Biol* **25:** 1577-1585

Schaeffer D, Reis FP, Johnson SJ, Arraiano CM, van Hoof A (2012) The CR3 motif of Rrp44p is important for interaction with the core exosome and exosome function. *Nucleic Acids Res* **40:** 9298-9307

Schaeffer D, Tsanova B, Barbas A, Reis FP, Dastidar EG, Sanchez-Rotunno M, Arraiano CM, van Hoof A (2009) The exosome contains domains with specific endoribonuclease, exoribonuclease and cytoplasmic mRNA decay activities. *Nat Struct Mol Biol* **16:** 56-62

Schilders G, Raijmakers R, Malmegrim KC, Vande Walle L, Saelens X, Vree Egberts W, van Venrooij WJ, Vandenabeele P, Pruijn GJ (2007a) Caspase-mediated cleavage of the exosome subunit PM/Scl-75 during apoptosis. *Arthritis Res Ther* **9:** R12

Schilders G, Raijmakers R, Raats JM, Pruijn GJ (2005) MPP6 is an exosome-associated RNA-binding protein involved in 5.8S rRNA maturation. *Nucleic Acids Res* **33:** 6795-6804

Schilders G, van Dijk E, Pruijn GJ (2007b) C1D and hMtr4p associate with the human exosome subunit PM/Scl-100 and are involved in pre-rRNA processing. *Nucleic Acids Res* **35:** 2564-2572

Schneider C, Leung E, Brown J, Tollervey D (2009) The N-terminal PIN domain of the exosome subunit Rrp44 harbors endonuclease activity and tethers Rrp44 to the yeast core exosome. *Nucleic Acids Res* **37:** 1127-1140

Slomovic S, Fremder E, Staals RH, Pruijn GJ, Schuster G (2010) Addition of poly(A) and poly(A)-rich tails during RNA degradation in the cytoplasm of human cells. *Proc Natl Acad Sci U S A* **107:** 7407-7412

Staals RH, Bronkhorst AW, Schilders G, Slomovic S, Schuster G, Heck AJ, Raijmakers R, Pruijn GJ (2010) Dis3-like 1: a novel exoribonuclease associated with the human exosome. *EMBO J* **29:** 2358-2367

Stead JA, Costello JL, Livingstone MJ, Mitchell P (2007) The PMC2NT domain of the catalytic exosome subunit Rrp6p provides the interface for binding with its cofactor Rrp47p, a nucleic acid-binding protein. *Nucleic Acids Res* **35:** 5556-5567

Steitz TA, Steitz JA (1993) A general two-metal-ion mechanism for catalytic RNA. *Proc Natl Acad Sci U S A* **90:** 6498-6502

Tomecki R, Kristiansen MS, Lykke-Andersen S, Chlebowski A, Larsen KM, Szczesny RJ, Drazkowska K, Pastula A, Andersen JS, Stepien PP, Dziembowski A, Jensen TH (2010) The human core exosome interacts with differentially localized processive RNases: hDIS3 and hDIS3L. *EMBO J* **29:** 2342-2357

van Dijk EL, Schilders G, Pruijn GJ (2007) Human cell growth requires a functional cytoplasmic exosome, which is involved in various mRNA decay pathways. *RNA* **13:** 1027-1035

van Hoof A, Lennertz P, Parker R (2000) Yeast exosome mutants accumulate 3'-extended polyadenylated forms of U4 small nuclear RNA and small nucleolar RNAs. *Mol Cell Biol* **20:** 441-452

Wasmuth EV, Lima CD (2012) Exo- and endoribonucleolytic activities of yeast cytoplasmic and nuclear RNA exosomes are dependent on the noncatalytic core and central channel. *Mol Cell* **48:** 133-144

Zuo Y, Wang Y, Malhotra A (2005) Crystal structure of Escherichia coli RNase D, an exoribonuclease involved in structured RNA processing. *Structure* **13:** 973-984

CHAPTER 6

hDis3L2 is a cytoplasmic exoribonuclease with an exosome-independent role in maintaining cell viability

Raymond H.J. Staals, Christian Buell, Ger J.M. Pruijn*

Department of Biomolecular Chemistry, Nijmegen Center for Molecular Life Sciences and Institute for Molecules and Materials, Radboud University Nijmegen, Nijmegen, The Netherlands

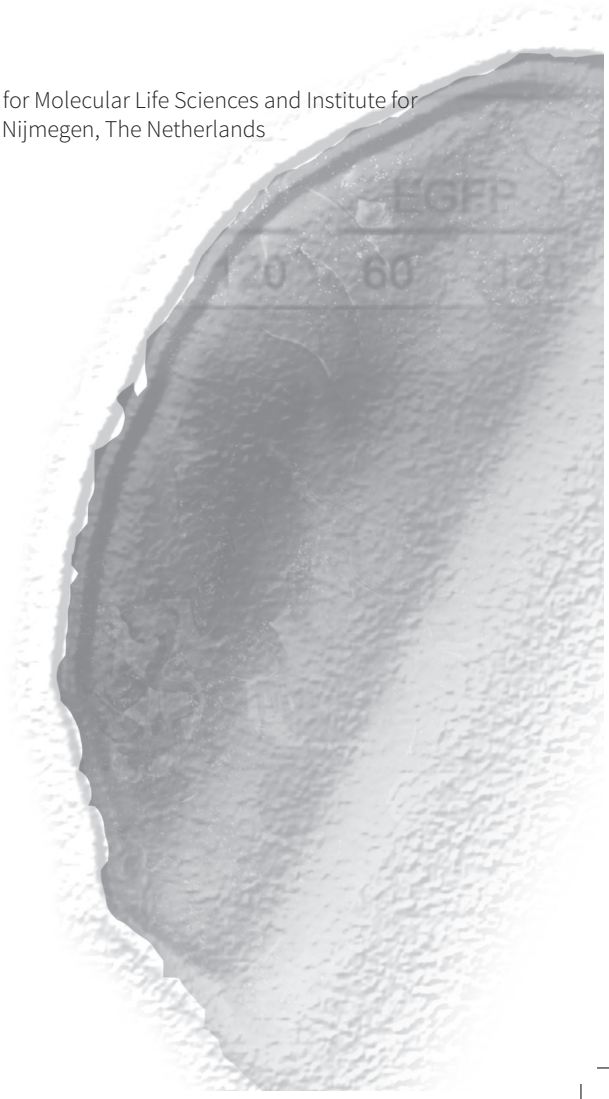

Abstract

Eukaryotic RNA degradation is mediated by a complex network of cooperating as well as independently operating enzymes. Although many different proteins and factors have been discovered over the years, the recurrent involvement of the RNA exosome makes it one of the most important protein complexes in RNA metabolism. Rather than degrading the RNA substrates itself, the eukaryotic exosome functions as a scaffold for the association of different exo- and endonucleases. Several exosome-associated nucleases have been identified and characterized, including PM/Scl-100 (or Rrp6), hDis3 and hDis3L1. The human genome encodes yet another protein with homology to Dis3-like ribonucleases, which is called hDis3L2. Here, we show that hDis3L2 is a cytoplasmic exoribonuclease that, in contrast to hDis3 and hDis3L1, is not detectably associated with the exosome. Furthermore, our data show that overexpression of hDis3L2 severely changes the cell morphology. The putative role of hDis3L2 in controlling important stages in cell division as well as the impact of hDis3L2 mutations on human health will be discussed.

Introduction

In the previous chapters it was shown that the human exosome functions as a scaffold for the association of different exoribonucleases. Both PM/Scl-100 and hDis3L1 have a strong affinity for binding the exosome and contribute to the activity that is associated with this complex. The interaction of hDis3 was found to be weaker and it is still not clear whether hDis3 is of major functional importance for exosome-mediated processes in human cells. In addition to these two Dis3(-like) proteins, the human genome appears to encode yet another protein with homology to the yeast Dis3, which is called hDis3L2.

The hDis3 and hDis3L1 proteins and their association with the exosome have been characterized previously (Lykke-Andersen *et al*, 2011; Staals *et al*, 2010; Tomecki *et al*, 2010), but the biochemical and biological features of hDis3L2 are still enigmatic. The first indications for a biological role of hDis3L2 were obtained in studies aimed at the gene(s) causing Perlman syndrome (a rare overgrowth disorder present at birth, which is frequently accompanied by a high risk of the formation of Wilms' tumors in the kidney). Perlman syndrome patients appeared to express mutants of the hDis3L2 protein, resulting in a plethora of mitotic abnormalities (Astuti *et al*, 2012). These mutant hDis3L2 proteins are due to missense and splice-site mutations, as well as exonic deletions in the germline. One of the exonic deletions (exon 9) was recently shown to arise from two independent non-allelic homologous recombination events between two L1 elements, which belong to the family of long interspersed elements (LINEs), some of which are active retrotransposons in the human genome (Higashimoto *et al*, 2013).

The first Dis3 protein was identified in *Schizosaccharomyces pombe* in a study addressing conditional mutants with defects in sister (Dis) chromatid separation (Ohkura *et al*, 1988).

The complete deletion of the Dis3 locus was found to be lethal. Furthermore, *S. pombe* Dis3 appeared to play a role in kinetochore formation and the subsequent interaction of the microtubule with the kinetochore, just prior to the anaphase (Murakami *et al*, 2007). It was suggested that *S. pombe* Dis3 mediates the silencing of the heterochromatic regions surrounding the centromere, which is important for these phenomena. In fact, temporal silencing of a particular RNA species by Dis3 has been shown to be a major cue for other fundamental cellular processes, as it appeared to be important for stages in development and meiosis as well (Cairrao *et al*, 2005; Hou *et al*, 2012; Wang *et al*, 2008).
The involvement of these Dis3(-like) proteins in such fundamentally important cellular processes underlines the need to characterize these nucleases and their activities in detail. Here, we demonstrate that hDis3L2 is a cytoplasmic protein with exoribonuclease activity and provide indirect evidence that at least a subset of its RNA substrates is involved in controlling essential mitotic events.

Results

The hDis3L2 gene is located on chromosome 2 and sequence databases indicate the existence of at least five transcript variants (accession numbers NM_152383.4, NM_001257281.1, NM_001257282.1, NR_046476.1 and NR_046477.1). The 'canonical' transcript encodes a polypeptide of 885 amino acids, with a calculated molecular mass of 99.3 kDa; the other transcripts represent shorter isoforms, which are truncated in the C-terminal region. The hDis3L2 amino acid sequence shows 23% identity with the yeast Dis3 sequence and orthologs can be found in most eukaryotic species, including fungi, mammals, vertebrates and possibly plants as well. The protein was initially believed to be absent in the fungal kingdom, since no Dis3L2 orthologs were found in the yeast *Saccharomyces cerevisiae*. However, BLAST database searches have recently indicated that *S. cerevisiae* is just one of the few examples in the fungal kingdom without a clear Dis3L2 ortholog, emphasizing the dangers of focusing on one particular model organism (Malecki *et al*, 2013).
Pfam database searches revealed the presence of a RNB domain in Dis3L2, which was originally identified in *Escherichia coli* RNase II, suggesting a role for this protein in RNA degradation. A comparison with the other two human Dis3(-like) proteins revealed some interesting differences. Both hDis3 and hDis3L1 contain three OB-fold-containing domains (CSD1, CSD2 and S1), but only the CSD2 domain can be discerned in the hDis3L2 protein (Chapter 3, Supplementary Figure S1). Furthermore, the N-terminal region of hDis3L2 does not contain a PIN(-like) domain, like hDis3 and hDis3L1, although the latter was recently shown to lack PIN domain-associated endoribonuclease activity (Staals *et al*, 2010; Tomecki *et al*, 2010). The PIN domain was also shown to mediate the interaction of Dis3 with the exosome in yeast, suggesting that hDis3L2 is incapable to associate with the exosome complex. Instead,

protein-protein interaction databases (Peri *et al*, 2004; Stark *et al*, 2006) point to interactions of hDis3L2 with COPS6 (signalosome complex subunit 6), FEZ1 (fasciculation and elongation protein zeta-1), VIM (vimentin), CBX2 (chromobox protein homolog 2) and UBC (ubiquitin C), although the biological significance of these interactions remains to be investigated.

Since the presence of an RNB domain suggests a potential role in RNA degradation, we set out to investigate whether hDis3L2 has ribonuclease activity. The coding sequence of the canonical hDis3L2 isoform was isolated from a HEp-2 cDNA library by PCR (the isolation from HeLa and human teratocarcinoma cDNA libraries failed). The hDis3L2 coding sequence was cloned into two mammalian expression vectors, either in-frame with an N-terminal VSV-G tag or fused to the 3' end of an EGFP-encoding sequence. The integrity of the constructs was confirmed by DNA sequence analysis. HEp-2 cells were transfected with these constructs, either by electroporation or using the Fugene transfection reagent and the expression was monitored 24 or 48 hours later by western blotting (Figure 1). The results showed that, in contrast to EGFP-hDis3L1 (which was included as a positive control) no expression of the tagged hDis3L2 protein could be detected, irrespective of the tag or the transfection procedure. Note that the band stained with anti-VSV-tag antibodies in material from the VSV-hDis3L2 transfected cells (Figure 1B) represents a background reactivity of the anti-VSV-tag antibodies. Other attempts to obtain hDis3L2 expression by transient transfection of COS-1 cells or by boosting the expression by the addition of sodium butyrate to the medium also did not lead to detectable hDis3L2 expression (data now shown). As an alternative for the transfected cells, an *in vitro* transcription-translation system (rabbit reticulocyte lysate) was used to produce the VSV-hDis3L2 protein. Also in this expression system hDis3L2 was not detectably expressed, in contrast to hDis3L1, which resulted in a M_r 120,000 polypeptide in SDS-PAGE, in agreement with the calculated molecular mass (Figure 2).

These results suggested that either the production of the tagged hDis3L2 proteins was very low, for example due to inefficient transcription and/or translation, or that the translation products were rapidly degraded. A third explanation might be that the expressed protein is highly toxic for cultured cells as well as the *in vitro* transcription-translation system. To explore these possibilities in more detail, COS-1 and HEp-2 cells were transfected with constructs encoding either EGFP-hDis3L2, VSV-hDis3L2 or EGFP-hDis3L1 (as a positive control) and the expression of the tagged proteins was studied by fluorescence microscopy, using anti-VSV antibodies in case of the VSV-tagged protein. In agreement with previous findings (Staals *et al*, 2010; Tomecki *et al*, 2010), EGFP-hDis3L1 was expressed in many cells and accumulated in the cytoplasm, displaying a diffuse staining pattern (Figure 3A,B). In contrast, only very few of the cells transfected with the EGFP-hDis3L2 and VSV-hDis3L2 constructs showed a detectable level of fluorescence, indeed suggesting that elevating the expression of hDis3L2 has severe effects on cell physiology. The cells in which tagged hDis3L2 expression was observed often displayed altered morphologies, some reminiscent of apoptosis (data not shown) and others

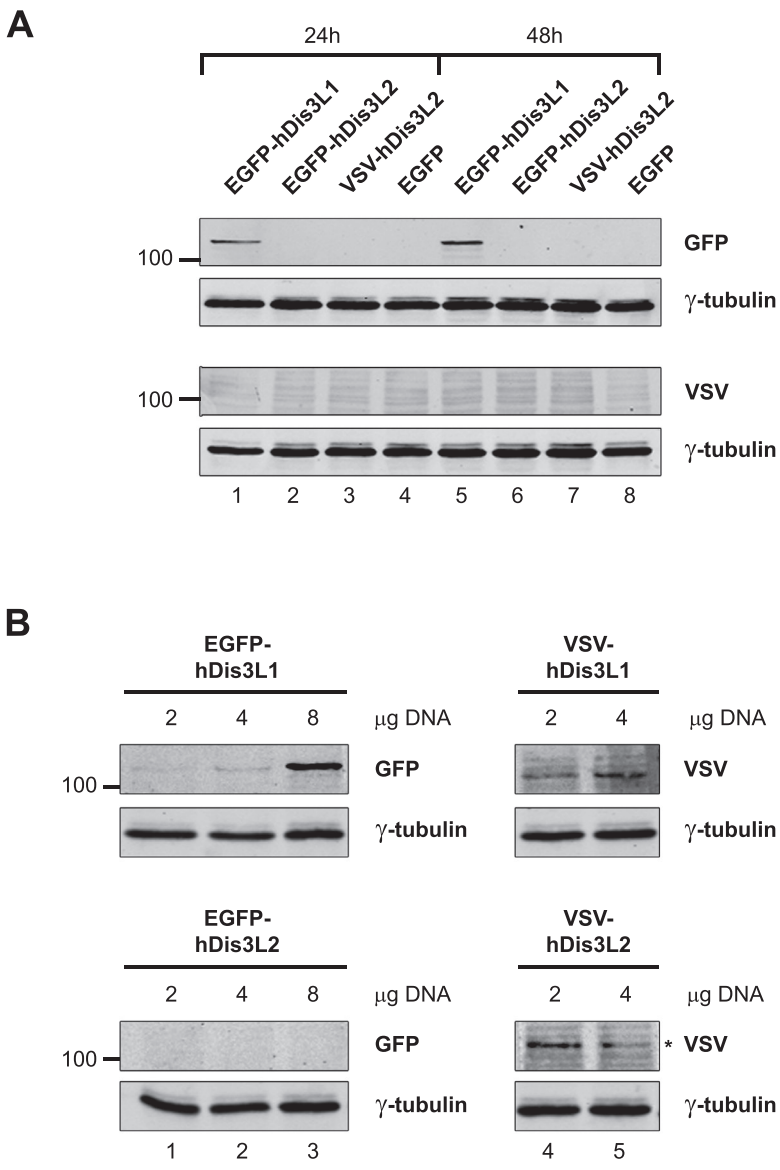

Figure 1. Expression of EGFP- or VSV-tagged hDis3L1 and hDis3L2 in HEp-2 cells.

HEp-2 cells were transfected with expression constructs encoding EGFP, EGFP-hDis3L1, VSV-hDis3L1, VSV-hDis3L2 or EGFP-hDis3L2 using electroporation (A) or the Fugene 6 transfection reagent with different amounts of plasmid DNA, as indicated above the panels (B). Total cell extracts were prepared (24 or 48 hours after electroporation or 48 hours after Fugene transfection), separated by SDS–PAGE and analysed by western blotting using polyclonal anti-GFP and monoclonal anti-VSV-tag antibodies to visualize the expression of tagged hDis3L1 and hDis3L2. Monoclonal anti-γ-tubulin antibodies were used as loading control. The asterisk indicates the presence of an unknown protein that was recognized by the anti-VSV-tag antibodies. The position of a 100 kDa marker in the gels is indicated on the left.

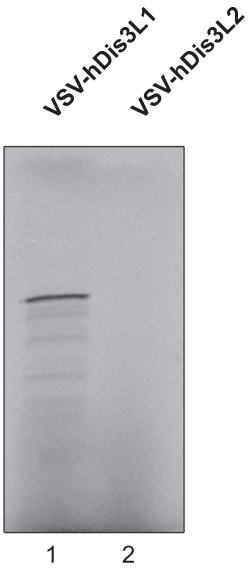

Figure 2. *In vitro* transcription and translation of VSV-hDis3L1 and VSV-hDis3L2.

VSV-hDis3L1 and VSV-hDis3L2 were expressed *in vitro* using a coupled transcription-translation system supplemented with ^{35}S-methionine. Translation products were visualized by separation on SDS-PAGE followed by autoradiography.

characterized by oversized nuclei. In these cells EGFP-hDis3L2 appeared to accumulate either in cytoplasmic speckles or was more diffusely distributed in the cytoplasm (Figure 3C,D). Cells expressing VSV-hDis3L2 with a relatively normal morphology contained the highest concentrations of VSV-hDis3L2 in small cytoplasmic speckles (Figure 3E,F). Despite the very small number of cells with detectable expression of the tagged protein and the disturbed cell morphologies, these results suggest that hDis3L2 resides in the cytoplasm, which is in agreement with observations from other laboratories (Astuti *et al*, 2012; Lubas *et al*, 2013; Malecki *et al*, 2013). Taken together, these results suggest that a small increase in the expression level of hDis3L2 may have severe consequences for cell viability. This might be due to the uncontrolled enzymatic activity of hDis3L2, but may also be caused by other phenomena. Interestingly, HEp-2 cells transfected with siRNAs to knock-down endogenous hDis3L2 protein levels displayed slightly elevated cell growth rates (data not shown).

Previously, it was shown that FLAG-tagged hDis3L2 was detectably expressed in stably transfected HEK293 cells (Astuti *et al*, 2012). Although rather speculative, the stable integration probably resulted in less dramatic increases in cellular Dis3L2 levels, thereby allowing detectable expression. Lysates from these cells were used to study the ribonuclease activity of the FLAG-tagged protein. More specifically, lysates from the HEK293 cells stably transfected with a construct encoding FLAG-tagged hDis3L2, or the corresponding FLAG-tag encoding vector, were used to immunoprecipitate the tagged protein using anti-FLAG-tag antibodies,

after which the precipitates were incubated with a radiolabeled RNA substrate in the presence of different concentrations of Mg^{2+}. While no activity was observed for the material from cell lines expressing the FLAG-tag alone, the FLAG-hDis3L2 containing precipitate efficiently converted the substrate RNA to small products (Figure 4). No degradation intermediates were detected, which is consistent with processive exonucleolytic degradation of the substrate. The highest activity was observed with no or relatively low magnesium concentrations, although also in the presence of relatively high concentrations the substrate was degraded. These results suggest that hDis3L2 acts as a Mg^{2+}-independent exoribonuclease.

Due to the similarity of hDis3L2 with hDis3 and hDis3L1, the exosome complex might be associated with hDis3L2. However, an analysis of exosome proteins copurifying with FLAG-tagged hDis3L2 by western blotting using anti-hRrp40 antibodies did not lead to the detection of hRrp40 (data not shown).

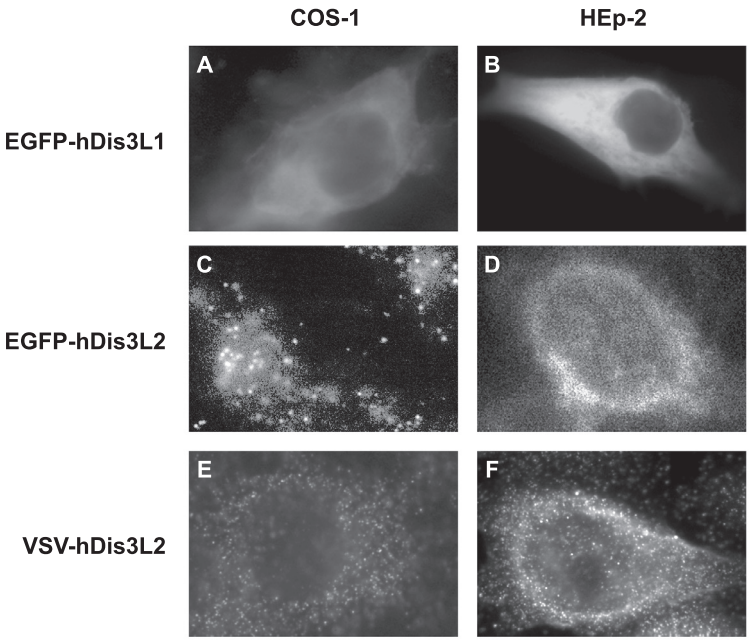

Figure 3. Localization of EGFP- or VSV-tagged hDis3L1 and hDis3L2 in HEp-2 and COS-1 cells.

COS-1 (A, C and E) and HEp-2 (B, D and F) cells were transfected with expression constructs encoding EGFP-hDis3L1 (A-B), EGFP-hDis3L2 (C-D) or VSV-hDis3L2 (E-F). Forty-eight hours after transfection the cells were fixed and EGFP-fusion proteins were visualized directly by fluorescence microscopy. The VSV-tagged proteins were visualized by incubating the cells with anti-VSV-tag antibodies after fixation and permeabilization, followed by Alexa Fluor 555-conjugated goat anti-mouse antibodies and fluorescence microscopy.

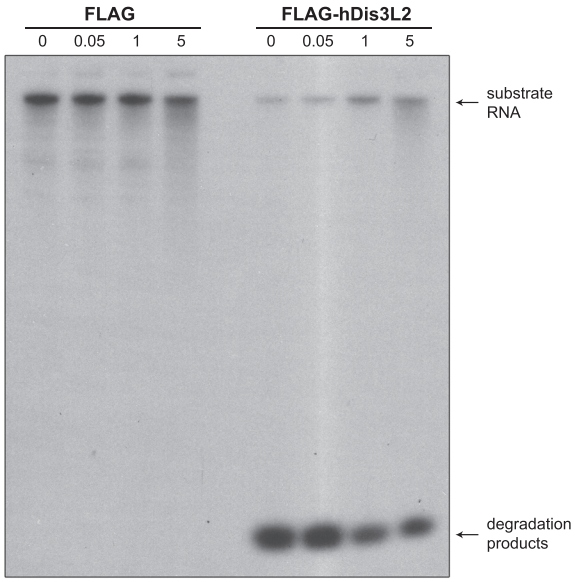

Figure 4. RNA degradation by Dis3L2 *in vitro.*

Cell lysates from stably transfected HEK293 cells expressing either the FLAG-tag alone (FLAG) or FLAG-tagged hDis3L2 (FLAG-hDis3L2) were subjected to immunoprecipitation with anti-FLAG antibodies. Precipitated proteins were incubated with a 267 nucleotide radiolabelled RNA substrate and the reaction products were subsequently analysed by denaturing polyacrylamide gel electrophoresis followed by autoradiography. The incubations were performed in the presence of various concentrations of Mg^{2+} (indicated in mM above the lanes).

Discussion

The results presented here indicate that hDis3L2 is an exosome-independent, cytoplasmic ribonuclease. hDis3L2 displayed exoribonuclease activity *in vitro* which does not seem to require Mg^{2+} (Figure 4). It should be noted that traces of Mg^{2+} might have been introduced in the reaction mixture that was used to analyse the activity in the absence of magnesium, e.g. via the (purification of the) RNA substrate. For the exoribonuclease activity of the structurally related proteins hDis3 and hDis3L1, Mg^{2+} has been previously shown to be required, albeit at low concentrations (Staals *et al*, 2010; Tomecki *et al*, 2010). Akin to hDis3 and hDis3L1, the active site of hDis3L2 is expected to be situated in its RNB domain, as deletion mutants abrogating this domain diminished its activity (Astuti *et al*, 2012). Since the same stable cell lines were used in this study, these findings also make it less likely that other (co-purifying) proteins are responsible for the observed activity in our RNA degradation assay.

In contrast to hDis3 and hDis3L1, hDis3L2 does not seem to be associated with the exosome core. First, no co-immunoprecipitation of the exosome with (FLAG-tagged) hDis3L2 was observed, which is substantiated by recently published data from other laboratories (Lubas *et al*, 2013; Malecki *et al*, 2013). Second, hDis3L2 lacks a PIN domain, which mediates the

interaction of Dis3 with the exosome (Schaeffer *et al*, 2012; Schneider *et al*, 2009). Finally, previous analyses of purified exosome complexes failed to identify hDis3L2 as a copurifying protein, even when sensitive approaches such as SILAC were applied (Chen *et al*, 2001; Staals *et al*, 2010; Tomecki *et al*, 2010). These observations argue against an exosome-dependent role of hDis3L2 in RNA metabolism.

None of the attempts to express tagged hDis3L2 in transiently transfected mammalian cells (HEp-2 and COS-1) to levels that are detectable by western blotting using total cell lysates was successful. One explanation for these observations might be that the (over)expression of the recombinant protein has severe effects on cell viability. When individual cells were examined by fluorescence microscopy, only very few cells showed detectable expression of the fluorescently tagged hDis3L2 protein. It is not likely that this is due to low transfection efficiencies, because EGFP-hDis3L1 and VSV-hDis3L1, which were analyzed in parallel, were readily expressed. Since also the morphology of most of the cells with detectable hDis3L2 expression was unusual, elevated expression levels of hDis3L2 indeed seem to be detrimental for cell survival. The expression data in the BIOGPS database (Wu *et al*, 2009) suggest that hDis3L2 is ubiquitously expressed in human tissues. Although this expression profile does not allow a proper comparison of the expression levels between different tissues, it is possible that the expression of Dis3L2 *in vivo* is tightly regulated. A possible explanation for our observed unusual cell morphologies can therefore be the disturbance of these tightly controlled hDis3L2 protein levels (e.g. by exogenous hDis3L2 expression).

As explained in the introduction, the importance of Dis3 for proper mitotic progression has been known since its discovery in yeast, where the protein was shown to have roles in chromatid disjoining and kinetochore formation (Murakami *et al*, 2007; Ohkura *et al*, 1988). The evidence in favor for a role of hDis3L2 in controlling the proper expression levels of several cell-cycle related mRNAs is currently building up. Firstly, mRNA levels of important proteins required for proper mitotic progression were found to be affected in cells where hDis3L2 protein levels were knocked down by RNAi (Astuti *et al*, 2012). Most notably, proteins involved in centrosome duplication (TTK), chromatid separation (securin) and several proteins controlling mitotic checkpoints (Aurora B, phosphorylated CDC25C, cyclin B1 and RAD21) were affected. Interestingly, the knockdown of hDis3L2 also resulted in aberrant cell morphologies, which could be a consequence of the aforementioned disturbed protein levels. Secondly, recent RNA-seq data have demonstrated that depletion of hDis3L2 resulted in the stabilization of many cell-cycle related mRNAs (Lubas *et al*, 2013). These findings suggest that the observed aberrant cell morphologies in hDis3L2 overexpressing cells (Figure 3) might be a result of a disturbance in the expression levels of cell-cycle and/or mitosis-related proteins, as both depletion and overexpression of proteins involved in these processes can affect cell morphology.

These data indicate that some RNA substrates of hDis3L2 are mRNAs encoding proteins with important functions in the cell cycle, making hDis3L2 a potential tumor suppressor. In line with this is the observation that cells with depleted hDis3L2 protein levels have a growth advantage over wild-type cells (Astuti *et al*, 2012). Furthermore, the observation that germline mutations in the hDis3L2 gene were found to be the cause of the Perlman syndrome further supports the role of hDis3L2 as a tumor suppressor. A possible link between the mutations in hDis3L2 and the development of the Perlman syndrome has recently been found by the identification of one of its substrates: the pre-let-7 miRNA (Chang *et al*, 2013). Silencing of this particular miRNA is especially important in stem cells, keeping them in an undifferentiated and proliferative state, while it is relieved in somatic cells (Yu *et al*, 2007). Lastly, recent studies have revealed a genetic link between human height variation and sequence variations in chromosomal loci containing the hDis3L2 gene (Estrada *et al*, 2009; Gudbjartsson *et al*, 2008; Okada *et al*, 2010). Further studies will be required to investigate whether hDis3L2 is involved.

Recently, a novel exoribonuclease homologous to hDis3L2 was identified in *Schizosaccharomyces pombe* (Malecki *et al*, 2013). *S. pombe* Dis3L2 was shown to be involved in an exosome-independent 3'-5' mRNA decay pathway occurring at or near P-bodies. P-bodies are granule-like cytoplasmic foci where translationally-silenced mRNAs and many different enzymes for various mRNA decay pathways are concentrated (Kulkarni *et al*, 2010). One of these enzymes is hXrn1, an important exoribonuclease responsible for 5'-3' mRNA decay (Sheth and Parker, 2003). Although 3'-5' mRNA decay was initially assumed to contribute little to the mRNA decay associated with these foci, this possibility now needs to be reinvestigated with the discovery of Dis3L2, which provides a source of 3'-5' ribonuclease activity. It appears that Xrn1 and Dis3L2 operate redundantly in mRNA decay substrates, as deletion of Dis3L2 was found to be synthetically lethal with a Xrn1 deletion (Malecki *et al*, 2013). In addition, hDis3L2 was recently shown to physically interact with hXrn1 and depletion of either hDis3L2 or hXrn1 stabilized an overlapping pool of RNAs (Lubas *et al*, 2013), indicating that at least some of their RNA substrates are indeed shared.

It will be interesting to investigate whether the observed cytoplasmic speckles in Dis3L2 overexpressing HEp-2 cells (Figure 3) also represent P-bodies. Since no P-body marker (such as DCP2) was included in our analysis, we cannot differentiate between this and other plausible explanations for the observed speckled staining pattern, such as protein aggregates, or stress granules. Co-localization experiments with P-body markers, e.g. by fluorescence microscopy, are needed to shed more light on this issue. It will also be interesting to investigate whether hDis3L2 overexpression affects the abundance of these P-bodies, because depletion of hDis3L2 was shown to increase the number of P-bodies per cell (Lubas *et al*, 2013).

In summary, the significance of RNA degradation by Dis3L2 for cellular RNA metabolism has just begun to become apparent and future experiments will provide more insight in the biochemical function of this exciting novel exoribonuclease.

Materials and methods

cDNA cloning and generation of the hDis3L2 expression constructs

The complete coding sequence of the largest isoform of hDis3L2 (RefSeq accession number: NM_152383.4) was isolated from a custom HEp-2, oligo(dT)-primed cDNA library by PCR using the following oligonucleotides:
5' - ACGCGTGGATCCAATGAGCCATCCTGACTACAG - 3' and
5' - CCCGAGGACTCAAGCACCAGCCCCGGGTGAGTCGAC- 3'.
The resulting PCR product was subsequently cloned into the pCR4-TOPO vector according to the manufacturer's guidelines (Invitrogen). The sequence of the selected clone was confirmed by DNA sequencing. N-terminal EGFP- and VSV-tagged hDis3L2 expression constructs were made by inserting the coding sequence into the pEGFP-C3 (Clontech) and pCI-neo-5'-VSV (Raijmakers *et al*, 2002) vectors, respectively, using the appropriate restriction sites that were added in the cDNA cloning primers.

Transient transfection of HEp-2 and COS-1 cells

Transfection of HEp-2 and COS-1 cells with the constructs encoding EGFP- and VSV-tagged hDis3L1 or hDis3L2 using the transfection reagent Fugene 6 (Roche) was performed in a 6-well cell culture format according to the manufacturer's recommendations using either 2, 4 or 8 μg of plasmid DNA per 5 x 10^5 cells. The transfection of the cells by electroporation was performed essentially as described before (Staals *et al*, 2010), with the exception that for the COS-1 cells, ice-cold PBS (phosphate-buffered saline) was used to resuspend the cells, after which the cells were electroporated at 300V and 125μF. Twenty-four or forty-eight hours after transfection the cells were harvested by trypsinization, resuspended in lysis-buffer (25 mM Tris-HCl, pH 7.5, 100 mM KCl, 1 mM EDTA, 0.5 mM PMSF, 0.05% NP-40, 1 mM DTT) and sonicated 3 times 30 seconds on ice using a Branson micro-tip.

Fluorescence microscopy

To study the subcellular localization of the tagged hDis3L1 and hDisL2 proteins, HEp-2 and COS-1 cells were transfected as described above, seeded on glass coverslips and fixed after

forty-eight hours with 3.7% paraformaldehyde. EGFP fusion proteins were visualized directly, while the VSV-tagged proteins were detected indirectly by incubation with a monoclonal anti-VSV antibody after permeabilization of the cells, followed by Alexa Fluor 555-conjugated goat anti-mouse antibodies (Invitrogen). Incubations with antibodies were performed in PBS supplemented with 1% sheep serum. The localization of EGFP- and VSV-tagged proteins was visualized by fluorescence microscopy.

Immunoblotting

For the detection of proteins on western blots, polyclonal rabbit antibodies (anti-GFP, anti-γ-tubulin "GTU-88" (Abcam)) and monoclonal mouse antibodies (anti-VSV-tag) were diluted in blocking buffer (5% non-fat dry milk, PBS, 0.05% NP-40). Blots were incubated with these antibodies for 1 h at room temperature. Bound antibodies were detected by incubation with IRDye 800CW-conjungated polyclonal goat anti-mouse or goat anti-rabbit antibodies (Li-Cor) for 1 h in blocking buffer and visualization using an Odyssey Infrared Imaging System (Li-Cor).

In vitro transcription and translation of Dis3L1 and Dis3L2

In vitro transcription and translation of hDis3L1 and hDis3L2 were performed by using the VSV-tagged expression constructs (described above) and the TnT Coupled Reticulocyte Lysate System (Promega), supplemented with ^{35}S-methionine using the manufacturer's recommendations.

RNA degradation assays

Cell pellets derived from the stable HEK293 cell clones expressing the FLAG-tag alone or the FLAG-tagged wild-type hDis3L2 were resuspended in six volumes of lysis buffer containing a protease inhibitor cocktail (Roche) and were incubated for 30 min on ice, sonicated and centrifuged at 13,000g at 4 °C for 30 min. Monoclonal mouse antibody to the FLAG-tag pre-coupled to protein A–agarose beads (Sigma) was added, and precipitates were washed twice with IPP500 (500 mM NaCl, 10 mM Tris-HCl, pH 8.0 and 0.05% NP-40) and twice with IPP150 (150 mM NaCl, 10 mM Tris-HCl, pH 8.0 and 0.05% NP-40). Cell extracts were incubated with the antibody-coupled beads overnight at 4 °C. Beads were washed twice with IPP150 and twice in RNA degradation buffer (20 mM HEPES-KOH, pH 7.5, 50 mM KCl and 1 mM DTT), containing different concentrations of Mg^{2+} (as indicated in Figure 4). RNA degradation assays were performed using a radiolabeled 267-nucleotide RNA substrate (the human 5.8S rRNA sequence and the most 5' 100 nucleotides of ITS2), which was obtained by *in vitro* transcription in the presence of α-^{32}P-UTP (Perkin-Elmer). After gel purification of the RNA substrate, it was incubated for 2 h with the immunoprecipitated material at 37 °C in RNA degradation buffer containing $MgCl_2$ concentrations as indicated. Reactions were stopped by the addition of 2 volumes RNA loading buffer (9 M urea, 0.1% bromophenol blue and 0.1% xylene cyanol)

supplemented with 20% phenol. Samples were analyzed by denaturing polyacrylamide gel electrophoresis followed by autoradiography.

References

Astuti D, Morris MR, Cooper WN, Staals RH, Wake NC, Fews GA, Gill H, Gentle D, Shuib S, Ricketts CJ, Cole T, van Essen AJ, van Lingen RA, Neri G, Opitz JM, Rump P, Stolte-Dijkstra I, Muller F, Pruijn GJ, Latif F, Maher ER (2012) Germline mutations in DIS3L2 cause the Perlman syndrome of overgrowth and Wilms tumor susceptibility. *Nat Genet* **44:** 277-284

Cairrao F, Arraiano C, Newbury S (2005) Drosophila gene tazman, an orthologue of the yeast exosome component Rrp44p/Dis3, is differentially expressed during development. *Dev Dyn* **232:** 733-737

Chang HM, Triboulet R, Thornton JE, Gregory RI (2013) A role for the Perlman syndrome exonuclease Dis3l2 in the Lin28-let-7 pathway. *Nature* **497:** 244-248

Chen CY, Gherzi R, Ong SE, Chan EL, Raijmakers R, Pruijn GJ, Stoecklin G, Moroni C, Mann M, Karin M (2001) AU binding proteins recruit the exosome to degrade ARE-containing mRNAs. *Cell* **107:** 451-464

Estrada K, Krawczak M, Schreiber S, van Duijn K, Stolk L, van Meurs JB, Liu F, Penninx BW, Smit JH, Vogelzangs N, Hottenga JJ, Willemsen G, de Geus EJ, Lorentzon M, von Eller-Eberstein H, Lips P, Schoor N, Pop V, de Keijzer J, Hofman A, Aulchenko YS, Oostra BA, Ohlsson C, Boomsma DI, Uitterlinden AG, van Duijn CM, Rivadeneira F, Kayser M (2009) A genome-wide association study of northwestern Europeans involves the C-type natriuretic peptide signaling pathway in the etiology of human height variation. *Hum Mol Genet* **18:** 3516-3524

Gudbjartsson DF, Walters GB, Thorleifsson G, Stefansson H, Halldorsson BV, Zusmanovich P, Sulem P, Thorlacius S, Gylfason A, Steinberg S, Helgadottir A, Ingason A, Steinthorsdottir V, Olafsdottir EJ, Olafsdottir GH, Jonsson T, Borch-Johnsen K, Hansen T, Andersen G, Jorgensen T, Pedersen O, Aben KK, Witjes JA, Swinkels DW, den Heijer M, Franke B, Verbeek AL, Becker DM, Yanek LR, Becker LC, Tryggvadottir L, Rafnar T, Gulcher J, Kiemeney LA, Kong A, Thorsteinsdottir U, Stefansson K (2008) Many sequence variants affecting diversity of adult human height. *Nat Genet* **40:** 609-615

Higashimoto K, Maeda T, Okada J, Ohtsuka Y, Sasaki K, Hirose A, Nomiyama M, Takayanagi T, Fukuzawa R, Yatsuki H, Koide K, Nishioka K, Joh K, Watanabe Y, Yoshiura K, Soejima H (2013) Homozygous deletion of DIS3L2 exon 9 due to non-allelic homologous recombination between LINE-1s in a Japanese patient with Perlman syndrome. *Eur J Hum Genet* **21:** 1316-1319

Hou D, Ruiz M, Andrulis ED (2012) The ribonuclease Dis3 is an essential regulator of the developmental transcriptome. *BMC Genomics* **13:** 359

Kulkarni M, Ozgur S, Stoecklin G (2010) On track with P-bodies. *Biochem Soc Trans* **38:** 242-251

Lubas M, Damgaard CK, Tomecki R, Cysewski D, Jensen TH, Dziembowski A (2013) Exonuclease hDIS3L2 specifies an exosome-independent 3'-5' degradation pathway of human cytoplasmic mRNA. *EMBO J* **32:** 1855-1868

Lykke-Andersen S, Tomecki R, Jensen TH, Dziembowski A (2011) The eukaryotic RNA exosome: same scaffold but variable catalytic subunits. *RNA Biol* **8:** 61-66

Malecki M, Viegas SC, Carneiro T, Golik P, Dressaire C, Ferreira MG, Arraiano CM (2013) The exoribonuclease Dis3L2 defines a novel eukaryotic RNA degradation pathway. *EMBO J* **32:** 1842-1854

Murakami H, Goto DB, Toda T, Chen ES, Grewal SI, Martienssen RA, Yanagida M (2007) Ribonuclease activity of Dis3 is required for mitotic progression and provides a possible link between heterochromatin and kinetochore function. *PLoS One* **2:** e317

Ohkura H, Adachi Y, Kinoshita N, Niwa O, Toda T, Yanagida M (1988) Cold-sensitive and caffeine-supersensitive mutants of the Schizosaccharomyces pombe dis genes implicated in sister chromatid separation during mitosis. *EMBO J* **7:** 1465-1473

Okada Y, Kamatani Y, Takahashi A, Matsuda K, Hosono N, Ohmiya H, Daigo Y, Yamamoto K, Kubo M, Nakamura Y, Kamatani N (2010) A genome-wide association study in 19 633 Japanese subjects identified LHX3-QSOX2 and IGF1 as adult height loci. *Hum Mol Genet* **19:** 2303-2312

Peri S, Navarro JD, Kristiansen TZ, Amanchy R, Surendranath V, Muthusamy B, Gandhi TK, Chandrika KN, Deshpande N, Suresh S, Rashmi BP, Shanker K, Padma N, Niranjan V, Harsha HC, Talreja N, Vrushabendra BM, Ramya MA, Yatish AJ, Joy M, Shivashankar HN, Kavitha MP, Menezes M, Choudhury DR, Ghosh N, Saravana R, Chandran S, Mohan S, Jonnalagadda CK, Prasad CK, Kumar-Sinha C, Deshpande KS, Pandey A (2004) Human protein reference database as a discovery resource for proteomics. *Nucleic Acids Res* **32:** D497-501

Raijmakers R, Egberts WV, van Venrooij WJ, Pruijn GJ (2002) Protein-protein interactions between human exosome components support the assembly of RNase PH-type subunits into a six-membered PNPase-like ring. *J Mol Biol* **323:** 653-663

Schaeffer D, Reis FP, Johnson SJ, Arraiano CM, van Hoof A (2012) The CR3 motif of Rrp44p is important for interaction with the core exosome and exosome function. *Nucleic Acids Res* **40:** 9298-9307

Schneider C, Leung E, Brown J, Tollervey D (2009) The N-terminal PIN domain of the exosome subunit Rrp44 harbors endonuclease activity and tethers Rrp44 to the yeast core exosome. *Nucleic Acids Res* **37:** 1127-1140

Sheth U, Parker R (2003) Decapping and decay of messenger RNA occur in cytoplasmic processing bodies. *Science* **300:** 805-808

Staals RH, Bronkhorst AW, Schilders G, Slomovic S, Schuster G, Heck AJ, Raijmakers R, Pruijn GJ (2010) Dis3-like 1: a novel exoribonuclease associated with the human exosome. *EMBO J* **29:** 2358-2367

Stark C, Breitkreutz BJ, Reguly T, Boucher L, Breitkreutz A, Tyers M (2006) BioGRID: a general repository for interaction datasets. *Nucleic Acids Res* **34:** D535-539

Tomecki R, Kristiansen MS, Lykke-Andersen S, Chlebowski A, Larsen KM, Szczesny RJ, Drazkowska K, Pastula A, Andersen JS, Stepien PP, Dziembowski A, Jensen TH (2010) The human core exosome interacts with differentially localized processive RNases: hDIS3 and hDIS3L. *EMBO J* **29:** 2342-2357

Wang SW, Stevenson AL, Kearsey SE, Watt S, Bahler J (2008) Global role for polyadenylation-assisted nuclear RNA degradation in posttranscriptional gene silencing. *Mol Cell Biol* **28:** 656-665

Wu C, Orozco C, Boyer J, Leglise M, Goodale J, Batalov S, Hodge CL, Haase J, Janes J, Huss JW, 3rd, Su AI (2009) BioGPS: an extensible and customizable portal for querying and organizing gene annotation resources. *Genome Biol* **10:** R130

Yu J, Vodyanik MA, Smuga-Otto K, Antosiewicz-Bourget J, Frane JL, Tian S, Nie J, Jonsdottir GA, Ruotti V, Stewart R, Slukvin, II, Thomson JA (2007) Induced pluripotent stem cell lines derived from human somatic cells. *Science* **318:** 1917-1920

CHAPTER 7

The human 3'-5' exoribonuclease hDis3 is associated with the pre-mRNA splicing machinery

Raymond H.J. Staals[a], Geurt Schilders[a], Wilma Vree Egberts, Ger J.M. Pruijn

Department of Biomolecular Chemistry, Nijmegen Center for Molecular Life Sciences and Institute for Molecules and Materials, Radboud University Nijmegen, Nijmegen, The Netherlands

[a] These authors contributed equally

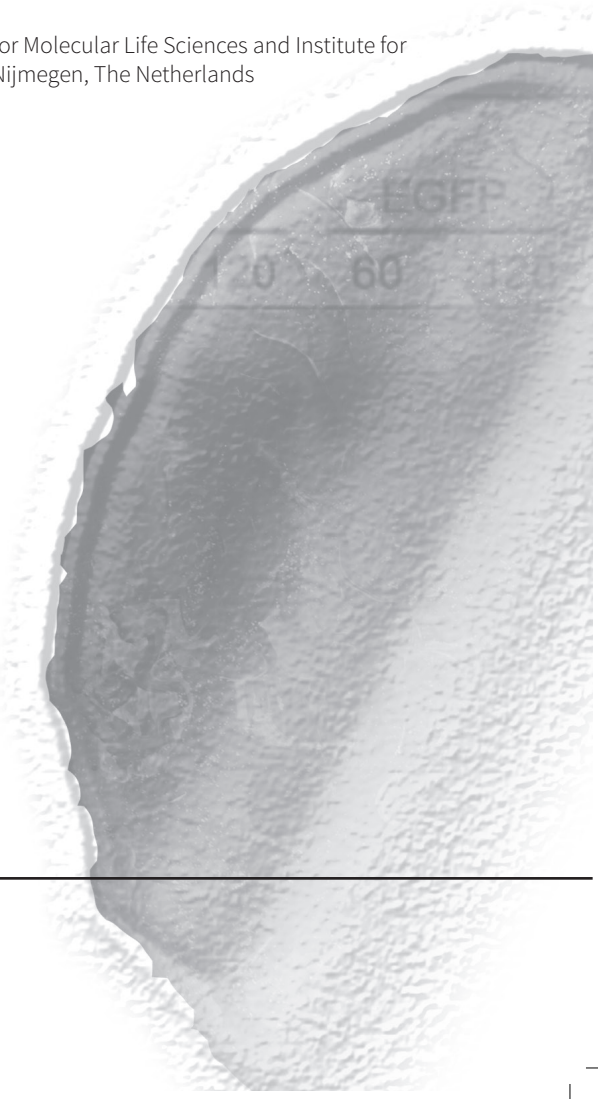

Submitted for publication

Abstract

The exosome is a multi-subunit complex, which is involved in 3'-5' processing or degradation of different classes of RNA. The human exosome contains nine components which are shared by the cytoplasmic and nuclear complex and are therefore termed 'core' components. In yeast Dis3/Rrp44, a member of the RNase R family of exoribonucleases, is stably associated with the exosome core. In this study, we addressed the ribonucleolytic activity of its human orthologue, hDis3 using in vitro activity assays. This revealed that hDis3 functions as a hydrolytic 3'-5' exoribonuclease, capable of degrading both structured and unstructured RNA substrates. Previous studies indicated that hDis3 is not (stably) associated with the exosome core, arguing for an exosome-independent role for hDis3 in RNA metabolism. To obtain more insight into processes mediated by hDis3, we identified proteins interacting with hDis3 by LC-MS/MS analysis of proteins co-purifying with hDis3 from HEp-2 cell extracts. The results showed that hDis3 interacts with many proteins involved in pre-mRNA splicing and pre-RNA processing. The interaction with one of these, SF3a60, was confirmed by coimmunoprecipitation experiments. We performed a global analysis of the effects of hDis3 depletion on steady-state mRNA levels. Although a relatively small subgroup of mRNAs appeared to be similarly affected as observed after depletion of an exosome core component or an exosome-associated ribonuclease (PM/Scl-100), the results are consistent with an exosome-independent role of hDis3 in pre-mRNA splicing.

Introduction

In the last decade major advances have been made with regard to the function, composition and structure of the RNA exosome, a multi-subunit complex containing 3'-5' exoribonuclease activity. The exosome has been demonstrated to be required for a variety of processes including the 3'-end processing of nuclear RNAs such as the 5.8S ribosomal RNA and small nucle(ol)ar RNAs, as well as the degradation of aberrant rRNAs, tRNAs and pre-mRNAs in the nucleus, whereas in the cytoplasm the exosome was shown to be required for the rapid decay of unstable mRNAs containing AU-rich sequence elements, as well as regular mRNA turnover (Chlebowski *et al*, 2013; Lykke-Andersen *et al*, 2009; Sloan *et al*, 2012). Next to the degradation of these 'canonical' RNAs, transcripts arising from pervasive transcription have also been shown to be targets for the exosome (Davis and Ares, 2006; Neil *et al*, 2009; Preker *et al*, 2008). Finally, exosome complexes were demonstrated to participate in several aspects in RNAi, such as the processing of miRNAs (Flynt *et al*, 2010) and the degradation of mRNAs that have been targeted for destruction by RISC (Orban and Izaurralde, 2005).

The eukaryotic exosome consists of at least nine components which are shared by the nuclear and cytoplasmic complex and are therefore often termed 'core' components. Six subunits (Rrp41, Rrp42, Rrp43/OIP2, Rrp45/PM/Scl-75, Rrp46, Mtr3) share homology with the bacterial 3'-5' exoribonuclease RNase PH and were shown to form a hexameric ring structure. Three

additional subunits show similarity to S1 and KH RNA-binding proteins (Rrp40p, Rrp4p and Csl4p) and form a second ring bound to one side of the hexameric ring (Liu *et al*, 2006). In the yeast *Saccharomyces cerevisiae*, an additional protein, Dis3/Rrp44, has been demonstrated to bind to the other side of the hexameric ring structure, although its interaction with the exosome core is unstable at high salt conditions (Bonneau *et al*, 2009; Schneider *et al*, 2009; Staals *et al*, 2010; Tomecki *et al*, 2010; Wang *et al*, 2007). Interestingly, Dis3 has been reported to be the major active 3'-5' exoribonuclease of the yeast exosome and to be essential for the recognition of specific RNA substrates (Dziembowski *et al*, 2007; Schneider *et al*, 2009). Moreover, it has been shown that Dis3 is essential for cell survival (Mitchell *et al*, 1997). Dis3 shares sequence similarity to RNase R, a member of the RNase II family of exoribonucleases which can processively degrade a single-stranded RNA substrate in the 3' to 5' direction resulting in the release of nucleotide 5' monophosphates (Amblar *et al*, 2006). In addition, the yeast Dis3 protein has been demonstrated to possess endoribonuclease activity, which is dependent on the PIN domain located in the N-terminal region (Lebreton *et al*, 2008). This PIN domain is also responsible for the interaction with the exosome core (Dziembowski *et al*, 2007; Schneider *et al*, 2009).

Another protein which was shown to be stably associated with the exosome core is Rrp6, a hydrolytic 3'-5' exoribonuclease which belongs to the RNase D family. Rrp6 is associated with nuclear exosomes in yeast, whereas its human counterpart, PM/Scl-100, appears to be present in the cytoplasm as well (Brouwer *et al*, 2001; Lejeune *et al*, 2003; van Dijk *et al*, 2007). Besides the differences in localization of the yeast and human Rrp6/PM/Scl-100, the capacity to degrade structured RNA substrates appeared to be slightly different as well (Januszyk *et al*, 2011).

Like in yeast, the human nine subunit exosome core was found to be catalytically inactive (Liu *et al*, 2006). As such, the human exosome core was postulated to function as a scaffold for the interaction with ribonucleases akin to the situation in yeast. Interestingly, the human genome encodes three putative homologues of yeast Dis3, which are termed hDis3 (958 aa), Dis3-like exonuclease 1 (hDis3L1 or hDis3L, 1001 aa) and Dis3-like exonuclease 2 (hDis3L2, 885 aa) (Astuti *et al*, 2012; Staals *et al*, 2010; Tomecki *et al*, 2010). Of these three proteins, hDis3 shows the highest level of sequence similarity with yeast Dis3 (Figure 1). Further analysis of the sequences by pattern and profile searches revealed a conserved PIN domain in the yeast and human Dis3 proteins, while several residues crucial for the endonucleolytic potential of this domain were absent in hDis3L1 and hDis3L2 (Staals *et al*, 2010; Tomecki *et al*, 2010). All Dis3 proteins contain a highly conserved RNB domain, which has been shown to be essential for their 3'-5' exoribonuclease activity (Astuti *et al*, 2012; Dziembowski *et al*, 2007; Staals *et al*, 2010; Tomecki *et al*, 2010). A putative nuclear localization signal was identified in the C-terminal region of hDis3: PKKKKM (aa 949 to 954).

The unstable interaction with the exosome core (Staals *et al*, 2010; Tomecki *et al*, 2010) argues for an exosome-independent role of hDis3 in RNA metabolism. To obtain more insight

in the role of hDis3 in cellular processes, we characterized its enzymatic activity, studied its interaction with other proteins and performed a global analysis of mRNAs affected by a reduction of hDis3 levels.

Results

Dis3 expression in primate cell lines

The human Dis3 polypeptide has a molecular mass of 109 kDa and a theoretical isoelectric point of 6.7. Nucleotide sequence database searches revealed a putative isoform of hDis3 in which amino acids 78-129 are replaced by VSAWRPGTWASVASSLRLPGSL, most likely as a result of an alternative splicing event (GenBank acc. number: NM_001128226). This results in a hDis3 isoform with a molecular mass of 105 kDa. Interestingly, the alternative elements are located within the PIN domain and thus may affect the endonucleolytic activity of this domain and/or the binding to the exosome core.

A polyclonal antibody to hDis3 detected two polypeptides in HEp-2 cell lysates, migrating at approximately 110 kDa and 85 kDa in SDS-PAGE gels (Figure 2A, lane 1). siRNA-mediated knockdown of hDis3 resulted in a significant reduction of the 110 kDa signal (Figure 2A, lane 3), indicating that the 110 kDa band represents hDis3 and that the 85 kDa band is probably due to cross-reactivity of the antiserum. As controls, siRNAs for EGFP and the exosome-associated protein MPP6 were used, and these did not detectably affect hDis3 expression levels (Figure 2A, lanes 1 and 2).

To further investigate the expression of hDis3, extracts of several different primate cell lines were analyzed by western blotting. The 110 kDa Dis3 protein appeared to be expressed at similar levels in all cells analyzed (Jurkat, a human T lymphocyte cell line; COS-1, a monkey kidney cell line; HEK293, a human embryonic kidney cell line; HEp-2, a human epithelial cell line; HL60, a human promyelocytic cell line; Figure 2B). Searching the BioGPS database (Wu *et al*, 2009) revealed that hDis3 expression was detected in all of the 79 different human tissues that were analysed at the mRNA level, indicating that hDis3 is indeed ubiquitously expressed. The RT-PCR primers used to generate this dataset cannot differentiate between the

Figure 1. Yeast and human Dis3 and Dis3-like sequence alignment.

A multiple alignment of the amino acid sequences of yeast Dis3 (yDis3), human Dis3 (hDis3), human Dis3-like 1 (hDis3L1) and human Dis3-like 2 (hDis3L2) was generated by the MUSCLE algorithm. The secondary structure of hDis3L1, as predicted by PsiPred, is depicted below the sequence alignment; β-strands are represented with green arrows and α-helices with red bars. Protein domains predicted by SMART are indicated by colored boxes surrounding the sequences. The putative NLS of hDis3, "PKKKKM", is indicated as well. The graphical presentation of the alignments was generated with Jalview (Waterhouse *et al*, 2009) using the default color scheme used for alignments in Clustal X.

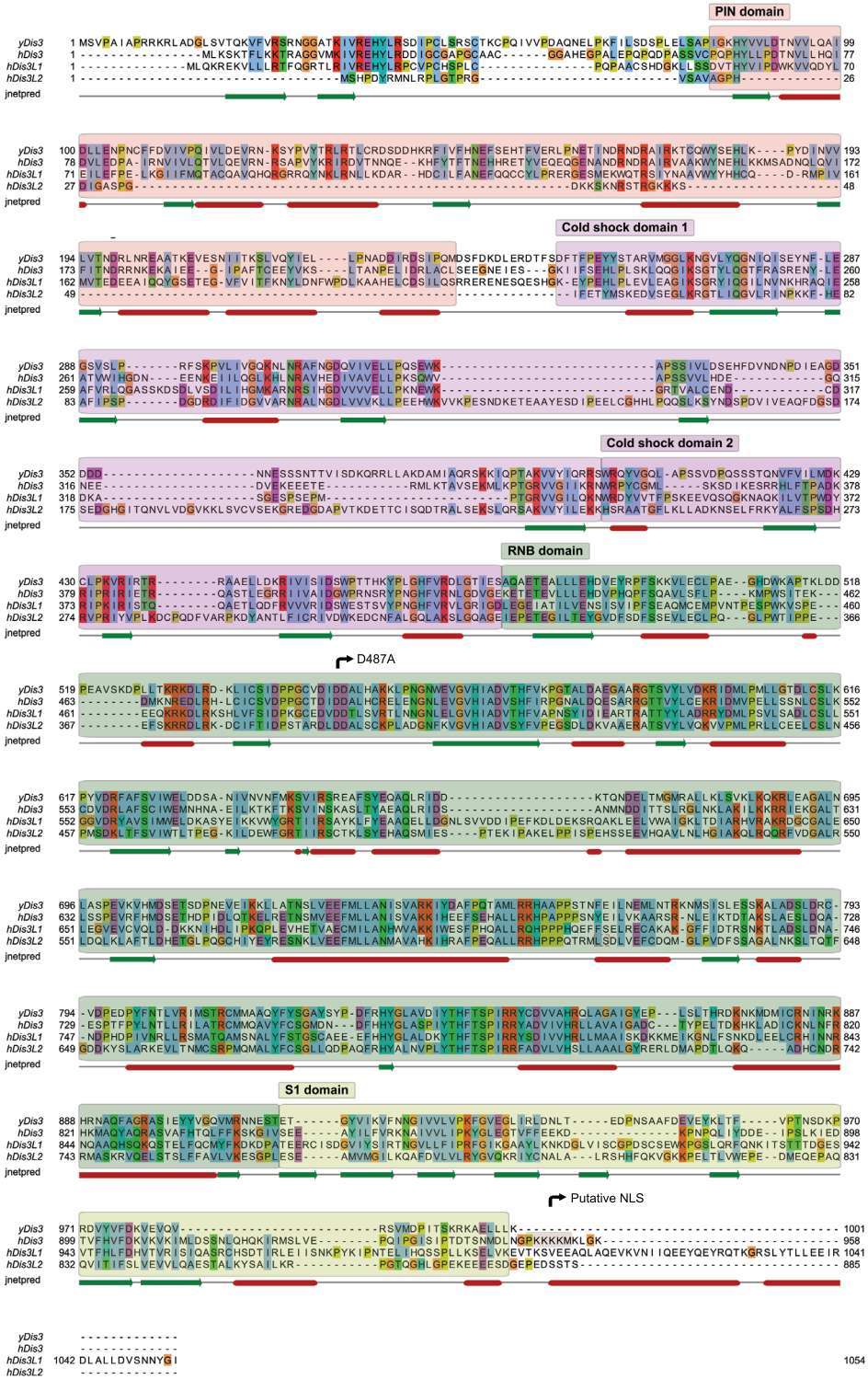
PIN domain
Cold shock domain 1
Cold shock domain 2
RNB domain
D487A
S1 domain
Putative NLS
yDis3
hDis3
hDis3L1
hDis3L2
jnetpred

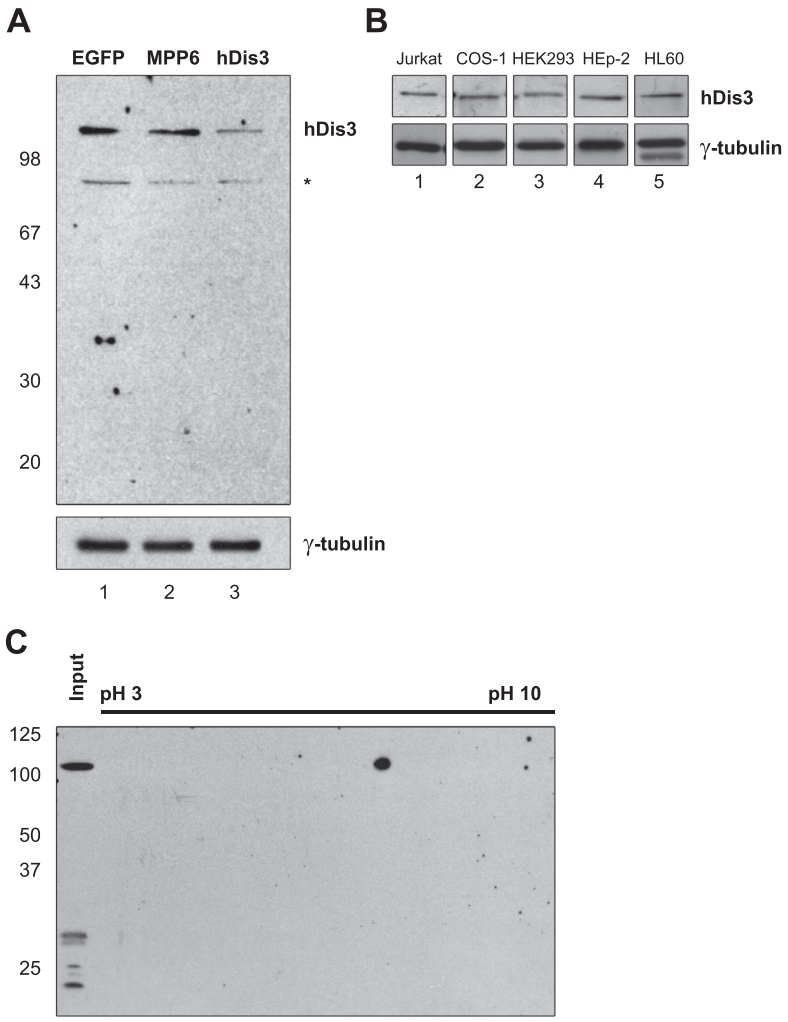

Figure 2. The human Dis3 protein is an unmodified 110 kDa protein, which is ubiquitously expressed in various primate cell lines.

A) Total cell extracts of HEp-2 cells transiently transfected with siRNAs directed against EGFP (lane 1), MPP6 (lane 2) or hDis3 (lane 3) were separated by SDS-PAGE and analyzed by western blotting, using anti-hDis3 antibodies. A monoclonal anti-γ-tubulin antibody was used as a control. The position of molecular weight markers (in kDa) are indicated on the left. (B) Total cell extracts of Jurkat, COS-1, HEK293, HEp-2 and HL60 cells were analyzed by western blot using the anti-hDis3 antibodies. (C) A total cell extract of HeLa cells was fractionated by isoelectric focusing using a non-linear gradient from pH 3.0 to pH 10.0, followed by SDS-PAGE and western blotting. Subsequently, the human Dis3 protein was identified by immunoblotting using anti-hDis3 antibodies. A sample of the HeLa cell extract ("Input") was separated in parallel during SDS-PAGE as a reference.

'canonical' hDis3 transcript and the splice variant described above. Searching for sequences specific for the shorter isoform in EST databases suggested that this isoform is expressed in testis, brain and lymph node tissues, suggesting that this isoform is not ubiquitously expressed. Two-dimensional IEF/SDS-PAGE analysis with a HeLa total cell extract, followed by immunoblotting resulted in the detection of only a single spot, suggesting that the majority of hDis3 molecules is not modified by post-translational modifications affecting the charge of the protein (Figure 2C). Also here, only 1 band was visible, most likely representing the longer isoform.

hDis3 is a hydrolytic 3'-5' exoribonuclease

To study the exonucleolytic activity of the hDis3 protein, lysates of HEp-2 cells transiently transfected with EGFP or EGFP-hDis3 were subjected to immunoprecipitation with anti-GFP antibodies. Subsequently, the immunoprecipitated material was used in an *in vitro* exoribonuclease assay using either low (0.02 mM, Figure 3A) or high (5 mM, Figure 3B) $MgCl_2$ concentrations. The immunoaffinity-purified EGFP-hDis3 (Figure 3A, lanes 5-7) appeared to be highly efficient in degrading a structured RNA substrate, the 5.8S rRNA joined to the first 50 nts of the ITS2 (internal transcribed spacer 2) of the rRNA precursor. The ribonuclease activity associated with EGFP-hDis3 was strongly reduced in the presence of relatively high $MgCl_2$ (5mM) concentrations (Figure 3B, lanes 5-7), which resembles the Mg^{2+}-requirements found for hDis3L1 (Staals *et al*, 2010) and Dis3L2 (Chapter 6).

Based upon the sequence similarity of hDis3 and RNase II it is expected that hDis3 is a hydrolytic enzyme. In order to discriminate between phosphorolytic and hydrolytic exoribonuclease activity, which results in the production of nucleotide diphosphates and monophosphates, respectively, the reaction products of the EGFP-hDis3 immunoprecipitates were analyzed by thin-layer chromatography (Figure 3C). The results showed that only UMP was produced (note that only radiolabeled UTP was used to generate the substrate RNA), indicating that hDis3 is indeed a hydrolytic 3'-5' exoribonuclease.

To rule out the possibility that the observed 3'-5' exoribonuclease activity associated with EGFP-hDis3 was due to a co-purified exoribonuclease, a substitution mutant of hDis3 was generated in which a conserved aspartic acid (position 487) was replaced by an alanine (D487A, see Figure 1). This residue was chosen because it is predicted to be part of the catalytic site of hDis3 and has been shown to be essential for the exoribonuclease activity (Dziembowski *et al*, 2007; Tomecki *et al*, 2010). EGFP-hDis3-D487A was immunoprecipitated with anti-GFP antibodies from transiently transfected HEp-2 cells and incubated with the substrate RNA in the presence of 0.02 mM $MgCl_2$. The results in Figure 4A show that this mutation completely abolished the exoribonuclease activity of EGFP-hDis3. The lack of activity is not due to differences in expression levels, because both the wild-type and mutant hDis3 fusion proteins were expressed to comparable levels (Figure 4B). From these results we conclude that hDis3 indeed acts as a hydrolytic 3'-5' exoribonuclease.

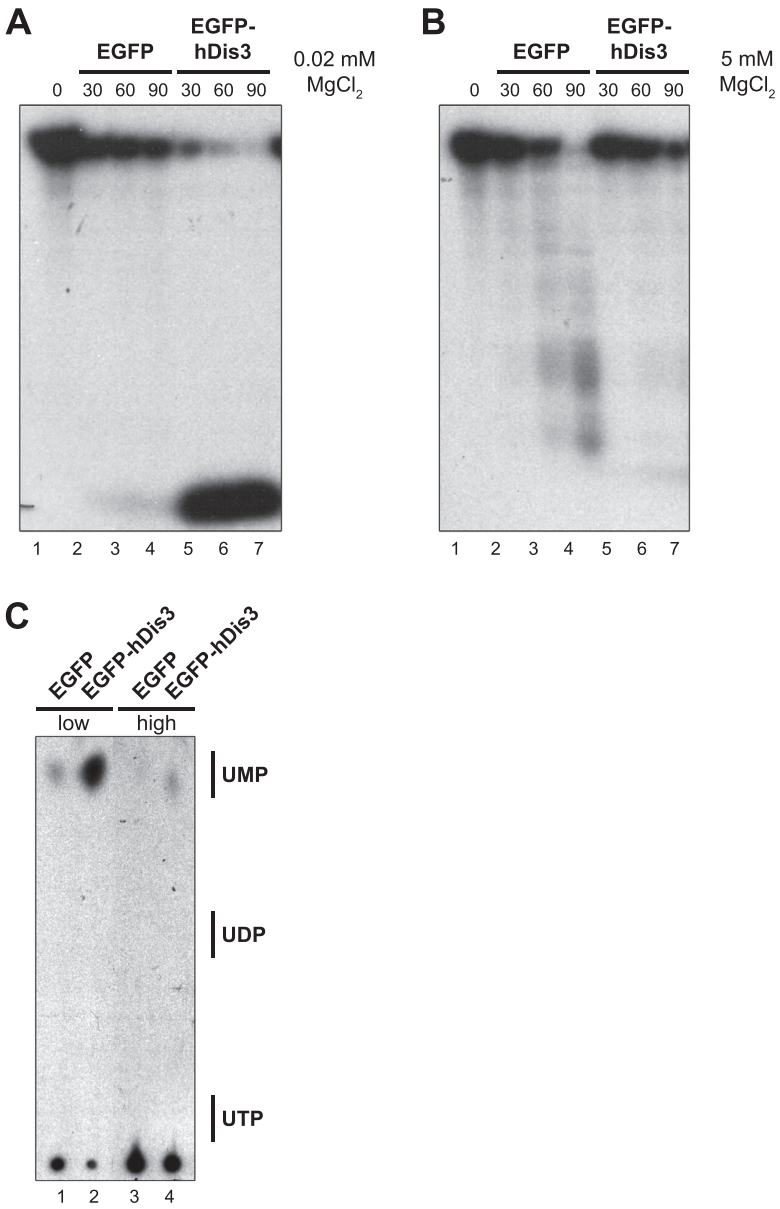

Figure 3. hDis3 is associated with hydrolytic exoribonuclease activity.

(A) Total cell extracts were prepared from transiently transfected HEp-2 cells expressing EGFP or EGFP-hDis3. Using anti-GFP antibodies, the precipitated complexes were analyzed for exoribonuclease activity by incubating a randomly ^{32}P-labelled substrate RNA at different $MgCl_2$ concentrations at 37°C. Samples were taken at 30, 60 and 90 minutes and analyzed by denaturing gel electrophoresis. The untreated RNA-substrate (input) was uses as a control. (B) Thin layer chromatography analysis of the reaction products of EGFP and EGFP-hDis3 obtained after incubation for 90 minutes at low (0.02 mM) or high (5.0 mM) $MgCl_2$. Unlabeled UMP, UDP and UTP were visualized by UV-shadowing which were used as markers and are indicated on the right.

The RNA substrate used in the experiments described above was degraded very efficiently in a processive manner. This 5.8S rRNA containing molecule has a relatively high GC content (~63%). To investigate whether hDis3 displays substrate specificity, several other RNAs were used in the *in vitro* assay, including 5'-end labeled poly(A) and poly(U) homopolynucleotides and a randomly labeled U3 snoRNA. In all cases the wild type hDis3 degraded the RNA substrates in a processive manner, whereas the hDis3-D487A mutant did not detectably affect these RNAs (Figure 4C). In contrast to the uniform sizes of the degradation products obtained with the 5.8S rRNA, poly(A) and poly(U) substrates, the U3 snoRNA substrate was converted to differently-sized degradation products. The migration distance on the gel suggests that these products are very small in size, arguing against the possibility that this is a result of secondary structures in the U3 snoRNA substrate. These data indicate that hDis3 is capable to degrade various RNAs irrespective of the nucleotide sequence.

Knockdown of hDis3 results in reduced cell growth

Previously, it has been shown that human exosome core components such as hRrp41 are essential for normal cell proliferation (van Dijk *et al*, 2007). Also in yeast it has been demonstrated that exosome core components, as well as Dis3, are essential for cell survival (Mitchell *et al*, 1997). This prompted us to investigate the effect of hDis3 depletion on cell growth. HEp-2 cells were transfected with siRNAs specific for hDis3, hRrp41, PM/Scl-100, and EGFP, and proliferation was determined by cell counting at several time points (24, 48 and 72 hours) after transfection. Knockdown of hRrp41 strongly inhibited cell growth, whereas moderately reduced growth rates were observed upon knockdown of hDis3 and PM/Scl-100 (Figure 5). The results suggest that although hDis3 and PM/Scl-100 are required for efficient cell growth, they are probably not essential for this process.

hDis3 associates with splicing factor SF3a60 in an RNA independent manner

The relatively weak association of hDis3 with the exosome core under physiological conditions suggested that it exerts at least some of its activities independently of the exosome. To obtain more insight into an exosome-independent role of hDis3 in human cells, VSV-tagged hDis3 was purified from transiently transfected HEp-2 cells using anti-VSV antibodies. After separation by SDS-PAGE and subsequent in-gel digestion, the (co-)precipitated proteins were analyzed by LC-MS/MS. As a control, material from extracts of HEp-2 cells transfected with the 'empty' VSV-tag encoding plasmid was analyzed in parallel. The identified proteins co-purifying with VSV-hDis3 are listed in Table 1. Strikingly, many of these proteins are involved in one of the different stages of pre-RNA processing and/or pre-mRNA splicing in the nucleus. To confirm the interaction of hDis3 with proteins involved in nuclear RNA metabolism, immunoprecipitations were performed using a total HEp-2 cell extract and antibodies directed against several proteins involved in pre-mRNA processing: hnRNP H (heterogeneous

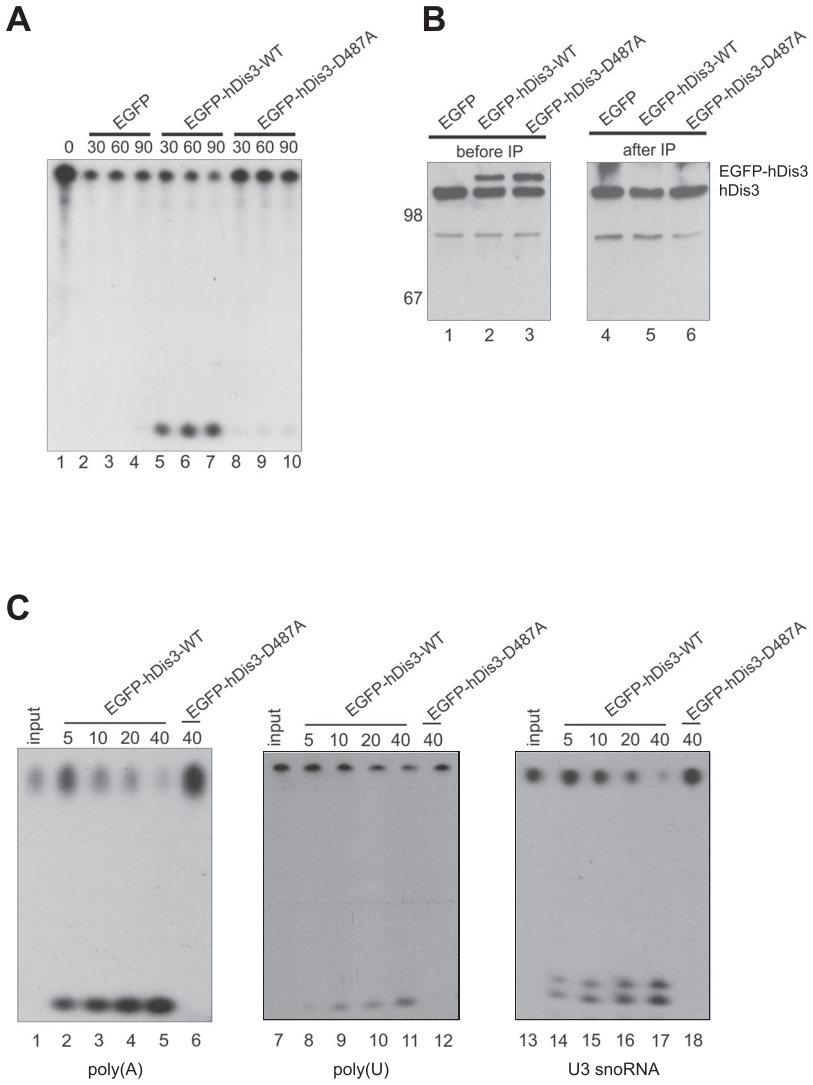

Figure 4. hDis3 is a processive, 3'-5' exoribonuclease, which no apparent substrate specificities.

(A) EGFP (control), EGFP-hDis3 and EGFP-hDis3-D487A were purified from transiently transfected HEp-2 cells with anti-GFP antibodies and analyzed in an *in vitro* exoribonuclease assay using 0.02mM $MgCl_2$. Samples were taken at 30, 60 and 90 minutes and analyzed by denaturing gel electrophoresis. The untreated RNA-substrate (input) was loaded as a control. (B) SDS-PAGE analysis of expressed EGFP-hDis3-WT and EGFP-hDis3-D487A using anti-hDis3 antibodies. In lanes 1-3 cell extracts were loaded before immunoprecipitation (IP) with anti-GFP-antibodies, whereas in lanes 4-6 cell extracts were loaded after IP with anti-GFP-antibodies. (C) EGFP-hDis3-WT and EGFP-hDis3-D487A were purified from transiently transfected HEp-2 cells with anti-GFP antibodies and analyzed in an in vitro exoribonuclease assay using 0.02mM $MgCl_2$ and radiolabeled poly(A), poly(U) and U3 snoRNA as RNA substrates. Samples were taken at 5, 10, 20 and 40 minutes and analyzed by denaturing gel electrophoresis. The untreated RNA-substrate (input) was loaded as a control.

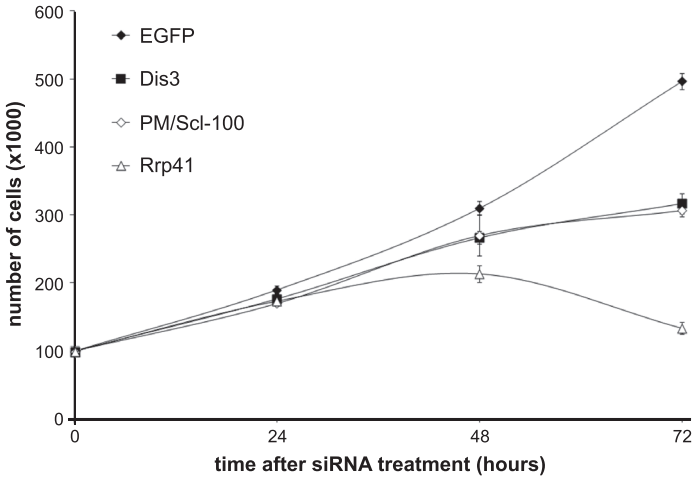

Figure 5. Dis3 is not essential for cell proliferation.

The exoribonucleases hDis3, PM/Scl-100 and an exosome core subunit (hRrp41) were downregulated by siRNA transfection and the effects on proliferation of the HEp-2 cells was assessed by cell counting. Knockdown of EGFP was used as a control. Cells were harvested and counted 24, 48, and 72 h after siRNA treatment.

nuclear ribonucleoprotein H), PABP1 (polyadenylate-binding protein 1) and SF3a60 (splicing factor 3A subunit 3). In parallel, the exosome complex was immunoprecipitated by antibodies to hRrp40 and an immunoprecipitation with NRS (normal rabbit serum) served as a negative control. Co-precipitation of hDis3 was visualized by probing western blots with anti-hDis3 antibodies. Like hRrp40, hnRNP H and PABP1 did not detectably interact with hDis3 (Figure 6A). In contrast, hDis3 efficiently co-precipitated with SF3a60. To provide further evidence for the hDis3-SF3a60 interaction, the reverse experiment was performed with material from HEp-2 cells transiently transfected with VSV-hDis3, VSV-hRrp46 or the 'empty' VSV-tag encoding plasmid. The cell extracts were subjected to immunoprecipitation with anti-VSV antibodies and the precipitated complexes were analyzed by western blotting using the anti-SF3a60 antibody. Indeed SF3a60 co-precipitated with VSV-hDis3, whereas no SF3a60 was detected in material immunoprecipitated from the control cell extracts (Figure 6B).
To investigate whether the interaction between hDis3 and SF3a60 is dependent on RNA, immunoprecipitations were performed with HEp-2 cell extracts pretreated with RNase A and RNase T1. Antibodies to SF3a60 co-precipitated hDis3 irrespective of pretreatment of the cell extracts with RNases (Figure 6C). These results indicate that hDis3 interacts with SF3a60 in an RNA-independent manner.

Global mRNA analysis upon hDis3 depletion

The results described above indicate that hDis3 displays exoribonuclease activity, which does not seem to be (stably) associated with the exosome. Instead, the activity of hDis3 seems to

Table 1. Proteins identified by LC-MS/MS in immunoaffinity-purified VSV-hDis3

UniProt ID	UniProt AC	Description	Class	MW (kDa)	Unique spectra	Total spectra	Coverage (%)
RRP44_HUMAN	Q9Y2L1	Exosome complex exonuclease RRP44	Dis3	109	7	16	8.5
ROA2_HUMAN	P22626	Heterogeneous nuclear ribonucleoproteins A2/B1	hnRNP	37	10	35	23.0
HNRL1_HUMAN	Q9BUJ2	Heterogeneous nuclear ribonucleoprotein U-like protein 1	hnRNP	96	8	21	11.0
HNRPK_HUMAN	P61978	Heterogeneous nuclear ribonucleoprotein K	hnRNP	51	8	11	18.0
ROA1_HUMAN	P09651	Heterogeneous nuclear ribonucleoprotein A1	hnRNP	39	3	7	9.1
HNRH3_HUMAN	P31942	Heterogeneous nuclear ribonucleoprotein H3	hnRNP	37	4	6	10.0
HNRDL_HUMAN	O14979	Heterogeneous nuclear ribonucleoprotein D-like	hnRNP	46	4	6	9.0
ROAA_HUMAN	Q99729	Heterogeneous nuclear ribonucleoprotein A/B	hnRNP	36	6	6	20.0
HNRH1_HUMAN	P31943	Heterogeneous nuclear ribonucleoprotein H	hnRNP	49	4	4	13.0
ROA3_HUMAN	P51991	Heterogeneous nuclear ribonucleoprotein A3	hnRNP	40	3	3	14.0
HNRPG_HUMAN	P38159	Heterogeneous nuclear ribonucleoprotein G	hnRNP	42	3	3	6.9
FUS_HUMAN	P35637	RNA-binding protein FUS	(poly)nucleotide binding	53	19	88	18.0
GBB1_HUMAN	P62873	Guanine nucleotide-binding protein G(I)/G(S)/G(T) subunit beta-1	(poly)nucleotide binding	37	6	28	18.0
GNAI2_HUMAN	P04899	Guanine nucleotide-binding protein G(i), alpha-2 subunit	(poly)nucleotide binding	40	6	13	15.0
5NTD_HUMAN	P21589	5’-Nucleotidase	(poly)nucleotide binding	63	5	12	10.0
EWS_HUMAN	Q01844	RNA-binding protein EWS	(poly)nucleotide binding	68	4	9	7.6
DDX5_HUMAN	P17844	Probable ATP-dependent RNA helicase DDX5	(poly)nucleotide binding	69	4	4	6.7
PCBP1_HUMAN	Q15365	Poly(rC)-binding protein 1	(poly)nucleotide binding	37	3	3	11.0

PABP1_HUMAN	P11940	Polyadenylate-binding protein 1	(poly)nucleotide binding	71	2	2	3.6
SNRPA_HUMAN	P09012	U1 small nuclear ribonucleoprotein A	(poly)nucleotide binding	31	2	2	13.0
RBM25_HUMAN	P49756	Probable RNA-binding protein 25	(poly)nucleotide binding	94	1	1	1.0
SYHC_HUMAN	P12081	Histidyl-tRNA synthetase, cytoplasmic	other	57	8	30	20.0
IMA2_HUMAN	P52292	Importin subunit alpha-2	other	58	5	5	10.0
EF1A1_HUMAN	P68104	Elongation factor 1-alpha 1	other	50	2	4	4.3
TIF1B_HUMAN	Q13263	Transcription intermediary factor 1-beta	other	89	4	4	5.1
NOLC1_HUMAN	Q14978	Nucleolar phosphoprotein p130	other	74	2	2	3.6
IMB1_HUMAN	Q14974	Importin subunit beta-1	other	97	1	1	1.4
RAGP1_HUMAN	P46060	Ran GTPase-activating protein 1	other	64	1	1	1.9
SF3A3_HUMAN	Q12874	Splicing factor 3A subunit 3 (=SF3a60)	splicing	59	3	3	4.2
SFRS3_HUMAN	P84103	Splicing factor, arginine/serine-rich 3	splicing	19	1	1	10.0

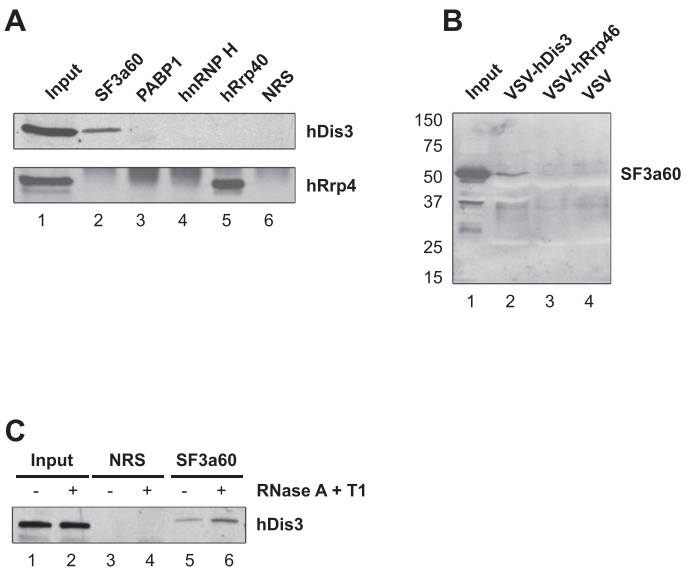

Figure 6. Dis3 interacts with SF3a60 in an RNA-independent manner.

(A) Total HEp-2 cell extracts were used for immunoprecipitations using anti-SF3a60 (lane 2), anti-PABP-1 (lane 3), anti-hnRNP H (lane 4) and anti-hRrp40 (lane 5). A normal rabbit serum (NRS) was used as a control (lane 6). Precipitated proteins were analyzed by western blotting using anti-hDis3 antibodies (upper part) or anti-hRrp4 antibodies (lower part). Input material (10%) of the extract was loaded in lane 1 as a control. (B) HEp-2 cells were transiently transfected with VSV-hDis3, VSV-hRrp46 and VSV (control) constructs and the expressed VSV-tagged proteins were purified with anti-VSV antibodies. The precipitated protein complexes were analyzed by western blotting using anti-SF3a60 antibodies. A total HEp-2 cell extract (10%) was loaded in lane 1. The positions of molecular mass markers (kDa) are indicated on the left. (C) HEp-2 cell extracts, either treated with or without RNase A and RNase T1, were used for immunoprecipitations using anti-SF3a60 antibodies (lanes 5-6) or a normal rabbit serum (NRS) as a control (lanes 3-4). The precipitated proteins were analyzed by western blotting using anti-hDis3 antibodies. Input material (10%) of the treated or untreated extracts was loaded in lanes 1 and 2, respectively.

be associated with the splicing factor SF3a60, hinting at a possible role of hDis3 in pre-(m) RNA processing and/or surveillance events. As such, this putative exosome-independent activity is likely to affect at least in part other substrates than those degraded/processed in an exosome-dependent fashion. To investigate this issue, changes in mRNA levels resulting from knocking down hDis3, hRrp41 (resulting in destabilization of the exosome core complex) and PM/Scl-100 were determined by microarray analyses. Forty hours after siRNA transfection reduced protein levels were demonstrated by western blotting (data not shown). After RNA isolation from extracts of these cells, oligo(dT)-primed cDNAs were analyzed by a microarray containing probes for 21,000 human protein-coding genes. The number of upregulated and downregulated mRNAs ($p<0.05$) was similar for each of the depletions, although depletion of PM/Scl-100 resulted in a slightly lower number of affected transcripts (Figure 7A). After clustering of the significantly affected transcripts, a heat map was generated (Figure 7B).

This revealed that a number of mRNAs were similarly affected upon depletion of all three proteins, but that the overlap for hRrp41 and PM/Scl-100 was much larger than that for either of these proteins with hDis3.

Previous results (association with SF3a60 and the nuclear localization of hDis3) indicated that the activity of hDis3 might be associated to the pre-RNA processing events occurring in the nucleus. If hDis3 through its association with the splicing machinery is involved in pre-mRNA splicing, the depletion of hDis3 might cause a decrease in mature mRNAs. In view of the experimental approach to deplete hDis3, mRNAs with a high turnover rate are expected to be more strongly affected than relatively stable mRNAs. To investigate this, we categorized the expected half-lives of ~5200 mRNAs (Yang *et al*, 2003), and determined the ratio of up- and downregulated mRNAs identified by the microarray analysis for these categories (Figure 7C). This analysis revealed that mRNAs with a high turnover rate were stabilized upon depletion of hRrp41 or PM/Scl-100 when compared to relatively stable mRNAs. Depletion of hDis3, however, did not seem to affect the stability of mRNAs with a high turnover rate, because the ratio of up- and downregulated mRNAs was similar for all three categories.

Taken together, the mRNA population affected by hDis3 depletion shows only a limited overlap with the mRNAs up- or downregulated by hRrp41 and PM/Scl-100 depletion, consistent with an exosome-independent function of hDis3 in mRNA metabolism. In addition, no relation between the turnover rate of mRNAs and hDis3 functioning was observed, in contrast to the exosome and the associated PM/Scl-100 exonuclease, which appear to be more strongly involved in the degradation of relatively instable mRNAs.

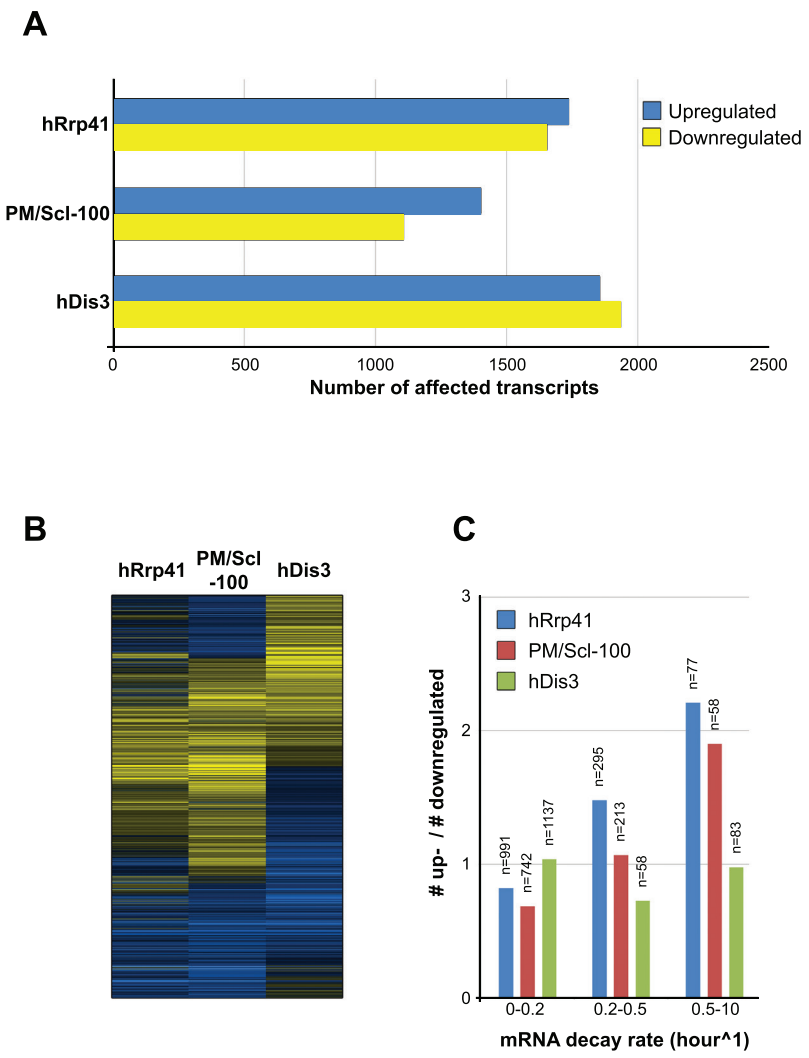

Figure 7. Global changes of mRNA levels due to hRrp41, PM/Scl-100 or hDis3 downregulation.

(A) Absolute number of significantly affected mRNA transcripts, resulting from the knockdown of hRrp41, PM/Scl-100 or hDis3. The blue bars represent the number of transcripts that were significantly ($p<0.05$) upregulated, while the yellow bars represent the significantly downregulated transcripts. (B) Heatmap of mRNAs that were significantly ($p<0.05$) affected by hRrp41, PM/Scl-100 or hDis3 depletion. Clustering of the data was performed using the self-organizing maps algorithm. Blue bars represent upregulated transcripts and yellow bars represent downregulated transcripts. (C) The mRNA decay rates (transcripts per hour) were categorized to include slow (0-0.2), moderate (0.2-0.5) and fast (0.5-10) decaying mRNAs. The ratio of the number of upregulated to downregulated mRNAs (belonging to a particular mRNA decay category) was calculated for each of the depleted proteins. The number of transcripts that were used to calculate these ratios are indicated above the bars.

Discussion

The presence of three distinct Dis3(-like) genes in humans indicates that the ribonuclease activity of the exosome is more complex than in yeast, in which Dis3 has been identified as a major exosome-associated ribonuclease. In this study we explored the functional activities of hDis3, which in agreement with previous studies displays only relatively weak interactions with the exosome core (Staals *et al*, 2010; Tomecki *et al*, 2010). In contrast to the yeast Dis3 protein, hDis3 does not appear to be essential for cell proliferation. The RNA-independent association of hDis3 with the pre-mRNA splicing factor SF3a60 points to a role for this human Dis3 variant in pre-mRNA processing.

The exoribonuclease activity of hDis3

The EGFP-hDis3 fusion protein efficiently degraded several different RNA substrates with no apparent sequence-specificity (Figure 4). The exoribonuclease activity of hDis3 appeared to be processive and not substantially hampered by secondary structures in the RNA substrate, since no intermediate RNA degradation products were observed, similar to what has been reported for yeast Dis3 (Dziembowski *et al*, 2007). For the yeast Dis3 protein it was demonstrated that the energy required to unwind such structures is provided by the hydrolysis of the substrate strand, which might also be the case for hDis3 (Lee *et al*, 2012).
The ribonuclease activity associated with the immunoaffinity-purified hDis3 preparations, which are devoid of detectable exosome proteins, strongly suggests that hDis3 is an active 3'-5' exoribonuclease acting independently of the exosome. A recent study showed that the activity of yeast Dis3 is modulated by its association with the exosome core complex (Wasmuth and Lima, 2012). Since the human Dis3 protein does not appear to be stably associated to the human exosome, it likely that the activity of hDis3 is regulated by other yet unknown mechanisms. In addition to enzymatic activity regulatory mechanisms, the proper subcellular localization will affect the population of substrates that can be converted by hDis3. However, little is known on the intracellular transport of the hDis3 protein. The clustering of basic residues in the C-terminal region (Figure 1) suggests that this region may contain a nuclear localization signal. Indeed, removal of this part of hDis3 showed that this region is important for its nuclear accumulation and fusion of this part to a reporter protein resulted in nuclear accumulation of the reporter (data not shown). In addition, we found that ectopically expressed VSV-hDis3 interacted with the importin beta-1 subunit (Table 1). Consistent with these data, in both yeast and *Drosophila melanogaster*, an interaction of Dis3 with a member of the importin protein family has also been reported (Graham *et al*, 2009; Mamolen *et al*, 2010; Synowsky *et al*, 2009). Taken together, these results strongly suggest that hDis3 is actively transported to the nucleus.

Association of Dis3 with SF3a60

Since our results indicate that the human Dis3 protein can function in an exosome-independent manner, we set out to find other proteins associated with hDis3 to gain more insight into its biological role. The results showed that hDis3 is associated with SF3a60 (also referred to as SF3a3) and potentially other proteins involved in pre-RNA processing. SF3a60 is a constituent of the SF3A splicing factor, which is required for pre-spliceosome formation and assembly of the 17S U2 snRNP (Nesic and Kramer, 2001; Tanackovic and Kramer, 2005). The SF3A splicing factor contributes to U2-type branch site recognition and is essential for pre-mRNA splicing in humans (Tanackovic and Kramer, 2005). Consistent with the subcellular localization of hDis3, SF3A is localized in the nucleoplasm and excluded from the nucleoli (Huang *et al*, 2011).

Considering the enzymatic activity of hDis3, it is tempting to speculate that hDis3 is involved in RNA processing and/or nuclear RNA surveillance pathways associated with the major spliceosome. The disturbance of the correct assembly of the spliceosome or the stalling of splicing might trigger an mRNA surveillance mechanism involving hDis3 and SF3a60 leading to degradation of the pre-mRNA. On the other hand, the activity of hDis3 might also be directly involved in RNA processing, where SF3a60 could recruit hDis3 to the 3' end of (debranched) introns, followed by 3'-5' degradation.

If hDis3 indeed has a role in pre-mRNA processing in the nucleus, hDis3 down-regulation may retard the maturation of these RNAs and the subsequent export to the cytoplasm. It is therefore anticipated that such perturbation would decrease rather than increase the level of mature mRNAs in the cytoplasm. This could (partly) explain the lower ratio of up- versus downregulated mRNAs in our microarray analyses when hDis3 levels were reduced than that observed after the depletion of exosome(-associated) proteins.

In support of our hypothesis that hDis3 is actively involved in pre-mRNA processing and/or surveillance pathways are two studies that recently addressed the possible RNA substrates of Dis3 in yeast, either by sequence analysis of UV-crosslinked RNAs, or by transcriptome-wide tiling microarrays (Gudipati *et al*, 2012; Schneider *et al*, 2012). In both studies, Dis3 was found to be associated with the intronic regions of the nuclear pre-mRNAs. These studies showed that more than half of the pre-(m)RNAs are degraded in a Dis3-dependent manner before splicing could finish. This surprising observation indicates that the level of mature RNA is the result of competition between processing and degradation and that pre-RNAs that fail to mature timely are quickly degraded by Dis3.

The interaction of hDis3 with components of the splicing machinery formed on pre-mRNA has been observed before (Rappsilber *et al*, 2002), although the role of hDis3 was not addressed. Its interaction with SF3a60 might therefore provide more clues to pinpoint its exact role. For instance, it has been shown that SF3a60 is involved in efficient linking of active transcription to proteins and/or complexes involved in post-initiation processes such as pre-mRNA splicing (Sims *et al*, 2007). The presence of hDis3 in these protein assemblies might therefore be an important source of endo- and/or exoribonuclease activity that might be

required for these processes. Interestingly, it has recently been postulated that the activity of the nuclear exosome is recruited to a subcomplex of the major spliceosome: the U4/U6.U5 tri-snRNP (Nag and Steitz, 2012). It was proposed that this activity might also be important for pre-mRNA processing and/or degradation of aberrant transcripts. Therefore, studying the identity and regulation of the ribonuclease activities associated with nuclear pre-mRNA processing in more detail is interesting, yet challenging.

Finally, it is noteworthy to mention that the interaction between hDis3 and SF3a60 does not automatically point towards a role for hDis3 in splicing events, as splicing complexes have been implicated in other processes as well, as exemplified by the splicing factor Spf30. This protein also associates with spliceosomes (including the U2 snRNP) and was shown to play a role in heterochromatin assembly and the silencing of these and centromeric regions of the chromosome in fission yeast (Bernard *et al*, 2010). The authors proposed a model where Spf30 is recruited towards these silenced regions in a Dis3-dependent manner. Together with the exosome, these proteins were found to be required for the silencing of these regions, as (polyadenylated) centromeric transcripts accumulated when Dis3, the exosome or Spf30 was mutated. The putative role of hDis3 in the surveillance of pre-mRNA molecules, its exact role in the splicing process and/or other processes requiring SF3a60 now awaits further investigations.

In conclusion, the results of this study demonstrate that the human Dis3 protein displays somewhat different features when compared to its closest homologue in yeast. In contrast to the essential role of Dis3 in cell survival in yeast, human cells survive hDis3 depletion, as witnessed by the moderate growth defects that were observed. However, the possibility that this relatively mild phenotype is a result of an incomplete knockdown should not be disregarded. The finding that hDis3 is confined to the nucleoplasm together with the recent discovery of two additional homologues that are expressed in higher eukaryotes, hDis3L1 and hDis3L2 (Staals *et al*, 2010; Tomecki *et al*, 2010), suggest a functional diversification of the different hDis3(-like) proteins. hDis3L1 has been reported to associate stably with the cytoplasmic exosome core and plays a role in the degradation of rRNAs and other cytoplasmic RNAs. hDis3L2 is not associated with the exosome core and appears to be involved in controlling the levels of specific RNAs that are important for mitotic progression (Astuti *et al*, 2012) and proliferation (Chang *et al*, 2013). In addition, hDis3L2 was found to be located at or near P-bodies, where it was shown to be involved in polyuridylation-stimulated RNA decay (Lubas *et al*, 2013; Malecki *et al*, 2013). The functions of hDis3 still remain to be elucidated, although the results presented here point towards a role in pre-mRNA processing and/or surveillance.

Methods

Bioinformatics

Prediction of functional domains was done using the Pfam protein family database (Punta *et al*, 2012). Sequence database searching was performed by BLAST using GenBank databases containing either ESTs or genomic sequence information. The graphical presentation of the multiple sequence alignments was generated with Jalview (Waterhouse *et al*, 2009) using the default color scheme used for alignments in Clustal X.

hDis3 expression constructs

The cDNA encoding hDis3 (GenBank accession number: NP 055768) was kindly provided by Dr. T. Nishimoto and the hDis3 coding sequence was subsequently cloned into the pCI-neo-5′-VSV and pEGFP-C3 vectors. The mutant hDis3 protein in which the aspartic acid at position 487 was changed into an alanine was created by using the Quick Change Site-directed mutagenesis kit (Stratagene), to generate the EGFP-hDis3-D487A construct.

Transient transfection and preparation of cell extracts

HEp-2 cells were grown to 70% confluency in DMEM containing 10% fetal calf serum (FCS) (DMEM+). For immunoprecipitation, approximately 10 x 10^6 cells were transfected with 30 μg of plasmid DNA in 850 μl of DMEM+ by electroporation at 260 V and 950 μF using a Gene-Pulsar II (Bio-Rad). After transfection, cells were seeded in 75-cm^2 culture flasks and cultured overnight in DMEM+. The trypsinized cells were washed with PBS, after which total cell extracts were prepared by resuspending the cells in lysis buffer (25 mM Tris-HCl, pH 7.5, 150 mM KCl, 1 mM EDTA, 0.5 mM PMSF, 1 mM DTT and 0.05% NP-40) and sonicated using a Branson microtip, followed by centrifugation for 5 min at 16,000 x *g*.

Immunoprecipitation

Polyclonal antibodies from rabbits (anti-SF3a60, anti-hRrp40, anti-GFP, anti-PABP-1 and anti-hnRNP H) and human autoimmune patients (α-PM/Scl-positive and α-PM/Scl-negative) were coupled to protein-A agarose beads (Kem-en-Tec) in IPP500 (500 mM NaCl, 10 mM Tris-HCl, pH 8.0, 0.05% NP-40) by incubation for 1 h at room temperature. Similar conditions were used to couple monoclonal mouse anti-VSV-tag antibodies to protein G-agarose beads. Beads were washed twice with IPP500, and twice with IPP150 (composition similar to IPP500, but containing 150 mM instead of 500 mM NaCl). For each immunoprecipitation equal amounts of cell extract were incubated with the antibody-coupled beads for 2 h at 4° C in the absence or presence of RNase A (10 g/ml) and RNase T1 (100 U/ml). Subsequently, beads were washed four times with IPP150, and co-immunoprecipitated proteins were analyzed by western blot analysis or used in an exoribonuclease activity assay.

Western blot analysis

For western blot analysis, proteins were separated by SDS-PAGE, and transferred to nitrocellulose membranes. In order to visualize the proteins, blots were incubated with the mouse monoclonal antibodies anti-hRrp4 (Modiquest) and anti-γ-tubulin, or with the mouse polyclonal antibody anti-hDis3 (Abnova), or with the rabbit polyclonal antibodies anti-hRrp40 and anti-SF3a60 in blocking buffer (5% skimmed milk, PBS, 0.05% NP-40). The anti-hDis3 antibody recognizes the C-terminal part (amino acids 851 to 956) of hDis3. As secondary antibody, horseradish peroxidase-conjugated goat anti-mouse IgG or goat anti-rabbit IgG (Dako Immunoglobulins) was used, 2500-fold diluted in blocking buffer. Bound antibodies were visualized by chemiluminescence.

2D isoelectric focusing / SDS-PAGE

A total cell extract of HeLa cells (approximately 100 μg) was separated in one dimension by isoelectric focusing using IPG strips with a non-linear pH gradient from 3 to 10 (Amersham Biosciences), followed by separation in the second dimension by SDS-PAGE. Separated proteins were transferred to nitrocellulose membranes by western blotting.

Exoribonuclease activity assay

Immunoprecipitated material (bound to the protein A or protein G agarose beads) were washed once with buffer A (10 mM Tris-HCl, pH 7.5, 50 mM KCl, 5 mM $MgCl_2$, 1 mM Na_2HPO_4, 0.5 mM $MnCl_2$, 0.5 mM DTT) or buffer B (same composition as buffer A only containing 0.2 mM $MgCl_2$). ^{32}P-labeled RNA substrate (approx. 100 ng) was added to the immunoprecipitated material, and the suspension was incubated at 37 °C. Formamide loading buffer was added to 10 μl samples taken at different time points, heated for 2 minutes at 70 °C and placed on ice. Reaction products were analyzed by denaturing polyacrylamide gel electrophoresis (15% acrylamide, 7M urea in 0.5x TBE) followed by autoradiography. Two RNA substrates were generated by *in vitro* transcription in the presence of ^{32}P-labeled UTP. The human 5.8S rRNA containing in addition 50 nts of the ITS2 at the 3'-end was generated by linearizing the corresponding plasmid construct with BamHI followed by *in vitro* transcription using T7 RNA polymerase. The U3 snoRNA was transcribed *in vitro* using T7 RNA polymerase and a KpnI-linearized pUC19-U3CD plasmid as template, as described previously (Granneman *et al*, 2002). Poly(A) and poly(U) RNA substrates were 5'-end labeled using T4 polynucleotide kinase and [γ-^{32}P]ATP (Schilders *et al*, 2007). Labeled RNAs were separated by denaturing polyacrylamide gel electrophoresis, after which the corresponding band was excised and eluted from the gel.

RNA interference and cell growth assay

An siRNA duplex (containing 3' dTdT overhangs) was generated based upon the coding region of the human Dis3 sequence described above: 5'- GCCUACAGGUAGAGUUGUAdTdT-3'. The siRNAs for human MPP6, PM/Scl-100, and hRrp41 were identical to those described previously (Lejeune *et al*, 2003; Schilders *et al*, 2005; van Dijk *et al*, 2007). For the siRNA treatment, approximately 3 x 10^5 HEp-2 cells were transfected with 100 pmol of siRNA using Oligofectamine transfection reagent (Invitrogen) as described by the manufacturer with the exception that during transfection 10% FCS was present in the medium. As a control, cells were transfected with a siRNA directed against EGFP. For the analysis of effects on cell growth, cells were harvested and counted with a Coulter A^C-T series analyzer.

Microarray analysis

HEp-2 cells seeded in 6-well plates were transfected with siRNAs targeting hRrp41, PM/Scl-100 or hDis3, essentially as described above. MilliQ water instead of siRNA solution was used in a control transfection. After 40 hours incubation the cells were harvested by trypsinization and centrifugation and the cells were resuspended in Trizol (Invitrogen) for isolation of total RNA, according to the manufacturer's recommendations. Subsequently, the total RNA was further purified by the RNeasy kit (Qiagen). Roughly 10 ug of total RNA was used for cDNA synthesis and hybridization on a custom microarray chip (UMCU human oligo v2.0), containing 21,000 different human mRNA probes (van de Peppel *et al*, 2003). Each knockdown was performed independently in duplicate and two microarrays were used per knockdown for the dye-swap correction (Cy3/Cy5). Significantly changed transcripts ($p<0.05$) were expressed as fold-changes relative to the control (EGFP) siRNA transfection. Data was further processed in Excel. Clustering of the significantly affected transcripts was performed with Cluster (Eisen *et al*, 1998), using the self-organizing maps algorithm. Heat maps of the resulting clustered data were made in Treeview (Saldanha, 2004). mRNA decay rates were extracted from Supplementary Table 9 from the Yang et al. study (Yang *et al*, 2003) and mapped to its corresponding Uniprot accession number for comparison with the microarray data.

LC-MS/MS

The gel containing the immunoaffinity-purified VSV-hDis3 was cut into 19 slices, proteins were reduced with 1,4-dithiothreitol (6.5 mM) and alkylated with iodoacetamide reagent (54 mM). After thorough washing, the gel slices were rehydrated in trypsin solution (10 ng/μl) on ice. After addition of 30 μl of NH_4HCO_3 (50 mM, pH 8.5), samples were digested for 16 h at 37°C. The supernatant of the digest was collected and the gel slices were washed for 15 min in 5% formic acid at room temperature, after which the supernatant was combined with the earlier fraction and stored at −20°C. All LC-MS/MS analyses were performed on an LTQ-Orbitrap mass spectrometer (Thermo, San Jose, CA) connected to an Agilent 1200 series nano-LC system. Peptides were fractionated on C18 with a multi-step gradient of 0.6%

HAc (solution A) and 0.6% HAc/80% acetonitrile (solution B). The mass spectrometer was operated in the data-dependent mode to automatically switch between MS and MS/MS. Raw MS data were converted to peak lists using Bioworks Browser software, version 3.1.1. All spectra were searched with Mascot against all human proteins in the Swissprot (v56.2) database with a precursor mass tolerance of 15 ppm and a product mass tolerance of 0.9 Da with trypsin as an enzyme, allowing two miscleavages. Carbamidomethyl of cysteine was specified as a fixed modification. Deamidation of asparagine and glutamine, oxidation of methionine, acetylation of the n-terminus and phosphorylation of serine, threonine and tyrosine were specified in Mascot as variable modifications. Identifications were processed using Scaffold (Proteome Software) version 4.0.4. Peptide identifications were accepted if they could be established at greater than 95.0% probability by the Peptide Prophet algorithm and at a minimum Mascot score of 25. Protein identifications were accepted if they could be established at greater than 99.0% probability, as assigned by the Protein Prophet algorithm.

References

Amblar M, Barbas A, Fialho AM, Arraiano CM (2006) Characterization of the functional domains of Escherichia coli RNase II. *J Mol Biol* **360:** 921-933

Astuti D, Morris MR, Cooper WN, Staals RH, Wake NC, Fews GA, Gill H, Gentle D, Shuib S, Ricketts CJ, Cole T, van Essen AJ, van Lingen RA, Neri G, Opitz JM, Rump P, Stolte-Dijkstra I, Muller F, Pruijn GJ, Latif F, Maher ER (2012) Germline mutations in DIS3L2 cause the Perlman syndrome of overgrowth and Wilms tumor susceptibility. *Nat Genet* **44:** 277-284

Bernard P, Drogat J, Dheur S, Genier S, Javerzat JP (2010) Splicing factor Spf30 assists exosome-mediated gene silencing in fission yeast. *Mol Cell Biol* **30:** 1145-1157

Bonneau F, Basquin J, Ebert J, Lorentzen E, Conti E (2009) The yeast exosome functions as a macromolecular cage to channel RNA substrates for degradation. *Cell* **139:** 547-559

Brouwer R, Allmang C, Raijmakers R, van Aarssen Y, Egberts WV, Petfalski E, van Venrooij WJ, Tollervey D, Pruijn GJ (2001) Three novel components of the human exosome. *J Biol Chem* **276:** 6177-6184

Chang HM, Triboulet R, Thornton JE, Gregory RI (2013) A role for the Perlman syndrome exonuclease Dis3l2 in the Lin28-let-7 pathway. *Nature* **497:** 244-248

Chlebowski A, Lubas M, Jensen TH, Dziembowski A (2013) RNA decay machines: the exosome. *Biochim Biophys Acta* **1829:** 552-560

Davis CA, Ares M, Jr. (2006) Accumulation of unstable promoter-associated transcripts upon loss of the nuclear exosome subunit Rrp6p in Saccharomyces cerevisiae. *Proc Natl Acad Sci U S A* **103:** 3262-3267

Dziembowski A, Lorentzen E, Conti E, Seraphin B (2007) A single subunit, Dis3, is essentially responsible for yeast exosome core activity. *Nat Struct Mol Biol* **14:** 15-22

Eisen MB, Spellman PT, Brown PO, Botstein D (1998) Cluster analysis and display of genome-wide expression patterns. *Proc Natl Acad Sci U S A* **95:** 14863-14868

Flynt AS, Greimann JC, Chung WJ, Lima CD, Lai EC (2010) MicroRNA biogenesis via splicing and exosome-mediated trimming in Drosophila. *Mol Cell* **38:** 900-907

Graham AC, Davis SM, Andrulis ED (2009) Interdependent nucleocytoplasmic trafficking and interactions of Dis3 with Rrp6, the core exosome and importin-alpha3. *Traffic* **10:** 499-513

Granneman S, Pruijn GJ, Horstman W, van Venrooij WJ, Luhrmann R, Watkins NJ (2002) The hU3-55K protein requires 15.5K binding to the box B/C motif as well as flanking RNA elements for its association with the U3 small nucleolar RNA in Vitro. *J Biol Chem* **277:** 48490-48500

Gudipati RK, Xu Z, Lebreton A, Seraphin B, Steinmetz LM, Jacquier A, Libri D (2012) Extensive degradation of RNA precursors by the exosome in wild-type cells. *Mol Cell* **48:** 409-421

Huang CJ, Ferfoglia F, Raleff F, Kramer A (2011) Interaction domains and nuclear targeting signals in subunits of the U2 small nuclear ribonucleoprotein particle-associated splicing factor SF3a. *J Biol Chem* **286:** 13106-13114

Januszyk K, Liu Q, Lima CD (2011) Activities of human RRP6 and structure of the human RRP6 catalytic domain. *RNA* **17:** 1566-1577

Lebreton A, Tomecki R, Dziembowski A, Seraphin B (2008) Endonucleolytic RNA cleavage by a eukaryotic exosome. *Nature* **456:** 993-996

Lee G, Bratkowski MA, Ding F, Ke A, Ha T (2012) Elastic coupling between RNA degradation and unwinding by an exoribonuclease. *Science* **336:** 1726-1729

Lejeune F, Li X, Maquat LE (2003) Nonsense-mediated mRNA decay in mammalian cells involves decapping, deadenylating, and exonucleolytic activities. *Mol Cell* **12:** 675-687

Liu Q, Greimann JC, Lima CD (2006) Reconstitution, activities, and structure of the eukaryotic RNA exosome. *Cell* **127:** 1223-1237

Lubas M, Damgaard CK, Tomecki R, Cysewski D, Jensen TH, Dziembowski A (2013) Exonuclease hDIS3L2 specifies an exosome-independent 3'-5' degradation pathway of human cytoplasmic mRNA. *EMBO J* **32:** 1855-1868

Lykke-Andersen S, Brodersen DE, Jensen TH (2009) Origins and activities of the eukaryotic exosome. *J Cell Sci* **122:** 1487-1494

Malecki M, Viegas SC, Carneiro T, Golik P, Dressaire C, Ferreira MG, Arraiano CM (2013) The exoribonuclease Dis3L2 defines a novel eukaryotic RNA degradation pathway. *EMBO J* **32:** 1842-1854

Mamolen M, Smith A, Andrulis ED (2010) Drosophila melanogaster Dis3 N-terminal domains are required for ribonuclease activities, nuclear localization and exosome interactions. *Nucleic Acids Res* **38:** 5507-5517

Mitchell P, Petfalski E, Shevchenko A, Mann M, Tollervey D (1997) The exosome: a conserved eukaryotic RNA processing complex containing multiple 3'-->5' exoribonucleases. *Cell* **91:** 457-466

Nag A, Steitz JA (2012) Tri-snRNP-associated proteins interact with subunits of the TRAMP and nuclear exosome complexes, linking RNA decay and pre-mRNA splicing. *RNA Biol* **9:** 334-342

Neil H, Malabat C, d'Aubenton-Carafa Y, Xu Z, Steinmetz LM, Jacquier A (2009) Widespread bidirectional promoters are the major source of cryptic transcripts in yeast. *Nature* **457:** 1038-1042

Nesic D, Kramer A (2001) Domains in human splicing factors SF3a60 and SF3a66 required for binding to SF3a120, assembly of the 17S U2 snRNP, and prespliceosome formation. *Mol Cell Biol* **21:** 6406-6417

Orban TI, Izaurralde E (2005) Decay of mRNAs targeted by RISC requires XRN1, the Ski complex, and the exosome. *RNA* **11:** 459-469

Preker P, Nielsen J, Kammler S, Lykke-Andersen S, Christensen MS, Mapendano CK, Schierup MH, Jensen TH (2008) RNA exosome depletion reveals transcription upstream of active human promoters. *Science* **322:** 1851-1854

Punta M, Coggill PC, Eberhardt RY, Mistry J, Tate J, Boursnell C, Pang N, Forslund K, Ceric G, Clements J, Heger A, Holm L, Sonnhammer EL, Eddy SR, Bateman A, Finn RD (2012) The Pfam protein families database. *Nucleic Acids Res* **40:** D290-301

Rappsilber J, Ryder U, Lamond AI, Mann M (2002) Large-scale proteomic analysis of the human spliceosome. *Genome Res* **12:** 1231-1245

Saldanha AJ (2004) Java Treeview--extensible visualization of microarray data. *Bioinformatics* **20:** 3246-3248

Schilders G, Raijmakers R, Raats JM, Pruijn GJ (2005) MPP6 is an exosome-associated RNA-binding protein involved in 5.8S rRNA maturation. *Nucleic Acids Res* **33:** 6795-6804

Schilders G, van Dijk E, Pruijn GJ (2007) C1D and hMtr4p associate with the human exosome subunit PM/Scl-100 and are involved in pre-rRNA processing. *Nucleic Acids Res* **35:** 2564-2572

Schneider C, Kudla G, Wlotzka W, Tuck A, Tollervey D (2012) Transcriptome-wide analysis of exosome targets. *Mol Cell* **48:** 422-433

Schneider C, Leung E, Brown J, Tollervey D (2009) The N-terminal PIN domain of the exosome subunit Rrp44 harbors endonuclease activity and tethers Rrp44 to the yeast core exosome. *Nucleic Acids Res* **37:** 1127-1140

Sims RJ, 3rd, Millhouse S, Chen CF, Lewis BA, Erdjument-Bromage H, Tempst P, Manley JL, Reinberg D (2007) Recognition of trimethylated histone H3 lysine 4 facilitates the recruitment of transcription postinitiation factors and pre-mRNA splicing. *Mol Cell* **28:** 665-676

Sloan KE, Schneider C, Watkins NJ (2012) Comparison of the yeast and human nuclear exosome complexes. *Biochem Soc Trans* **40:** 850-855

Staals RH, Bronkhorst AW, Schilders G, Slomovic S, Schuster G, Heck AJ, Raijmakers R, Pruijn GJ (2010) Dis3-like 1: a novel exoribonuclease associated with the human exosome. *EMBO J* **29:** 2358-2367

Synowsky SA, van Wijk M, Raijmakers R, Heck AJ (2009) Comparative multiplexed mass spectrometric analyses of endogenously expressed yeast nuclear and cytoplasmic exosomes. *J Mol Biol* **385:** 1300-1313

Tanackovic G, Kramer A (2005) Human splicing factor SF3a, but not SF1, is essential for pre-mRNA splicing in vivo. *Mol Biol Cell* **16:** 1366-1377

Tomecki R, Kristiansen MS, Lykke-Andersen S, Chlebowski A, Larsen KM, Szczesny RJ, Drazkowska K, Pastula A, Andersen JS, Stepien PP, Dziembowski A, Jensen TH (2010) The human core exosome interacts with differentially localized processive RNases: hDIS3 and hDIS3L. *EMBO J* **29:** 2342-2357

van de Peppel J, Kemmeren P, van Bakel H, Radonjic M, van Leenen D, Holstege FC (2003) Monitoring global messenger RNA changes in externally controlled microarray experiments. *EMBO Rep* **4:** 387-393

van Dijk EL, Schilders G, Pruijn GJ (2007) Human cell growth requires a functional cytoplasmic exosome, which is involved in various mRNA decay pathways. *RNA* **13:** 1027-1035

Wang HW, Wang J, Ding F, Callahan K, Bratkowski MA, Butler JS, Nogales E, Ke A (2007) Architecture of the yeast Rrp44 exosome complex suggests routes of RNA recruitment for 3' end processing. *Proc Natl Acad Sci U S A* **104:** 16844-16849

Wasmuth EV, Lima CD (2012) Exo- and endoribonucleolytic activities of yeast cytoplasmic and nuclear RNA exosomes are dependent on the noncatalytic core and central channel. *Mol Cell* **48:** 133-144

Waterhouse AM, Procter JB, Martin DM, Clamp M, Barton GJ (2009) Jalview Version 2--a multiple sequence alignment editor and analysis workbench. *Bioinformatics* **25:** 1189-1191

Wu C, Orozco C, Boyer J, Leglise M, Goodale J, Batalov S, Hodge CL, Haase J, Janes J, Huss JW, 3rd, Su AI (2009) BioGPS: an extensible and customizable portal for querying and organizing gene annotation resources. *Genome Biol* **10:** R130

Yang E, van Nimwegen E, Zavolan M, Rajewsky N, Schroeder M, Magnasco M, Darnell JE, Jr. (2003) Decay rates of human mRNAs: correlation with functional characteristics and sequence attributes. *Genome Res* **13:** 1863-1872

CHAPTER 8

General Discussion

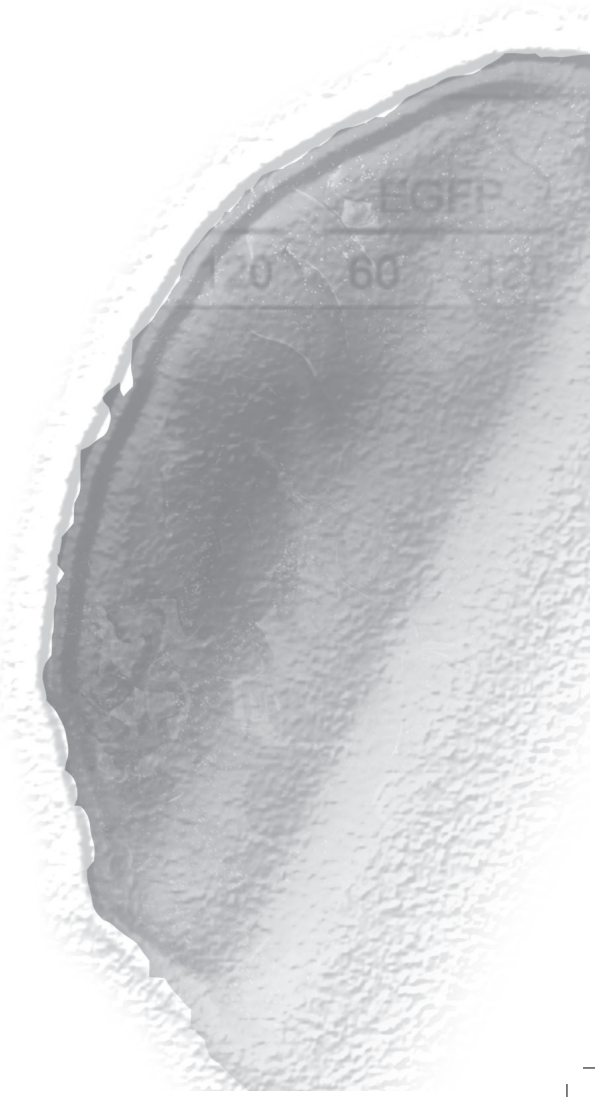

Introduction

Almost two decades after its initial discovery in yeast, it is now well established that the exosome fulfills a fundamental role in many aspects of cellular RNA metabolism. Perhaps owing to its crucial role in the maturation and degradation of rRNA species (which are estimated to constitute as much as 75% of the total RNA population present in a living cell), the exosome is an evolutionary indispensable source of ribonuclease activity, which is reflected by the lethality that is associated with exosome-related knockouts (Allmang *et al*, 1999a; Allmang *et al*, 1999b). Additionally, the omnipresence of exosome complexes and its structural analogues in all three domains of life (covered in Chapter 1), emphasizes this view even further. Despite the evolutionary pressure to retain the catalytic activity associated with the exosome complex, two decades of exosome-research have taught us that the way how this activity is achieved can be markedly different among species.

The core of the exosome is a collection of proteins with potential 3'-5' exoribonuclease and RNA-binding activities that are clustered within one moderately-sized protein complex of ~286 kDa (Liu *et al*, 2006). This complex can be subdivided in two moieties. Firstly, there is the ring-like structure, which is composed of six proteins that share homology with the bacterial 3'-5' phosphorolytic exoribonuclease RNase PH. Secondly, three proteins harboring KH and/or S1 RNA-binding domains are located on one side of the ring structure. These RNA-binding proteins are thought to form the entrance to a central channel in the exosome core, which spans the proteins that make up the ring-like structure. The width of this channel has been estimated to be just large enough to accommodate a single-stranded RNA molecule. Collectively, these proteins are dubbed the "exosome core" complex, as this particular structural setup has been conserved from eubacteria (when considering exosome-like complexes, such as PNPase) to archaea and eukaryotes. However, this is where the analogy between the complexes from different prokaryotic and eukaryotic lineages stops, as recent insights have shown that the *modus operandi* of the activity of the exosome complex in higher eukaryotes is differently organized.

The activity of the archaeal exosome complex resembles that of the eubacterial PNPase: the RNA substrate is guided towards and into the central channel where the active site is located. In the archaeal exosome complex, this active site is formed by the two RNase-PH-like proteins Rrp41 and Rrp42, which are located within the ring-structure (Lorentzen *et al*, 2005). Studies addressing the structure and activity of the yeast and human complexes, however, resulted in the remarkable conclusion that the eukaryotic exosome core is catalytically inert (Liu *et al*, 2006), suggesting that eukaryotic exosome complexes have lost the phosphorolytic activity associated with the $(Rrp41\text{-}Rrp42)_3$ hexamer. Indeed, sequence analysis of archaeal and eukaryotic Rrp41 revealed that key residues involved in phosphate binding (Chapter 1, Figure 3) were not conserved in eukaryotes. An exception is the Rrp41 protein from plants, consistent with the phosphorolytic activity that was found to be associated with the plant

exosome core (Chekanova *et al*, 2000). The activity that was previously found to be associated with the yeast and human exosome complexes must therefore be provided by auxiliary proteins. Indeed, two different ribonucleases were identified and found to associate with the exosome core complex, thereby endowing it with ribonuclease activity: Rrp6 (PM/Scl-100 in humans) and Dis3 (Allmang *et al*, 1999b; Dziembowski *et al*, 2007). Similar to the subcellular distribution of the exosome core complex, yeast Dis3 was found in both the nuclear and the cytoplasmic compartments, making it a major source of ribonuclease activity for the yeast exosome (Dziembowski *et al*, 2007; Liu *et al*, 2006; Schaeffer *et al*, 2009). This role could not be attributed to Rrp6, since the protein only appeared to be present in the nucleus (Allmang *et al*, 1999b), suggesting that it exclusively operates in concert with the nuclear exosome. Since homologues of both proteins (PM/Scl-100 and hDis3) were also present in humans, it was predicted that the activity of the human exosome complex was provided by these two proteins in a similar fashion. The subcellular distribution of PM/Scl-100 overlaps with that of yeast Rrp6 in that it seems to be abundant to the nucleus (with the highest concentrations found in the nucleoli). On the other hand, and in contrast to yeast Rrp6, low amounts of PM/Scl-100 have also been reported to be situated in the cytoplasm of human (Lejeune *et al*, 2003; Schilders *et al*, 2007; van Dijk *et al*, 2007), fly (Graham *et al*, 2009a) and protozoan (Haile *et al*, 2007) cells. This fraction might represent a free pool of PM/Scl-100 and/or PM/Scl-100 associated with the cytoplasmic exosome. More importantly, the subcellular distribution of hDis3 was markedly different from that of yeast Dis3, with high levels only in the nucleoplasm and exclusion from the nucleoli and cytoplasm (Chapter 7). Moreover, previous attempts to co-purify the human exosome with hDis3 repeatedly failed (Allmang *et al*, 1999a; Chen *et al*, 2001; Raijmakers *et al*, 2002). In other words, while nuclear exosome activity could potentially originate from either PM/Scl-100 or hDis3, the source of activity for the cytoplasmic exosome was still enigmatic.

Ribonuclease activity of the human exosome

This thesis focused on how the ribonuclease activities associated with the human exosome complex, which led to the identification and characterization of two additional members of the Dis3 family, which are not present in the yeast *Saccharomyces cerevisiae* and which are termed hDis3L1 and hDis3L2. In Chapter 3, we described the initial characterization of the hDis3L1 protein, which revealed that hDis3L1 is a hydrolytic 3'-5' exoribonuclease, the activity of which was found to be associated with the exosome core. Moreover, hDis3L1 appeared to reside exclusively within the cytoplasm, which explains at least in part the exoribonuclease activity associated with the cytoplasmic exosome complex. Finally, we showed that also hDis3 can interact with the exosome core structure, although this particular interaction appeared to be less stable compared to the interactions of hDis3L1 and PM/Scl-100 with the exosome core. In Chapter 4, we addressed (one of) the cellular function(s) of hDis3L1 by siRNA-mediated silencing. This approach revealed not only that hDis3L1 participates in cytoplasmic degradation of rRNA and mRNA species, but also uncovered a novel RNA

degradation route that involves the transient polyadenylation of rRNA and mRNA fragments that are destined for degradation. Since previous results indicated that three different exoribonucleases (PM/Scl-100, hDis3 and hDis3L1) could associate with the exosome, we set out to investigate the conditions and their influence on ribonuclease activity of these enzymes when bound to the exosome complex. The results from Chapter 5 showed that the regulation of activity of the exosome could be mediated by the Mg^{2+}-concentration and ionic strength and that exosome-associated levels of hDis3L1 and PM/Scl-100 may influence one another. The results of this thesis provide a better understanding on how the activity of the human exosome is organized (Figure 1), especially when the cytoplasmic exosome is considered. The identification and characterization of multiple Dis3(-like) proteins not only revealed that the activity of the human exosome is differently organized when compared to its yeast counterpart, but also have major implications for cytoplasmic RNA processing and degradation processes that have previously been ascribed to the exosome core. This will be discussed in more detail below.

Exosomes and Dis3(-like) proteins in cytoplasmic RNA degradation

Over the years, many functions have been ascribed to the cytoplasmic exosome, most of which are focused on the turnover and surveillance of mRNA species. Especially for mRNAs with high turnover rates, the levels of mRNAs are strongly dependent on mRNA decay (Garneau *et al*, 2007). Generally speaking, mRNAs can be either degraded in a 5'-3' fashion

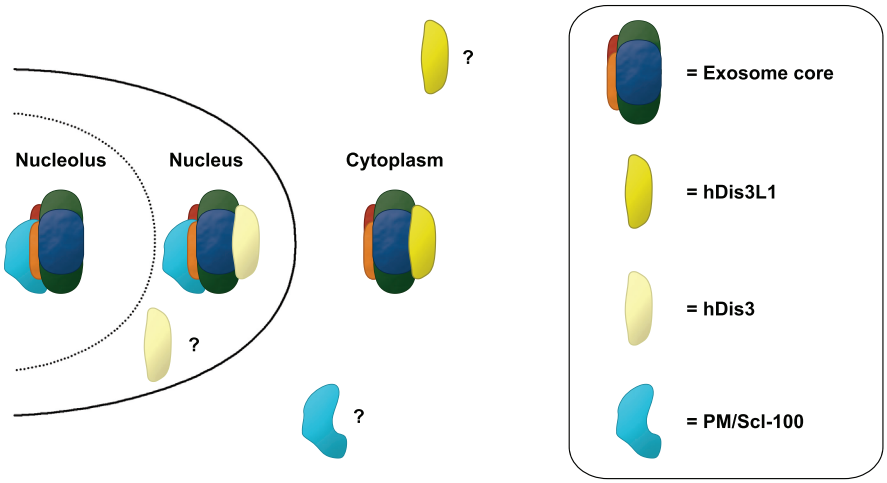

Figure 1. Subcellular distribution of the exosome-associated ribonucleases.

Schematic representation of the subcellular distribution of the human exosome in association with PM/Scl-100, hDis3 and hDis3L1. Non-exosome-associated pools of hDis3, hDis3L1 and PM/Scl-100 may exist in the nucleoplasm and cytoplasm, respectively (indicated with question marks).

by Xrn1, or enter the 3'-5' degradation route that involves the exosome and/or Ski complexes (Anderson and Parker, 1998; van Dijk *et al*, 2007; van Hoof *et al*, 2000). Also in cases where 3'-5 degradation is stimulated by the *cis*-acting AU-rich elements in mammalian unstable mRNA transcripts, the cytoplasmic exosome plays a central role (Chen *et al*, 2001). The surveillance of mRNAs represents a process in which aberrant forms of messengers are recognized and promptly degraded. As already mentioned in Chapter 1, many different surveillance mechanisms involving the exosome are in place to detect different abnormalities within the mRNA body: NMD (nonsense mediated decay), NSD (nonstop mediated decay) and NGD (no-go decay) (Doma and Parker, 2006; Mitchell and Tollervey, 2003; van Hoof *et al*, 2002).

In view of the lack of catalytic activity of the human exosome core, the discovery of hDis3L1 as a novel ribonuclease associated with the cytoplasmic exosome opens new doors to investigate whether hDis3L1 is involved in any of these processes. The results presented in Chapters 3 and 4 show that hDis3L1 is involved in a novel cytoplasmic decay route for rRNA and mRNA species. The depletion of hDis3L1 resulted in the accumulation of polyadenylated degradation intermediates, indicating that these molecules are genuine hDis3L1 substrates. Surprisingly, the exosome core seemed to be dispensable for this process, since no noticeable accumulation of these cytoplasmic degradation intermediates was observed when the exosome core components hRrp40 or PM/Scl-75 were depleted. This result might indicate that hDis3L1 can function in an exosome-independent manner, although the possibility that (incomplete) depletion of hRrp40 and PM/Scl-75 did not result in complete destruction of the exosome core cannot be excluded completely. Nevertheless, codepletion of other exosome core subunits has been observed previously for PM/Scl-75 (van Dijk *et al*, 2007). Alternatively, the depletion of individual exosome core components does not always have the same outcome on RNA degradation, as it has been shown for ARE-mediated mRNA decay, in which PM/Scl-75 was found to have a more prominent role when compared to other core components (Stoecklin *et al*, 2006).

It will be interesting to know whether the Ski complex acts in collaboration with hDis3L1 to degrade cytoplasmic RNA substrates. In yeast the interaction of the Ski complex with the exosome core is bridged by the Ski7 protein (Araki *et al*, 2001; van Hoof *et al*, 2000), but no clear human homologues for this protein have been described so far. The C-terminal part of the Ski7 protein resembles the translation factors EF1-alpha and Hbs1 (Benard *et al*, 1999), and an ortholog of the latter is encoded in the human genome: HBS1-like protein (HBS1L). Interestingly, our proteomic analysis of purified exosome complexes (Chapter 3) identified a peptide sequence corresponding to this particular protein (data not shown). Although a single peptide might reflect a background signal, one has to keep in mind that the purified exosome used for the proteomic analysis was extensively washed with 1 M NaCl to reduce the co-purification of weakly interacting proteins as much as possible. Moreover, HBS1L has been found to co-purify with hDis3L1 in another study (Tomecki *et al*, 2010). Since the protein responsible for bridging the human exosome and Ski complexes is currently still unknown, HBS1L is certainly an attractive candidate for further investigations.

If hDis3L1 indeed is involved in the activities that have been ascribed to the cytoplasmic exosome, one important difference with the situation in yeast is that hDis3L1 lacks endoribonuclease activity. It is possible that this particular activity is of lower importance for at least some of these processes. Indeed, it has been reported that the endoribonuclease activity of yeast Dis3 is not required for some mRNA surveillance mechanisms (Schaeffer and van Hoof, 2011). Moreover, only the exoribonuclease mutant of yeast Dis3 was found to be synthetic lethal with a exoribonuclease mutant of Xrn1, while the endoribonuclease Dis3 mutant was not (Schneider *et al*, 2009). These results suggest that in cytoplasmic mRNA turnover and surveillance the endoribonuclease activity of Dis3(-homologues) is of minor importance and could explain why this particular activity was not conserved in hDis3L1. Future studies will hopefully address if and to what extent the exoribonuclease activity of hDis3L1 affects the different mRNA turnover and surveillance mechanisms.

Previously, it has been reported that a minor fraction of PM/Scl-100 is localized in the cytoplasm of human cells (Lejeune *et al*, 2003; van Dijk *et al*, 2007). Although this fraction might be associated with the exosome, preliminary co-immunoprecipitation data suggests otherwise (Chlebowski *et al*, 2013). We therefore favor the possibility that cytoplasmic PM/Scl-100 functions in an exosome-independent fashion, in agreement with previous suggestions (Graham *et al*, 2009b). In the latter study the Drosophila Rrp6 protein was proposed to have exosome-independent roles during the cell cycle and mitotic progression. Whether the cytoplasmic pool of non-exosome-associated PM/Scl-100 performs similar tasks in humans is currently not known.

Although not associated with the exosome core, Dis3L2 was recently shown to be the major ribonuclease responsible for an additional cytoplasmic 3'-5' mRNA degradation route in *Schizosaccharomyces pombe*, (Malecki *et al*, 2013). In this study, deletion of Dis3L2 was found to be synthetically lethal with a Xrn1 deletion, indicating that Dis3L2 fulfills important roles in (m)RNA metabolism. Furthermore, the Lsm1-Dis3L2 double knockout resulted in the accumulation of polyuridylated mRNAs, which were shown to be the preferred substrate for the *S. pombe* Dis3L2. It is likely that a similar mRNA degradation route is present in plants as well, and requires the SOV protein, which probably represents an ortholog of Dis3L2 (Zhang *et al*, 2010). The preferred targeting of RNA substrates containing an uridylated 3' end is also conserved in mice, as murine Dis3L2 was recently shown to degrade a member of the let-7 family of miRNAs in an uridylation-dependent manner (Chang *et al*, 2013). In fact, the division of Dis3 homologues into three different categories (Dis3, Dis3L1 and Dis3L2) seems to be widespread in eukaryotes, with *S. cerevisiae* being one of the few exceptions (Malecki *et al*, 2013).

Post-transcriptional modification of exosome core and associated proteins

The association of various exoribonucleases with the exosome core will not be the only mechanism by which the activity of the complex can be modulated. In addition, posttranslational modifications (PTMs) may be involved, because these are known to contribute to the regulation of enzymatic activities in general (Walsh *et al*, 2005). We therefore also searched within our human exosome proteomic dataset (Chapter 3) for PTMs of exosome core components and of exosome-associated proteins (hDis3L1, PM/Scl-100, MPP-6 and C1D). This did not reveal PTMs, which, at least in part, may be due to the relatively low sequence coverage for most of these proteins. As an alternative approach, we analyzed individual exosome core and exosome-associated proteins for the presence of PTMs by 2-dimensional isoelectric focusing - SDS-polyacrylamide gel electrophoresis (Figure 2). Multiple spots were observed for hRrp4, hRrp40, PM/Scl-75 and PM/Scl-100, suggesting that these proteins are indeed modified. Coincidentally, the proteins found to be modified in this analysis were also previously found to be targeted by autoantibodies in polymyositis/ scleroderma-overlap patients (Table 3, Chapter 1). PTMs have been postulated to play a role in the generation of neo-epitopes that may initiate an autoimmune response. As such, these PTMs might also be of clinical value. The identification and implication of these (and potential other) modifications will certainly be a challenging task for future studies addressing the catalytic and autoantigenic properties of the exosome.

Polyadenylation and polyuridylation-stimulated RNA degradation

Polyadenylation of RNAs is a widespread cellular mechanism that can have many different outcomes depending on which RNA is polyadenylated, the position of the RNA molecule at which the poly(A)-tail is added and in which species and/or cellular compartment this event takes place. Perhaps the most well-known example of eukaryotic polyadenylation is the posttranscriptional addition of poly(A)-tails to the 3' end of mRNAs as part of their maturation process, promoting transcript stability, nuclear export and translation efficiency (Guhaniyogi and Brewer, 2001), which is therefore also referred to as 'stable polyadenylation'. In contrast, the addition of poly(A)-tails to the 3' end of prokaryotic mRNAs is known to promote their degradation and indeed the resulting polyadenylated mRNAs are often very short-lived, giving rise to the term 'transient polyadenylation'.

Over the years, it has become clear that also eukaryotes employ transient polyadenylation for the rapid degradation of RNAs. As mentioned in Chapter 1, the nuclear TRAMP complex has been shown to add poly(A)-tails to RNAs during RNA quality control and 3'-end processing events, often in concert with Rrp6 and Dis3 (Wyers et al., 2005;LaCava et al., 2005;Vanacova et al., 2005;Kadaba et al., 2006). The rapid degradation of transiently polyadenylated RNA is probably one of the reasons why these molecules have escaped detection for many years. Now, by silencing the ribonuclease(s) responsible for their degradation, these transcripts accumulated, which facilitated their detection. This not only revealed new RNA degradation

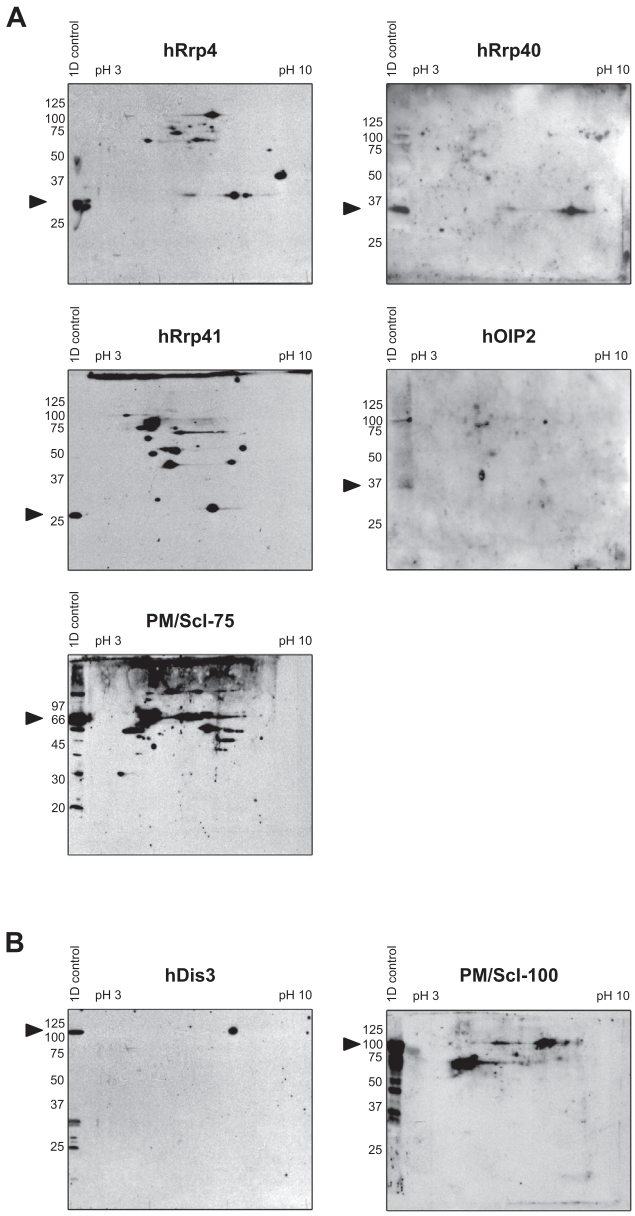

Figure 2. Two-dimensional isoelectric focusing – SDS-PAGE analyses of exosome core and exosome-associated proteins.

HeLa cell extracts (70 μg total protein) were separated by isoelectric focusing on 7 cm, non-linear IPG Immobiline Drystrips with a pH-range of 3 to 10, after which proteins were size-fractionated by SDS-PAGE. After western blotting of the 2D gels, proteins on the blots were stained with antibodies recognizing (A) the exosome core proteins hRrp4, hRrp40, hRrp41, hOIP2 and PM/Scl-75, or (B) the exosome-associated proteins hDis3 and PM/Scl-100. Positions of the respective proteins on the blots are indicated with arrowheads. The positions of molecular weight markers are indicated on the left of each panel. The "1D control" lane contains 20 μg total protein of the same HeLa cell extract, which was size-fractioned by SDS-PAGE without prior isoelectric focusing.

and processing pathways, such as that involving the nuclear TRAMP complex, but also identified new classes of RNAs, such as CUTs (cryptic unstable transcripts) in yeast, and PROMPTs (promotor upstream transcripts) in humans (Neil *et al*, 2009; Preker *et al*, 2008).
Likewise, by the silencing of hDis3L1, we identified a novel RNA degradation pathway in the cytoplasm that involves the transient poly(A)-rich tailing of degradation intermediates (Chapter 3 and 4). This mechanism might not be unique to humans, as a similar mechanism was recently shown to be present in algae as well, although the subcellular distribution of the polyadenylated 18S rRNA species studied in algae was not determined (Zhuang *et al*, 2013). Rather than exclusively consisting of adenosines, these tails were found to be heteropolymeric in nature, as the other three nucleotides were also detected within the tail sequence, albeit at a much lower frequency. One of the future challenges in this field will be to find the polymerase responsible for synthesis of these tails. In *S. pombe*, the addition of poly(U)-tails to mRNAs was shown to be dependent on the Cid1 protein, which has an orthologue in humans (Rissland and Norbury, 2009). Interestingly, these orthologues may also be responsible for the polyuridylation-stimulated histone mRNA degradation, a process that also involves the 3'-5' exoribonuclease activity of the exosome (Mullen and Marzluff, 2008).
As mentioned above, another example of 3'-end RNA tailing was recently demonstrated in two independent studies, where Dis3L2 functions to degrade polyuridylated cytoplasmic mRNA and miRNA species (Chang *et al*, 2013; Malecki *et al*, 2013), the tails of which were added by 2 members of the 3' terminal uridylyl transferase family (TUTases). It is, however, not known if these noncanoncial transferases are also involved in the uridylation of other RNA species.
In summary, 3'-end polyadenylation and polyuridylation serve as important cues in the degradation of many different classes of RNA, which is schematically illustrated in Figure 3. It is also important to note that these discoveries can have profound implications for conventional RT-PCR procedures utilizing oligo(dT) in reverse priming reactions to enrich for mRNAs species (Nam *et al*, 2002).

Exosomes and Dis3(-like) proteins in human disease

As discussed in Chapter 2, the identification of the human exosome was accelerated due to the discovery that the serum of patients with the polymyositis/scleroderma-overlap syndrome contained autoantibodies targeting several exosome(-associated) proteins. In fact, two exosome(-associated) proteins still owe their name to this phenomenon: PM/Scl-75 and PM/Scl-100. It is still an open question why exactly these proteins were found to be targeted by the immune system and how this relates to the phenotype of these patients. The same can be said about the exosome core component hRrp46, which was found to be immunogenic in patients with chronic myelogenous leukemia (Yang *et al*, 2002).
Several recent studies indicated that also mutations in exosome core (and associated) proteins can have a pathogenic role in human disease. Firstly, whole-genome sequencing

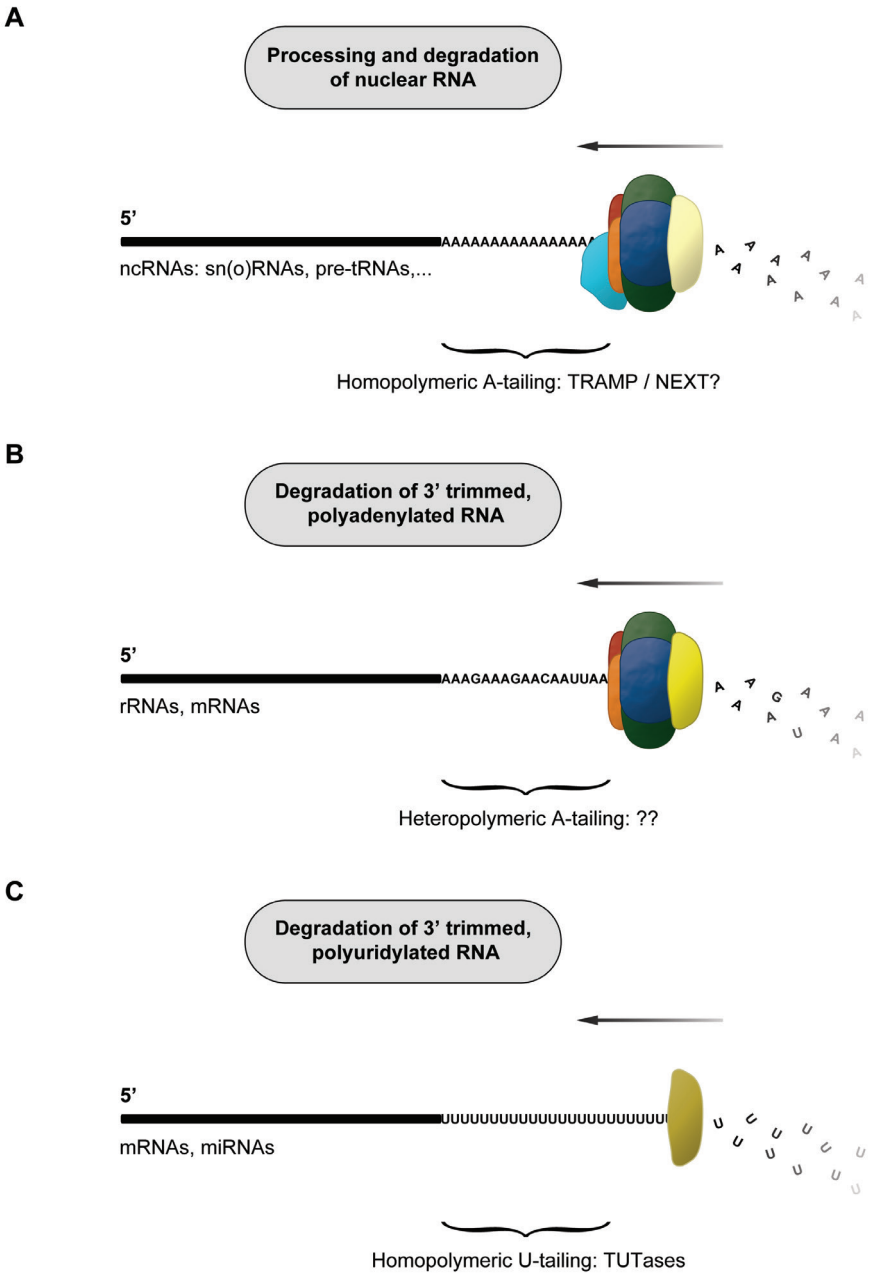

Figure 3. Polyadenylation- and polyuridylation-stimulated RNA degradation by exoribonucleases.

(A) In yeast, nuclear non-coding RNAs (ncRNAs) are polyadenylated by the TRAMP complex, followed by processing or degradation by the exosome associated with Rrp6 and Dis3. (B) Human cytoplasmic rRNA (and mRNA) degradation intermediates are tailed by an unknown polymerase, followed by hDis3L1-mediated degradation in association with the exosome. (C) Human pre-miRNAs are polyuridylated by TUTases, after which degradation is initiated by hDis3L2. In *S. pombe*, a similar mechanism is in place for the degradation of mRNA species.

of multiple myeloma patients revealed that 11% contained mutations in the h*DIS3* gene (Chapman *et al*, 2011). Interestingly, all of these mutations were found to cluster exclusively in the region encoding the RNB domain of hDis3 and about 50% of these or equivalent mutations were previously shown to severely diminish the exoribonuclease activity of the enzyme (Barbas *et al*, 2009; Schneider *et al*, 2007). Notably, no mutations in hDis3L1 were identified in this study. It will therefore be interesting to determine the substrate repertoire of hDis3 in order to identify genes that might be involved in tumor formation in these patients. Recently, this issue has been addressed by transcriptome-wide studies in yeast, but due to the dissimilarities between the yeast and human Dis3 proteins and the higher complexity of the human genome, these results cannot be extrapolated to humans in a simple way (Gudipati *et al*, 2012; Schneider *et al*, 2012).

Next to hDis3, mutant versions of its paralogue hDis3L2 have also been linked to tumor formation (Astuti *et al*, 2012). Patients that were diagnosed with the Perlman syndrome were found to contain germline mutations resulting in truncated versions of this protein. In parallel to the mutations found in the study of Chapman and colleagues (Chapman *et al*, 2011), all of these truncations affected the RNB domain, resulting in an inactive form of the protein. Although the full substrate repertoire of hDis3L2 is currently unknown, recent studies have identified at least a subset. In humans, hDis3L2 depletion was found to increase the half-life of several important mRNAs, many of which were involved in controlling the cell cycle (Lubas *et al*, 2013). The activity of hDis3L2 is probably not restricted to mRNAs, as evidenced by its role in the degradation of the pre-let-7 miRNA (Chang *et al*, 2013). It was shown that the Lin28A protein recruits the enzymes responsible for the uridylation of the pre-let-7 miRNA, thereby tagging it for degradation by hDis3L2. Note that this finding is consistent with the observed accumulation of uridylated RNAs in Dis3L2 depleted cells in *S. pombe* (Malecki *et al*, 2013). The Lin28A-mediated silencing of let-7 is known to be active in stem cells, keeping them in an undifferentiated and proliferative state, while it is relieved in somatic cells (Yu *et al*, 2007). Whether or not the Lin28A-mediated regulation of let-7 is relevant for the development of the Perlman syndrome awaits further characterization.

Exome sequencing of patients showing clinical symptoms reminiscent of pontocerebellar hypoplasia (PCH) revealed mutations in the human exosome core component hRrp40 (Wan *et al*, 2012). PCH is a collective term for several rare neurodegenerative disorders, which results in the impaired development of different brain tissues. The disease is inherited in an autosomal recessive fashion and the responsible gene had not been identified. All but one of the identified mutations in the hRrp40 gene were shown to be located in the hRrp40-coding sequence, often resulting in substitutions of conserved amino acids of the N-terminal domain and the KH and S1 RNA-binding domains. hRrp40 is one of the 'cap' proteins that are stacked on the ring-structure, which have been proposed to mediate the recruitment of substrate RNA and to guide this towards the central channel (Oddone *et al*, 2007). hRrp40 also seems to be of structural importance, as it stabilizes the integrity of the ring-structure (Liu *et al*, 2006).

Curiously, two of the identified mutations in hRrp40 occur at highly conserved residues that were proposed to be of importance for the latter function.

Concluding remarks and future perspectives

The exosome is a remarkably versatile protein complex, involved in many different aspects of RNA metabolism. In fact, it is believed that almost every type of RNA will encounter the exosome somewhere within its lifecycle. Not surprisingly, the list of substrate RNAs of the exosome is astonishing, and will undisputedly grow as additional functions of the exosome will be explored. The identification of hDis3 and hDis3L1 as important ribonucleases for the activity of the exosome will certainly facilitate this process even further (e.g. by observing the stabilization of substrate RNAs after depletion of hDis3 and/or hDis3L1). In addition, there are several interesting reports about unexpected functions of the exosome, such as its involvement in controlling the eukaryotic circadian clock (Guo *et al*, 2009) and its role in promoting antibody diversity by regulating the activation-induced cytidine deaminase in immunoglobulin heavy-chain class switch recombination and somatic hypermutation (Basu *et al*, 2011). Finally, exosome core components can have individual non-exosome associated roles, as for example has been reported for hRrp46, which appeared to be involved in the clearance of apoptotic DNA (Yang *et al*, 2010).

The involvement in so many different (and sometimes essential) cellular processes, together with its relationship with several human diseases, indicates that the exosome is not only an important topic for fundamental research, but is also of major importance from a clinical perspective. Deciphering how the versatile activities of the exosome are modulated is therefore a key topic for the upcoming years.

References

Allmang C, Kufel J, Chanfreau G, Mitchell P, Petfalski E, Tollervey D (1999a) Functions of the exosome in rRNA, snoRNA and snRNA synthesis. *EMBO J* **18:** 5399-5410

Allmang C, Petfalski E, Podtelejnikov A, Mann M, Tollervey D, Mitchell P (1999b) The yeast exosome and human PM-Scl are related complexes of 3' --> 5' exonucleases. *Genes Dev* **13:** 2148-2158

Anderson JS, Parker RP (1998) The 3' to 5' degradation of yeast mRNAs is a general mechanism for mRNA turnover that requires the SKI2 DEVH box protein and 3' to 5' exonucleases of the exosome complex. *EMBO J* **17:** 1497-1506

Araki Y, Takahashi S, Kobayashi T, Kajiho H, Hoshino S, Katada T (2001) Ski7p G protein interacts with the exosome and the Ski complex for 3'-to-5' mRNA decay in yeast. *EMBO J* **20:** 4684-4693

Astuti D, Morris MR, Cooper WN, Staals RH, Wake NC, Fews GA, Gill H, Gentle D, Shuib S, Ricketts CJ, Cole T, van Essen AJ, van Lingen RA, Neri G, Opitz JM, Rump P, Stolte-Dijkstra I, Muller F, Pruijn GJ, Latif F, Maher ER (2012) Germline mutations in DIS3L2 cause the Perlman syndrome of overgrowth and Wilms tumor susceptibility. *Nat Genet* **44:** 277-284

Barbas A, Matos RG, Amblar M, Lopez-Vinas E, Gomez-Puertas P, Arraiano CM (2009) Determination of key residues for catalysis and RNA cleavage specificity: one mutation turns RNase II into a "SUPER-ENZYME". *J Biol Chem* **284:** 20486-20498

Basu U, Meng FL, Keim C, Grinstein V, Pefanis E, Eccleston J, Zhang T, Myers D, Wasserman CR, Wesemann DR, Januszyk K, Gregory RI, Deng H, Lima CD, Alt FW (2011) The RNA exosome targets the AID cytidine deaminase to both strands of transcribed duplex DNA substrates. *Cell* **144:** 353-363

Benard L, Carroll K, Valle RC, Masison DC, Wickner RB (1999) The ski7 antiviral protein is an EF1-alpha homolog that blocks expression of non-Poly(A) mRNA in Saccharomyces cerevisiae. *J Virol* **73:** 2893-2900

Chang HM, Triboulet R, Thornton JE, Gregory RI (2013) A role for the Perlman syndrome exonuclease Dis3l2 in the Lin28-let-7 pathway. *Nature* **497:** 244-248

Chapman MA, Lawrence MS, Keats JJ, Cibulskis K, Sougnez C, Schinzel AC, Harview CL, Brunet JP, Ahmann GJ, Adli M, Anderson KC, Ardlie KG, Auclair D, Baker A, Bergsagel PL, Bernstein BE, Drier Y, Fonseca R, Gabriel SB, Hofmeister CC, Jagannath S, Jakubowiak AJ, Krishnan A, Levy J, Liefeld T, Lonial S, Mahan S, Mfuko B, Monti S, Perkins LM, Onofrio R, Pugh TJ, Rajkumar SV, Ramos AH, Siegel DS, Sivachenko A, Stewart AK, Trudel S, Vij R, Voet D, Winckler W, Zimmerman T, Carpten J, Trent J, Hahn WC, Garraway LA, Meyerson M, Lander ES, Getz G, Golub TR (2011) Initial genome sequencing and analysis of multiple myeloma. *Nature* **471:** 467-472

Chekanova JA, Shaw RJ, Wills MA, Belostotsky DA (2000) Poly(A) tail-dependent exonuclease AtRrp41p from Arabidopsis thaliana rescues 5.8 S rRNA processing and mRNA decay defects of the yeast ski6 mutant and is found in an exosome-sized complex in plant and yeast cells. *J Biol Chem* **275:** 33158-33166

Chen CY, Gherzi R, Ong SE, Chan EL, Raijmakers R, Pruijn GJ, Stoecklin G, Moroni C, Mann M, Karin M (2001) AU binding proteins recruit the exosome to degrade ARE-containing mRNAs. *Cell* **107:** 451-464

Chlebowski A, Lubas M, Jensen TH, Dziembowski A (2013) RNA decay machines: the exosome. *Biochim Biophys Acta* **1829:** 552-560

Doma MK, Parker R (2006) Endonucleolytic cleavage of eukaryotic mRNAs with stalls in translation elongation. *Nature* **440:** 561-564

Dziembowski A, Lorentzen E, Conti E, Seraphin B (2007) A single subunit, Dis3, is essentially responsible for yeast exosome core activity. *Nat Struct Mol Biol* **14:** 15-22

Garneau NL, Wilusz J, Wilusz CJ (2007) The highways and byways of mRNA decay. *Nat Rev Mol Cell Biol* **8:** 113-126

Graham AC, Davis SM, Andrulis ED (2009a) Interdependent nucleocytoplasmic trafficking and interactions of Dis3 with Rrp6, the core exosome and importin-alpha3. *Traffic* **10:** 499-513

Graham AC, Kiss DL, Andrulis ED (2009b) Core exosome-independent roles for Rrp6 in cell cycle progression. *Mol Biol Cell* **20:** 2242-2253

Gudipati RK, Xu Z, Lebreton A, Seraphin B, Steinmetz LM, Jacquier A, Libri D (2012) Extensive degradation of RNA precursors by the exosome in wild-type cells. *Mol Cell* **48:** 409-421

Guhaniyogi J, Brewer G (2001) Regulation of mRNA stability in mammalian cells. *Gene* **265:** 11-23

Guo J, Cheng P, Yuan H, Liu Y (2009) The exosome regulates circadian gene expression in a posttranscriptional negative feedback loop. *Cell* **138:** 1236-1246

Haile S, Cristodero M, Clayton C, Estevez AM (2007) The subcellular localisation of trypanosome RRP6 and its association with the exosome. *Mol Biochem Parasitol* **151:** 52-58

Lejeune F, Li X, Maquat LE (2003) Nonsense-mediated mRNA decay in mammalian cells involves decapping, deadenylating, and exonucleolytic activities. *Mol Cell* **12:** 675-687

Liu Q, Greimann JC, Lima CD (2006) Reconstitution, activities, and structure of the eukaryotic RNA exosome. *Cell* **127:** 1223-1237

Lorentzen E, Walter P, Fribourg S, Evguenieva-Hackenberg E, Klug G, Conti E (2005) The archaeal exosome core is a hexameric ring structure with three catalytic subunits. *Nat Struct Mol Biol* **12:** 575-581

Lubas M, Damgaard CK, Tomecki R, Cysewski D, Jensen TH, Dziembowski A (2013) Exonuclease hDIS3L2 specifies an exosome-independent 3'-5' degradation pathway of human cytoplasmic mRNA. *EMBO J* **32:** 1855-1868

Malecki M, Viegas SC, Carneiro T, Golik P, Dressaire C, Ferreira MG, Arraiano CM (2013) The exoribonuclease Dis3L2 defines a novel eukaryotic RNA degradation pathway. *EMBO J* **32:** 1842-1854

Mitchell P, Tollervey D (2003) An NMD pathway in yeast involving accelerated deadenylation and exosome-mediated 3'-->5' degradation. *Mol Cell* **11:** 1405-1413

Mullen TE, Marzluff WF (2008) Degradation of histone mRNA requires oligouridylation followed by decapping and simultaneous degradation of the mRNA both 5' to 3' and 3' to 5'. *Genes Dev* **22:** 50-65

Nam DK, Lee S, Zhou G, Cao X, Wang C, Clark T, Chen J, Rowley JD, Wang SM (2002) Oligo(dT) primer generates a high frequency of truncated cDNAs through internal poly(A) priming during reverse transcription. *Proc Natl Acad Sci U S A* **99:** 6152-6156

Neil H, Malabat C, d'Aubenton-Carafa Y, Xu Z, Steinmetz LM, Jacquier A (2009) Widespread bidirectional promoters are the major source of cryptic transcripts in yeast. *Nature* **457:** 1038-1042

Oddone A, Lorentzen E, Basquin J, Gasch A, Rybin V, Conti E, Sattler M (2007) Structural and biochemical characterization of the yeast exosome component Rrp40. *EMBO Rep* **8:** 63-69

Preker P, Nielsen J, Kammler S, Lykke-Andersen S, Christensen MS, Mapendano CK, Schierup MH, Jensen TH (2008) RNA exosome depletion reveals transcription upstream of active human promoters. *Science* **322:** 1851-1854

Raijmakers R, Egberts WV, van Venrooij WJ, Pruijn GJ (2002) Protein-protein interactions between human exosome components support the assembly of RNase PH-type subunits into a six-membered PNPase-like ring. *J Mol Biol* **323:** 653-663

Rissland OS, Norbury CJ (2009) Decapping is preceded by 3' uridylation in a novel pathway of bulk mRNA turnover. *Nat Struct Mol Biol* **16:** 616-623

Schaeffer D, Tsanova B, Barbas A, Reis FP, Dastidar EG, Sanchez-Rotunno M, Arraiano CM, van Hoof A (2009) The exosome contains domains with specific endoribonuclease, exoribonuclease and cytoplasmic mRNA decay activities. *Nat Struct Mol Biol* **16:** 56-62

Schaeffer D, van Hoof A (2011) Different nuclease requirements for exosome-mediated degradation of normal and nonstop mRNAs. *Proc Natl Acad Sci U S A* **108:** 2366-2371

Schilders G, van Dijk E, Pruijn GJ (2007) C1D and hMtr4p associate with the human exosome subunit PM/Scl-100 and are involved in pre-rRNA processing. *Nucleic Acids Res* **35:** 2564-2572

Schneider C, Anderson JT, Tollervey D (2007) The exosome subunit Rrp44 plays a direct role in RNA substrate recognition. *Mol Cell* **27:** 324-331

Schneider C, Kudla G, Wlotzka W, Tuck A, Tollervey D (2012) Transcriptome-wide analysis of exosome targets. *Mol Cell* **48:** 422-433

Schneider C, Leung E, Brown J, Tollervey D (2009) The N-terminal PIN domain of the exosome subunit Rrp44 harbors endonuclease activity and tethers Rrp44 to the yeast core exosome. *Nucleic Acids Res* **37:** 1127-1140

Stoecklin G, Mayo T, Anderson P (2006) ARE-mRNA degradation requires the 5'-3' decay pathway. *EMBO Rep* **7:** 72-77

Tomecki R, Kristiansen MS, Lykke-Andersen S, Chlebowski A, Larsen KM, Szczesny RJ, Drazkowska K, Pastula A, Andersen JS, Stepien PP, Dziembowski A, Jensen TH (2010) The human core exosome interacts with differentially localized processive RNases: hDIS3 and hDIS3L. *EMBO J* **29:** 2342-2357

van Dijk EL, Schilders G, Pruijn GJ (2007) Human cell growth requires a functional cytoplasmic exosome, which is involved in various mRNA decay pathways. *RNA* **13:** 1027-1035

van Hoof A, Frischmeyer PA, Dietz HC, Parker R (2002) Exosome-mediated recognition and degradation of mRNAs lacking a termination codon. *Science* **295:** 2262-2264

van Hoof A, Staples RR, Baker RE, Parker R (2000) Function of the ski4p (Csl4p) and Ski7p proteins in 3'-to-5' degradation of mRNA. *Mol Cell Biol* **20:** 8230-8243

Walsh CT, Garneau-Tsodikova S, Gatto GJ, Jr. (2005) Protein posttranslational modifications: the chemistry of proteome diversifications. *Angew Chem Int Ed Engl* **44:** 7342-7372

Wan J, Yourshaw M, Mamsa H, Rudnik-Schoneborn S, Menezes MP, Hong JE, Leong DW, Senderek J, Salman MS, Chitayat D, Seeman P, von Moers A, Graul-Neumann L, Kornberg AJ, Castro-Gago M, Sobrido MJ, Sanefuji M, Shieh PB, Salamon N, Kim RC, Vinters HV, Chen Z, Zerres K, Ryan MM, Nelson SF, Jen JC (2012) Mutations in the RNA exosome component gene EXOSC3 cause pontocerebellar hypoplasia and spinal motor neuron degeneration. *Nat Genet* **44:** 704-708

Yang CC, Wang YT, Hsiao YY, Doudeva LG, Kuo PH, Chow SY, Yuan HS (2010) Structural and biochemical characterization of CRN-5 and Rrp46: an exosome component participating in apoptotic DNA degradation. *RNA* **16:** 1748-1759

Yang XF, Wu CJ, Chen L, Alyea EP, Canning C, Kantoff P, Soiffer RJ, Dranoff G, Ritz J (2002) CML28 is a broadly immunogenic antigen, which is overexpressed in tumor cells. *Cancer Res* **62:** 5517-5522

Yu J, Vodyanik MA, Smuga-Otto K, Antosiewicz-Bourget J, Frane JL, Tian S, Nie J, Jonsdottir GA, Ruotti V, Stewart R, Slukvin, II, Thomson JA (2007) Induced pluripotent stem cell lines derived from human somatic cells. *Science* **318:** 1917-1920

Zhang W, Murphy C, Sieburth LE (2010) Conserved RNaseII domain protein functions in cytoplasmic mRNA decay and suppresses Arabidopsis decapping mutant phenotypes. *Proc Natl Acad Sci U S A* **107:** 15981-15985

Zhuang YY, Zhang H, Lin SJ (2013) Polyadenylation of 18S rRNA in algae. *Journal of Phycology* **49:** 570-579

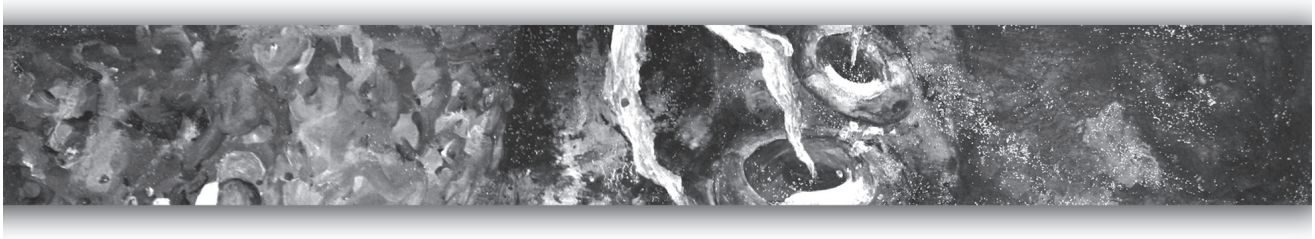

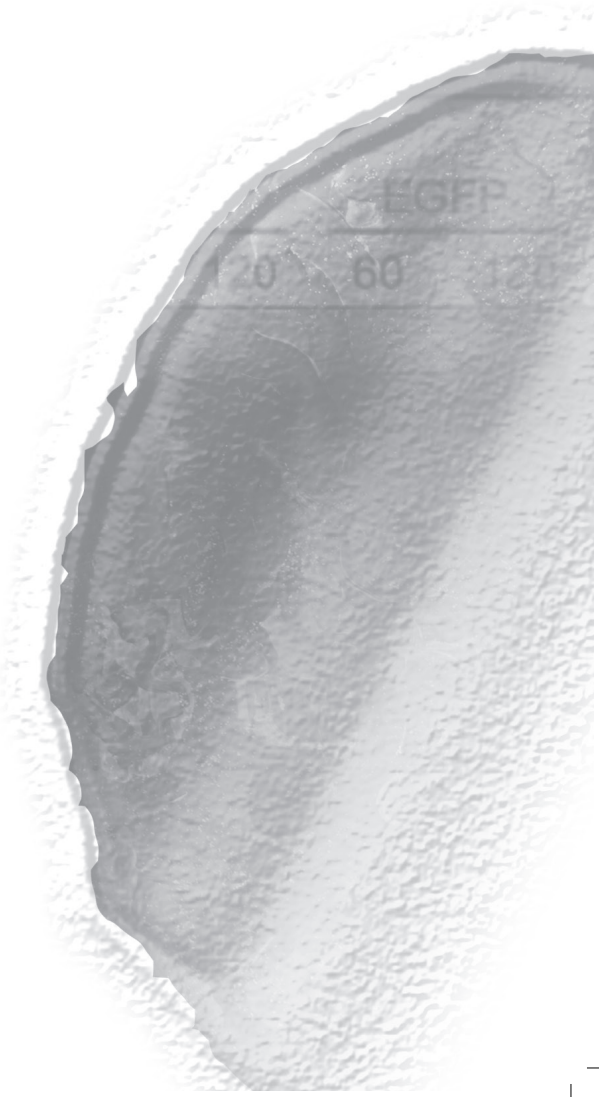

Summary

RNA metabolism is the collective term for all the different processes involving changes of RNA molecules during their lifecycle. Following transcription, many RNAs undergo maturation steps, during which the RNAs are processed and modified. In eukaryotes, several quality control pathways exist to coordinate these processes and to monitor the integrity of (mature) RNAs. The (partial) degradation of RNA is an indispensable step in many of these processes. A central role in these processes is played by the exosome, a multisubunit protein complex with ribonuclease (RNA degradation) activity. Since the term exosome is now also widely used for cell-derived vesicles that are present in biological fluids and cell culture media, the intracellular RNA degrading complex is frequently indicated with 'RNA exosome'.

A key advancement in our understanding of the eukaryotic exosome was the observation that the complex was devoid of intrinsic ribonuclease activity. Instead, the catalytic activity of the exosome is introduced by a set of ribonucleases, which can associate with the complex. For the well-characterized exosome in yeast, two of these ribonucleases were readily identified: yRrp6 and yDis3. Shortly thereafter, their human counterparts were identified as well: PM/Scl-100 and hDis3, respectively. Opposed to PM/Scl-100, the association of hDis3 with the human exosome remained elusive for many years. Furthermore, both these proteins are predominantly localized in the nucleus, while exosome complexes can be found in both the cytoplasm and the nucleus. These observations suggested that the activity of the human exosome is differently organized.

The objective of this study was to establish how the activity of the human exosome is accomplished and to determine which proteins and factors contribute to its activity. On one hand, the results of this study will be of importance from a fundamental, scientific point of view. For example, the experimental manipulation of newly identified ribonucleases associated with the exosome may facilitate the detection of novel substrates (or their degradation intermediates), potentially revealing new RNA degradation and/or processing pathways in human cells. On the other hand, the results of this study can be of medical importance, because several diseases are associated with dysfunctioning of (ribo)nucleases, or with the targeting of (ribo)nucleases by the immune system.

In **Chapter 1** we describe the discovery of the exosome from a historical perspective and provide a functional and structural comparison of exosome and exosome-like complexes in the three different domains of life. The current knowledge of important exosome-interacting proteins together with their contribution to several exosome-related functions is discussed as well.

The association of exosome complexes with several medical conditions is covered in **Chapter 2**. The occurrence of autoantibodies targeting exosome components and exosome-associated proteins in autoimmune disease patients will be discussed, which concurrently facilitated the identification of the exosome complex in humans. In addition, the current knowledge on aberrant expression of exosome and exosome-associated proteins in cancer patients is described.

The abovementioned nuclear localization of the ribonucleases PM/Scl-100 and hDis3 raised the question whether other ribonucleases are involved in the catalytic activities associated with the cytoplasmic human exosome complex. This question is addressed in **Chapter 3**. By analyzing immunoaffinity-purified exosome complexes by mass spectrometry, we identified a novel exosome-associated ribonuclease called hDis3-like exonuclease 1 (hDis3L1). We showed that hDis3L1 localized exclusively to the cytoplasm and that it is stably associated with the exosome complex. In addition, we demonstrate that the association of hDis3 with the exosome is relatively weak. Characterization of the enzymatic activity of hDis3L1 showed that the protein has exoribonuclease activity and contributes to the activity of the exosome. In contrast to hDis3, hDis3L1 lacks endoribonuclease activity, consistent with the lack of conservation of catalytically important residues in the N-terminal PIN domain.

In **Chapter 4** we address one of the biological roles of hDis3L1. Analyses of RNA degradation intermediates in the cytoplasm of human cells revealed hetero- and homopolymeric adenylated tails at internal positions of substrate RNAs. These polyadenylated degradation intermediates accumulated when protein levels of hDis3L1 were knocked down, which suggests that hDis3L1 is involved in polyadenylation-stimulated degradation of RNA in the cytoplasm. While polyadenylation-stimulated RNA degradation was known to occur in prokaryotes, organelles and nuclei of eukaryotic cells, the results of this study indicate that RNA degradation occurs by a similar mechanism in the cytoplasm as well.

In the study described in **Chapter 5**, we investigated the contributions of PM/Scl-100, hDis3 and the newly discovered hDis3L1 to the activity of the exosome complex as a whole. The results showed that the activities of hDis3 and hDis3L1 are most prominent at relatively low Mg^{2+} concentrations, in contrast to the activity of PM/Scl-100, which is dependent on much higher Mg^{2+} concentrations. Furthermore, the data suggested that the activity of PM/Scl-100 is modulated by other (yet unkown) exosome-association proteins. SiRNA-mediated knock-down studies with these three ribonucleases showed that their expression levels influence each other and that the association of hDis3L1 and PM/Scl-100 with the exosome might be mutually exclusive. These observations have important implications for the regulation of exosome complexes *in vivo*.

Analysis of the genomes of human and other higher eukaryotes revealed that they encode yet another protein with homology to the Dis3-like ribonucleases, which is called Dis3-like exonuclease 2, or hDis3L2 in humans. In **Chapter 6** we show that hDis3L2 is not detectaby associatied with the exosome, as revealed by co-immunopurification experiments. Overexpression of hDis3L2 in HEp-2 cells had a severe impact on cell morphology and viability, suggesting that cellular hDis3L2 levels are tightly regulated. *In vitro* activity assays showed that hDis3L2, like the other Dis3-like proteins, contains ribonuclease activity. Based on the results from the experiments described in this chapter and literature data we conclude with a discussion about the possible functional roles of hDis3L2.

The weak association of hDis3 with the exosome argues that hDis3 might have (additional) exosome-independent roles as well. In the experiments described in **Chapter 7**, we explored

the role of hDis3 outside the context of the exosome. We show that hDis3 associates with proteins involved in pre-mRNA splicing and processing. Furthermore, microarray analyses revealed that hDis3 affects the levels of a different set of mRNAs compared to the exosome, substantiating the different substrate repertoire of hDis3.

Finally, in **Chapter 8**, we summarize and integrate the most important results of this study and discuss what impact they have on our understanding of the human exosome. We conclude that the activity of the exosome is largely determined by the localization of the exosome-associating ribonucleases. This implies that hDis3 and PM/Scl-100 are predominantly responsible for the activities of the exosome in the nucleus. With the identification of hDis3L1, we have found an important mediator of the ribonuclease activity associated with the cytoplasmic exosome. The characterization of hDis3L1 also revealed a novel, hDis3L1-dependent RNA degradation pathway in the cytoplasm. It is possible that other cytoplasmic activities attributed to the exosome are mediated by this ribonuclease as well. Furthermore, we showed that the regulation of the activity of the exosome can be modulated by the microenvironment and possibly other, yet unknown exosome-associated proteins. The presence of the three different Dis3 homologues in other eukaryotes suggests that these conclusions might be applicable to exosomes in other eukaryotic species as well.

Samenvatting

RNA metabolisme is een collectieve term die alle verschillende processen omvat met betrekking tot veranderingen aan RNA moleculen tijdens hun levenscyclus. Na transcriptie ondergaan veel RNA's maturatie stappen, die het RNA bewerken en veranderen. In eukaryoten bestaan er een aantal kwaliteitscontroles die deze processen coördineren en de integriteit van het (mature) RNA monitoren. Bij veel van deze processen is het (deels) afbreken van RNA een onmisbare stap. Het exosoom, een eiwitcomplex met ribonuclease (RNA-afbraak) activiteit, speelt hierin een belangrijke rol. Omdat de term exosoom nu ook veel gebruikt wordt voor de van cellen afgesplitste blaasjes, die aanwezig zijn in biologische vloeistoffen en in media van celculturen, wordt dit intracellulaire, RNA-afbrekende eiwitcomplex vaak aangeduid als het 'RNA exosoom'.

Een belangrijke vooruitgang in het begrijpen van het eukaryote exosoom was de observatie dat het complex zelf geen intrinsieke ribonuclease-activiteit heeft. De katalytische activiteit van het exosoom wordt in plaats daarvan verzorgd door een set van ribonucleases die associëren met het complex. Twee van deze ribonucleases werden al snel geïdentificeerd in het goed gekarakteriseerde exosoomcomplex van gist: yRrp6 en yDis3. Kort hierna werden de tegenhangers hiervan ook in menselijke cellen geïdentificeerd: PM/Scl-100 en hDis3. In tegenstelling tot PM/Scl-100 bleef de associatie van het hDis3 eiwit gedurende vele jaren maar moeilijk aantoonbaar. Daarnaast bevinden deze twee eiwitten zich voornamelijk in de kern, terwijl exosoomcomplexen in zowel de kern als het cytoplasma te vinden zijn. Deze observaties suggereerden dat de activiteit van het humane exosoom anders georganiseerd is.

Het doel van deze studie was om vast te stellen hoe de activiteit van het humane exosoom tot stand gebracht wordt en om te bepalen welke eiwitten en factoren bijdragen aan de activiteit van het exosoom. Enerzijds zijn de resultaten van deze studie belangrijk vanuit een fundamenteel wetenschappelijk oogpunt. Zo is het mogelijk om door het experimenteel manipuleren van nieuw geïdentificeerde, exosoom-geassocieerde ribonucleases nieuwe RNA-substraten (of de afbraakproducten daarvan) en mogelijk nieuwe afbraak- en/of bewerkingsroutes in humane cellen bloot te leggen. Anderzijds kunnen de resultaten van deze studie van medisch belang zijn, omdat enkele ziekten geassocieerd zijn met een ontregeling van (ribo)nucleases, of met een immuunrespons tegen deze (ribo)nucleases.

In **Hoofdstuk 1** beschrijven we de ontdekking van het exooom vanuit een historisch perspectief en geven we een functionele en structurele vergelijking van het exosoom en 'exosoom-achtige' complexen in de drie levensdomeinen. Onze huidige kennis van belangrijke exosoom-interacterende eiwitten samen met hun bijdragen aan enkele exosoom-gerelateerde functies worden ook bediscussieerd.

De relatie van exosoomcomplexen met betrekking tot een aantal medische aandoeningen wordt behandeld in **Hoofdstuk 2**. De aanwezigheid van autoantilichamen gericht tegen exosoomcomponenten en exosoom-geassocieerde eiwitten in auto-immuunpatiënten zal worden behandeld. Deze ontdekking heeft tegelijkertijd de identificatie van het humane

exosoom gefaciliteerd. Daarnaast wordt de huidige kennis met betrekking tot de afwijkende expressie van exosoom en exosoom-geassocieerde eiwitten in kankerpatiënten besproken.
De bovengenoemde lokalisatie van de ribonucleases PM/Scl-100 en hDis3 in de celkern wierp de vraag op of andere ribonucleases mogelijk betrokken zijn bij de katalytische activiteit die geassocieerd is met het cytoplasmatische humane exosoomcomplex. Deze vraag wordt behandeld in **Hoofdstuk 3**. Door het analyseren van immuno-affiniteits opgezuiverde exosoomcomplexen met behulp van massaspectrometrie hebben we een nieuwe exosoom-geassocieerde ribonuclease gevonden, genaamd hDis3-like exoribonuclease 1 (hDis3L1). We hebben laten zien dat hDis3L1 zich exclusief in het cytoplasma bevindt en dat het stabiel met het exosoomcomplex geassocieerd is. Daarnaast laten we zien dat hDis3 relatief zwak aan het exosoom bindt. Uit enzymatische activiteitsanalyses van hDis3L1 bleek dat dit eiwit over exoribonuclease-activiteit beschikt en bijdraagt aan de activiteit van het exosoom. In tegenstelling tot hDis3 heeft hDis3L1 geen endonuclease activiteit, wat in overeenstemming is met het gebrek aan belangrijke, evolutionair-geconserveerde katalytische residuen in het N-terminale PIN domein van dit eiwit.
In **Hoofdstuk 4** richten we ons op een van de biologische rollen van hDis3L1. Analyses van RNA-afbraakintermediairen in het cytoplasma van humane cellen lieten zien dat er heterogene en homogene gepolyadenyleerde staarten op interne posities in het RNA zaten. Deze gepolyadenyleerde afbraakintermediairen hoopten zich op wanneer het eiwitniveau van hDis3L1 omlaag werd gebracht, hetgeen suggereerde dat hDis3L1 betrokken is bij de door polyadenylatie-gestimuleerde afbraak van RNA in het cytoplasma. Alhoewel het bekend is dat polyadenylatie-gestimuleerde RNA-afbraak optreedt in prokaryoten, organellen en kernen van eukaryote cellen, lieten de resultaten van deze studie zien dat RNA-afbraak ook in het cytoplasma via een vergelijkbaar mechanisme verloopt.
In de in **Hoofdstuk 5** beschreven studie hebben we de bijdragen aan de activiteit van het exosoom van PM/Scl-100, hDis3 en het nieuw ontdekte hDis3L1 eiwit onderzocht. De resultaten lieten zien dat de activiteit van hDis3 en hDis3L1 met name bevorderd wordt door lage Mg^{2+}-concentraties, in tegenstelling tot de activiteit van PM/Scl-100, die afhankelijk is van relatief hoge Mg^{2+}-concentraties. Daarnaast lieten de resultaten zien dat de activiteit van PM/Scl-100 gereguleerd kan worden door andere (nog onbekende) exosoom-geassocieerde eiwitten. Ten slotte hebben we middels siRNA-experimenten met de drie ribonucleases laten zien dat de expressieniveau's elkaar kunnen beïnvloeden en dat de binding van hDis3L1 of PM/Scl-100 aan het exosoom de binding van de ander wellicht uitsluit. Deze waarnemingen hebben belangrijke consequenties voor de regulatie van exosoomcomplexen *in vivo*.
Uit analyse van het humane genoom en andere genomen van hogere eukaryoten bleek dat deze nog voor een ander eiwit coderen dat structureel verwant is aan de Dis3-like ribonucleases, dat Dis3-like exonuclease 2, of hDis3L2 (in menselijke cellen) wordt genoemd.
In **Hoofdstuk 6** laten we door middel van co-immuunprecipitatie experimenten zien dat hDis3L2 niet detecteerbaar associeert met het exosoom. Overexpressie van hDis3L2 in HEp-2-cellen had ernstige effecten op de morfologie en viabiliteit van de cellen, wat suggereert dat

cellulaire hDis3L2 niveaus strikt gereguleerd zijn. *In vitro* activiteitsexperimenten lieten zien dat hDis3L2, net als de andere Dis3-like eiwitten, ribonuclease-activiteit heeft. Door middel van de huidige literatuur en de resultaten uit dit hoofdstuk eindigen we met een discussie over de mogelijke biochemische en celbiologische functies van hDis3L2.

De zwakke binding van hDis3 aan het exosoom wijst erop dat hDis3 mogelijk ook (additionele) exosoom-onafhankelijke rollen heeft. Met behulp van de experimenten in **Hoofdstuk 7** hebben we daarom de rol van hDis3 buiten de context van het exosoom onderzocht. We hebben laten zien dat hDis3 associeert met eiwitten die betrokken zijn met pre-mRNA splicing en 'processing'. Daarnaast hebben microarray-analyses uitgewezen dat hDis3 de niveaus van een andere set van mRNAs beïnvloedt in vergelijking met die van het exosoom. Dit versterkt onze hypothese dat hDis3 een ander substraatrepertoire heeft.

Ten slotte worden in **Hoofdstuk 8** de meest belangrijke resultaten van deze studies samengevat en geïntegreerd en wordt de invloed hiervan op onze kennis van het humane exosoom bediscussieerd. De activiteit van het exosoom wordt voor een belangrijk deel bepaald door de lokalisatie van de met het exosoom geassocieerde ribonucleases. Dit betekent dat hDis3 en PM/Scl-100 voornamelijk verantwoordelijk zullen zijn voor de activiteiten van het exosoom in de celkern. Met de identificatie van hDis3L1 hebben we een belangrijk ribonuclease voor exosoomcomplexen in het cytoplasma gevonden. Deze ontdekking heeft daarnaast ook een nieuwe, door hDis3L1-gemedieerde, afbraakroute voor RNAs in het cytoplasma blootgelegd. Het is mogelijk dat een deel van de andere aan het cytoplasmatische exosoom toegeschreven activiteiten ook afhankelijk zijn van deze ribonuclease. Verder hebben we laten zien dat de activiteiten van het exosoom gereguleerd kunnen worden door het micromilieu en mogelijkerwijs door andere, nog onbekende exosoom-bindende eiwitten. De aanwezigheid van de drie verschillende Dis3-homologen in andere eukaryote cellen suggereert dat deze conclusies mogelijk ook voor exosoomcomplexen in andere eukaryote organismen van toepassing zijn.

Curriculum vitae

Raymond H.J. Staals werd geboren op 16 oktober 1979 te Grubbenvorst. In 1998 behaalde hij zijn VWO-diploma aan het Blariacumcollege te Venlo, waarna hij begon aan de studie Biologie aan de Universiteit van Utrecht. Tijdens deze studie heeft hij twee wetenschappelijke stages gelopen. Zijn eerste stage was op de afdeling Ecofysiologie van Planten van de Universiteit van Utrecht, onder begeleiding van dr. A.J.M. Peeters. Zijn tweede stage was op de afdeling Medische Oncologie in het Josephine Nefkens Instituut, Erasmus Medisch Centrum te Rotterdam, onder begeleiding van dr. E.A.C. Wiemer. Het doctoraalexamen Biologie heeft hij gehaald in augustus 2006. Tussen 2005 en 2006 heeft hij gewerkt op het Blariacumcollege te Venlo als leraar biologie (bovenbouw van het HAVO en VWO). Van 2006 tot 2011 heeft hij gewerkt als promovendus op de afdeling Biomoleculaire Chemie van de Radboud Universiteit Nijmegen, onder begeleiding van prof. dr. G.J.M. Pruijn. Gedurende deze periode werd het onderzoek verricht dat is beschreven in dit proefschrift. Van 2011 tot 2014 heeft hij gewerkt als Research Fellow in het Laboratorium voor Microbiologie op de Universiteit van Wageningen, onder begeleiding van prof. dr. J. van der Oost. Begin 2014 heeft hij de Health Science Career Development Postdoctoral Fellowship van de Universiteit van Otago gehonoreerd gekregen. Sinds maart 2014 is hij werkzaam als Assistant Research Fellow in het Fineran laboratorium (Department of Microbiology and Immunology) op de Universiteit van Otago in Nieuw-Zeeland.

List of publications

Staals RH*, Zhu Y*, Taylor DW*, Kornfeld JE, Sharma K, Barendregt A, Koehorst JJ, Vlot M, Neupane N, Varossieau K, Sakamoto K, Suzuki T, Dohmae N, Yokoyama S, Schaap PJ, Urlaub H, Heck AJR, Nogales E, Doudna JA, Shinkai A, van der Oost J (2014) RNA-targeting by the Type III-A CRISPR-Cas Csm complex of *Thermus thermophilus*. *Mol Cell* 20 (in press)

Richter C*, Dy RL*, McKenzie RE*, Watson BN, Taylor C, Chang JT, McNeil MB, **Staals RH**, Fineran PC (2014) Priming in the Type I-F CRISPR-Cas system triggers strand-independent spacer acquisition, bi-directionally from the primed protospacer. *Nucleic Acids Res* 42: 8516-8526

Niemela EH*, Oghabian A*, **Staals RH**, Greco D, Pruijn GJ, Frilander MJ (2014) Global analysis of the nuclear processing of transcripts with unspliced U12-type introns by the exosome. *Nucleic Acids Res* 42: 7358-7369

Fineran PC, Gerritzen MJ, Suarez-Diez M, Kunne T, Boekhorst J, van Hijum SA, **Staals RH**, Brouns SJ (2014) Degenerate target sites mediate rapid primed CRISPR adaptation. *Proc Natl Acad Sci U S A* 111: E1629-1638

Louwen R, **Staals RH**, Endtz HP, van Baarlen P, van der Oost J (2014) The role of CRISPR-Cas systems in virulence of pathogenic bacteria. *Microbiol Mol Biol Rev* 78: 74-88

Staals RH*, Agari Y*, Maki-Yonekura S*, Zhu Y, Taylor DW, van Duijn E, Barendregt A, Vlot M, Koehorst JJ, Sakamoto K, Masuda A, Dohmae N, Schaap PJ, Doudna JA, Heck AJ, Yonekura K, van der Oost J, Shinkai A (2013) Structure and activity of the RNA-targeting Type III-B CRISPR-Cas complex of *Thermus thermophilus*. *Mol Cell* 52: 135-145

Westra ER*, **Staals RH***, Gort G, Hogh S, Neumann S, de la Cruz F, Fineran PC, Brouns SJ (2013) CRISPR-Cas systems preferentially target the leading regions of MOBF conjugative plasmids. *RNA Biol* 10: 749-761

Staals RH, Brouns SJ (2013) Distribution and Mechanism of the Type I CRISPR-Cas Systems. In *CRISPR-Cas Systems*, pp 145-169. Springer

Westra ER, Swarts DC, **Staals RH**, Jore MM, Brouns SJ, van der Oost J (2012) The CRISPRs, they are a-changin': how prokaryotes generate adaptive immunity. *Annu Rev Genet* 46: 311-339

Westra ER, van Erp PB, Kunne T, Wong SP, **Staals RH**, Seegers CL, Bollen S, Jore MM, Semenova E, Severinov K, de Vos WM, Dame RT, de Vries R, Brouns SJ, van der Oost J (2012) CRISPR immunity relies on the consecutive binding and degradation of negatively supercoiled invader DNA by Cascade and Cas3. *Mol Cell* 46: 595-605

Astuti D*, Morris MR*, Cooper WN, **Staals RH**, Wake NC, Fews GA, Gill H, Gentle D, Shuib S, Ricketts CJ, Cole T, van Essen AJ, van Lingen RA, Neri G, Opitz JM, Rump P, Stolte-Dijkstra I, Muller F, Pruijn GJ, Latif F, Maher ER (2012) Germline mutations in DIS3L2 cause the Perlman syndrome of overgrowth and Wilms tumor susceptibility. *Nat Genet* 44: 277-284

Staals RH, Bronkhorst AW, Schilders G, Slomovic S, Schuster G, Heck AJ, Raijmakers R, Pruijn GJ (2010) Dis3-like 1: a novel exoribonuclease associated with the human exosome. *EMBO J* 29: 2358-2367

Slomovic S*, Fremder E*, **Staals RH**, Pruijn GJ, Schuster G (2010) Addition of poly(A) and poly(A)-rich tails during RNA degradation in the cytoplasm of human cells. *Proc Natl Acad Sci U S A* 107: 7407-7412

Staals RH, Pruijn GJ (2010) The human exosome and disease. *Adv Exp Med Biol* 702: 132-142

Vreeburg RA, Benschop JJ, Peeters AJ, Colmer TD, Ammerlaan AH, Staal M, Elzenga TM, **Staals RH**, Darley CP, McQueen-Mason SJ, Voesenek LA (2005) Ethylene regulates fast apoplastic acidification and expansin A transcription during submergence-induced petiole elongation in *Rumex palustris*. *Plant J* 43: 597-610

*These authors contributed equally to this work

Dankwoord

Dit is vaak het meest gelezen onderdeel van een proefschrift en daardoor misschien wel het belangrijkste, zeker wanneer je beseft dat zonder de hulp van de onderstaande personen dit boekje nooit het levenslicht zou hebben gezien.

Ik wil graag beginnen met mijn promotor Ger Pruijn. Ger, dank je wel dat je ondanks de lange tijd die het geduurd heeft, altijd voor me klaar stond. Ik heb enorm veel van je geleerd, zeker wat betreft het schrijven van wetenschappelijk-correcte manuscripten en het kritisch bestuderen van mijn onderzoeksresultaten. Ik heb je vaak in mijn gedachten vergeleken met bèta-actine. Ik zal dit uitleggen. Niet alleen is bèta-actine essentieel voor de structurele integriteit, het wordt ook vaak gebruikt om zaken te normaliseren. Dat laatste had ik af en toe nodig als ik bij je langskwam met, in mijn ogen, tegenvallende resultaten, waar je vaak weer een positieve draai aan wist te geven. Andersom kon je me voorzien van kritiek op de momenten dat ik dacht dat ik iets onomstotelijk had aangetoond.

Els, wat was het altijd fijn om te weten dat ik voor werkelijk alles bij je terecht kon. Misschien in eerste instantie voor een goed gesprek, maar ook als er iets geregeld moest worden. Ik kon er gewoon blind op vertrouwen dat dingen altijd correct door jou werden afgehandeld: dank je wel voor alle hulp en steun!

Lettie, Walther en Wilbert, bedankt dat ik gebruik heb mogen maken van jullie ruime ervaring in de wetenschap, ik heb er veel baat bij gehad en denk nog vaak terug aan onze gesprekken. Ik sta nog steeds beschikbaar, mochten jullie hulp nodig hebben bij eventuele computerproblemen.

I would like to thank Professor Schuster and Professor Maher and members of their labs for the excellent collaborations we had. This has been a fantastic experience for me to see what you can achieve when working together on a project. De samenwerking met het lab van Professor Heck is een bijzondere. Met de identificatie van Dis3-like 1, is jullie werk doorslaggevend geweest voor het vinden van de ‘rode draad’ in mijn promotie traject. Ik ben er trots op dat we nu nog steeds samenwerken in het CRISPR veld en hoop dat we dit in de toekomst blijven doen; bedankt voor alles!

Ik had het geluk dat ik bij aanvang van mijn promotietraject op een rijdende ‘exosoom trein’ kon springen. Deze trein werd gerund door Erwin, Geurt en Wilma, maar we hadden ook een extra bemanningslid aan boord genaamd Reinout, die ondanks dat hij officieel op een andere trein werkzaam was, ons vaak voorzag van zijn enorme exosoom kennis. Ik wil jullie alle vier bedanken voor jullie hulp en advies voor het opzetten en uitvoeren van goed doordachte exosoom experimenten, maar ook voor het creëren van een leuke sfeer op het lab en daarbuiten.

Wat betreft de sfeer op het lab, wil ik graag een persoon in bijzonder noemen: Remon, aka 'de sloper uit Oss'. Het is bijna onwerkelijk dat we, ondanks alle ongein op het lab en daarbuiten, in staat zijn geweest om het boekje af te maken. Ik heb mede door jou een ontzettend leuke tijd op BMC gehad, waarvoor dank! Mariska, super leuk dat je er vaak bij was als we weer eens wat buiten BMC gingen doen. Ik kom snel eens even kijken naar jullie mooie nieuwe woning!

Verder wil ik ook graag al mijn andere collega's van 2.55 bedanken dat ze het zo lang met mij hebben weten vol te houden op het lab: ("guy") Sandy, ("soulless") Joyce, ("ja") Chantal, ("large mouth") Tamara, Carla O., Helma, Judith, en Annemarie. Sandy, RNA buddeh, gelukkig ben je een Facebook-fanaat en kan ik af en toe meelezen hoe leuk je het daar in de States hebt: you go guy! Joyce, je hebt behoorlijk wat zielige (ha!) grapjes moeten incasseren,maar je was gelukkig zelf ook niet op je mondje gevallen. Chantal, bedankt voor je vele goede (*kuch*) tips wat betreft de muziekkeuze op het lab en sorry dat we je van 'zeauveel' dingen hebben beschuldigd. Ook jouw promotie zal nu niet meer lang op zich laten wachten. Tamara, ik weet dat je prima Nederlands kunt lezen, dus bij dezen: bedankt voor de super leuke tijd in en buiten het lab! Heb me altijd rot kunnen lachen om de vele bizarre gesprekken die we hebben gehad en wil je nogmaals bedanken voor de leuke vakantie in Kroatië; hopelijk kom je me nog eens bezoeken in Nieuw-Zeeland. Carla O., gelukkig beschik je zelf over een gezonde portie humor en kon je de Remon en Raymond terror vaak met een rake opmerking de kop in drukken. Bedankt voor de excellente organisatie en hulp in het lab! Helma, ik vond het leuk om je als U-genoot te hebben en te mogen profiteren van je (RNA) kennis. Judith en Annemarie, bedankt dat jullie zo'n leuke buren voor me waren. Judith, bedankt voor je hulp aan hoofdstuk 5: dit waren geen gemakkelijke experimenten, maar je hebt het toch maar weer voor elkaar gekregen, super!

Natuurlijk wil ik het 2.35 lab ook niet vergeten. Marina, thanks for the interesting conversation we had about science and non-science related topics. Elina, many thanks for organizing all the great (dinner) parties and for sending me your thesis all the way to New Zealand. I'm was very pleased to be able to provide (a minor) contribution to one of your chapters and wish you all the best in Finland! Sanne en Carla, ik ken weinig mensen die elke dag met zo'n vrolijk humeur op het lab staan; daar kan deze 'grumpy cat' nog een hoop van leren! Sander en Lonneke, bedankt voor de leuke sfeer op het lab en het 'über'-gezellig maken van de congressen die we samen hebben bezocht. Siebe (en/of Teo?), heb enorm kunnen genieten van je droge humor en je no-nonsense mentaliteit, bedankt voor al je hulp en advies voor mijn experimenten.

Een groot deel van het werk dat beschreven staat in dit proefschrift is mede tot stand gekomen door de inzet van een aantal excellente studenten die ik heb mogen begeleiden tijdens mijn promotietijd: Marie-Christine, Walter, Christian, Manuela, Victoria en Peter. Wat heb ik toch ontzettend geboft met jullie! Naast het feit dat ik het super leuk heb gevonden om met jullie samen te werken, hebben jullie allemaal een zeer belangrijke bijdrage geleverd aan de verschillende onderwerpen. Bedankt voor al jullie inzet en de ontzettend leuke tijd!

Natuurlijk is het ook belangrijk om ook wat ontspanning te vinden na het werk of in het weekend. Marieke en Dave, bedankt dat jullie deur altijd open stond voor een gezellig avondje of weekend! Janneke, bedankt voor de leuke tijd in Grave, en al is het anders gelopen dan we hadden gedacht, uiteindelijk is het allemaal goed gekomen en heeft het ons (ook letterlijk) verder gebracht.

Maurice en Karlijn, ik vind het nog steeds erg bijzonder dat jullie mij peetoom van Emma hebben gemaakt: ik ben hier ontzettend blij mee! Ik zou willen dat ik wat vaker langs kon komen, maar de afstand van bijna 20.000 kilometer maakt dat op dit moment een beetje lastig. Ik hoop dit in de komende jaren goed te maken. Hetzelfde geldt voor Lucien. Als bijna-afgestudeerde ga je binnenkort immers ook het 'dokters pad' op en ben daarom benieuwd hoe je dat zult ervaren. Als ik zie wat je allemaal voor talenten in huis hebt, weet ik zeker dat je ook dit tot een goed einde zal gaan brengen. Bedankt voor je bijdrage aan de cover: die is prachtig geworden! Vond het fijn dat jullie alle drie (Emma interesseert het geloof ik nog niet zo) altijd geïnteresseerd waren, ondanks dat het vaak moeilijk te begrijpen was waar ik nou precies mee bezig was!

Last but not least: mum en ded. Ik vind het erg moeilijk om de juiste woorden te vinden om goed duidelijk te kunnen maken hoeveel jullie voor me betekenen. Jullie stonden, en staan nog steeds, altijd voor mij klaar wat er ook gebeurde. Zo hebben jullie me altijd gestimuleerd om gewoon te gaan voor de dingen die ik graag wilde doen, zelfs toen dit betekende dat ik aan de andere kant van de wereld zou gaan wonen. Zonder jullie hulp en steun had ik het dan ook nooit zo ver kunnen schoppen en daar ben ik jullie oneindig dankbaar voor!!